

RESERVOIR MANAGEMENT STRATEGY FOR EAST
RANDOLPH FIELD, RANDOLPH TOWNSHIP, PORTAGE
COUNTY, OHIO

August 1997

By
L. Eugene Safley
S. Phillip Salamy
Mark A. Young
Michael L. Fowler
James L. Wing
John B. Thomas
Jim Mills
Dan Wood

July 1998

Performed Under Contract No. DE-AC22-94PC91008

BDM Oklahoma, Inc
Bartlesville, Oklahoma

**National Petroleum Technology Office
U. S. DEPARTMENT OF ENERGY
Tulsa, Oklahoma**

MASIER YOU

DISTRIBUTION OF THIS DOCUMENT IS UNLIMITED



DISCLAIMER

This report was prepared as an account of work sponsored by an agency of the United States Government. Neither the United States Government nor any agency thereof, nor any of their employees, makes any warranty, expressed or implied, or assumes any legal liability or responsibility for the accuracy, completeness, or usefulness of any information, apparatus, product, or process disclosed, or represents that its use would not infringe privately owned rights. Reference herein to any specific commercial product, process, or service by trade name, trademark, manufacturer, or otherwise does not necessarily constitute or imply its endorsement, recommendation, or favoring by the United States Government or any agency thereof. The views and opinions of authors expressed herein do not necessarily state or reflect those of the United States Government.

This report has been reproduced directly from the best available copy.

Available to DOE and DOE contractors from the Office of Scientific and Technical Information, P.O. Box 62, Oak Ridge, TN 37831; prices available from (615) 576-8401.

Available to the public from the National Technical Information Service, U.S. Department of Commerce, 5285 Port Royal Rd., Springfield VA 22161

DISCLAIMER

Portions of this document may be illegible in electronic image products. Images are produced from the best available original document.

**RESERVOIR MANAGEMENT STRATEGY FOR EAST RANDOLPH
FIELD, RANDOLPH TOWNSHIP, PORTAGE COUNTY, OHIO**

for

**Management and Operating Contract
for the Department of Energy's
National Oil and Related Programs**

Work Performed Under Contract No.
DE-AC22-94PC91008

Prepared for
U.S. Department of Energy
Assistant Secretary for Fossil energy
Edith Allison, Project Manager
National Petroleum Technology Office

DISCLAIMER

This report was prepared as an account of work sponsored by an agency of the United States Government. Neither the United States Government nor any agency thereof, nor any of their employees, makes any warranty, expressed or implied, or assumes any legal liability or responsibility for the accuracy, completeness, or usefulness of any information, apparatus, product, or process disclosed, or represents that its use would not infringe privately owned rights. Reference herein to any specific commercial product, process, or service by trade name, trademark, manufacturer, or otherwise does not necessarily constitute or imply its endorsement, recommendation, or favoring by the United States Government or any agency thereof. The views and opinions of authors expressed herein do not necessarily state or reflect those of the United States Government or any agency thereof.

BDM-Oklahoma, Inc.
P.O. Box 2565
Bartlesville, Oklahoma 74005

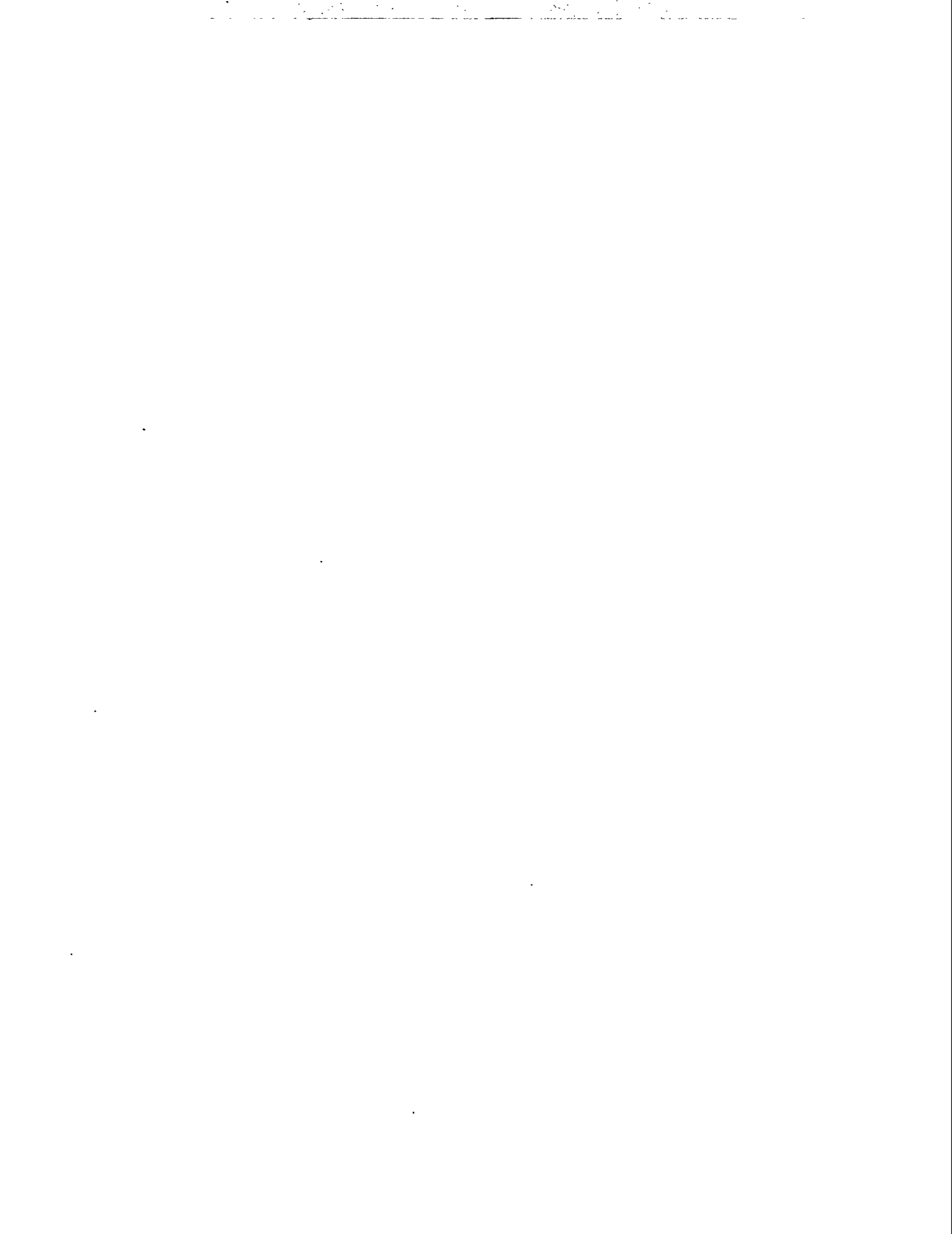


TABLE OF CONTENTS

1.0	INTRODUCTION.....	1
1.1	Program Description	1
1.2	East Randolph Field Reservoir Management Demonstration Project.....	2
2.0	RESERVOIR MANAGEMENT STRATEGY.....	5
2.1	Reservoir Management Process	5
2.2	Improved Recovery Process	5
2.3	Well Spacing	6
2.4	Data Collection and Integration	7
2.5	Production Aspects.....	8
3.0	EAST RANDOLPH FIELD RESERVOIR CHARACTERIZATION	9
3.1	Data Available and Previous Work	9
3.2	Geological Analyses	13
3.2.1	Structural Interpretation	13
3.2.2	Stratigraphic Interpretation	17
3.2.2.1	Log Analysis	17
3.2.2.2	Geologic Mapping Interpretation	19
3.2.3	Core Analyses.....	27
3.2.3.1	Conventional Core Analysis.....	27
3.2.3.2	Special Core Analysis	31
3.2.3.3	Core Description and Petrographic Analyses	37
3.2.4	Depositional Environment Interpretation	47
3.2.5	Production Mapping Interpretation	48
3.3	Reservoir Engineering Analysis	56
3.3.1	Preliminary Data Analysis	56
3.3.2	Pressure Buildup Analysis.....	57
3.3.3	PVT Data Analysis.....	58
3.3.4	Relative Permeability and Capillary Pressure Data Collection	59
3.3.5	Volumetrics and Material Balance Calculations	63
4.0	RESERVOIR SIMULATION.....	65
4.1	Single-Well Model Simulation of the McGuire No. 1 Well.....	65
4.2	Pilot Area Simulation.....	72

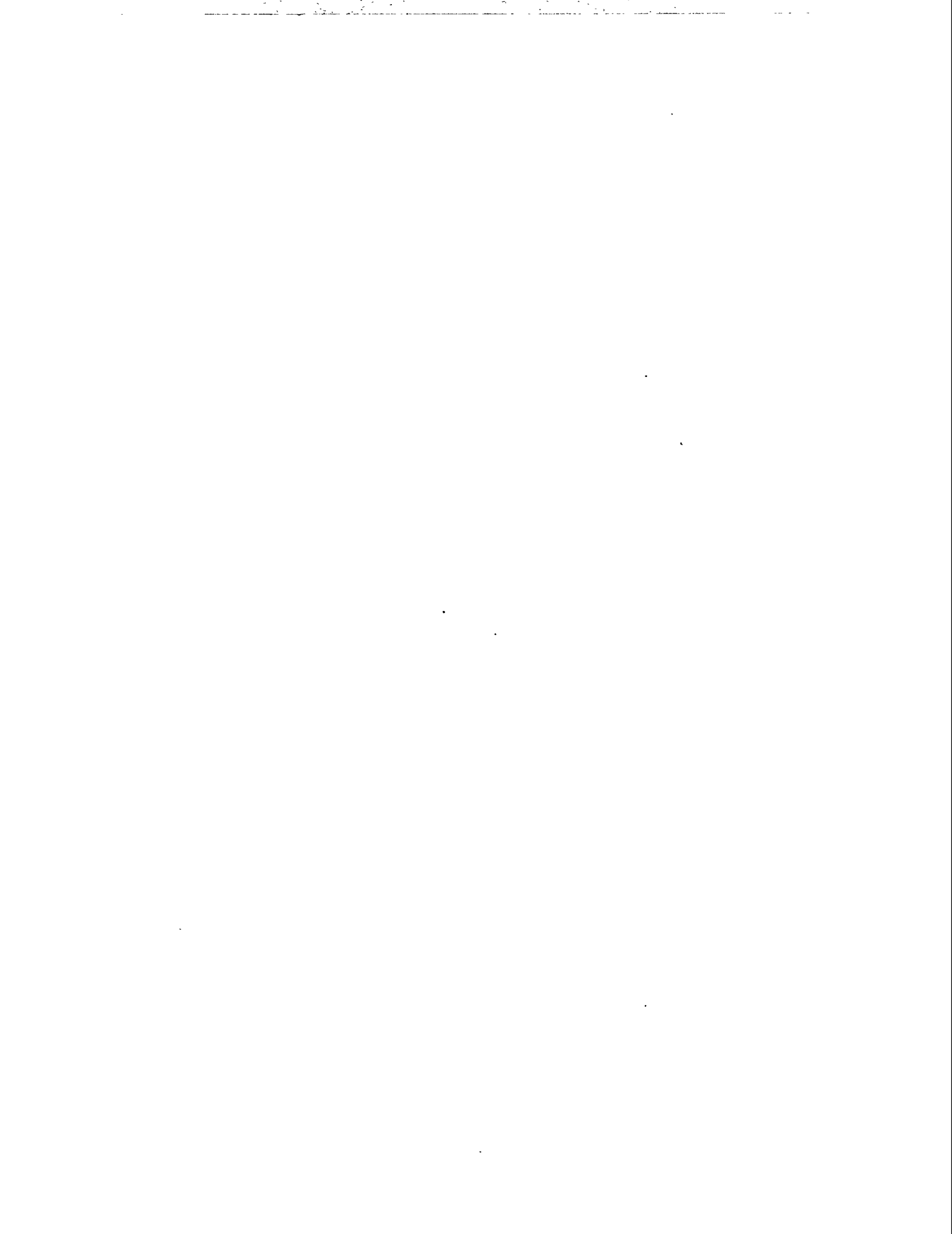
4.3	Full-Field Simulation	72
4.3.1	Model Development	72
4.3.2	History Matching	73
4.3.3	Recovery Process Predictions	75
5.0	PRODUCTION ANALYSES	79
6.0	ECONOMIC ANALYSES	83
6.1	Base Case Economics	83
6.2	Waterflood Economics	85
6.3	Gas Injection Economics	86
7.0	APPLICATION OF RESERVOIR MANAGEMENT CONCEPTS	89
7.1	Defining Reservoir Management Approach	89
7.1.1	Introduction	89
7.1.2	Reservoir System	89
7.1.3	Available Technologies	90
7.1.4	Business Environment	91
7.2	Plan Building Process	92
7.3	Summary of the Plan-Building Process for East Randolph Field	93
8.0	TECHNOLOGY TRANSFER	97
9.0	REFERENCES	99

Appendices

A	SPECIAL CORE ANALYSES	103
B	SPE 37334	133
C	SPE 37333	147

TABLES

3-1	Routine Permeability and Porosity Results.....	32
3-2	Petrophysical Properties of Selected Plugs at 100 and 4,250 psig Net Confining Pressure	36
3-3	East Randolph Field Reservoir Properties.....	56
3-4	Results of Pressure Buildup Data Analysis for the McGuire No. 1 Well	58
3-5	Summary of PVT Data Analysis.....	59
3-6	Volumetric OOIP Analysis by Reservoir Zone for East Randolph Field	63
6-1	Economic Assumptions	84
6-2	Base Case Economic Results for a July 1, 1996 Start Date.....	84
6-3	Waterflooding Case Economic Results for a July 1, 1996 Start Date	85
6-4	Gas Injection Case Economic Results for a July 1, 1996 Start Date	86



FIGURES

3-1	East Randolph Field Location Map	9
3-1	East Randolph Field Location Map	9
3-2	Gamma Ray-Neutron/Density Type Log for East Randolph Field	11
3-3	Cross Section Locations for East Randolph Field.....	15
3-4	Structure Top of the Rose Run with Location of Northwest-Trending Normal Faults .	16
3-5	Crossplot of Core Porosity vs. Permeability for Cored Wells in East Randolph Field..	19
3-6	Net Sand Thickness of Rose Run Zone 3B Using a 6% Porosity Cutoff	21
3-7	Average Porosity in Rose Run Zone 3B with Bubbled Cumulative Oil Production....	22
3-8	Average Water Saturation Rose Run Zone 3B with Bubbled Cumulative Water Production	23
3-9	Average Water Saturation Rose Run Zone 3B with Bubbled Cumulative Water Production	24
3-10	Average Porosity of Rose Run Zone 3A with Bubbled Cumulative Oil Production ...	25
3-11	Average Water Saturation of Rose Run Zone 3A with Bubbled Cumulative Water Production	26
3-12	Rose Run Zone 2 Net Sandstone Thickness Using a 6% Porosity Cutoff	28
3-13	Rose Run Zone 2 Average Porosity with Bubbled Cumulative Gas Production.....	29
3-14	Rose Run Zone 2 Average Water Saturation with Bubbled Cumulative Water Production	30
3-15	Gas Permeabilities from OMNI and BDM-OK Labs. BDM measurements were performed with 100 psig confining pressure.....	33
3-16	Gas Permeabilities from Routine Property Measurements by Depth	34
3-17	Porosities from Routine Property Measurements by Depth.....	34
3-18	Changes in Pore Volumes with Stress Interpreted from Squeeze-Out Measurements .	35
3-19	Comparison of Brine Permeability Measurements (4,250 psig Confining Pressure) with Air Permeability Measurements (100 psig Confining Pressure).....	36
3-20	Core Photographs of Rose Run Zone 3B Taken from McGuire No. 2 Core. Plain light	38
3-21	Core Photographs of Rose Run Zone 3B Taken from McGuire No. 2 core. Fluorescent light	39
3-22	Core Photograph of Rose Run Zone 3A Taken from McGuire No. 2 Core. Plain light	40
3-23	Core Photograph of Rose Run Zone 3A Taken from McGuire No. 2 Core. Fluorescent light	41
3-24	Core Photograph of Rose Run Zone 2 Taken from McGuire No. 2 Core. Plain light	42
3-25	Core Photograph of Rose Run Zone 2 Taken from McGuire No. 2 Core. Fluorescent light	43

3-26	Photomicrographs in Plain (Left) and Polarized (Right) Light of Rose Run Zone 3B Taken from McGuire No. 2 Core Showing Lithology and Grain Size Distribution	45
3-27	Photomicrographs in Plain (Left) and Polarized (Right) Light of Rose Run Zone 3B Taken from the McGuire No. 2 Core Showing Types of Cement and Porosity Distribution	47
3-28	Contoured and Bubbled 9-Month Oil Production	49
3-29	Contoured and Bubbled 9-Month Gas Production	51
3-30	Contoured Average Producing GOR With Bubbled Cumulative Gas Production.	52
3-31	Producing WOR Map for the Rose Run.	53
3-32	Contoured Estimated Ultimate Recovery of Oil from East Randolph Field	54
3-33	Contoured Estimated Ultimate Recovery of Gas from East Randolph Field.	55
3-34	Pressure Buildup Analysis Using a Horner Plot for the McGuire No. 1 Well	57
3-35	Pressure Buildup Analysis Using ATCM for the McGuire No. 1 Well	58
3-36	Relative Permeability for Oil-brine System, McGuire No. 2 Zone 3A at 7328.3 ft	61
3-37	Centrifuge Oil-Brine Capillary Pressure, McGuire No. 2 Zone 3A at 7332.2 ft.	62
3-38	Waterflood Susceptibility Test, McGuire No. 2 Coreflood	62
3-39	Material Balance Pressure Match for East Randolph Field.	64
4-1	History Match of Cumulative Oil Production for the McGuire No. 1 Well	66
4-2	History Match of Cumulative Gas Production for the McGuire No. 1 Well	67
4-3	History Match of Cumulative Water Production for the McGuire No. 1 Well.	67
4-4	History Match of Cumulative Oil Production for the McGuire No. 1 Well (No Free Gas).	68
4-5	History Match of Cumulative Water Production for the McGuire No. 1 Well (No Free Gas).	68
4-6	History Match of Cumulative Gas Production for the McGuire No. 1 Well (No Free Gas).	69
4-7	Decline Curves for the McGuire No. 1 Well	69
4-8	Base Case Oil Rate Simulation vs. the Decline Curve Extrapolations.	70
4-9	Base Case Gas Rate Simulation vs. the Decline Curve Extrapolations	70
4-10	McGuire No. 1 Well Oil Production Waterflood.	71
4-11	McGuire No. 1 Well Cumulative Oil Production Waterflood Projection	71
4-12	Full-Field History Match of Cumulative Oil Production	73
4-13	Full-Field History Match of Cumulative Gas Production.	74
4-14	Full-Field History Match of Reservoir Pressure	74
4-15	East Randolph Field Oil Rate Production as Function of Recovery Process	76
4-16	East Randolph Field Cumulative Oil Production as Function of Recovery Process.	76
4-17	East Randolph Field Cumulative Gas Production as Function of Recovery Process	77
4-18	East Randolph Field Pressure Performance as Function of Recovery Process	78
6-1	Cumulative Undiscounted Net Case Flow Diagram for Improved Recovery Options in East Randolph Field	85

EXECUTIVE SUMMARY

The Reservoir Management Field Demonstration Program is a Department of Energy (DOE) program designed to demonstrate reservoir management techniques to independent oil operators. Projects are conducted as Cooperative Research and Development Agreements (CRADAs) with at least 50% industry cost sharing, and last approximately one year. The projects involve a significant regional oil resource and/or address a major technology need. The team members transfer information about the methods employed, value achieved, and project results to other operators through DOE and industry publications, project workshops, and presentations at regional conferences.

The primary objective of the project with Belden and Blake Corporation is to demonstrate that multidisciplinary reservoir management teams using appropriate software and methodologies can develop a comprehensive reservoir management strategy to improve the operational economics and optimize oil production from East Randolph field, Randolph Township, Portage County, Ohio. A secondary objective is to transfer information about technical results, methods used, and value received in developing the reservoir management strategy to independent operators active in the Appalachian Basin. Building an optimal reservoir management plan requires knowledge and consideration of (1) the reservoir system, (2) proven and currently evolving technologies, and (3) the business environment under which the reservoir management plan will be implemented.

The Upper Cambrian Rose Run sandstone is currently the most active exploratory play in the Appalachian Basin. The Rose Run sandstone, a member of the Upper Cambrian Knox Supergroup, ranges in thickness from 110 to 150 ft and consists of stacked sheet sandstone deposits separated by and interbedded with thin, low permeability dolomites and carbonaceous shales. The Rose Run subcrop extends from southern Ohio northeastward to northwest Pennsylvania, approximately parallel to the current structural configuration of the Appalachian Basin. Most production from the Rose Run is dry natural gas from structural and stratigraphic traps.

Since 1992, the East Randolph field has produced an estimated 450,000 bbl of oil and 1.5 bcf of gas from the Rose Run sandstone. The field consists of 32 active wells drilled on approximately 60-ac spacing. The predominant recovery mechanism is solution gas drive. Data available at the beginning of the project consisted of hard-copy wireline logs, completion reports and stimulation history for each well, analyses of whole core from nearby fields and of sidewall cores from East Randolph field, fluid analyses, pressure data, capillary pressure and relative permeability data from nearby fields, production data, and articles on geologic history and field development. Additional data needs were identified, and core data, specialized wireline logs, pressure buildup data, fluid analyses, and logs from infill wells were acquired.

Fracture analysis was investigated in the Rose Run using the Formation Micro-Imager logging tool and whole core analysis. Two dominant fracture trends were interpreted for the area: east-west and north-northwest-south-southeast. The east-west set predominates, and both trends are related to regional faulting associated with the Suffield fault system, which is the southern boundary of the field.

Petrophysical analysis of the Rose Run sandstone includes quantifying petrophysical properties from wireline logs, integrating core and petrographic data with geophysical log data, and mapping measured and calculated reservoir properties. Gamma ray logs were found to be of limited value for correlating productive sandstone intervals; instead, neutron/density logs were used. Resistivity logs were normalized using the Glenwood Shale as a regional marker before calculating water saturations.

The geologic data from well log interpretation and core analyses in East Randolph field were entered into GeoGraphix software for the construction and interpretation of maps of structure, net sandstone thickness, porosity, water saturation, gas-oil and water-oil ratios, and production. Cross sections were constructed for identification of faulting, structural compartmentalization, and permeability barriers, and the correlation of individual flow units. The three productive Rose Run sandstone zones in East Randolph field were deposited as linear sand bodies oriented parallel to depositional strike trending to the northeast-southwest. The average net sandstone thicknesses of the zones are 4–8 ft, with porosities averaging from 6% to 12%. The sandstones have sharp, conformable basal contacts into dolomite and gradational upper contacts. Downdip wells have higher water-oil ratios than updip wells.

Core analysis showed that reservoir quality is predominantly controlled by the amount of silica and carbonate cement and the extent of secondary dissolution porosity. The dominant mineral constituents are monocrystalline quartz, K-feldspar, plagioclase feldspar, and polycrystalline quartz. Most of the intergranular pores are small, poorly interconnected, and partially to completely occluded by quartz and dolomite cementation. Porosity enhancement is due to partial to complete dissolution of chemically unstable feldspar grains and rock fragments. The thicker sandstone intervals have better developed effective intergranular porosity and higher permeability. Interbedded dolomites may act as permeability barriers or baffles. Areas of faulting and fracturing may create localized fracture porosity.

The Rose Run sandstone was deposited as a lowstand deposit in a shallow subtidal to intertidal marine environment on a broad carbonate shelf during a sea level fall, and reworked during a subsequent highstand of sea level. Individual sandstone beds were deposited parallel to the active paleoshoreline as imbricate sheet sands. The repeated fining-upward cycles suggest deposition by waning storm-generated currents that was later reworked by current activity.

The highest oil production rates, cumulative oil production volumes, and estimated ultimate oil recovery correlate with the thickest net sands in the central part of the field. These sands have the highest porosity and permeability and lower water saturation. High initial gas-oil ratios suggest

an initial gas cap may have been present where zone 2 is best developed in the updip portion of the field.

Available reservoir and production data were gathered and analyzed to describe the field in terms of pressures, production rates, stimulation effectiveness, and reservoir quality. A single-well reservoir model was developed to run on BOAST3-PC using the minimal field data. Well stimulation data were evaluated, and fracture gradients for the wells were computed. The resulting single-well model was found to be unstable due to high producing gas-oil ratios and the lack of pressure-volume-temperature (PVT) analyses, pressure data, and sufficient core data.

In order to perform material balance calculations and do a simulation study, the reservoir pressure was measured to estimate reservoir properties. A 14-day pressure buildup test was conducted, and Horner technique and automatic curve matching were used to predict the effective reservoir permeability and formation damage, and to estimate the reservoir pressure. The need to understand the fluid properties, bubble point pressure, and solution gas-oil ratio, dictated the need to run PVT analyses on fluid samples from East Randolph field. Steady-state imbibition tests, second-drainage oil-water relative permeability measurements, oil-brine centrifuge tests, and a water susceptibility test were performed on core samples. The residual brine saturation ranged from 31.5% to 44.9% of pore volume. Residual oil saturations achieved during these tests ranged from 25% to 45%, yielding oil recovery rates from 30% to 58% of original oil-in-place (OOIP).

Material balance calculations using Dwight's OilWat/GasWat material balance software package were compared with the values obtained from volumetric calculation in GeoGraphix of net pay, porosity, and water saturation. At an initial gas-oil ratio of 0.20, the OOIP was calculated at 11.2 million stocktank bbl (stb), which correlates with the value based on volumetrics. Results of the pressure match indicated that a gas-oil ratio of 0.17 and an OOIP of 12 million stb exhibited a good pressure match. These results indicated that an initial gas saturation must be present in zone 2 in order to reach an acceptable match of gas production.

The development of the input data set for full-field simulation was started as more experimental and field data became available. The simulation grid is a rotated, nonuniform grid using three layers representing an area of the field 20,500 ft × 10,700 ft long and containing 25 wells. Values of net pay, porosity, and water saturation were generated for each grid block representing the study area. History matching the actual production and pressure data was accomplished by holding constant known field and experimental data, such as fluid properties and initial oil, water, and gas saturations. In order to simulate field performance, two different rock regions were modeled, each having different relative permeabilities and capillary pressures.

A baseline case was established by projecting the performance of the reservoir to economic limit. The economic limit was established using decline curve projections, a water-oil ratio of 99%, and field operation costs. Based on the baseline predictions to the economic limit, the projected cumulative oil production is 881,000 stb, with a cumulative gas production of 4,547 mmcf at an average reservoir pressure of 753 psi.

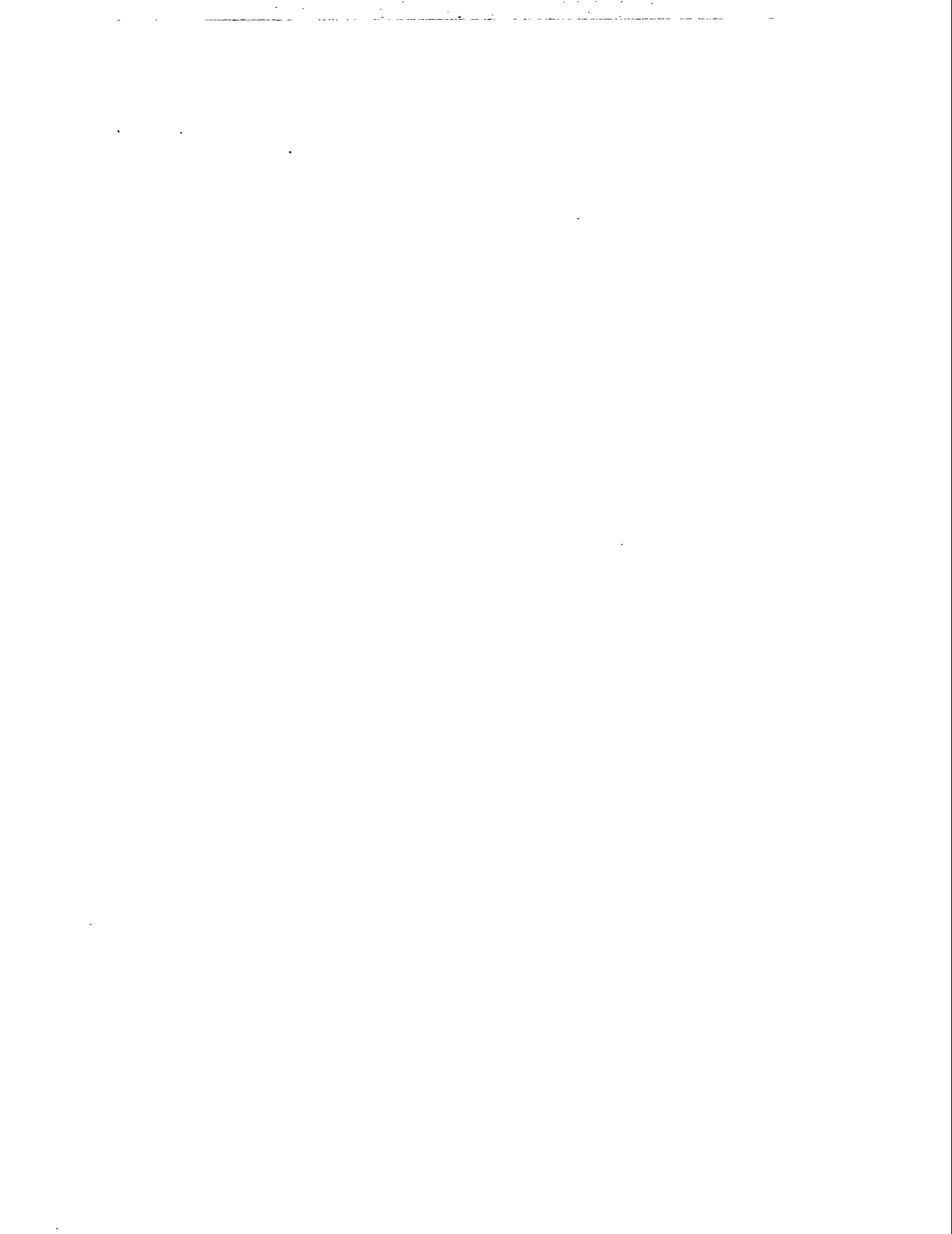
A total of 11 injection and 17 producing wells were used to project the potential for the various recovery processes. In the waterflood case, the average injection rate used in the simulation was 200 BWPD in each of 11 injection wells. This value was selected as result of performing various sensitivity analyses on the availability of injection water, the formation breakdown pressure, and the formation injectivity potential. Using an OOIP of 11 million stb, the waterflood projection to the economic limit indicates an oil recovery potential of 8.5%, compared to 8.0% for baseline prediction. Waterflooding, therefore, does not generate positive incremental cash flow above primary recovery. The low recovery due to waterflooding is attributed to low reservoir permeability, very low oil-water relative permeability, and the presence of a high gas saturation in zone 2.

In the gas re-injection case, the average injection rate was selected as a result of rate sensitivity analysis, gas availability, and reservoir limitations. An injection rate of 350 mcf/day in each of the 11 wells was used in simulating the gas re-injection recovery process. Simulation results indicate that the gas re-injection recovery process will result in reservoir pressure maintenance that will stabilize the pressure at approximately 2,400 psi, which is still above the reservoir saturation pressure of 2,070 psi. The field oil production rate was maintained at 350 bbl/day, compared to a sharp decline for both the baseline case and the waterflood case. Incremental oil recovery potential results were 16%, or 8% above baseline. Economic analysis indicates a positive cash flow for 17 years, or the economic life of the field.

Production problems investigated included paraffin buildup downhole, production lift methods, and hydraulic fracture treatments. Regularly treating wellbores with toluene was found to be successful in dissolving paraffin present in the micropores. Microbial techniques are another flexible, cost-effective way to remove paraffin and improve oil recovery without the use of environmentally toxic solvents and dispersants. Due to the relatively high fluid volumes produced from many wells, rod pumps have proved to be more beneficial than plunger lifts. Hydraulic fracture stimulation treatment results using crosslinked fluids show improved, sustainable oil production above those using CO₂ foam or polymer gels.

The project team was involved in several significant technology transfer activities that facilitated the transfer of information about the methods employed, value of using various technologies, and project results to other operators in the region. At the Fourth Annual Technical Canton Symposium, October 1996, John Thomas of Belden and Blake presented a paper, coauthored with Eugene Safley, on the geologic interpretations and core descriptions of the Rose Run sandstone. During the AAPG Eastern Regional Meeting in Charleston, West Virginia, in October 1996, representatives from BDM-Oklahoma presented a half-day workshop on the Reservoir Management Demonstration Program. In addition, Michael Fowler and Eugene Safley each presented a paper on various aspects of the Reservoir Management Demonstration Program and the geologic methods and interpretations conducted under the East Randolph field project. During the Eastern Regional SPE meeting in Columbus, Ohio, in October 1996, Michael Fowler presented an overview of various aspects of the Reservoir Management Demonstration Program. Phillip Salamy's presentation at this meeting focused on the reservoir engineering

aspects of the East Randolph field project. A paper focusing on the role of reservoir characterization in the reservoir management process was presented by Michael Fowler at the Fourth International Reservoir Characterization Conference in Houston, Texas, in March 1997. Eugene Safley will present the final results of the project at the AAPG Eastern Regional Meeting in Lexington, Kentucky in September 1997. Several of the papers presented at regional conferences are available on the Internet on the National Petroleum Technology Office homepage (www.npto.doe.gov) under the What's New link.



ACKNOWLEDGMENTS

This report was prepared for the U.S. Department of Energy National Petroleum Technology Office (NPTO) by BDM-Oklahoma under the Management and Operating Contract for DOE's National Oil and Related Programs (Contract Number DE-AC22-94PC91008). The authors and other researchers participating in the Reservoir Management Demonstration Program are appreciative of the U.S. Department of Energy's foresight in supporting this Reservoir Management Demonstration Project. The authors wish to acknowledge Edith C. Allison and Betty J. Felber of NPTO for their program guidance and useful discussions during the project. The authors would also like to express their thanks to Dr. Mike Madden, BDM-Oklahoma project manager, and Leo A. Schrider, Belden & Blake Corporation project manager, for allowing us to work on this project and for their helpful discussions. The authors are grateful for the support and data provided by Stacy Morrison with Belden & Blake Corporation and the employees of PEP Drilling Company. We are also grateful to BDM-Oklahoma Information Services Department for their editorial review and technical support.

1.0 INTRODUCTION

1.1 Program Description

The Reservoir Management Field Demonstration Program is a Department of Energy (DOE) program designed to demonstrate reservoir management techniques to independent oil operators. BDM-Oklahoma, management and operating contractor for DOE's National Oil Program, solicited letters of interest from operators interested in participating with BDM-Oklahoma in reservoir management demonstration projects. BDM-Oklahoma targeted small business operators who, while interested in reservoir management, have concerns about its cost-effectiveness and/or have limited practical experience in reservoir management projects. The multidisciplinary teams in the project consist of independent operators, BDM-Oklahoma staff, and persons from other organizations (universities, state geologic surveys, and consultants), as appropriate.

Projects are conducted as Cooperative Research and Development Agreements (CRADAs) with at least 50% industry cost sharing, and last approximately one year. The projects involve a significant regional oil resource and/or address a major technology need. The team members are transferring information about the methods employed, value achieved, and project results to other operators through DOE and industry publications, project workshops, and presentations at regional geological and engineering conferences. Project methods and results are also publicized on the National Petroleum Technology Office homepage on the World Wide Web (www.npto.doe.gov) and through activities of the Petroleum Technology Transfer Council (PTTC).

The primary objective of the Reservoir Management Field Demonstration Program is to demonstrate that multidisciplinary reservoir management teams using appropriate software and methodologies with efforts scaled to the size of the resource are a cost-effective method for:

- Increasing current profitability of field operations
- Forestalling abandonment of the reservoir
- Improving long-term economic recovery for the company

Multidisciplinary reservoir management should apply, as appropriate, expertise from many disciplines (geology, geophysics, engineering, environmental, operations, legal, accounting, administration, etc.) to field problems and opportunities. By teaming with the operators and performing reservoir management in actual field operations, industry will better understand and apply multidisciplinary reservoir management teams to improve operations. In this respect, both the operators and the DOE's National Oil Program will benefit.

The benefits to the National Oil Program include establishing valuable informal communication channels among industry, BDM-Oklahoma, and DOE; defining operator needs and constraints;

and broadening researchers' outlooks to guide future research programs. Benefits to the industry include strengthening the capabilities of regional infrastructures, improving the capabilities of specific operators through hands-on experience, addressing a significant resource or technology need, and developing practical advice and guidelines for assessing and applying cost-saving technologies.

The program entails six key activities:

- Developing the program plan
- Enhancing reservoir management capabilities of the reservoir management team members
- Evaluating operator letters of interest and negotiating CRADAs for the most beneficial projects
- Performing laboratory analyses and evaluating field operations to develop an appropriate reservoir management strategy
- Preparing a solicitation plan and documents for future demonstration projects
- Transferring technology, methods employed, value realized, and projects results to industry

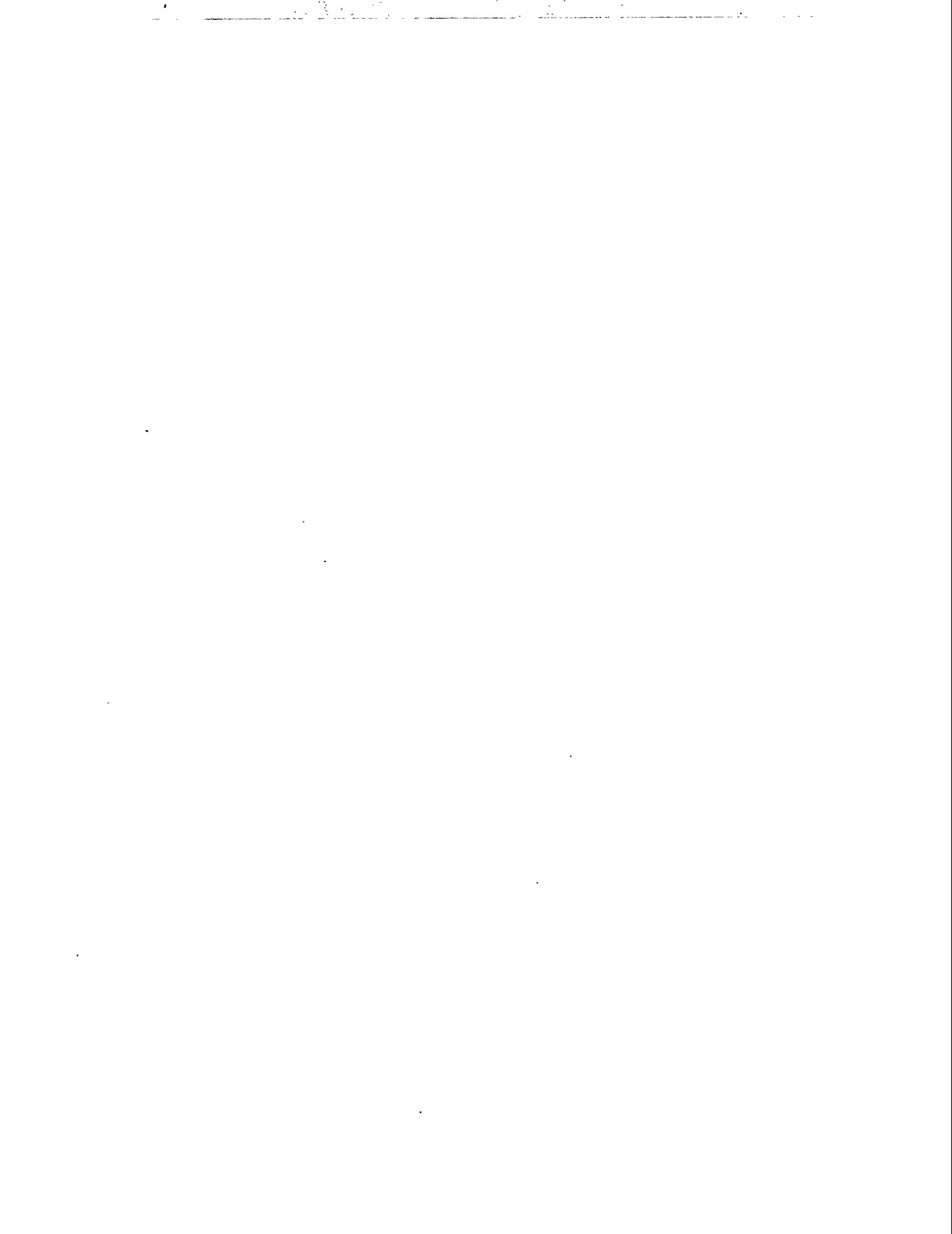
1.2 East Randolph Field Reservoir Management Demonstration Project

The primary objective of the Reservoir Management Demonstration Project with Belden and Blake Corporation is to develop a comprehensive reservoir management strategy to improve the operational economics and optimize oil production from East Randolph field, Randolph Township, Portage County, Ohio. This strategy identifies the viable improved recovery process options and defines related operational and facility requirements. In addition, strategies are addressed for field operation problems, such as paraffin buildup, hydraulic fracture stimulation, pumping system optimization, and production treatment requirements, with the goal of reducing operating costs and improving oil recovery.

A secondary objective is to transfer not only the technical results of this project to other operators of similar reservoirs, but to transfer information about the methods that were employed and the value of employing them in developing the reservoir management strategy. This transfer of information will enable all operators to consider these methods in developing their own optimum reservoir management strategies.

The initial efforts focused on detailed reservoir characterization of the Rose Run sandstone and the analysis of available production and reservoir data. The results of this effort included the identification of additional reservoir data required for reservoir simulation. Belden and Blake collected the required reservoir data by drilling and coring an infill well and performing

additional fluid and well tests. The data were used in the development of several geologic and reservoir models for use in simulating reservoir performance. Based on the simulation, improved recovery processes were identified and the reservoir management strategy was developed for the field based upon economic sensitivity analysis.



2.0 RESERVOIR MANAGEMENT STRATEGY

This section summarizes some of the major conclusions and recommendations from the Reservoir Management Demonstration Project in East Randolph field, including definitive conclusions based on the work conducted under this project, additional areas which should be investigated further, and activities which could be conducted during the remaining life of the field to address unanswered questions.

2.1 Reservoir Management Process

The purpose of this project was to develop a comprehensive reservoir management strategy to improve the operational economics and optimize oil recovery from East Randolph field. The strategy itself is not something that can be easily written down and stated emphatically like a cookbook set of instructions on what to do in the field over time. Rather, the entire project represented the ongoing process of reservoir management strategy development, revision, implementation, modification, and refinement. The reservoir management process is ongoing; this project marks neither the beginning nor the end of the reservoir management strategy development for East Randolph field. During the project many questions about the field were answered and some additional questions were posed. Some of these questions remain unanswered and may or may not need to be addressed further.

The continued success of East Randolph field is dependent upon the continued refinement of the reservoir management strategy for the field. The reservoir management process should continue as an interactive, interdisciplinary planning and implementation methodology for improving field performance. The integrated team approach that was used in this project is a proven methodology for solving large-scale problems and optimizing field performance. The reservoir engineers, geologists, and production engineers responsible for this field should continue to work closely together to identify opportunities for reducing costs and improving recovery.

2.2 Improved Recovery Process

At the beginning of this project, the reservoir management team felt that the viable improved recovery process for East Randolph field would most likely be implementation of a waterflood, with gas injection as a possibility. The reservoir simulation and economic analyses conducted under this study indicate that gas injection is the preferred strategy to pursue for improving recovery in this field. Primary recovery in East Randolph field will result in recovery of only 8% of OOIP, which is not unexpected given the reservoir characteristics. Waterflooding is uneconomic; it only results in the incremental recovery of an additional 0.5% of OOIP. Ultimate recovery can be economically doubled, however, through the implementation of a gas re-

injection process for pressure maintenance in the field. The simulation assumed that produced methane was re-injected into the field. The economic benefits of injecting lower cost nitrogen or flue gas should be investigated further. The optimum improved recovery strategy could be miscible/immiscible methane, nitrogen, or flue gas injection. An economic comparison between methane, flue gas, and nitrogen injection would illustrate the feasibility of injecting one gas versus the other. If the nitrogen or flue gas injection processes appear to be economically viable, additional simulation work may be necessary to define the optimum injection scenarios. Field issues, such as corrosion from flue gas and nitrogen re-injection for sales gas, must also be addressed.

Many questions remain to be answered before initiating a gas injection process in the field. One of the most important areas that should be investigated is the definition of the optimum gas injection rate for the field, which includes selecting the optimum number and location of the gas injection wells. A detailed simulation and economic sensitivity analysis would help to identify an optimum gas injection scenario.

One of the biggest hurdles that must be crossed prior to the implementation of a field-wide gas injection process is the formation of a unit or execution of joint development agreements between the various operators in the field. This has been a perpetual problem in the industry as waterflooding, pressure maintenance, and EOR strategies have been developed. Improved recovery process implementation usually benefits all of the interest owners, but individual owner equity must always be preserved or some operators will bear a disproportionate share of the cost burden or receive inequitable production benefits. Pressure maintenance in East Randolph field will undoubtedly benefit the interest owners, so they should share the cost burden of implementing and operating the project.

2.3 Well Spacing

The simulation work indicates that the current 60-ac well spacing is probably adequate for continued primary recovery because it appears that the field is being entirely pressure-depleted by the existing wellbores. Compartmentalization and directional permeability within the field could dictate the need for additional wells, but infill drilling decisions will require careful analyses to prevent accelerated recovery of currently producible reserves instead of the capture of additional reserves that would typically remain in the reservoir after primary recovery. Additional wells, however, may be necessary for the implementation of an improved recovery process. Additional simulation sensitivities would indicate the technical viability of infilling and would quantify acceleration versus incremental recovery; then, economic sensitivity analyses could be conducted. Under continued primary recovery, compartmentalization will be difficult to quantify due to the paucity of pressure data. If injection is initiated, responses in some wells and the lack of responses in other wells would be a direct indicator of compartmentalization.

2.4 Data Collection and Integration

The economic optimization of the oil recovery from East Randolph field will require the collection and analysis of additional reservoir and production data from the field. The cost-benefit of such data collection efforts should be ascertained and decisions should be made to obtain the data required to monitor and analyze individual well and field performance. As additional data are obtained, these data should be integrated into the reservoir model and simulation performed if necessary for refining the predictions.

Most importantly, additional pressure data should be obtained from the field on a routine basis. The effectiveness of the field recovery process cannot be assessed without performance data. Pressure data are absolutely necessary for monitoring and simulating the performance of East Randolph field. If gas injection is initiated, pressure data will be vital for determining the optimum gas injection rates and overall volume during the life of the project. A strategy should be devised for minimizing the cost of collecting this data. Initial reservoir pressures should be obtained from any infill wells drilled in the field. Shut-in pressures and fluid levels should be obtained on any wells that are shut in the field. Pressure build-up data should be obtained and analyzed from various wells in the field over the field life to correlate with production and injection responses. Pressure fall-off tests could be conducted on injection wells to avoid lost production. In short, a cost-effective pressure data collection strategy for the field should be developed.

Additional PVT data should also be considered to improve the understanding of the reservoir performance. Since the reservoir fluid properties used in the simulator were based on only one fluid sample collected during field development, it may be necessary to obtain some additional PVT data. The samples taken in conjunction with this project were collected in the high GOR area of the field, where the gas zone is present. PVT analysis on samples collected from the oil zone would help to refine the simulation.

The geologic factors which would influence the production and injection performance of the field should be assessed thoroughly. Data that has been obtained since the geological model was developed for the simulation effort should be incorporated to refine the geologic interpretation and reservoir model developed. Additional geologic data should be collected from the field as additional wells are drilled. Besides routine well logs, additional sidewall or whole core should be considered. Analysis of additional log and core data could help to further characterize the areal relationships of porosity, permeability, and fluid saturation in the field. Once again, cost-benefit analyses should be conducted for any additional data collection effort. Obtaining and analyzing additional geologic data from the field would help the operators gain a better understanding of the reservoir heterogeneities and production responses.

2.5 Production Aspects

One of the most important parts of this project was the analysis of the production aspects of the field, with particular emphasis on improving operating economics. Additional work should be done to define the factors which cause lost productivity in wells after shut-in periods. Also, paraffin deposition problems and well treatment methods should be investigated further. An optimum well treatment or stimulation methodology should be developed to maintain well productivity and minimize treatment costs. The results of the fracture stimulation investigations should be assessed to determine the optimum strategy for fracturing any additional wells drilled in the field.

3.0 EAST RANDOLPH FIELD RESERVOIR CHARACTERIZATION

3.1 Data Available and Previous Work

The Upper Cambrian Rose Run sandstone is currently the most active exploratory play in the Appalachian Basin. In Ohio during 1995, the Rose Run accounted for more than 65% of all exploratory wells and had a 38% success rate (McCormac and Wolfe 1996). The Rose Run sandstone subcrop extends from southern Ohio northeastward to northwest Pennsylvania (see Fig. 3-1).

The subcrop trends approximately parallel to the current structural configuration of the Appalachian Basin. Most production from the Rose Run is dry natural gas; oil production is very localized. The Rose Run sandstone produces from structural and stratigraphic traps. The major constraints on lateral continuity or heterogeneity are erosional truncation or lateral changes in porosity.

To effectively characterize the reservoir, an operator must integrate all available data from geological, geophysical, and engineering studies. This data will help to identify heterogeneities

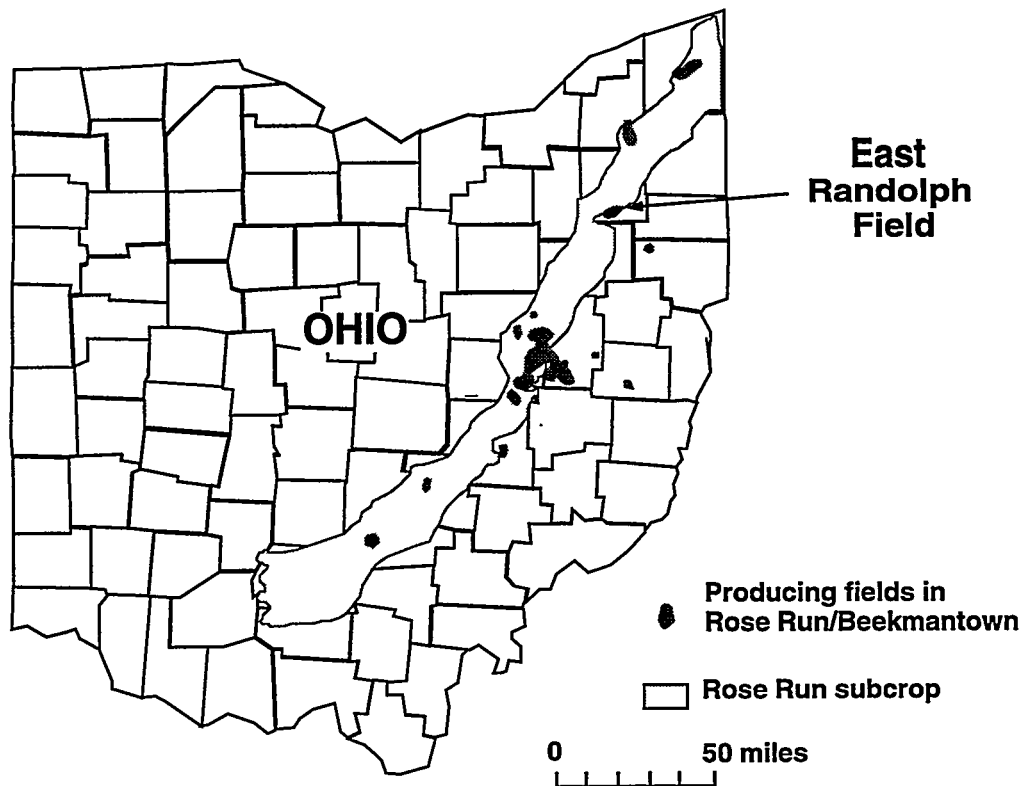


Figure 3-1 East Randolph Field Location Map

within the reservoir that may prevent oil from flowing to existing wellbores, and to understand the reservoir drive mechanisms and effects of field operations on production. An effective data acquisition and analysis program requires careful planning and well-coordinated team efforts throughout the life of the reservoir. By effectively and accurately characterizing the reservoir, an operator can determine the optimum improved recovery processes to improve production and reduce operating costs.

Objectives of reservoir characterization in this study were as follows:

- Integrate available log, core, fluid, and pressure data to interpret reservoir heterogeneity and effects of faults and fractures on production.
- Conduct additional routine and special core analyses and description.
- Obtain and interpret additional engineering data collected in the field.
- Develop single-well, pilot, and full-field reservoir models; and simulate reservoir performance to optimize future locations of infill wells.

In addition to infill drilling, two recovery processes (waterflooding and gas re-injection) were investigated. These recovery process are typically technically and economically feasible for independent operators to apply to small field sizes depending on reservoir conditions.

Reservoir data can be divided into three broad categories: (1) rock properties, (2) fluid properties, and (3) interaction between reservoir rock and fluid. Both static and dynamic measurements are required. Reservoir characterization requires data on a range of scales from basin and field-scale information to pore-size information, each of which must be collected with the appropriate tools (Jackson et al. 1993). Field-scale information establishes the spatial framework and general architecture of the reservoir facies. The reservoir architecture controls the interwell communication and is used for describing and predicting reservoir compartmentalization. Pore-scale information, which affects fluid flow properties, includes pore size, pore throat, grain size, and sorting. The major controls on these characteristics are the sediment source and the subsequent diagenetic processes of compaction, cementation, and dissolution. The amount and type of data needed for reservoir characterization are determined by the recovery process applied (Ringrose et al. 1991). As the field matures, the scale of the heterogeneities that needs to be considered for development and application of various improved oil recovery processes decreases.

The Rose Run sandstone is a member of the Upper Cambrian Knox Supergroup. The type log of the D'Agostine No. 1 well shows the typical gamma-ray, neutron, and density log responses for Upper Cambrian stratigraphy (see Fig. 3-2).

The Rose Run sandstone ranges in thickness from 110 to 150 ft and consists of stacked sheet sandstone deposits separated by and interbedded with thin, low-permeability dolomites and carbonaceous shales. The Rose Run sandstone in East Randolph field can be divided into five distinct sandstone zones from the top, zones 1,2,3A and 3B, and 4. Only zones 2, 3A, and 3B are productive in the East Randolph field. on the basis of log character. The Rose Run sandstone is

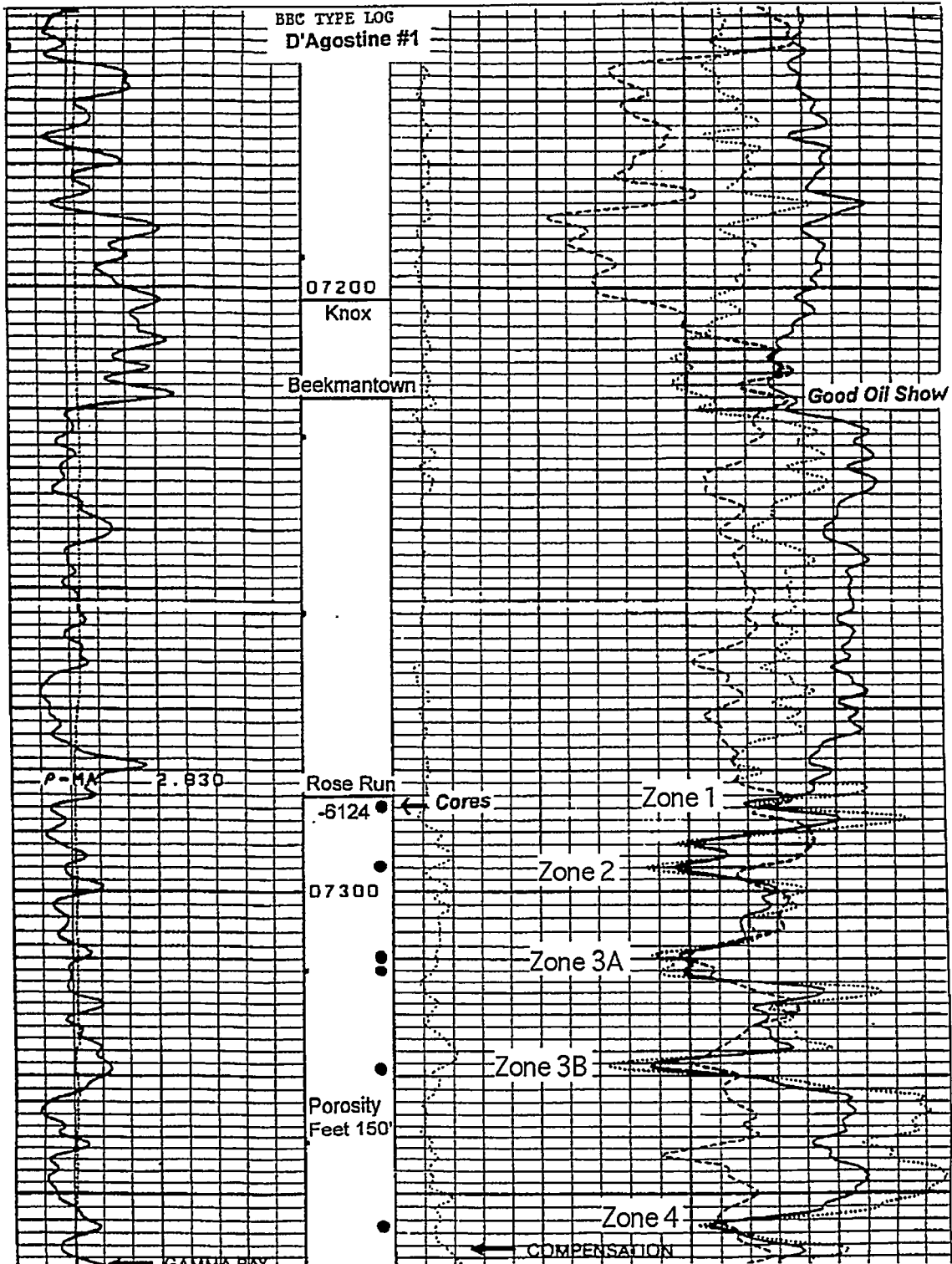


Figure 3-2 Gamma Ray-Neutron/Density Type Log for East Randolph Field

overlain by the Lower Ordovician Beekmantown Dolomite (which is capped by the Knox unconformity) and underlain by the Trepaleau Dolomite. Hydrocarbon traps for the Rose Run sandstone are a combination of structural and stratigraphic features (Coogan and Maki 1986).

Early reservoir studies characterized the Rose Run sandstone in eastern Ohio as a mappable, homogeneous sandstone unit present on erosional remnants below the Knox unconformity (Janssens 1973). Structural traps were the primary exploration target in the Rose Run. This interpretation was based on the limited amounts of core analyses and pressure data available. Operators have learned from subsequent studies that this interpretation is oversimplified (Riley et al. 1993). Recent studies indicate that the Rose Run sandstone consists of three to four individual flow units of varying reservoir quality separated by nonreservoir layers, usually low-permeability dolomite (Thomas and Safley 1996).

From 1992 to 1996, East Randolph field has produced an estimated 450,000 bbl of oil and 1.5 bcf of gas from the Rose Run sandstone. The field consists of 32 active wells drilled on approximately 60-ac spacing. The predominant recovery mechanism is solution gas drive. Several major issues have been identified as requiring attention in this and in other Rose Run fields in the area to improve characterization of the reservoir and determine future recovery potential. Reservoir pressure is rapidly declining and, at some point in the future, may fall below bubble point. Several of the wells have high producing gas-oil ratios; others are poor producers due to completion or stimulation problems, but have high remaining oil potential. Paraffin problems have been observed downhole in wellbores and in surface equipment.

Data on East Randolph field were received from Belden & Blake and PEP Drilling, each operators of multiple wells in the field. Data available consisted of hard copy wireline logs, completion reports and stimulation history of each well, core analyses of whole core from nearby fields and of sidewall cores from East Randolph field, fluid sample analyses, pressure data, capillary pressure data and relative permeability data from nearby fields, production data by well by month, and relevant articles on the geologic history and field development of the area. Much of the geologic data was input into the GeoGraphix Exploration System (GES).

GES is a powerful, affordable technical mapping and data management application which uses geological, geophysical, geographical, and engineering data for mapping and analysis. Within GES, a customizable, relational database consisting of more than 100 discrete fields organizes critical data into logical tables. The data may be entered by hand or downloaded from a variety of data providers. A series of layers is used to store and display logically related data. Specialized features include interactive gridding and contouring, 3-D visualization, digital log cross sections, 2-D and 3-D velocity modeling, deviated and horizontal wellbore profiles, and reservoir and economic predictions.

Additional data needs were identified to enable improved reservoir characterization and identification of future recovery options. A whole core from an infill well was required to provide rock property data for capillary pressure and relative permeability analyses. Schlumberger's Formation Micro-Imager (FMI) and Combinable Magnetic Resonance (CMR)

logs were needed to identify the extent and direction of fracturing of the reservoir to interpret directional permeability and the fluid saturations. PVT analyses and pressure buildup data were needed to characterize the fluid and rock properties at reservoir conditions. The drilling of six additional infill and extension wells helped to extend reservoir limits and provided additional well and log data.

The availability of reliable and detailed geologic and reservoir data can not be overemphasized, whether it is a new field or a mature field. Reservoir characterization can only be as effective and accurate as the quantity and quality of data available. Without reservoir data such as core, log, pressure, and fluid samples collected from most wells in the field from the time of field discovery through field abandonment, the operator may not fully understand the reservoir conditions present and the effectiveness of field operations. The opportunity for collecting a number of critical data (PVT, initial fluid properties, initial pressure, etc.) once lost can not be regained. Instead, assumptions must be made which may not accurately reflect the reservoir conditions at any time in the past.

There is never enough data to completely characterize a reservoir. Determining the value of additional data may not be known until it is acquired and analyzed. Data are not of equal value, and there is a hierarchy in data acquisition (Saleri et al. 1991). It may be possible to collect some data that may be representative for the field or parts of the field. Cost-benefit analyses should be done to determine the optimum quantity and quality and the long-term value of data collection to answer questions or solve field problems that may occur.

3.2 Geological Analyses

3.2.1 Structural Interpretation

Several studies (Harper 1989; Riley et al. 1993; Moyer 1995) discuss the complex structural history along the Akron-Suffield basement wrench fault system and the influence of the regional Knox unconformity on trapping mechanisms. Source areas for the Cambrian clastic influx were limited to topographic features of Precambrian Grenville metasediments to the northwest in the vicinity of the Canadian shield. The erosional truncation by the Knox unconformity causes the Upper Cambrian Knox interval to decrease in thickness to the northeast and southwest of the field. Irregular structural noses are caused by wrench faulting creating erosional remnants of the Knox group below the unconformity.

The Suffield fault, which forms the southern boundary of the field, and other extensional faults may have resulted from reactivation along zones of weakness defined by the Grenville thrust sheets during regional episodes of compression and extension during the Cambrian (Riley et al. 1993). Development of the Rome trough to the southeast was accompanied by down-to-the-southeast faulting and tectonic thickening of Upper Cambrian rocks, as seen on seismic reflection data. Reactivation of the Suffield fault during the Paleozoic caused repeated episodes of faulting and fracturing. Left lateral strike-slip movement has been interpreted along the fault.

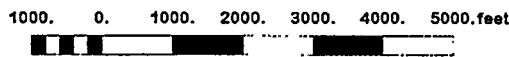
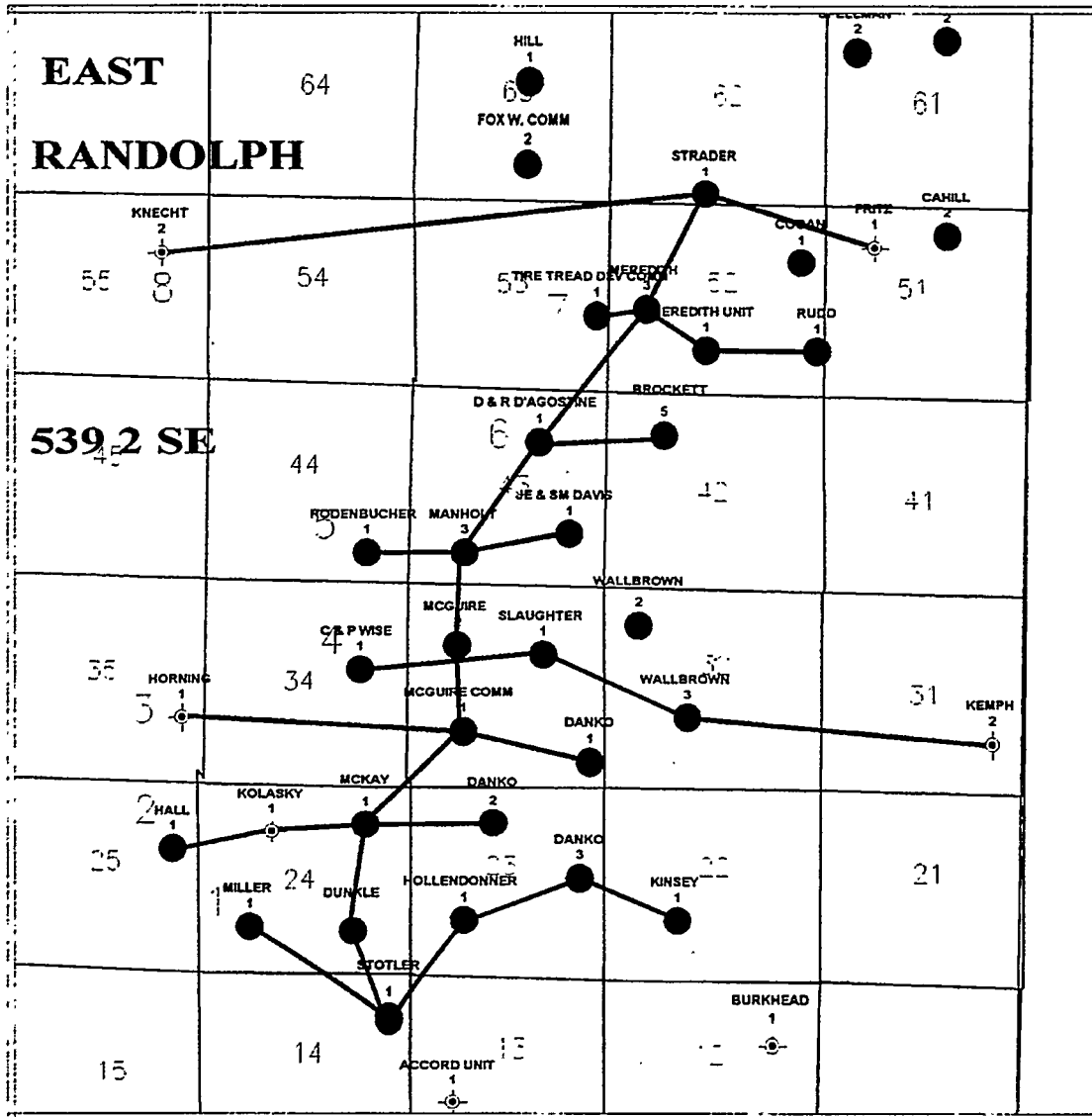
Across the Suffield fault to the south, seismic and log data indicate that the Beekmantown Dolomite is absent on the downthrown block.

Eight east-west and one north-south structural cross sections were constructed for identification of faulting and structural compartmentalization (see Fig. 3-3). Two stratigraphic cross sections were constructed for identification of permeability barriers and correlation of individual flow units. The Rose Run sandstone in East Randolph field strikes along a southwest to northeast trend and dips 1-2° to the south and east (see Fig. 3-4).

The productive intervals lie at a depth of approximately 7,200 ft. The wells are drilled on 40-60 ac spacing and aligned parallel to depositional strike. A series of high angle normal faults with 5-15 ft displacement parallel the major Suffield Fault and subdivide the field into separate fault blocks.

The influence of the Knox unconformity and the Akron-Suffield fault system on the reservoirs and the migration and entrapment of hydrocarbons in East Randolph Field is not fully understood (Riley et al. 1993). Paleotopographic relief on the Knox unconformity resembles karst towers, sinkholes, and intraformational breccias. The overlying Beekmantown Dolomite acts as the regional seal for Rose Run production. The series of northwest-southeast normal faults were interpreted by the changes in dip and thinning of interval thickness between wells (Tearpock and Bischke 1991). The fault displacement may not be enough to juxtapose tight dolomites against the permeable sandstones to cause permeability barriers or discontinuities. The presence and effect of any barriers were investigated by comparison of production, gas-oil ratios, and water-oil ratios across the fault zones described later in this report.

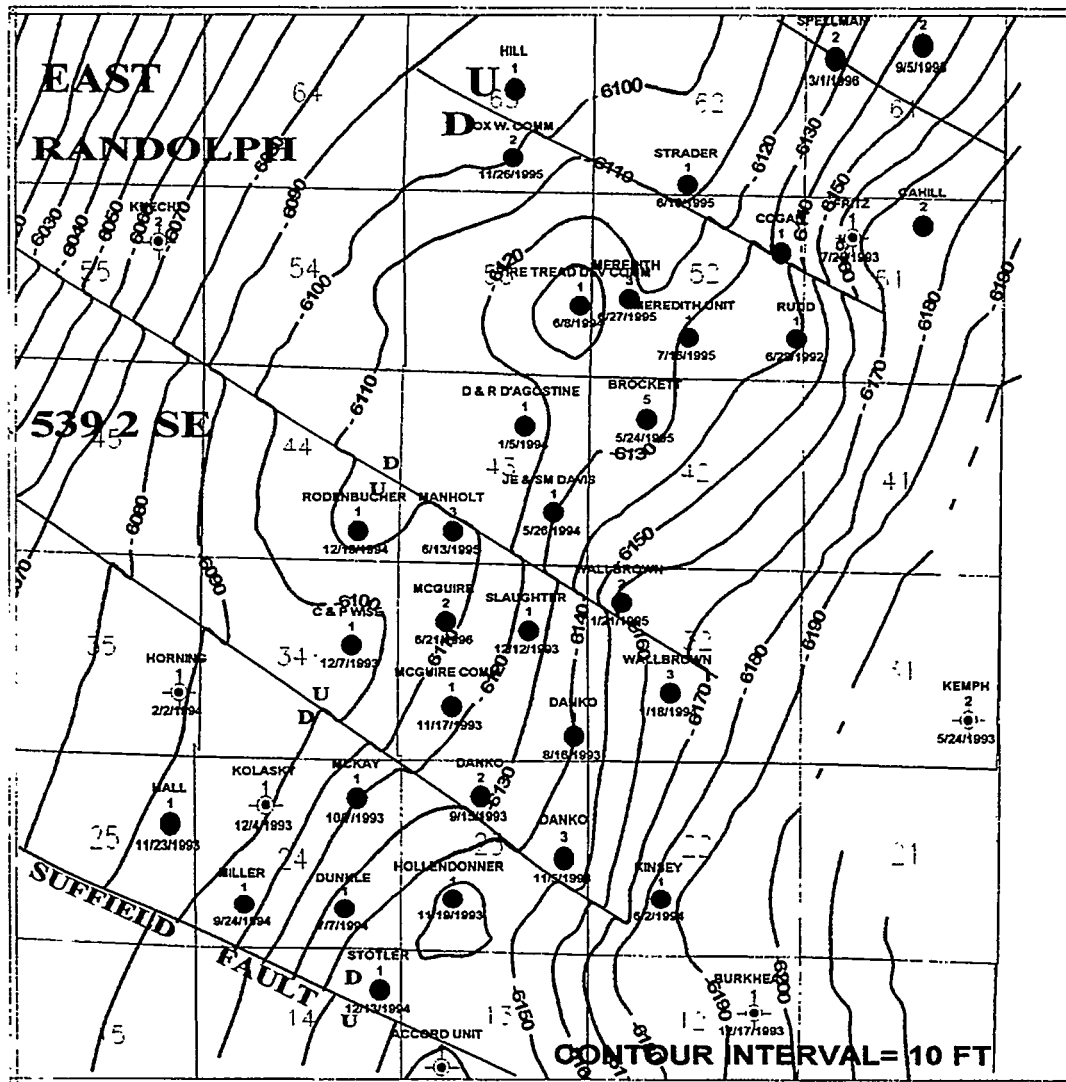
Fracture systems may be associated with the faulting and could affect fluid migration. Fracture trends identified on the surface by landsat and aerial photograph interpretations (Guo and George 1996) may not be representative of the fracture orientations that existed prior to the Knox unconformity. The possibility of additional sources of fracturing in post-Paleozoic time was great enough that the surface fracture patterns were not investigated. Fracture trends had been previously determined from core analysis of the overlying Silurian Clinton sandstone in Marboro field. Two dominant fracture trends were interpreted: east-west and north-northwest-south-southeast. The east-west set predominates and is related to regional faulting, parallel to the Suffield fault. The north-northwest-south-southeast trend represents conjugate shear fractures caused by the same faulting. The fractures are near vertical, with slickensides observed. Minor microfractures trend northeast-southwest. In view of the extremely low permeability of the rock matrix, natural fractures can be quite advantageous for primary oil production (Schridder et al. 1970). Depending on the abundance and degree of openness, natural fractures could jeopardize waterflooding by permitting early breakthrough. Fracture analysis was investigated in the Rose Run using the FMI logging tool and whole core analysis, as discussed later in this report.



LEGEND	
●	OIL WELL
☀	GAS WELL
⊙	DRY AND ABANDONED

BDM-Oklahoma, Inc.
EAST RANDOLPH FIELD CROSS SECTIONS ALL WELLS POSTED

Figure 3-3 Cross Section Locations for East Randolph Field



1000. 0. 1000. 2000. 3000. 4000. 5000. feet



LEGEND	
●	OIL WELL
☼	GAS WELL
○	DRY AND ABANDONED

BDM-Oklahoma, Inc.
EAST RANDOLPH FIELD STRUCTURE TOP OF ROSE RUN COMPLETION DATE

Figure 3-4 Structure Top of the Rose Run with Location of Northwest-Trending Normal Faults

3.2.2 Stratigraphic Interpretation

3.2.2.1 Log Analysis

Petrophysical analysis of the Rose Run sandstone includes quantifying petrophysical properties from wireline logs, integrating core and petrographic data with geophysical log data, and mapping measured and calculated reservoir properties. Available wireline logs from East Randolph field include gamma-ray, compensated neutron, density, and sonic logs and dual laterologs. CMR and FMI, two advanced logging tools, were run in an infill well. None of the logs from East Randolph field have been digitized.

Gamma-ray logs respond to natural radioactive isotopes present in the rocks and provide information on lithology and the shale content of the rock (Schlumberger 1989). K feldspar, which ranges from trace amounts up to 10% by weight, will be detected as clay by gamma-ray logs due to the presence of potassium in the mineral. Conversely, the clay mineral, kaolinite, which is present in trace amounts, will not be detected by gamma-ray logs due to the absence of potassium. Based on correlations with other wells and the presence of radioactive minerals within the Rose Run sandstone, the gamma ray log was found to be of limited value for correlating productive intervals from one well to the next.

Porosity values are used for determining rock void space and volumes of reservoir fluids. Neutron logs respond to hydrogen content of pore fluids, which is an index to porosity. The neutron log also is affected by the presence of hydrous minerals, such as mixed-layer illite/smectite. Porosity values calculated from neutron log response may be slightly higher than effective porosity in zones which contain higher amounts of smectitic minerals. The relatively low concentration of smectite in the Rose Run sandstones made neutron porosity correction unnecessary. Neutron log measurements are negatively affected by high gas saturation and read lower than actual porosity depending on the amount of gas saturation.

The density log measures the electron density of the formation. The Rose Run sandstones contain varying amounts of high-density carbonate minerals (primarily dolomite and ankerite). Appropriate bulk density values should be used when calculating density porosity values for intervals which contain carbonate minerals. Density log measurements are more optimistic in zones with high gas saturation. Such zones (e.g., Rose Run zone 2) can be identified by the crossover of the neutron and density porosity curves. For the Rose Run formation, mapped porosity values were determined by the average of the neutron and density porosity curves.

Hydrocarbon saturation values are used to define pay zones and determine the amount of oil in place. Archie's equation illustrates that water saturation is a function of formation porosity (ϕ), formation resistivity (R_t), cementation exponent (m), saturation exponent (n), formation water resistivity (R_w), and a constant (a).

$$S_w^n = aR_w / \phi^m R_t$$

The formation water resistivity used was 0.035 ohm·m, from a local Rose Run produced-water sample. Formation resistivity was determined from the dual laterolog. The fact that resistivity

logs from several logging service companies were used caused some concern for the correlation between wells of resistivity measurements and reliable water saturation measurements. To attempt to compensate for the various data vintages and logging companies, the logs were normalized using the overlying Glenwood Shale as a regional marker. Resistivity values were adjusted between adjacent wells so that the Glenwood Shale had similar resistivity values. The values measured for the Rose Run sandstone were then adjusted accordingly.

Parameters m and n are formation properties and ideally should be determined in the lab for each rock type (Dewan 1983). The value of m is a function of the degree of pore interconnectivity, or pore geometry. The value of n is a measurement of the degree of conductive fluid (i.e., water) for a constant porosity. Since the saturation exponent is measured at various water saturations, the interconnectedness is a function of pore geometry and rock and fluid properties. Because accurate determination of these parameters is usually cost prohibitive, local "known" values of these parameters may be used for quick-look log analysis. For more detailed log analyses, these values should be accurately determined. Reported values for m and n are very limited and range from 1.8 to 2.3 (Riley et al 1993). In the case of porous formations characterized by intergranular porosity, lab measurements have shown m to be 2.0 on average. Due to the fine grain-size and low permeability of the Rose Run, values of m and n used in the water saturation calculations were 1.8 and 1.7, respectively.

The CMR tool, which Schlumberger is currently applying in the Appalachian Basin, was run in the McGuire #2 infill well. This logging tool is designed to provide a continuous measurement of permeability independent of lithology to help determine irreducible water saturation in thin-bedded, low-permeability zones. The results of the CMR measurements confirm the special core analysis results (see Section 3.2.3) from core plugs from the McGuire No. 2 well. Zones 3A and 3B had an irreducible water saturation of 41% and 33%, respectively; zone 2 had an irreducible water saturation of 25%. Conventional log analysis from the McGuire No. 2 well indicated initial water saturation for zones 2, 3A, and 3B of 30%, 52%, and 62% respectively, indicating that water production is coming predominantly from zone 3B, but that zone 3A is a contributor in certain areas.

Fractures, which often occur in orthogonal networks, may be sealing or conductive depending on the direction and magnitude of in-situ stresses (Teufel and Lorenz 1992), and the degree of cementation of the fracture plane. An FMI log was run on the McGuire no. 2 well in an effort to identify open fractures and reservoir heterogeneities. Results of the log indicate the absence of natural fractures in the logged interval. This was somewhat surprising due to the amount of movement along the Suffield fault system during the Paleozoic. This suggests that fracturing associated with the regional faulting may be of limited extent. Hydraulically induced fracturing may intersect many small interconnected natural fractures and permit oil to flow to the wellbore at economic rates.

FMI images of the Rose Run zone 2 generally show parallel laminated to wavy laminated sandstone. FMI images of zone 3A and 3B show wavy laminated to cross laminated sandstones containing shale rip-up clasts. The dolomites interbeds are massive to laminated. The strike of the majority of the cross beds in the sandstones were measured to be between N30°E and N60°E.

An additional logging tool that was considered but not run was the Repeat Formation Tester (RFT). It was not run because the low porosity and permeability of the reservoir could lead to inaccurate pressure readings.

3.2.2.2 Geologic Mapping Interpretation

The distributions of the reservoir and nonreservoir rock types and of the reservoir fluids determine the geometry and heterogeneity of the reservoir model. Lithofacies maps, well log patterns, and regional correlations are combined to interpret the reservoir facies distribution. Recognition of the environment of deposition is important because the quality and three-dimensional distribution of the reservoir is greatly influenced by depositional conditions. These elements have a direct effect on the porosity, permeability, and saturation distribution required in the numerical simulation. Both lateral and vertical continuity of the sandstones must be known so that proper well spacing and patterns can be selected.

The geologic data from well log interpretation and core analyses in East Randolph field were entered into GeoGraphix software for the construction and interpretation of structure, net sandstone thickness, porosity, water saturation, gas-oil and water-oil ratios, and production maps. Net sandstone thickness maps use a 6% porosity cutoff based on core porosity-permeability crossplot interpretation from all available whole core and sidewall core data from the Rose Run sandstone (see Fig. 3-5).

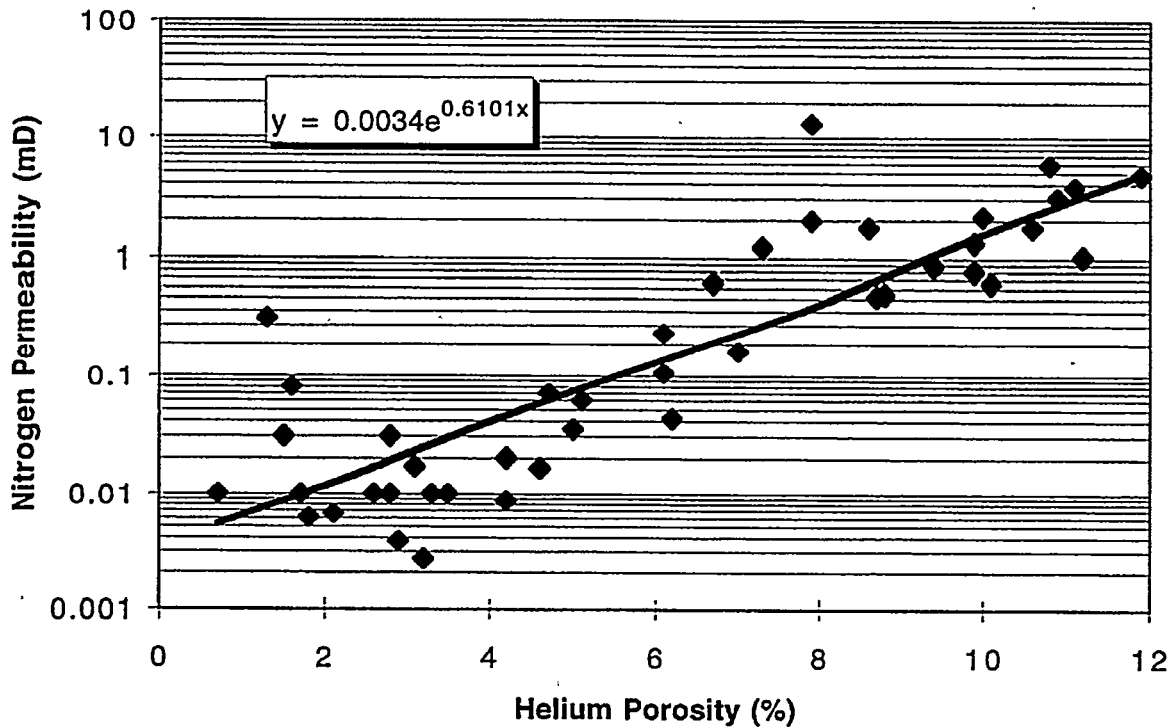


Figure 3-5 Crossplot of Core Porosity vs. Permeability for Cored Wells in East Randolph Field

The core porosity-permeability crossplot suggests that above a core porosity of 6%, permeability is more than 0.1 md. As permeability increases with increasing porosity, reservoir fluid migration occurs. Some of the scatter in data points is possibly due to microfractures causing higher permeability in the samples. Production data support the fact that hydrocarbons are produced from sandstones with porosity above 6%. The core porosity-log porosity crossplot, while exhibiting some scatter of data points, suggests an approximate one-to-one relationship between core and log porosities. The geologic maps were continuously revised with additional log and core data collected from infill and extension wells drilled during the project.

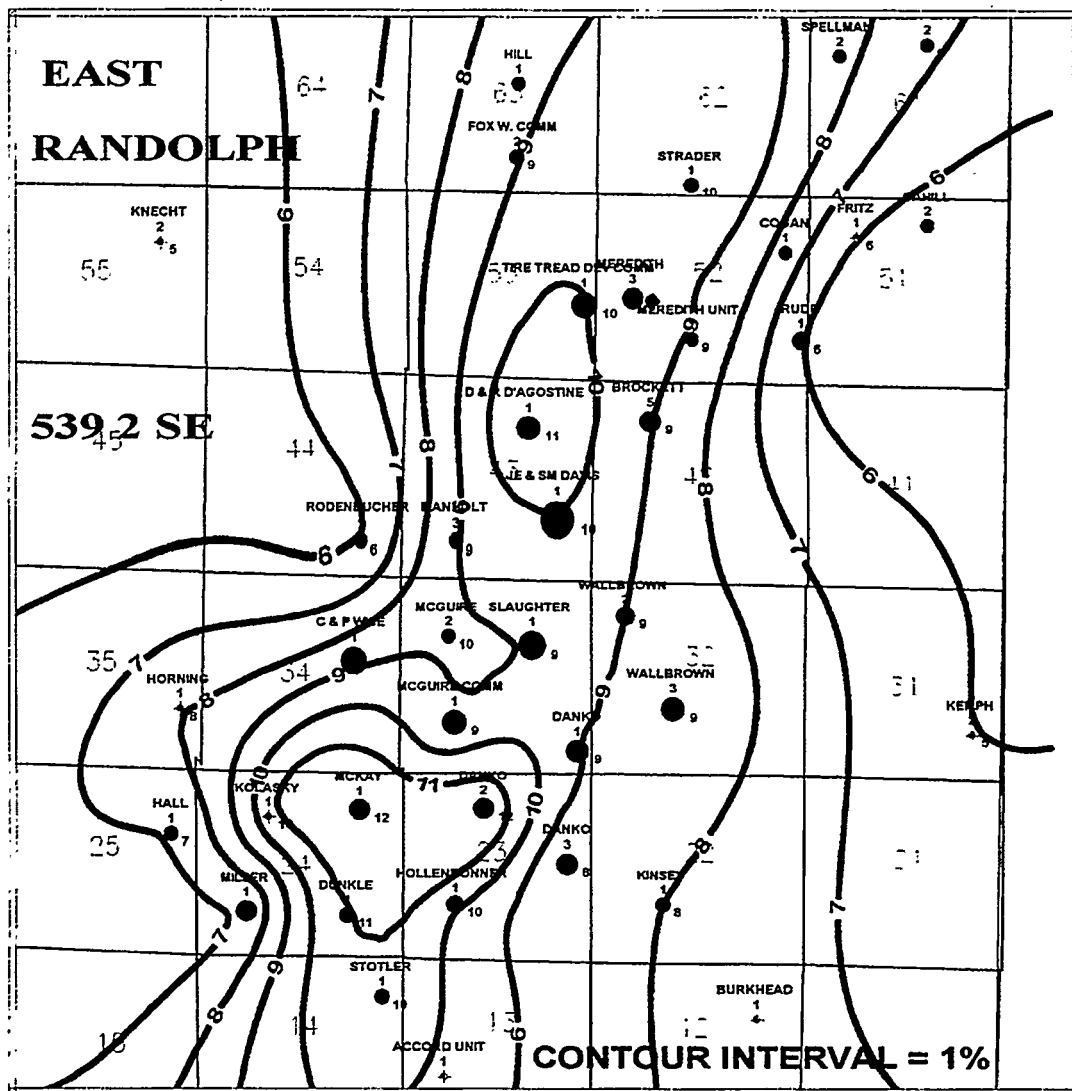
The lowermost Rose Run sandstone interval, zone 3B, consists of a linear sand body oriented parallel to depositional strike trending to the northeast-southwest (see Fig. 3-6). The zone was deposited over an irregular erosional topography on top of the Trempealeau Dolomite. Zone 3B typically consists of two distinct sandstone deposits separated by a thin dolomite interbed. Individual sandstone deposits are continuous locally, but discontinuous regionally. Sandstone thickness ranges from 3 ft up to 12 ft, with an average net sandstone thickness of approximately 8 ft using a 6% porosity cutoff. The average porosity of this zone from log analysis ranges from 6% to 12%. Porosity pinches out rapidly to the east and west, but is more continuous to the north (see Fig. 3-7).

The highest porosity occurs in the thickest sands. Based on log analysis the sandstone has a sharp, conformable basal contact into low porosity dolomite and a gradational upper contact. The high water productions, as depicted in the size of the bubbles in Figure 3-8, correlates best with the calculated water saturation for zone 3B.

Several wells along the southeast margin of the field are not completed in zone 3B due to the zone's high water saturation (up to 40%). Producing water-oil ratios also indicate that downdip wells completed in zone 3B have higher water ratios. It is possible that the value of the saturation exponent (n) used to calculate the water saturation is incorrect. Further laboratory analyses would be required to determine the proper value of n .

The Rose Run sandstone zone 3A is a linear sandstone body deposited as a single interval (see Fig. 3-9). Gross sandstone thickness ranges from 2 to 12 ft. Following the sea level rise that deposited dolomites overlying zone 3B, sandstone deposition appears to have shifted slightly to the west. The sandstone trends to the northeast-southwest with an average net sandstone thickness of approximately 7.5 ft (using a 6% porosity cutoff). The sandstone has a sharp lower contact with thin shales separating the underlying dolomites from the sandstones. The upper contact is conformable and gradational with interbedded sandstones and dolomites.

Average porosity from log analysis ranges from 6% to 10% (see Fig. 3-10). The porosity is highest in those wells having the thickest sandstone. Zone 3B is a possible source for some the sand in zone 3A. Water saturation ranges from 28% to 38%, increasing rapidly to the west and more gradually to the east (see Fig. 3-11). The tighter sandstones have correspondingly high water saturations.



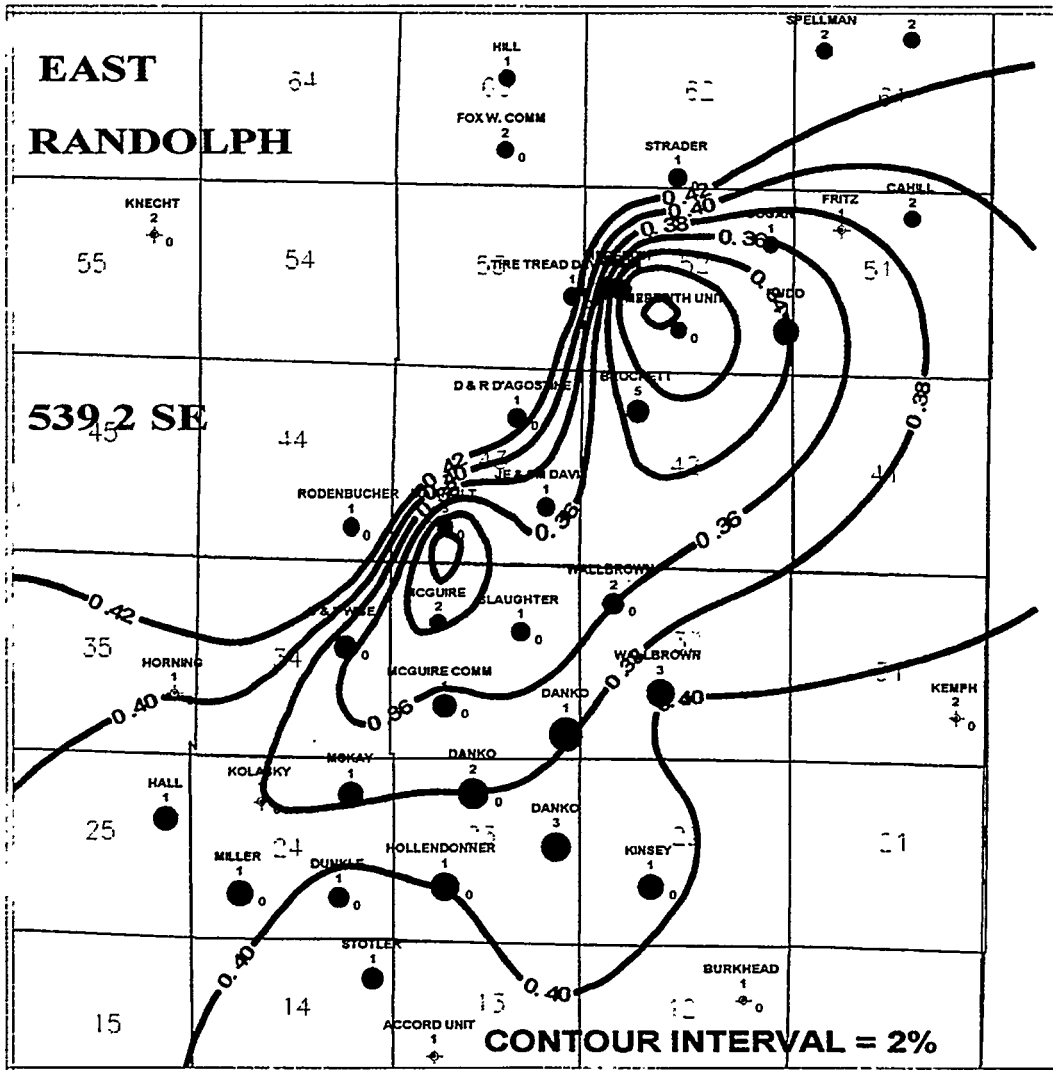
1000. 0. 1000. 2000. 3000. 4000. 5000. feet



LEGEND	
●	OIL WELL
☀	GAS WELL
○	DRY AND ABANDONED

BDM-Oklahoma, Inc.
EAST RANDOLPH FIELD AVERAGE POROSITY ZONE 3B BUBBLE CUM OIL PRODUCTION

Figure 3-6 Net Sand Thickness of Rose Run Zone 3B Using a 6% Porosity Cutoff



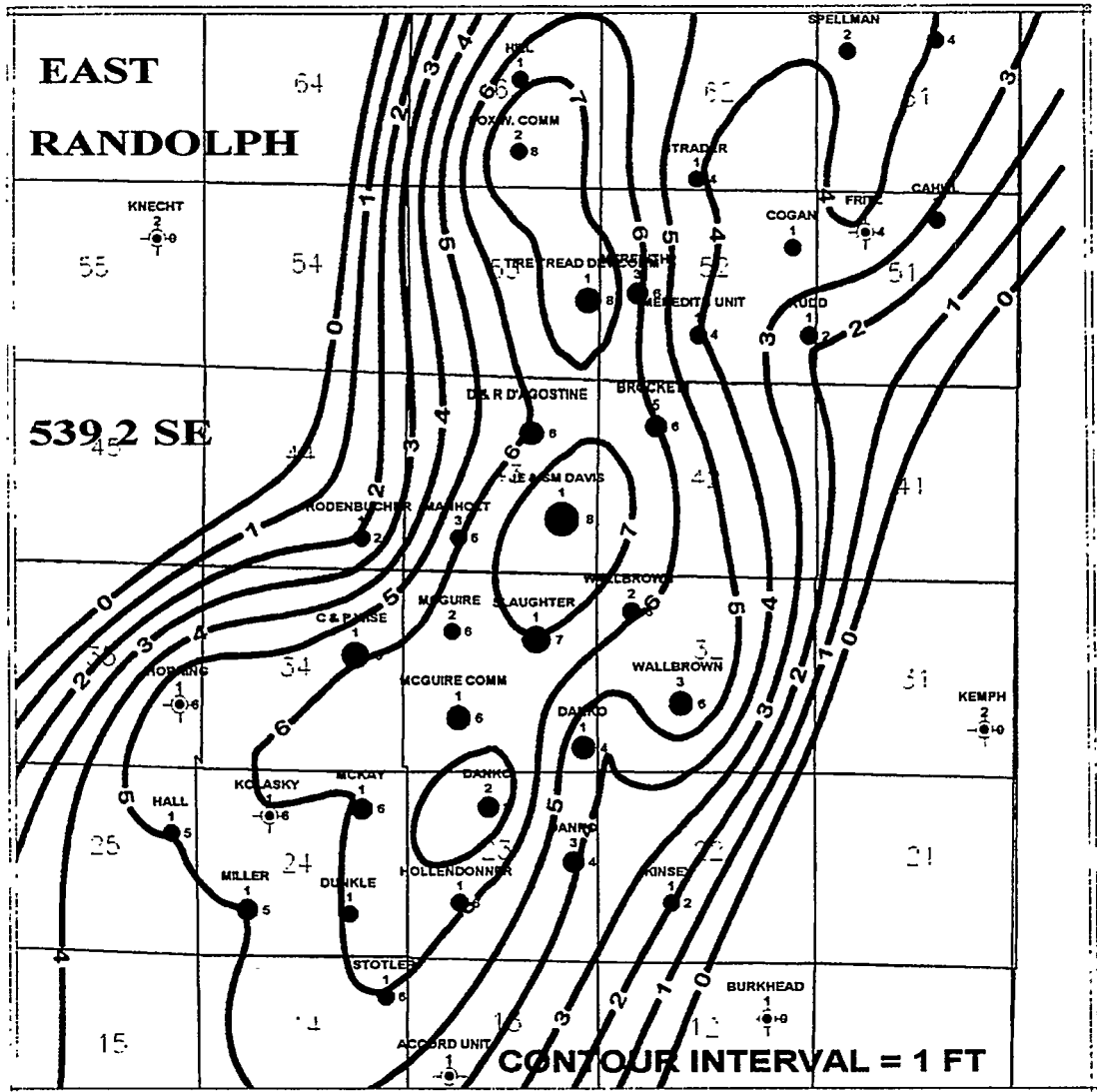
1000. 0. 1000. 2000. 3000. 4000. 5000. feet



LEGEND	
●	OIL WELL
☀	GAS WELL
⊕	DRY AND ABANDONED

BDM-Oklahoma, Inc.
EAST RANDOLPH FIELD
WATER SATURATION ZONE 3B
BUBBLE CUM WATER PRODUCTION

Figure 3-8 Average Water Saturation Rose Run Zone 3B with Bubbled Cumulative Water Production





1000. 0. 1000. 2000. 3000. 4000. 5000.feet



LEGEND

- OIL WELL
- GAS WELL
- DRY AND ABANDONED

BDM-Oklahoma, Inc.

EAST RANDOLPH FIELD
NET SAND THICKNESS ZONE 3A
BUBBLE CUM OIL PRODUCTION

Figure 3-9 Average Water Saturation Rose Run Zone 3B with Bubbled Cumulative Water Production

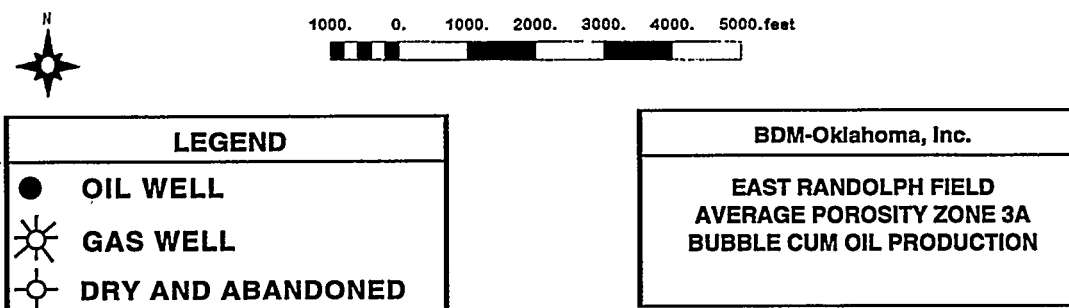
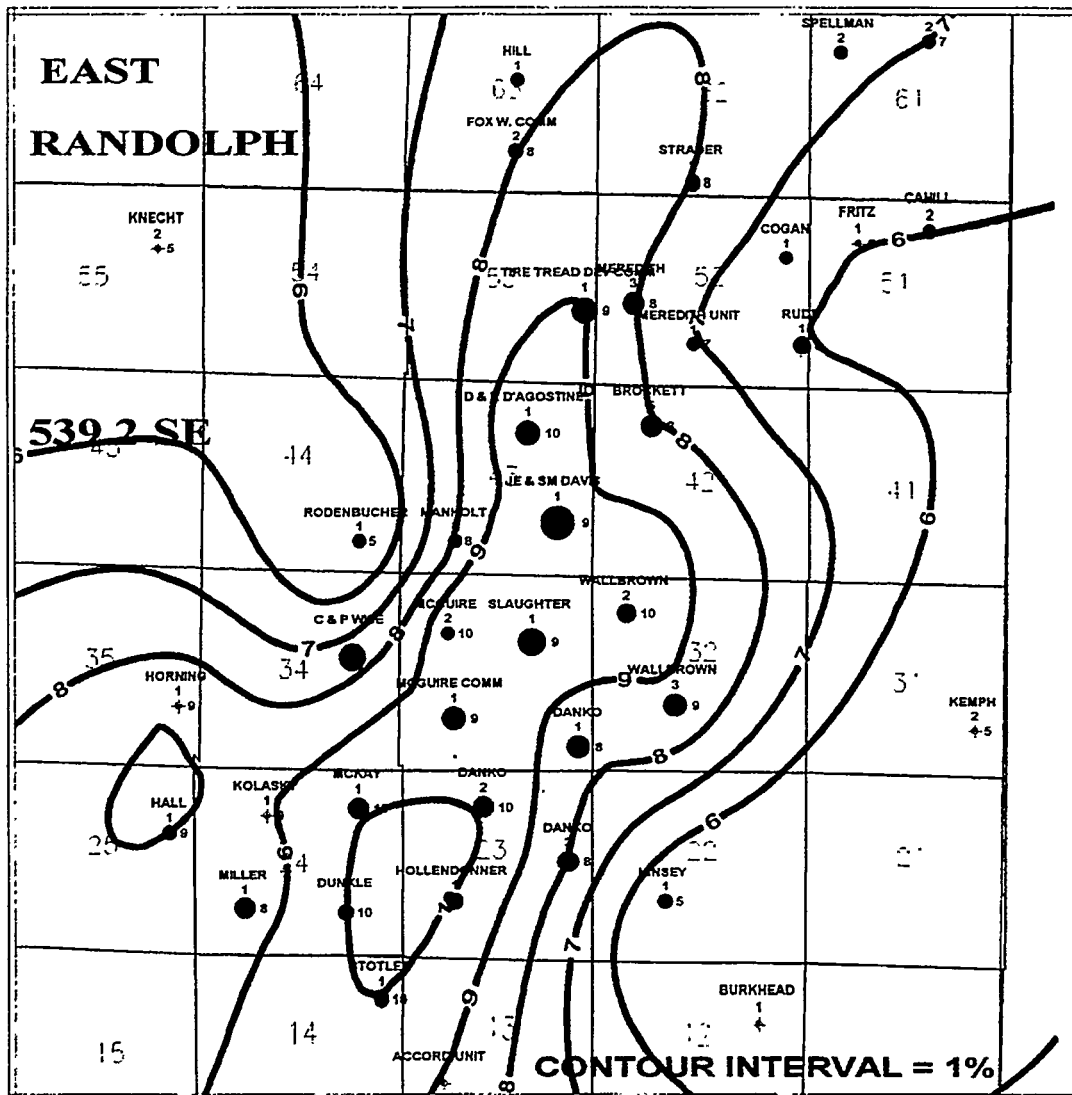
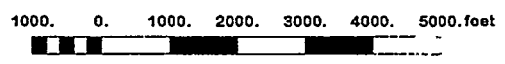
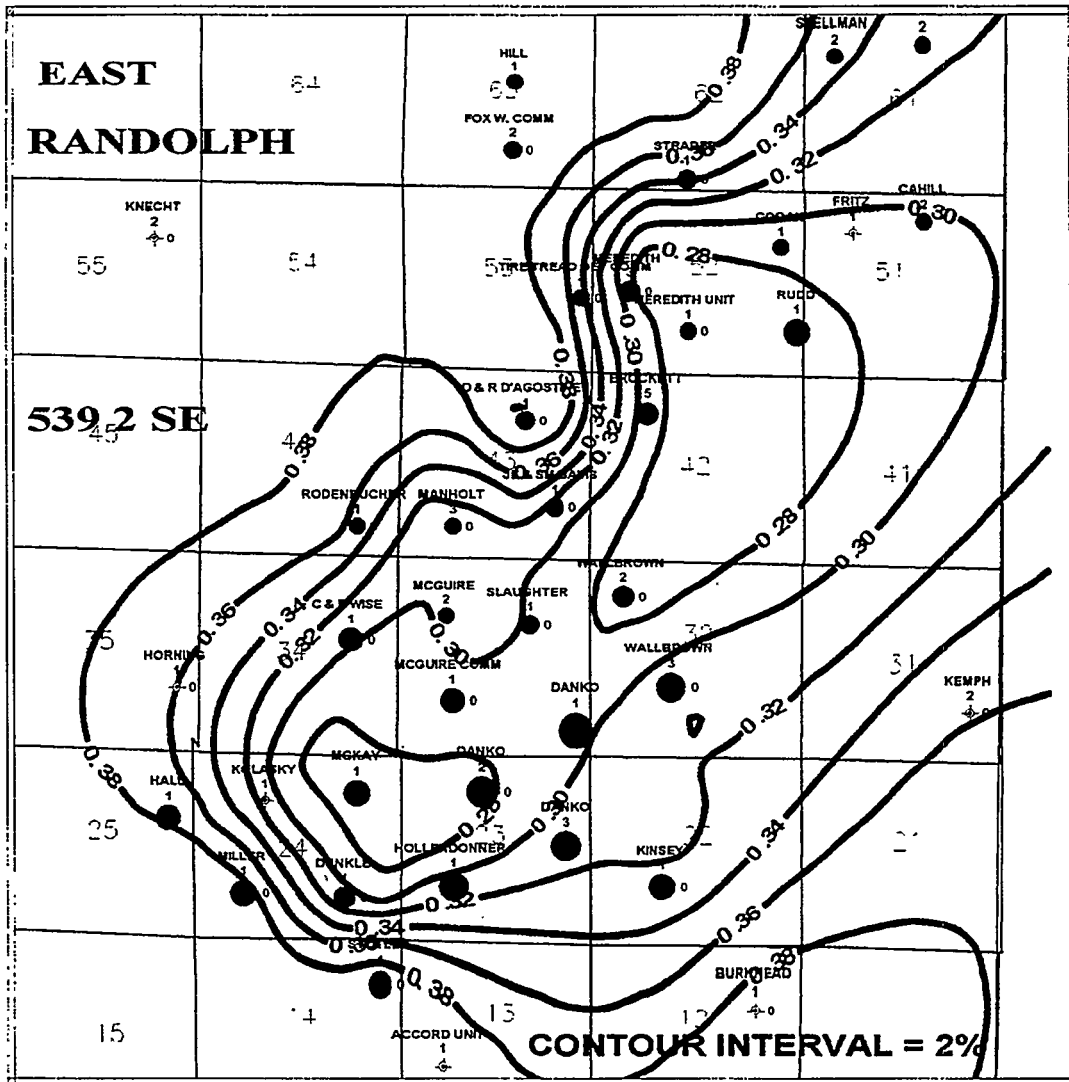


Figure 3-10 Average Porosity of Rose Run Zone 3A with Bubbled Cumulative Oil Production



LEGEND	
●	OIL WELL
☀	GAS WELL
○	DRY AND ABANDONED

BDM-Oklahoma, Inc.
 EAST RANDOLPH FIELD
 WATER SATURATION ZONE 3A
 BUBBLE CUM WATER PRODUCTION

Figure 3-11 Average Water Saturation of Rose Run Zone 3A with Bubbled Cumulative Water Production

The distribution of the sandstone body, the various porosities, and the fining-upward log character reflect changing current directions and variations in wave energy and sediment supply.

Rose Run sandstone Zone 2 has the most limited distribution of the productive zones in East Randolph field (see Fig. 3-12). The sand body is oriented northwest-southeast with an average net sandstone thickness of approximately 5 ft (using a 6% porosity cutoff). Porosity from log analyses varies from 4% to 6%, and pinches out rapidly to the west (see Fig. 3-13).

The amount of neutron-density crossover from log analysis measurements indicates that zone 2 has a high gas saturation. This accounts for the strong correlation between net sandstone thickness and porosity with cumulative gas production. The sandstone has a sharp lower contact with interbedded dolomite. Log analysis indicates a gradational upper contact into sandy dolomites. Underlying dolomites are typically massive and have low porosity. Water saturation ranges from 18% to 28% (see Fig. 3-14). This zone appears more channelized than underlying zones on the basis of sandstone thickness, porosity trends, and log characteristics.

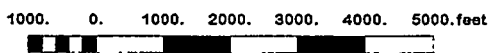
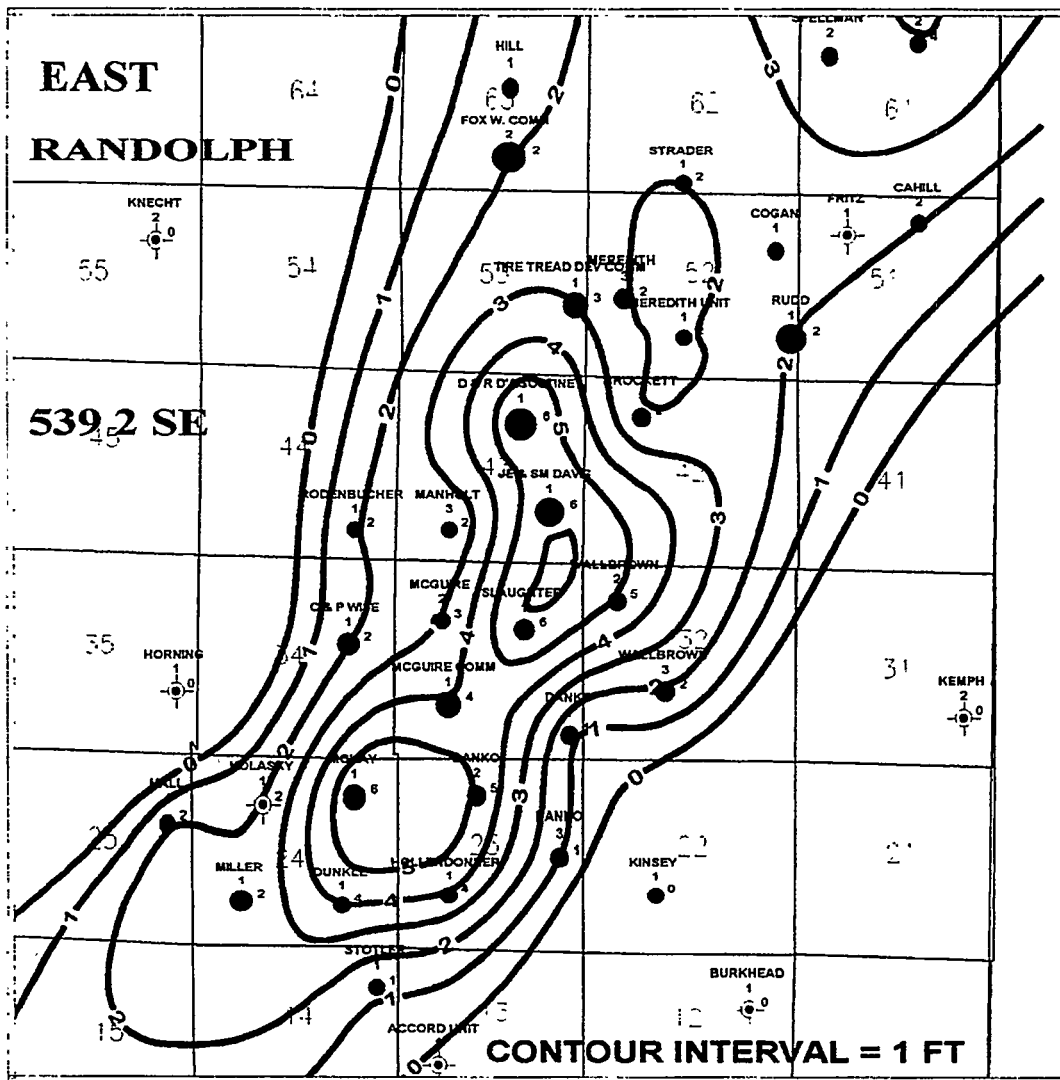
The uppermost sandstone member (zone 1) is laterally discontinuous and generally nonproductive in East Randolph field. The sandstone is up to 2 ft thick and has low porosity and permeability. Based on gas detection while drilling on air, which usually does not exceed 100 units, this zone contributes only small volumes of gas to total production from East Randolph field. West of East Randolph field, this sandstone becomes thicker and more porous, and is one of the productive intervals in the West Randolph gas field. Because of the lack of significant production and poor reservoir quality of this zone in East Randolph field, no maps were constructed showing its distribution.

Isopach mapping of the overlying Beekmantown Dolomite shows that the Rose Run sandstones were deposited in a depositional low. Where the Rose Run sandstones are best developed, the Beekmantown ranges in thickness from 40 to 100 ft. Thinner intervals of Beekmantown indicate structural highs where Rose Run sandstones were diverted around barriers or eroded away. The Beekmantown represents the seal for Rose Run production beneath the Knox unconformity.

3.2.3 Core Analyses

3.2.3.1 Conventional Core Analysis

Knowledge of the internal structure of the reservoir rock is important for log analysis; drilling, completion, and stimulation applications; and estimation of injection fluid/rock interactions. Core analysis allows the operator to determine the pore types, spatial distribution of porosity, and effects of diagenetic products on the productive capability of the rock. The key to understanding the various effects of lithology and diagenesis on reservoir quality is the interpretation and integration of data and results from a number of relatively independent analytical techniques.



LEGEND	
●	OIL WELL
☀	GAS WELL
⊙	DRY AND ABANDONED

BDM-Oklahoma, Inc.
EAST RANDOLPH FIELD NET SAND THICKNESS ZONE 2 BUBBLE CUM GAS PRODUCTION

Figure 3-12 Rose Run Zone 2 Net Sandstone Thickness Using a 6% Porosity Cutoff

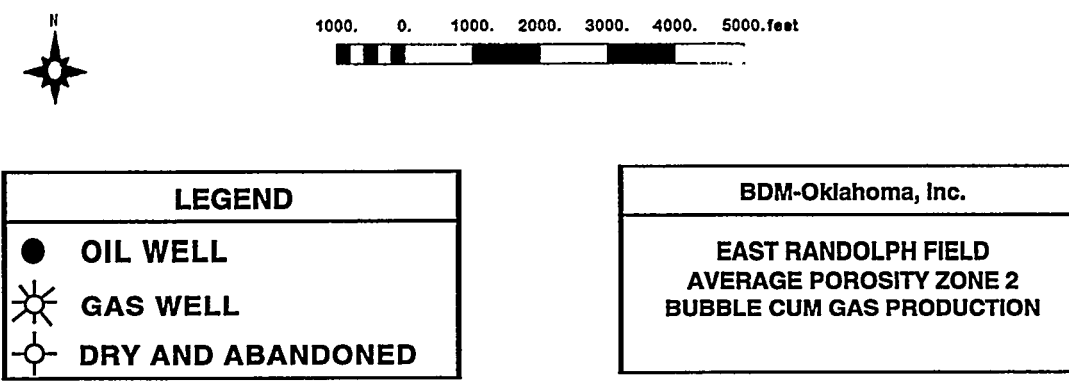
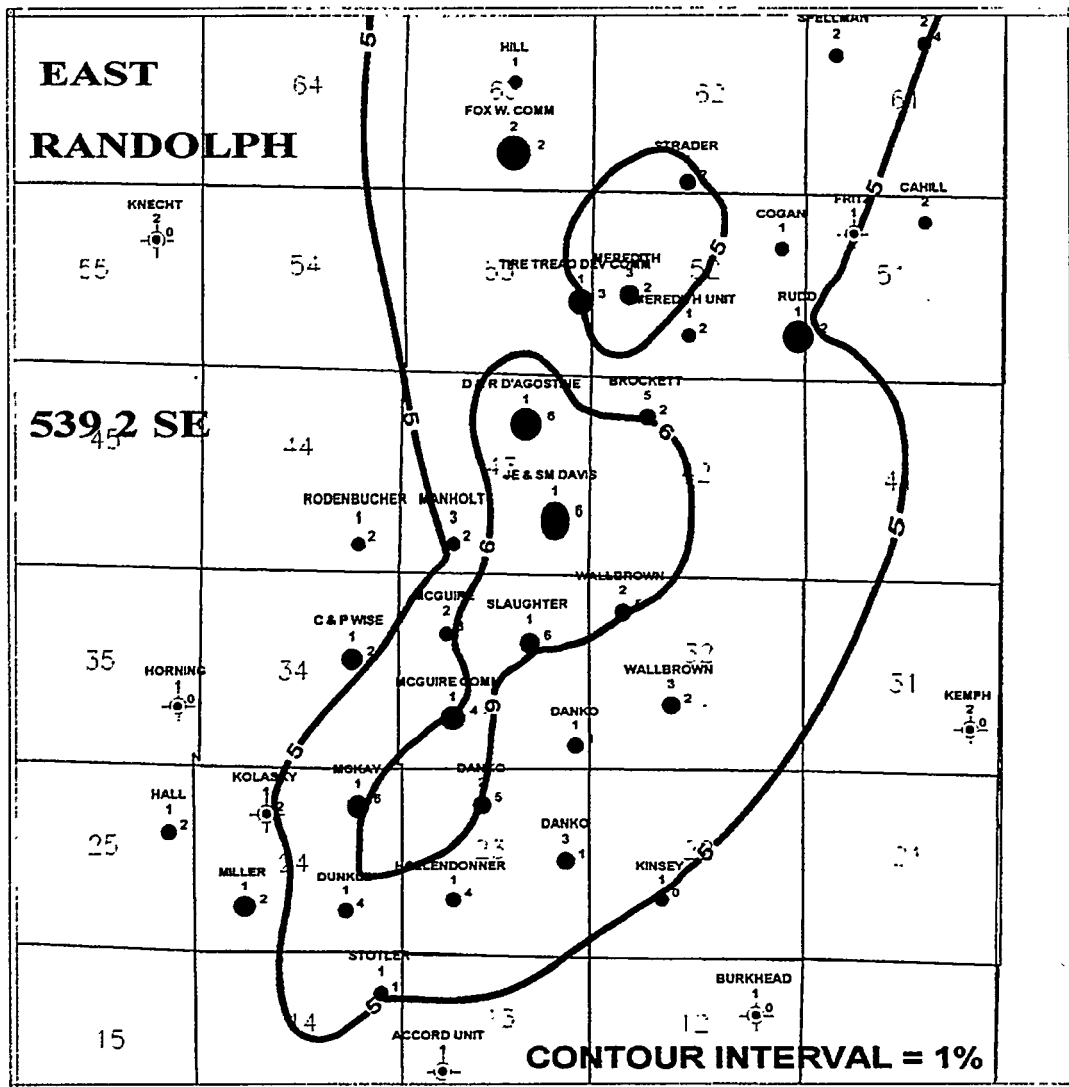
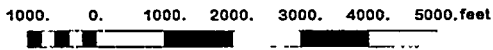
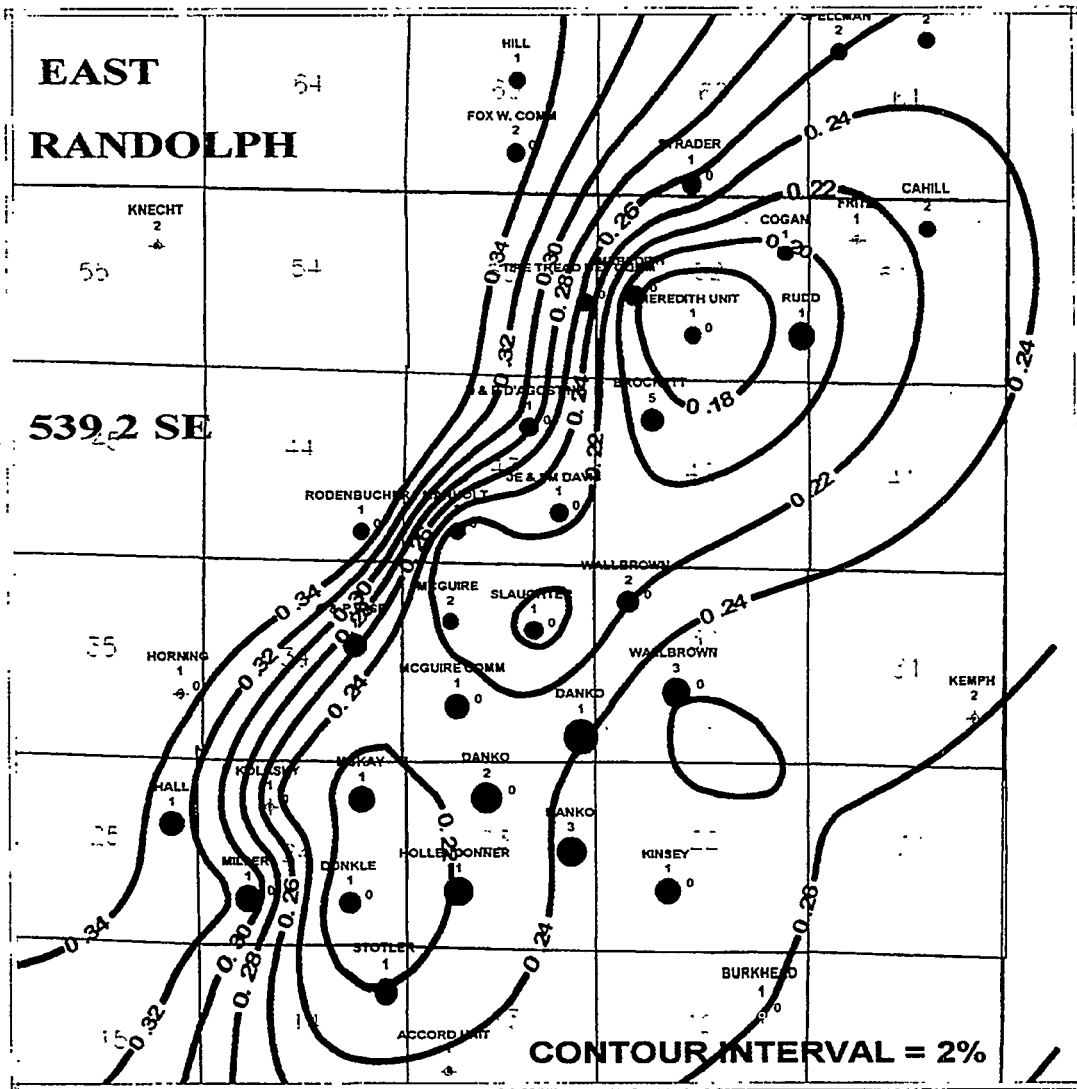


Figure 3-13 Rose Run Zone 2 Average Porosity with Bubbled Cumulative Gas Production



LEGEND	
●	OIL WELL
☀	GAS WELL
○	DRY AND ABANDONED

BDM-Oklahoma, Inc.	
EAST RANDOLPH FIELD	
WATER SATURATION ZONE 2	
BUBBLE CUM WATER PRODUCTION	

Figure 3-14 Rose Run Zone 2 Average Water Saturation with Bubbled Cumulative Water Production

Belden & Blake coordinated the bidding, retrieving, and shipping of the whole core acquired from the McGuire No. 2 infill well in East Randolph field. The well was cored from a depth of 7,318 to 7,372 ft, recovering 54 ft of 4-in. diameter core. Field problems in identifying the upper Rose Run sand (zone 1) during drilling resulted in coring operations beginning near the base of the zone 2 sand, missing much of the productive interval in that zone. OMNI Laboratories in Houston was selected by Belden & Blake to perform the conventional core analyses on Rose Run sandstone zones 3A and 3B. Core photographs in plain light and fluorescent light were taken to determine the distribution of oil saturation (white streaks and vugs) and dolomitization (mottled) within each of the zones. Based on comparison of the core gamma-ray log with the wireline log, the core depth was 4 ft shallower than the log (i.e., core depth + 4 ft = log depth).

The 1.0-in. diameter samples were cleaned in a cool solvent extraction system using toluene and methanol, then dried overnight in a vacuum oven at 90°C until a stable weight was established. Ambient permeability to air was measured using a confining pressure of 400 psi. Boyle's Law porosity and grain density using helium were measured, and fluid saturations were calculated. A permeability vs. porosity plot was drawn for the analyzed zone. A least-squares best-fit line through the data was drawn, and the resulting equation was calculated:

$$K = \text{antilog} (0.305 \cdot \phi_{\text{core}} - 2.825)$$

where K = maximum permeability (md) and ϕ_{core} = measured core porosity (%).

This relationship could change significantly with changes in pore sizes and pore size distribution. The relationship should be compared with other core porosity- permeability relationships to determine how the relationship varies across the field.

3.2.3.2 Special Core Analysis

Special core analyses were performed by Dan Maloney at BDM-Oklahoma on Rose Run sandstone zones 2, 3A, and 3B from the McGuire No. 2 core (Appendix A). BDM-Oklahoma cleaned plugs by multiple extraction/soak cycles using toluene and methanol solvents. Toluene was used to remove oil and paraffin from the plugs. Methanol was used to remove the toluene, which sometimes leaves outer plug surfaces oil-wet. The rigorous cleaning techniques employed by BDM-Oklahoma provided conventional permeability and porosity results that were, for some plug depths, higher than those measured by OMNI Laboratories.

Conventional permeability and porosity measurements were made using nitrogen (permeability) and helium (porosity) gases. Plugs were subjected to 100 psig confining pressure during the BDM-Oklahoma tests. Results are shown in Table 3-1, which also includes conventional property results from OMNI Laboratories for comparison.

Table 3-1 Routine Permeability and Porosity Results

Sample Depth, ft	Gas Permeability, md	Helium Porosity, %	Lab
7318.10	<0.01	0.7	BDM
7319.10	0.01	1.7	BDM
7321.45	0.06	5.1	OMNI
7322.20	0.17	7.0	OMNI
7323.10	8.58	2.1	BDM
7327.00	1.02	11.2	OMNI
7328.30	3.04	10.9	BDM
7328.50	1.74	8.6	OMNI
7330.30	12.99	7.9	BDM
7330.95	1.20	7.3	OMNI
7332.30	5.81	10.8	BDM
7332.80	0.80	9.9	OMNI
7333.10	3.76	11.1	BDM
7335.60	7.09	1.2	BDM
7336.00	<0.01	2.8	OMNI
7339.20	8.46	3.8	BDM
7339.90	<0.01	3.3	OMNI
7342.40	1.98	7.9	OMNI
7343.00	16.59	8.4	BDM
7344.00	11.60	0.9	BDM
7346.35	<0.01	2.6	OMNI
7348.30	2.13	10.0	BDM
7348.85	0.54	8.8	OMNI
7349.30	1.73	10.6	BDM
7349.80	<0.01	3.5	OMNI
7350.30	0.02	4.2	BDM
7352.30	<0.01	1.8	BDM

Figure 3-15 is a plot of data from Table 3-1 for plugs with permeabilities greater than or equal to 0.01 md. Four of the plugs (from depths of 7323.1, 7335.6, 7339.2, and 7344.0 ft) had porosities less than 4%, but gas permeabilities of about 10 md. Cracks were visually evident in two of the plugs (those from 7335.6 and 7344.0 ft). The other two plugs are suspected to contain cracks as well. Plugs 7323.1 and 7335.6 were essentially impermeable to brine when subjected to 4,250 psig confining pressures. From these considerations, it appears that samples with porosities less than about 4% have permeabilities of 0.01 md or less at reservoir conditions.

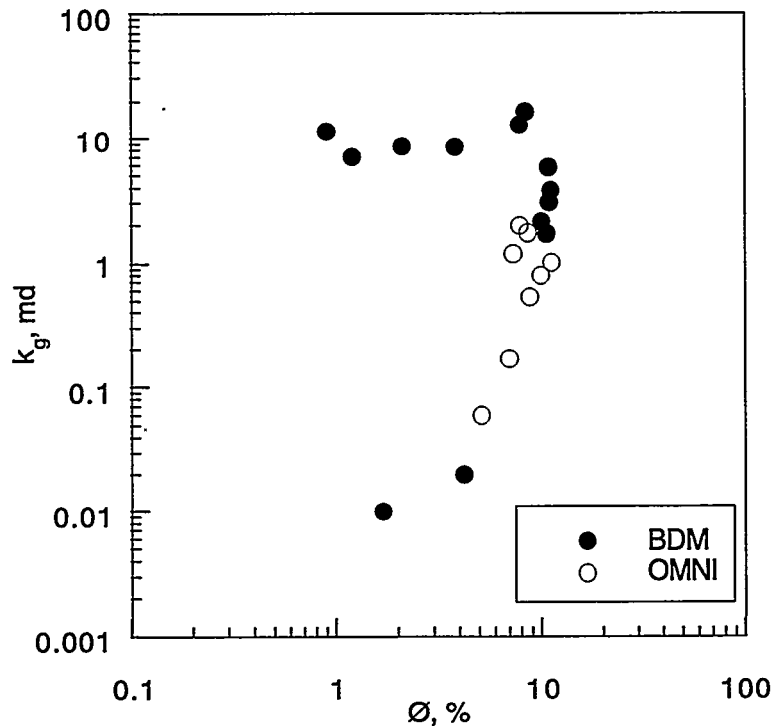


Figure 3-15 Gas Permeabilities from OMNI and BDM-OK Labs. BDM measurements were performed with 100 psig confining pressure.

Figures 3-16 and 3-17 show permeability and porosity data from both OMNI and BDM plotted against depth. Lines on the graphs that link data points are included to show changes in measured results with depth rather than to infer values between measurements. Results for plugs 7323.1, 7335.6, 7339.2, and 7344.0 are not included in these two figures because permeabilities for these samples are believed to be nonrepresentative. The high permeabilities and low porosities for these four plugs suggest the presence of high permeability cracks, as described in the previous paragraph. These cracks are probably closed at the reservoir stress conditions.

Eight core plugs were selected for brine permeability measurements. With increasing confining pressure, volumes of brine "squeezed out" of the plugs were measured. Brine volumes produced as the confining pressure was first increased from 0 psig to 300 psig were attributed primarily to surface effects when the coreholder sleeve and core end-pieces firmly seal against the rock sample. For stresses greater than 300 psig, brine volumes squeezed out of a plug were considered to result from pore volume compression.

Figure 3-18 shows apparent decrease in pore volume vs. confining pressure results for the eight core plugs. Results indicate that pore volumes for most of the plugs were reduced by 4% to 6% as the confining pressure changed from 300 psig to 4,250 psig. Pore volume in sample 7323.1 was significantly reduced due to the closing of microfractures with increasing confing pressures.

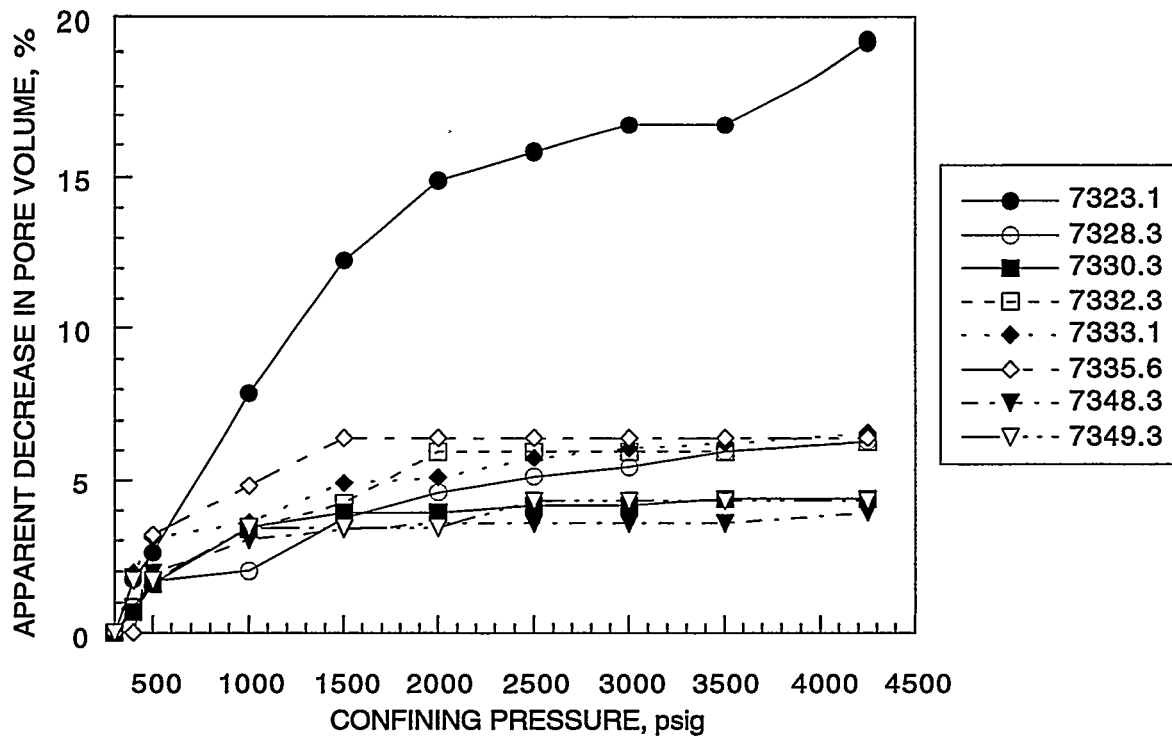


Figure 3-18 Changes in Pore Volumes with Stress Interpreted from Squeeze-Out Measurements

Brine permeability tests were performed with 4,250 psig net confining pressure applied to the plugs. Permeabilities for each plug were calculated using rate and pressure drop measurements from four different injection rates. Table 3-2 shows permeability and porosity measurements from routine (low-pressure) gas measurements as well as from brine permeability and porosity measurements at simulated reservoir stress conditions (4,250 psig net confining pressure).

Figure 3-19 shows measured brine permeabilities from 4,250 psig net confining pressure conditions plotted against gas permeabilities measured with 100 psig confining pressure. The correlation equation shown is useful for estimating brine permeabilities when only gas permeability data from conventional core analyses are available (within the range of measurements shown).

Table 3-2 Petrophysical Properties of Selected Plugs at 100 and 4,250 psig Net Confining Pressure

Plug	100 psig					4,250 psig		
	GV, cm ³	PV, cm ³	BV, cm ³	k _a , md	φ, %	PV, cm ³	k _w , md	φ, %
7318.1	53.463	0.36	53.819	<0.01	0.7			
7319.1	53.555	0.94	54.497	0.01	1.7			
7323.1	53.012	1.14	54.152	8.58	2.1	0.92	<0.010	1.7
7328.3	47.962	5.85	53.816	3.04	10.9	5.48	0.810	10.3
7330.3	50.027	4.32	54.347	13.00	7.9	4.13	1.920	7.6
7332.3	48.679	5.87	54.554	5.81	10.8	5.50	0.720	10.2
7333.1	48.723	6.07	54.793	3.76	11.1	5.67	0.424	10.4
7335.6	52.676	0.62	53.295	7.09	1.2	0.58	<0.010	1.1
7339.2	53.321	2.09	55.416	8.46	3.8			
7343.0	50.667	4.67	55.341	16.59	8.4			
7344.0	53.962	0.49	54.452	11.60	0.9			
7348.3	49.949	5.57	55.523	2.13	10.0	5.35	0.386	9.7
7349.3	48.820	5.78	54.601	1.73	10.6	5.53	0.147	10.2
7350.3	53.970	2.34	56.307	0.02	4.2			
7352.3	55.227	0.99	56.217	<0.01	1.8			

GV = grain volume k_a = gas permeability PV = pore volume
 k_w = brine permeability BV = bulk volume φ = porosity

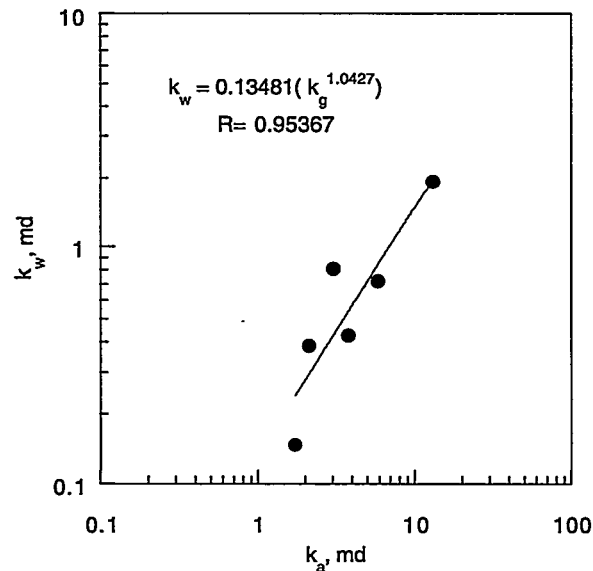


Figure 3-19 Comparison of Brine Permeability Measurements (4,250 psig Confining Pressure) with Air Permeability Measurements (100 psig Confining Pressure)

3.2.3.3 Core Description and Petrographic Analyses

Core description and petrographic analyses provides information on various depositional and diagenetic controls that include pore sizes and distribution, pore throat size, grain size, sorting, and mineralogy. Variations in grain and pore attributes define distinct zones with similar fluid flow characteristics. The major controls on these features are the sediment source and the subsequent diagenetic processes of compaction, dissolution and cementation.

The lowermost zone (3B) is a tightly cemented, light gray to medium gray, parallel laminated to ripple cross laminated, well sorted, arkosic sandstone (see Figs. 3-20 and 3-21). The sandstone lithology is classified as arkosic (Folk 1974). Individual laminations are defined by variations in grain size and varying amount of shaley material. The sandstone is interbedded with dolomitized wackestones and packstones and thinly laminated to flaser-bedded shale. The wavy laminated sandstones contain angular shale rip-up clasts and shale drapes. The sandstone is burrowed near the top. The upper contact is gradational with shale rip-ups present in the overlying mottled dolomite. Fluorescent lighting identifies those intervals (light colored in Figure 3-21) that are oil saturated and those intervals with abundant dolomite cementation (mottled).

From core analysis, zone 3B porosity ranges from 7.9% to 10.6%. Air permeability ranges from 0.54 md to 2.13 md; brine permeability ranges from 0.14 md to 0.38 md, approximately 10% of air permeability. Water saturation ranges from 49.2% to 70.7%, indicating a higher water saturation toward the base of the Rose Run interval. The low porosity often indicates extremely small capillary pore openings and accompanying high formation water saturation.

Zone 3A is a light to medium gray, sub- to well-rounded, moderately sorted arkosic sandstone (see Figs. 3-22 and 3-23). The sandstone is parallel laminated to low-angle, ripple cross laminated. Laminations are defined by variations in grain size and accentuated by higher concentrations of shaley material. The sandstones are interbedded with wavy laminated and flaser-bedded shales. Bioturbation, soft sediment deformation due to compaction and dewatering, and stylolites have distorted or destroyed the laminations in places. The basal contact into the underlying dolomite is sharp. The high oil saturation of this interval and the interbedded dolomite intervals is apparent in the core photograph with the fluorescent lighting.

The sandstone is fine grained at the base and becomes very fine grained with lower porosity near the top. Based on core analysis, porosity for zone 3A ranges from 7.3% to 11.1%. Air permeability ranges from 1.02 md to 12.9 md; brine permeability ranges from 0.42 md to 1.92 md, approximately 10% of air permeability. Water saturation ranges from 32.5% to 51.4%.

Zone 2 sandstones are light to medium gray, fine grained, well rounded, well sorted, and parallel laminated to cross laminated (see Figs. 3-24 and 3-25). Alternating light and medium gray laminations are defined by grain size differences and shale content. The sandstone is burrowed in places with the burrows filled with finer grained material than the surrounding sediments. Thin interbedded shales are parallel to ripple laminated and contain reddish oxidation, possible root traces, and bioturbation. Soft sediment deformation is present due to compaction and dewatering, with small microfractures healed with quartz cement.

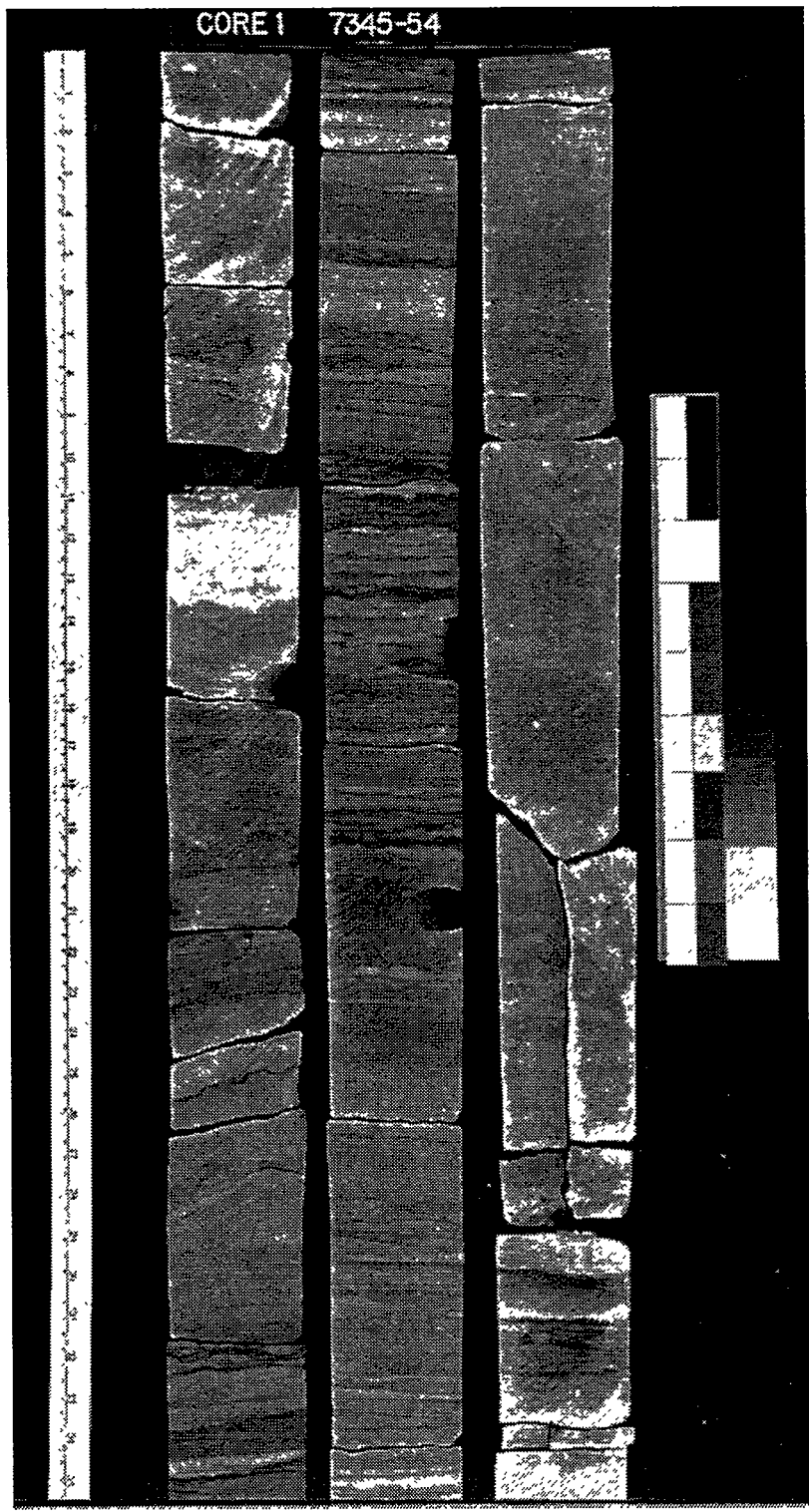


Figure 3-20 Core Photographs of Rose Run Zone 3B Taken from McGuire No. 2 Core. Plain light

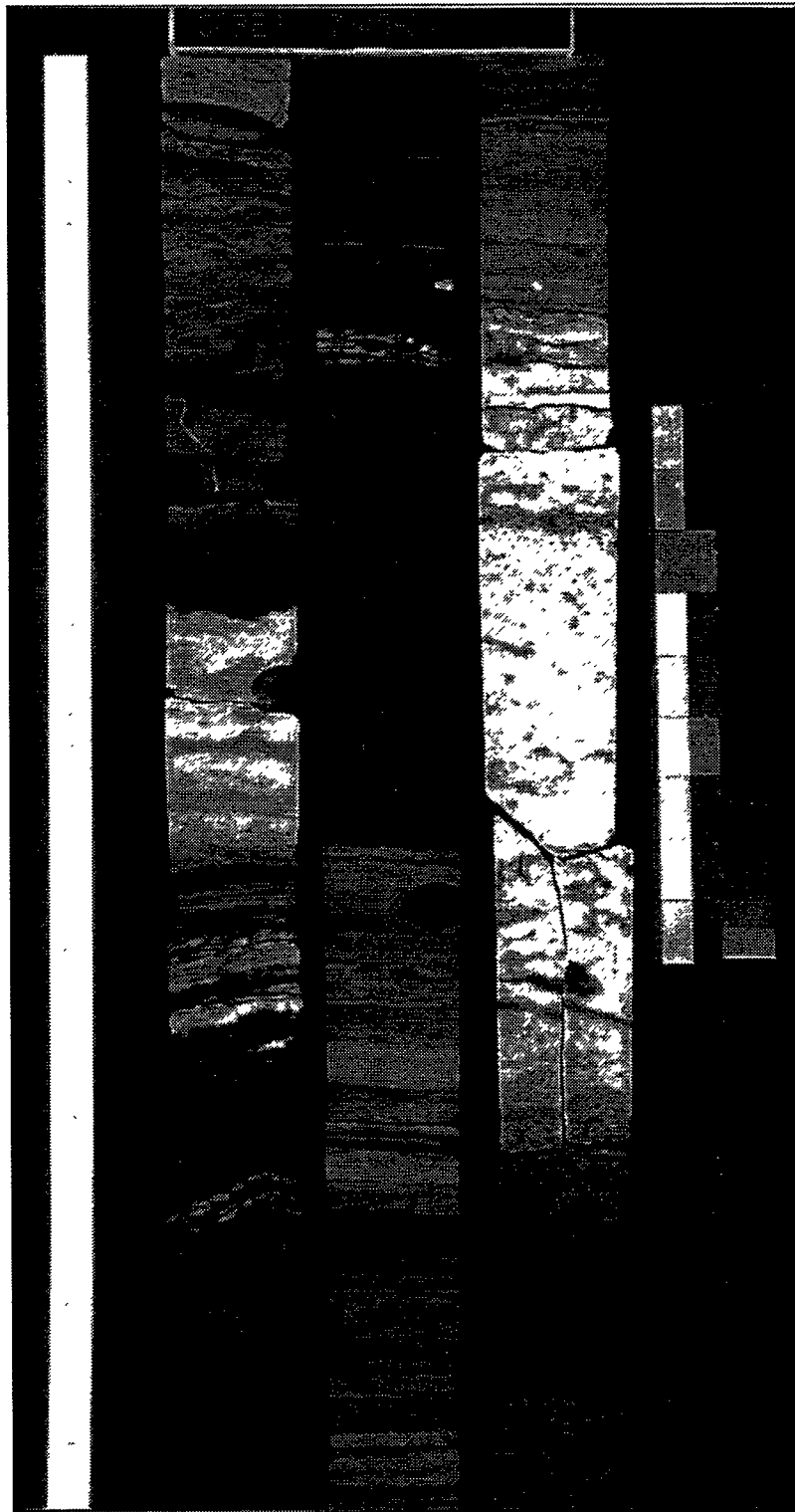


Figure 3-21 Core Photographs of Rose Run Zone 3B Taken from McGuire No. 2 core.
Fluorescent light

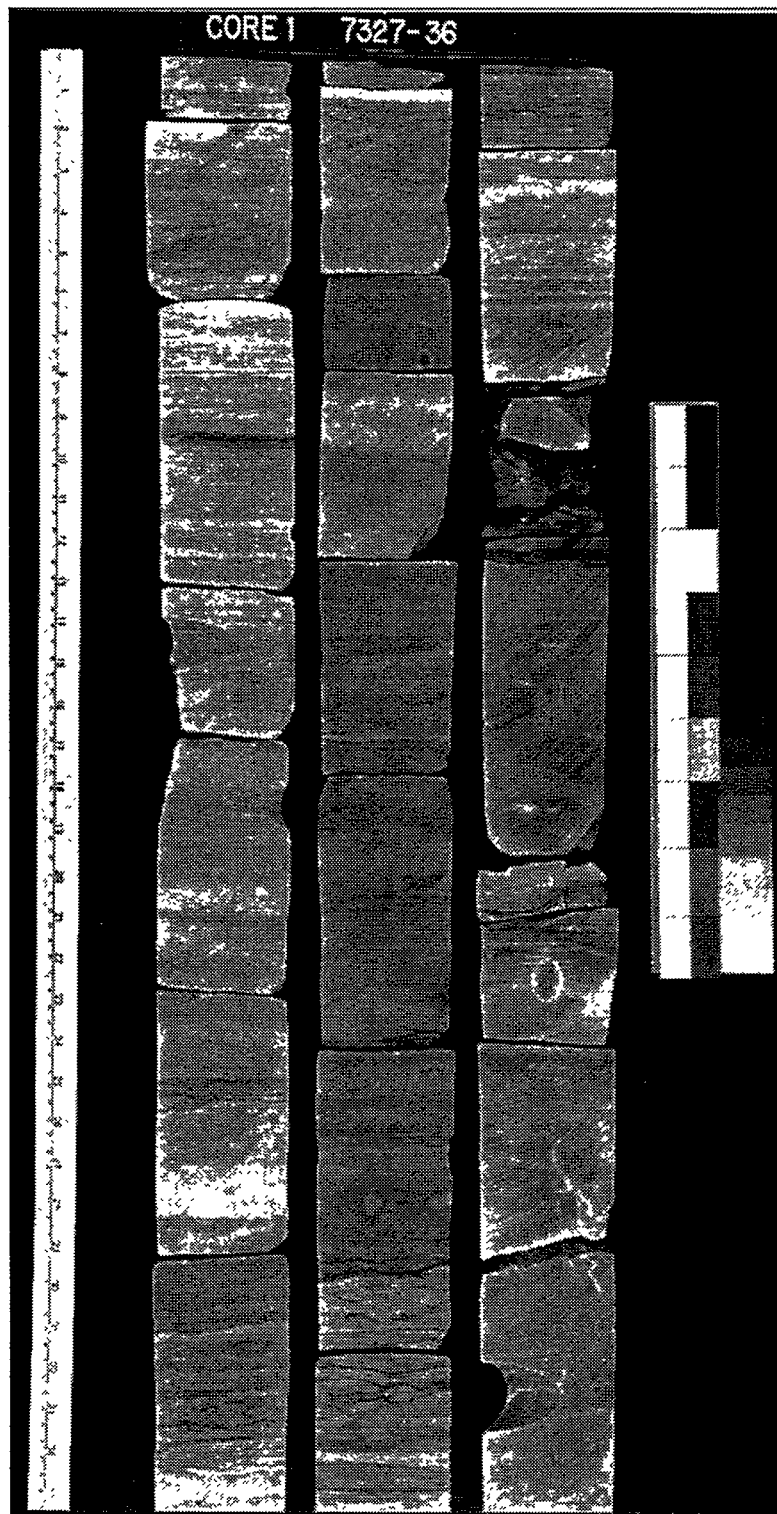


Figure 3-22 Core Photograph of Rose Run Zone 3A Taken from McGuire No. 2 Core.
Plain light

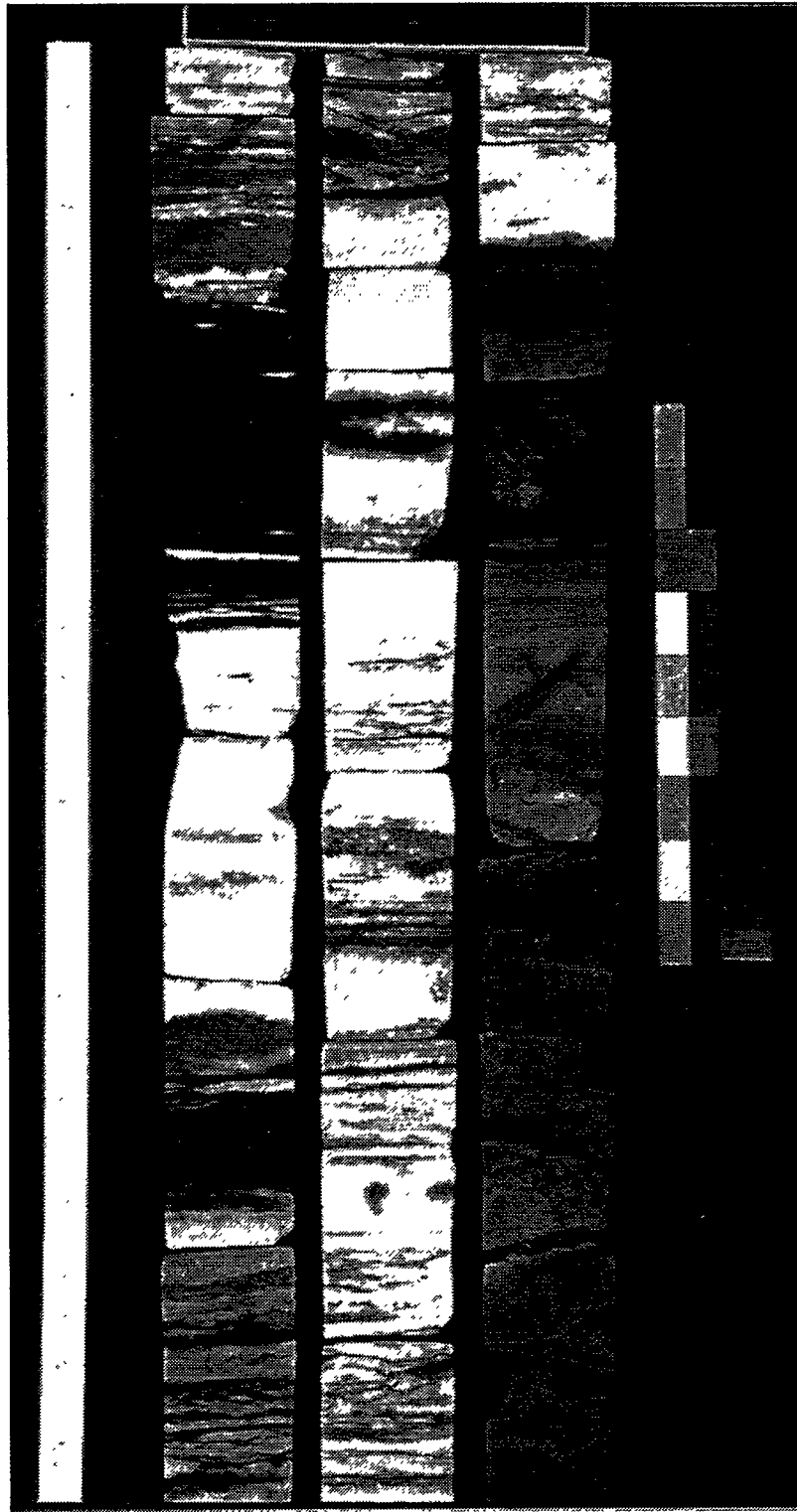


Figure 3-23 Core Photograph of Rose Run Zone 3A Taken from McGuire No. 2 Core.
Fluorescent light

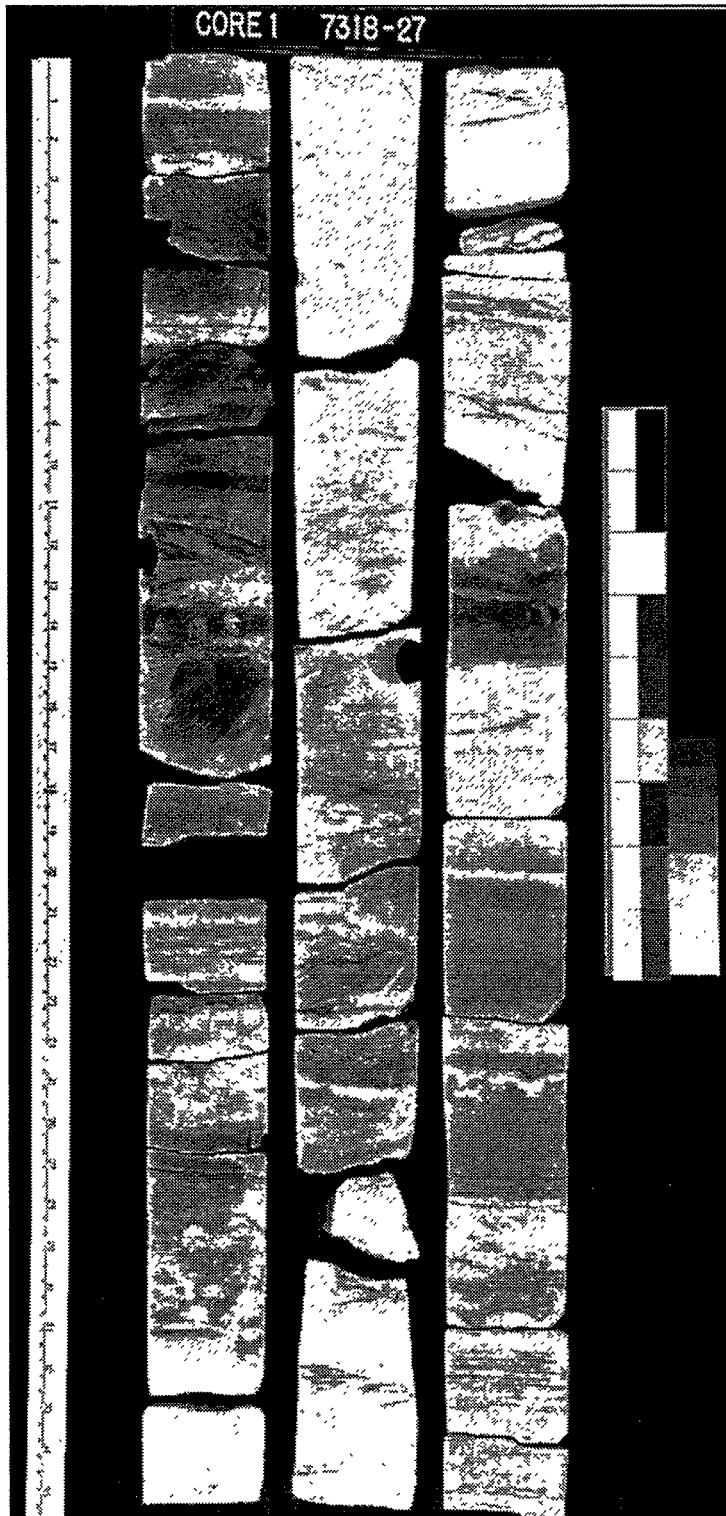


Figure 3-24 Core Photograph of Rose Run Zone 2 Taken from McGuire No. 2 Core. Plain light

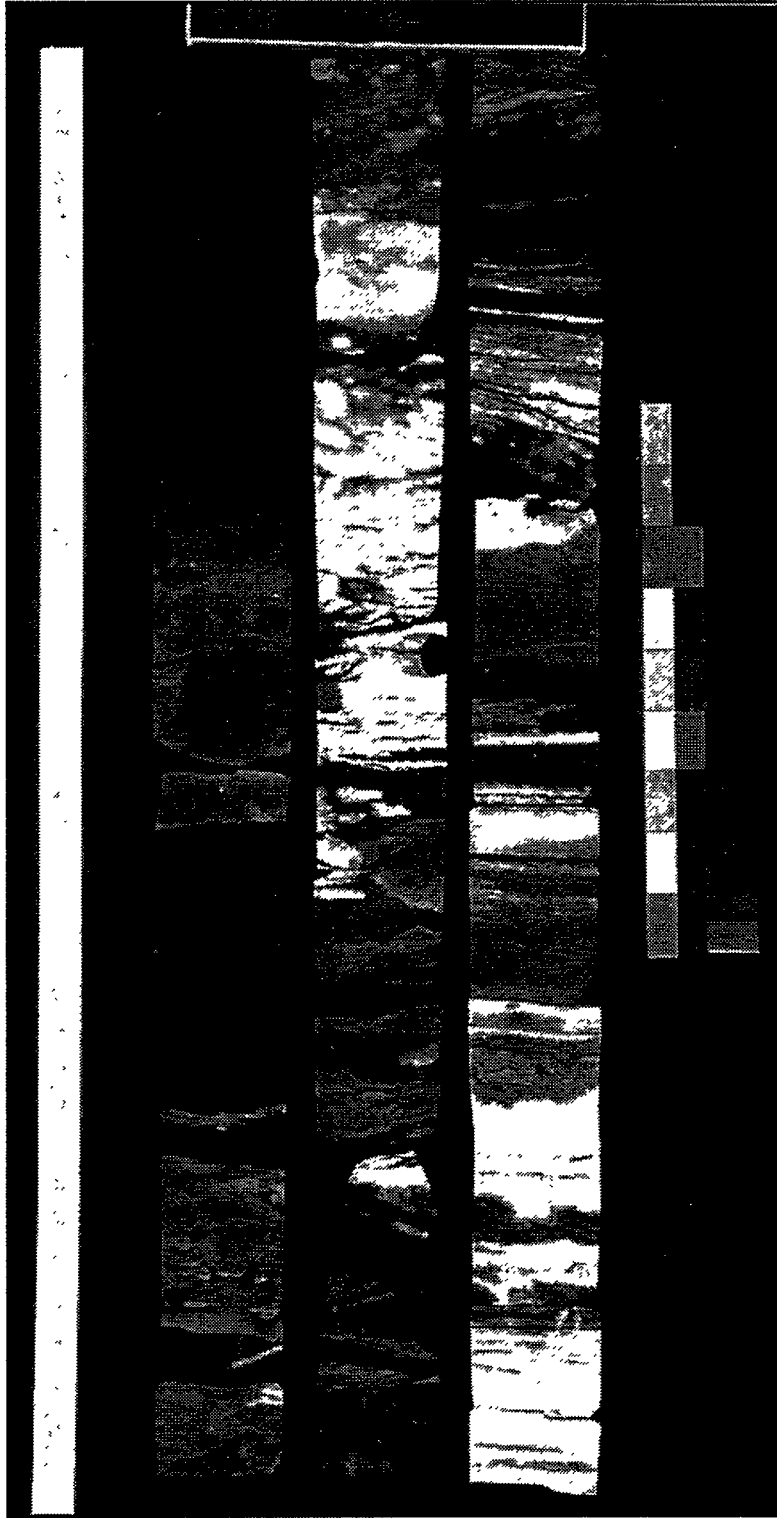


Figure 3-25 Core Photograph of Rose Run Zone 2 Taken from McGuire No. 2 Core.
Fluorescent light

No conventional porosity or permeability measurements were performed for zone 2 in the McGuire #2 core. Core porosity measurements for zone 2 from the D'Agostine No. 1 well range from 1.7% to 6.2%; air permeability ranges from 0.01 md to 0.42 md. Log porosity varies from 1% to 7%, with neutron-density crossover of 4% to 6%, suggesting high gas saturation.

Zone 1 had the poorest reservoir quality of all the sandstone zones. This zone varies laterally from a tightly cemented fine-grained quartz arenite to a sandy dolomite. Average porosity from logs in this zone is less than 6%. Permeability is also low, usually less than 0.1 md. Bedding is usually horizontal, with beds ranging in thickness from 6 in. to 2 ft. Hydrocarbon production from this unit is limited to a few wells where porosity exceeds 6%. Based on gas detection, which usually does not exceed 100 units when drilling on air, this zone contributes only small volumes of gas to total Rose Run production.

The interbedded dolostones are typically gray to brown, fine to medium crystalline, and parallel laminated. Erosional contacts with overlying sandstones contain dolomite and sandstone rip-up clasts. Ooids and peloids are present within several interbedded intervals. The dolomite is typically mottled with stylolites present locally. The dolomite typically has very low visible porosity. A few intervals have well-developed vuggy porosity. The interbedded dolomites act as baffles to fluid flow and create fluid-flow compartments within the Rose Run sequence.

Reservoir quality analysis, therefore, indicates that sandstone zones having the best reservoir quality tend to be located near the basal portion of each zone, and fine upward, usually grading into a nonreservoir, low-permeability dolomite or carbonaceous shale. The lenticularity of the sandstones and dolomite interbeds encourages horizontal flow and minimizes cross flow or channeling. The porosity variation across the field could adversely affect areal sweep efficiency. The repeated fining upward cycles of sandstone and dolomite suggest cyclical fluctuations of sea level and sediment supply.

Petrographic analyses, combined with lithofacies and petrophysical measurements, will aid in the interpretation of wireline data, determine diagenetic history, and evaluate controls on reservoir quality. Thin section petrography was performed on selected intervals from the McGuire No. 2 cored infill well. The objectives of the analyses were to characterize the grain size, texture, and mineralogy of the productive intervals; interpret the effects of diagenesis and cementation on porosity distribution; and integrate the core analyses with log analyses to refine the geologic model.

Most of the Rose Run sandstones petrographically analyzed are silica- or dolomite-cemented, moderately well-sorted to very well-sorted, subrounded to well-rounded, fine-grained sandstones (see Figure 3-26A).

The sandstones are typically parallel laminated to low-angle cross laminated. Individual laminations are often defined by variations in grain size (see Figure 3-26B). The dominant mineral constituents are monocrystalline quartz, K-feldspar, plagioclase feldspar, and polycrystalline quartz. Rock fragments are predominantly sedimentary in origin, with trace amounts of altered igneous lithics. Chert occurs in a few samples. Feldspar grains are generally

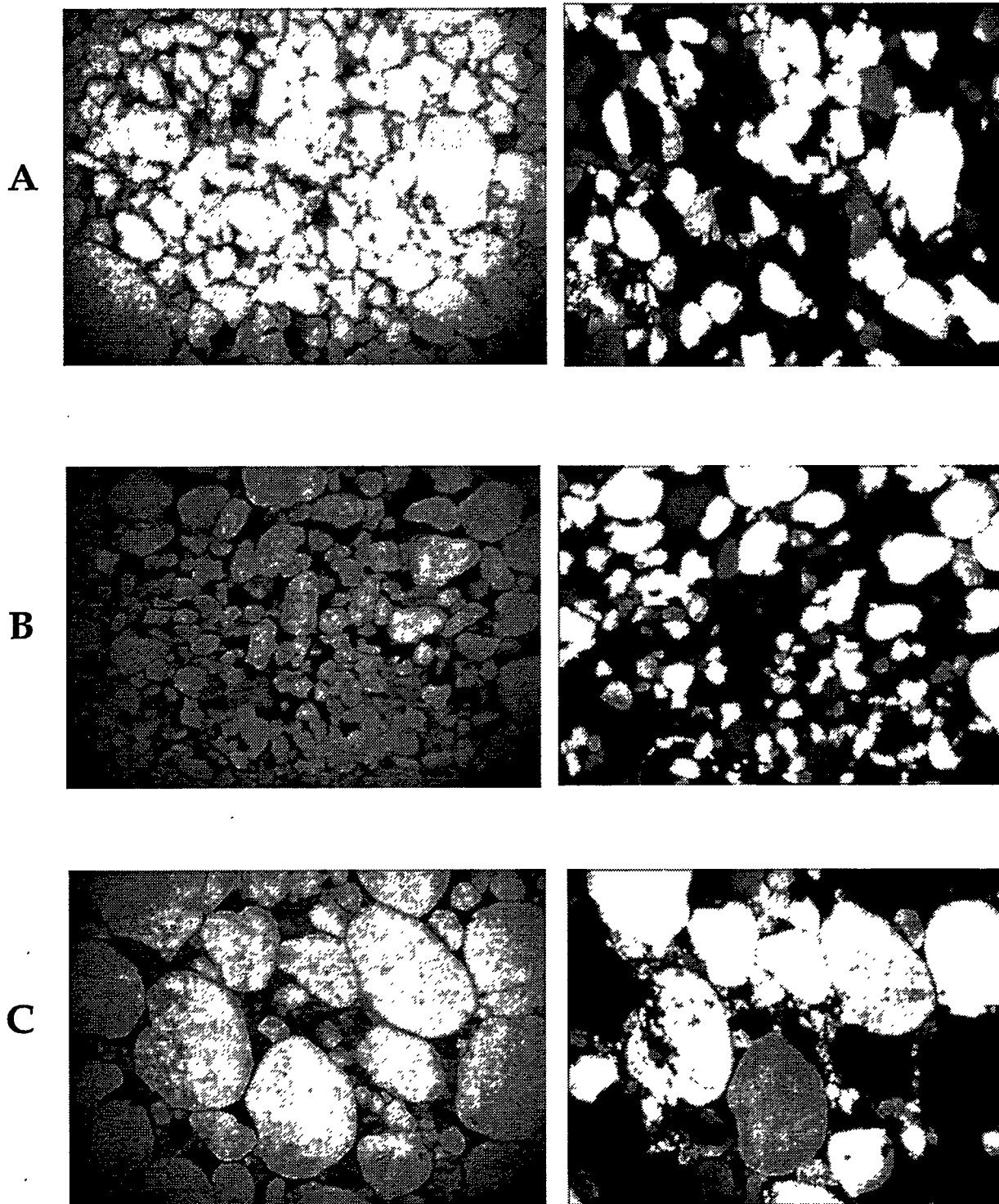


Figure 3-26 Photomicrographs in Plain (Left) and Polarized (Right) Light of Rose Run Zone 3B Taken from McGuire No. 2 Core Showing Lithology and Grain Size Distribution

partially to completely leached due to secondary dissolution. Glauconite is present in some samples near the contacts with dolostone interbeds.

Many of the Rose Run samples have a bimodal grain size distribution, suggesting grain transport from several different source areas (see Figure 3-26C). Most grain contacts are concave-convex or long with very few point contacts indicating burial compaction. The progressive improvement in rounding and sorting of the grains from zone 3B upward to zone 2 indicates some reworking of previous sand deposits. The high compositional maturity of the sandstones reflect their origin from crystalline Precambrian shield complexes and uplifted platform rocks and moderate reworking after deposition (Miall 1984).

Most primary intergranular porosity has been partially to completely occluded by quartz and dolomite cementation (see Figure 3-27A). Silica cement is the dominant cement in the sandstones (5%–20% of the rock). Brownish dust rims define some of the quartz overgrowth contacts with the detrital quartz grains. Quartz overgrowths restrict pore throat openings between larger pores and completely fill smaller pores. Dolomite and calcite comprise a major proportion (up to 30%) of the cement where silica cement is minimal. Other cements that are present in minor amounts include feldspar overgrowths and ankerite. Minor amounts of microporous authigenic illite is present in the Rose Run coating framework grains and lining and bridging pore spaces inhibiting the precipitation of quartz overgrowths (Cramer and Thomas 1994). Repression of the resistivity measurements can occur in those intervals where illite accounts for more than 10% of rock volume..

Primary intergranular porosity is the major porosity type present (see Figure 3-27B). Most of the intergranular pores between the framework grains are small and poorly interconnected. Porosity enhancement is due to secondary intergranular and moldic pores created from partial and complete dissolution of chemically unstable feldspar grains and rock fragments. In many samples, well-connected intergranular porosity distribution is restricted to distinct laminations. Microporosity is typically associated with authigenic clays or dissolution of unstable grains. Fracture porosity was rarely observed in the samples analyzed. Mechanical deformation due to compaction is evident in some samples, with fractured grains and stylolites being formed.

The reservoir quality of the sandstones varies from good to poor. The reservoir quality is predominantly controlled by the amount of silica cement, the amount of secondary carbonate cement, and the extent of secondary dissolution porosity. The thicker sandstone intervals in zones 3A and 3B have much better developed effective intergranular porosity and higher permeability. Thinner intervals tend to have higher amounts of silica and carbonate cement and less secondary dissolution, accounting for the reduced porosity and permeability. The interbedded dolomites may act as permeability barriers or baffles preventing effective communication between the sandstone flow units. This is most likely the case between zones 2 and 3A, less likely between zones 3A and 3B. Vuggy porosity in the dolomites is due to leaching of unstable grains by diffuse flow of meteoric water. Different stands in the water table could result in distinct vertical zonation of vuggy porosity that can be correlated on logs. Areas of faulting and fracturing may create localized fracture porosity, allowing cross communication between each of the sandstone flow units.

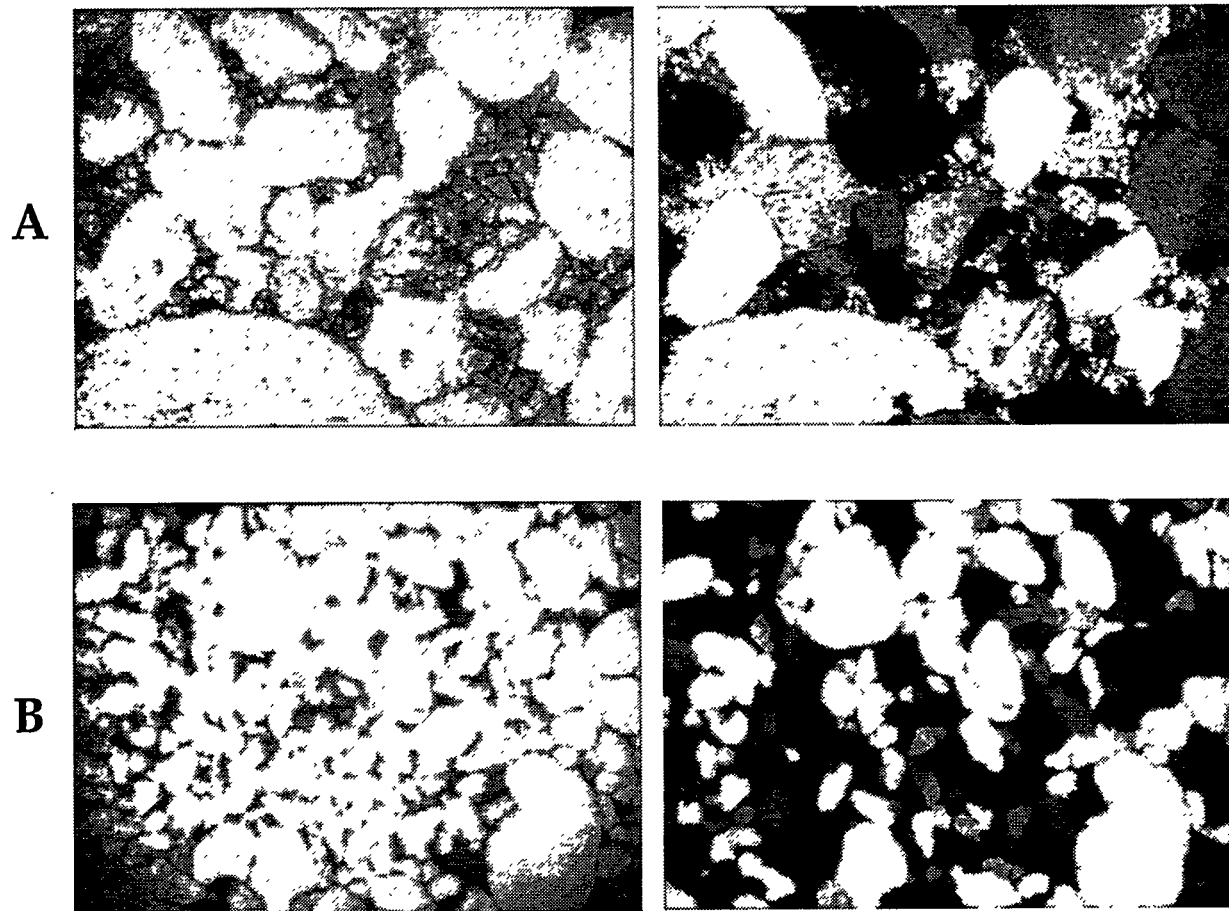


Figure 3-27 Photomicrographs in Plain (Left) and Polarized (Right) Light of Rose Run Zone 3B Taken from the McGuire No. 2 Core Showing Types of Cement and Porosity Distribution

3.2.4 Depositional Environment Interpretation

Upper Cambrian rocks in the Appalachian basin represent deposition on or adjacent to a broad, rimmed shelf of low relief. The Rose Run sandstone would represent Class 4, strandplain/barrier island reservoirs, in the DOE geological classification (Cole et al 1994). The Rose Run sandstones were deposited as lowstand deposits during third-order sea level falls and reworked during subsequent highstands of sea level (Read 1989). On the basis of grain size, lithology, and sedimentary structures, the sandstones are interpreted to have been deposited in a shallow subtidal to intertidal marine environment. Individual sandstone beds were deposited parallel to the active paleoshoreline as imbricate sheet sands. The repeated fining-upward cycles suggest deposition by waning storm-generated currents that was later reworked by current activity (Goldring and Bridges 1973; Johnson 1978). The segregation of grain size into different laminations is indicative of alternating sediment bedload and suspension deposition. The low-angle, often bi-directional, lenticular to trough cross laminations, indicates tidal-current bedload

transport with reversals of current flow direction (Klein 1970). The intercalated shaley flaser bedding results from the alternation of tidal-current bedload deposition with suspension settlement of mud laminae in the ripple troughs during slack water periods (Reinech and Wunderlich 1968). Escape burrows, soft sediment deformation, and disturbed laminations as a result of bioturbation are common within the intertidal zone (Shinn 1983; Wilson 1983).

The parallel-laminated, microcrystalline dolomites were deposited as shoaling-upward carbonate deposits across a broad carbonate shelf during sea level fluctuations. Ooids and peloids form in agitated marine waters within carbonate sand shoals in the subtidal to intertidal environment (Hine 1977). Burrowing organisms indicate normal saline open-marine water conditions. The sharp upper contacts of the dolomites and the repeated fining-upward cycles of sandstone suggest eustatic sea level changes and fluctuating terrigenous sediment supply.

3.2.5 Production Mapping Interpretation

Potential source rocks for pre-Knox unconformity hydrocarbons are not well constrained. Most oil production from the Knox Supergroup is distinguished by high gravity (41–55° API gravity). Cole et al. (1987) suggest that the oil and gas were generated from mature to overmature Ordovician Point Pleasant shales. These marine shales are dominantly oil-prone, with maturation levels that span the immature to peak oil-generation range. Total organic content values and production indices calculated from several Lower to Upper Cambrian formations in the Rome trough were found to have low to marginal source potential for gas generation (Ryder et al. 1992). Richer Cambrian source rocks may occur elsewhere in the Rome trough and may have reached higher thermal maturity. The hydrocarbons generated would have had to migrate from deep within the Appalachian basin. Migration into shallower reservoirs could have followed faults, fracture zones, unconformities, and other permeability pathways.

Since its discovery in 1992, East Randolph field has produced more than 450,000 bbl of oil and 1.5 bcf of gas from the Rose Run sandstone from 32 active wells. Historical trends of oil, gas, and water production provide important information about reservoir response to management strategies and provide information about reservoir compartmentalization. When reservoir compartment and sandstone heterogeneity data are incorporated, production information documents undrained or incompletely drained areas of the reservoir that can be targeted for infill drilling or secondary recovery processes.

Cumulative production maps are often biased due to the range in production times for the wells from only a few months to several years. Therefore production, gas-oil ratio, and water-oil ratio maps for East Randolph field were made for each well's first 6, 9, and 12 months of production to normalize the data and to account for the range in well completion dates and production data.

The highest oil production rates and cumulative oil production volumes per period correlate with the thickest Rose Run sandstones in the central part of the field (see Fig. 3–28). The thickest sandstones have the highest porosity and permeability and usually lower water saturations. Wells in the southern and eastern portion of the field have lower cumulative oil production per

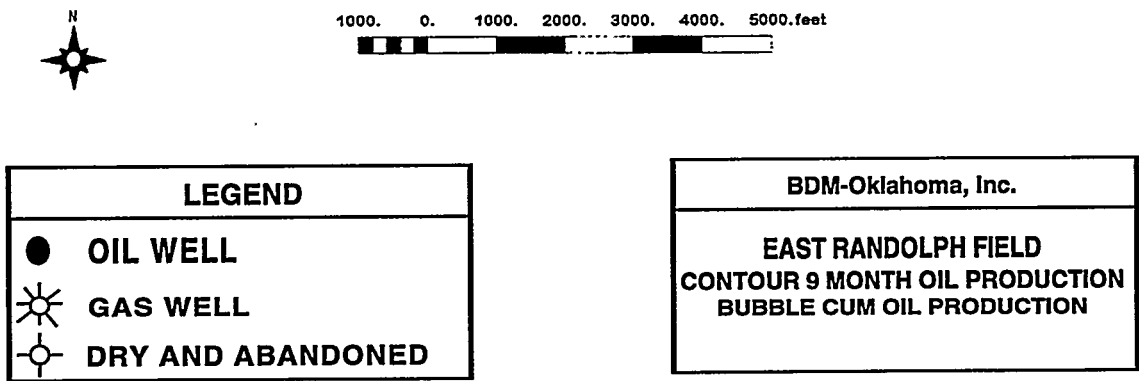
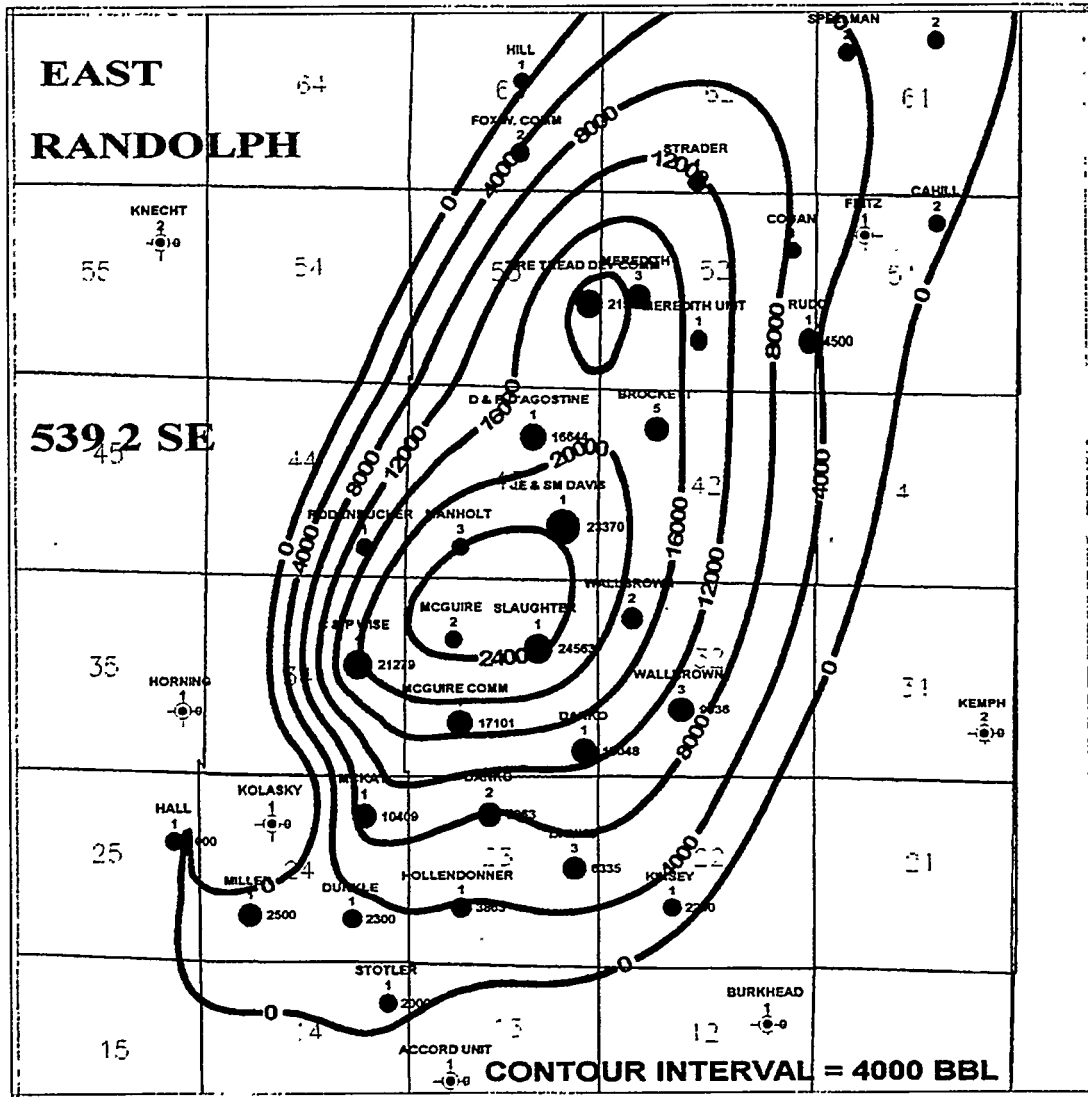


Figure 3-28 Contoured and Bubbled 9-Month Oil Production

period due to lower porosity, higher water saturation in zone 3B, and possibly completion differences. Several downdip wells along the eastern margin of the field have not been completed in zone 3B due to the high water saturation. The presence of the faults appears to have only limited, localized influence on the rate of production and on cumulative fluid recoveries.

Gas production volumes correlate best with net sandstone thickness and reservoir quality of zone 2 (see Fig. 3-29). High initial gas-oil ratios (GORs), calculated from first month production volumes, suggest an initial gas cap may have been present where zone 2 is best developed in the updip portion of the field. Producing GORs range from 1,713 standard cubic feet/barrel of oil (scf/bbl) to 4,288 scf/bbl (see Fig. 3-30).

The highest GORs lie along a northeast trend along the western margin of the field. The high GOR value in the Rudd No. 1 well in the northeastern portion of the field is an anomaly. It was the discovery well for the field and had high initial gas production with no offset producers for its first two years of production. High gas saturation in zone 2 has been recently observed when drilling through the zone and from log analyses. The high initial gas production rates of recent extension wells in the northern part of the field suggest they are producing from separate reservoir compartments under different reservoir conditions due to faulting or permeability barriers. No pressure data is available to confirm this interpretation at present.

Maps of producing water-oil ratios (WORs) were constructed to determine the distribution of water production and interpret its relationship to structure (see Fig. 3-31). Water production is not caused by a natural water drive in the reservoir, but is the result of water saturation in excess of irreducible water saturation for that zone. WORs vary from 0.03 to 2.7. The field average WOR is approximately 0.67. The highest WORs lie in the south-southeast, downdip portion of the field. High values are also associated with the northwest-trending faults in the southern portion of the field. Wells adjacent to the faults have producing WOR ranging from 0.58 to 2.70. Fracturing associated with the faulting may cause higher water production in wells where zone 3B has good reservoir quality. Although water production does not preclude waterflooding, a high WOR indicates that injection of additional water would have little or no beneficial effect.

On the basis of cumulative and daily production rates, gas-oil ratios, and water-oil ratios, there is limited evidence to suggest that the faults act as permeability barriers to fluid migration. In fact, the high water-oil ratios suggest that fracturing associated with the faults may aid in vertical and lateral fluid migration. The lack of fracturing observed in the McGuire No. 2 core or on the FMI log suggests fracturing may contribute only locally to production.

Estimated ultimate recoveries were calculated for every well in the field using decline curve analyses. The net sandstone thickness of zones 3A and 3B correlates well with the estimated ultimate oil recovery (see Fig. 3-32). The highest estimated ultimate oil recovery correspond to the thickest net sands in the central part of the field. Estimated ultimate recovery of gas corresponds best with the net sandstone thickness and reservoir quality of zone 2 (see Fig. 3-33). As the reservoir pressure continues to decline, additional gas will begin to come out of solution in zones 3A and 3B. It is important to stabilize reservoir pressure to be able to recover remaining reserves from these zones.

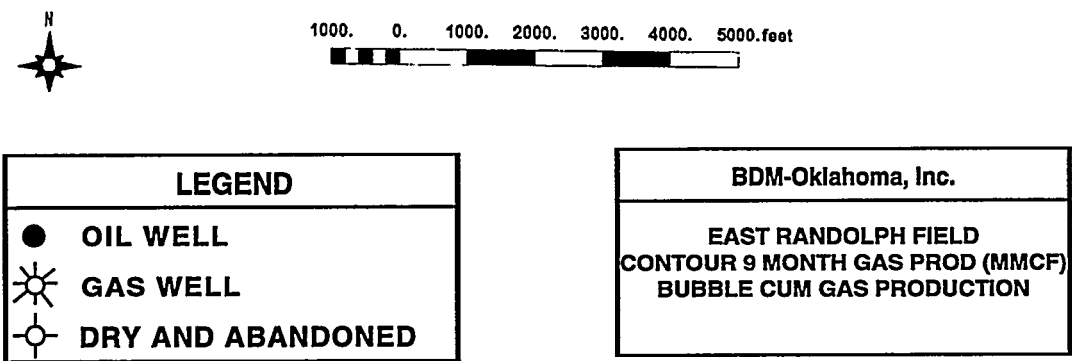
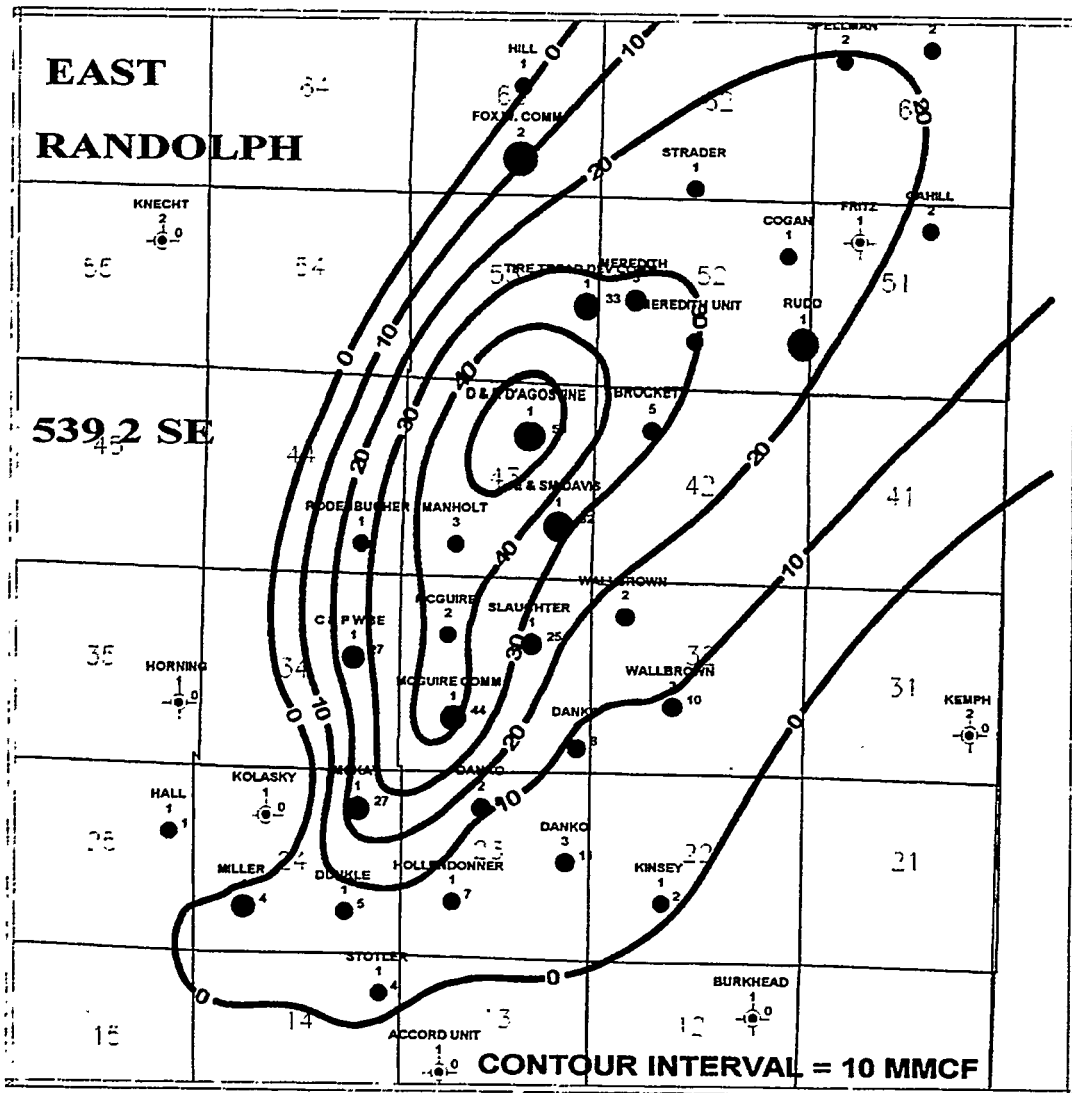


Figure 3-29 Contoured and Bubbled 9-Month Gas Production

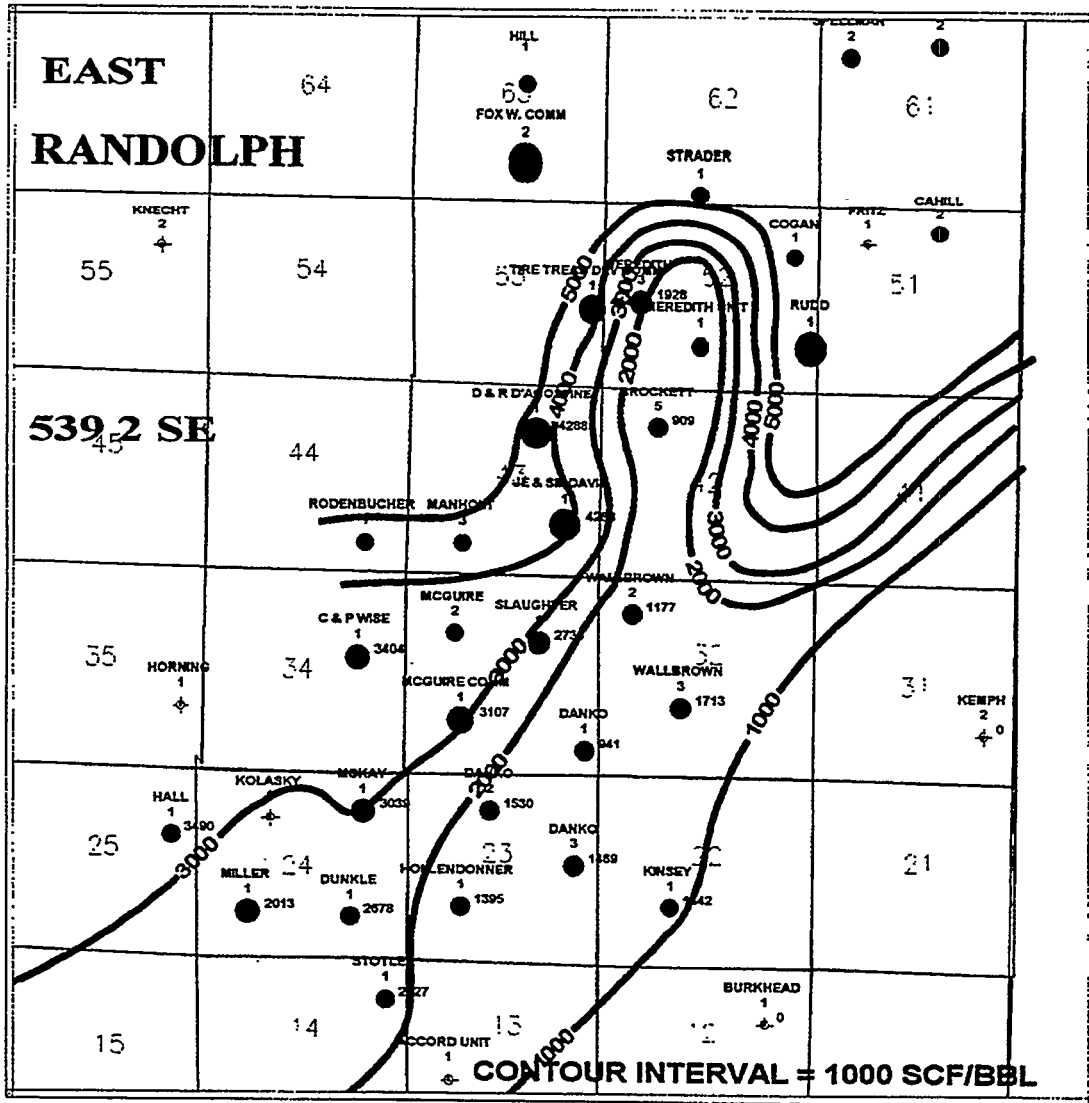
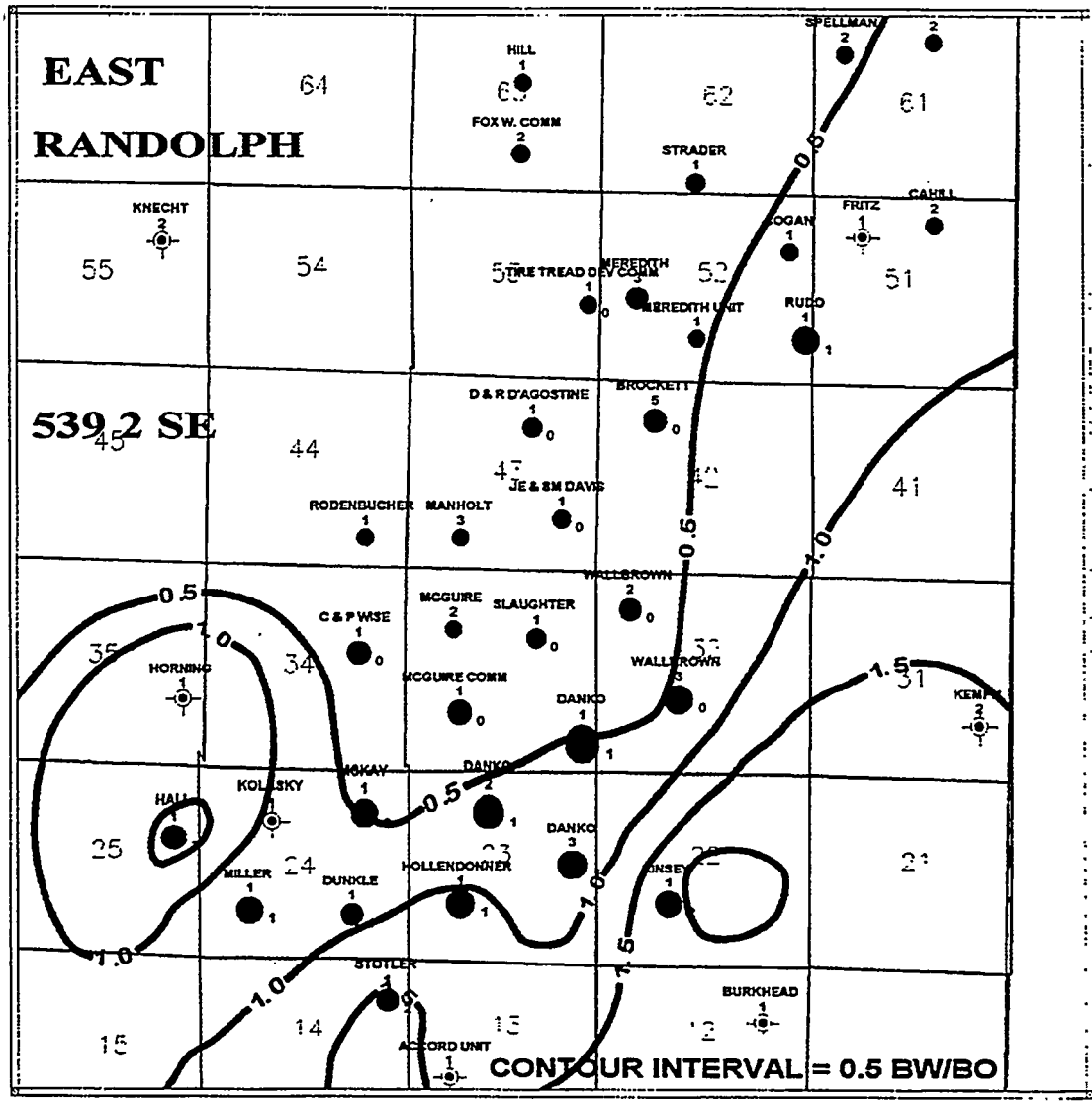


Figure 3-30 Contoured Average Producing GOR With Bubbled Cumulative Gas Production



<p>LEGEND</p> <ul style="list-style-type: none"> ● OIL WELL ☀ GAS WELL ⊖ DRY AND ABANDONED 	<p>BDM-Oklahoma, Inc.</p> <p>EAST RANDOLPH FIELD CONTOUR PRODUCING WATER/OIL RATIO BUBBLE CUM WATER PRODUCTION</p>
--	--

Figure 3-31 Producing WOR Map for the Rose Run

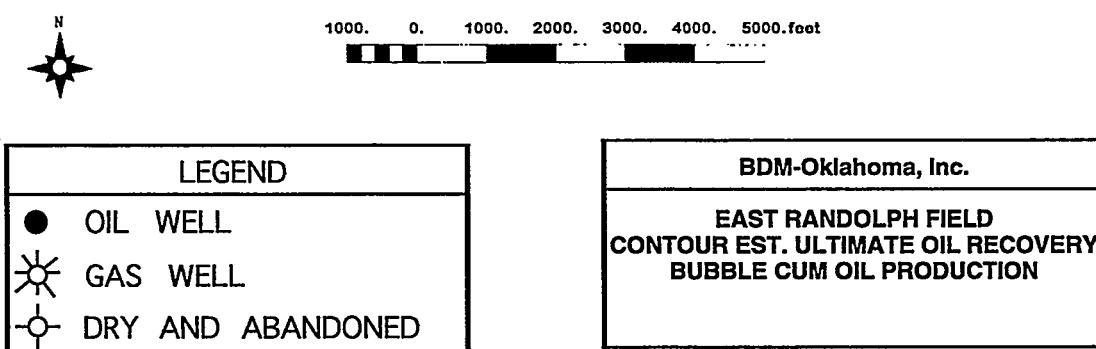
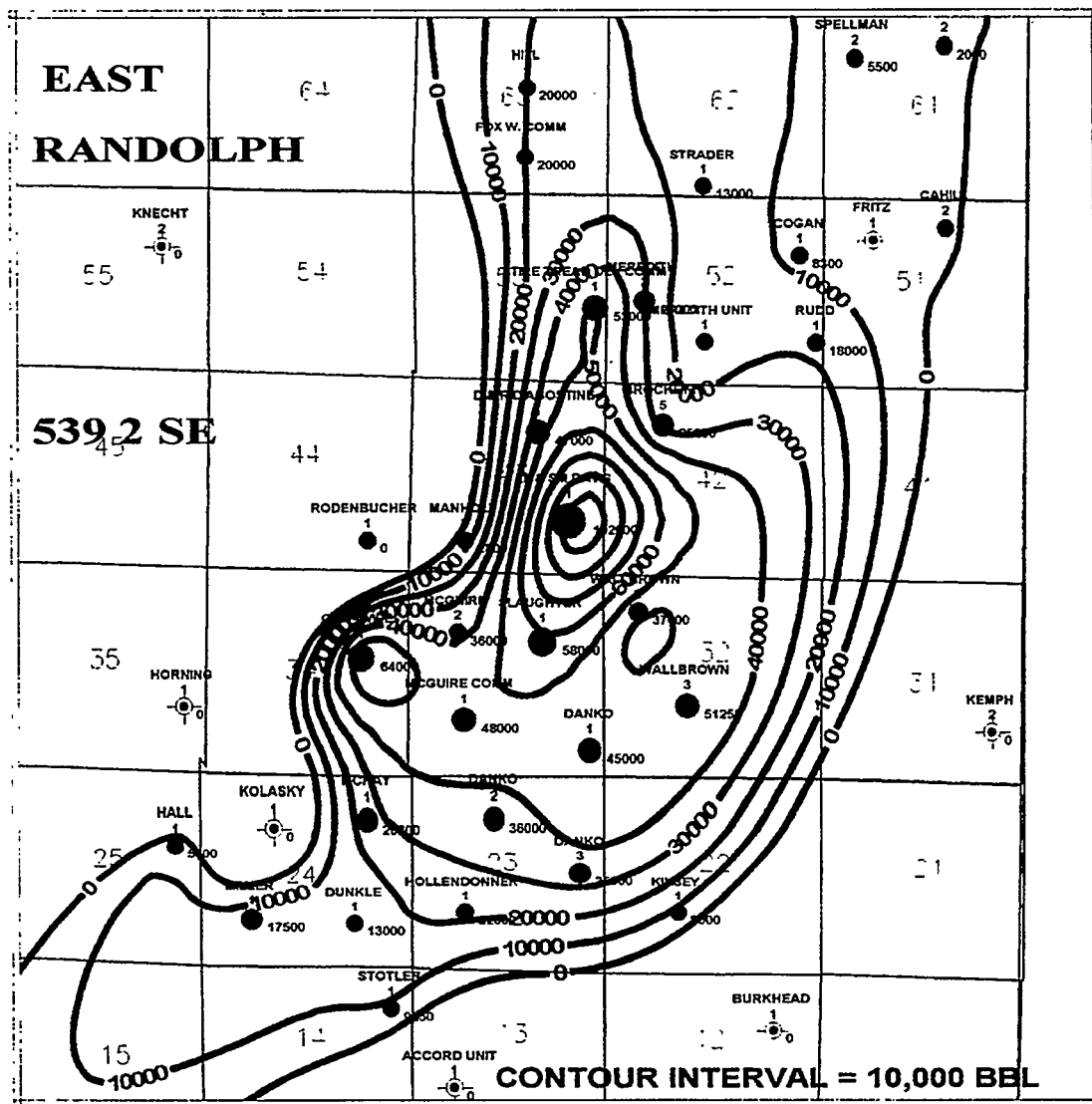
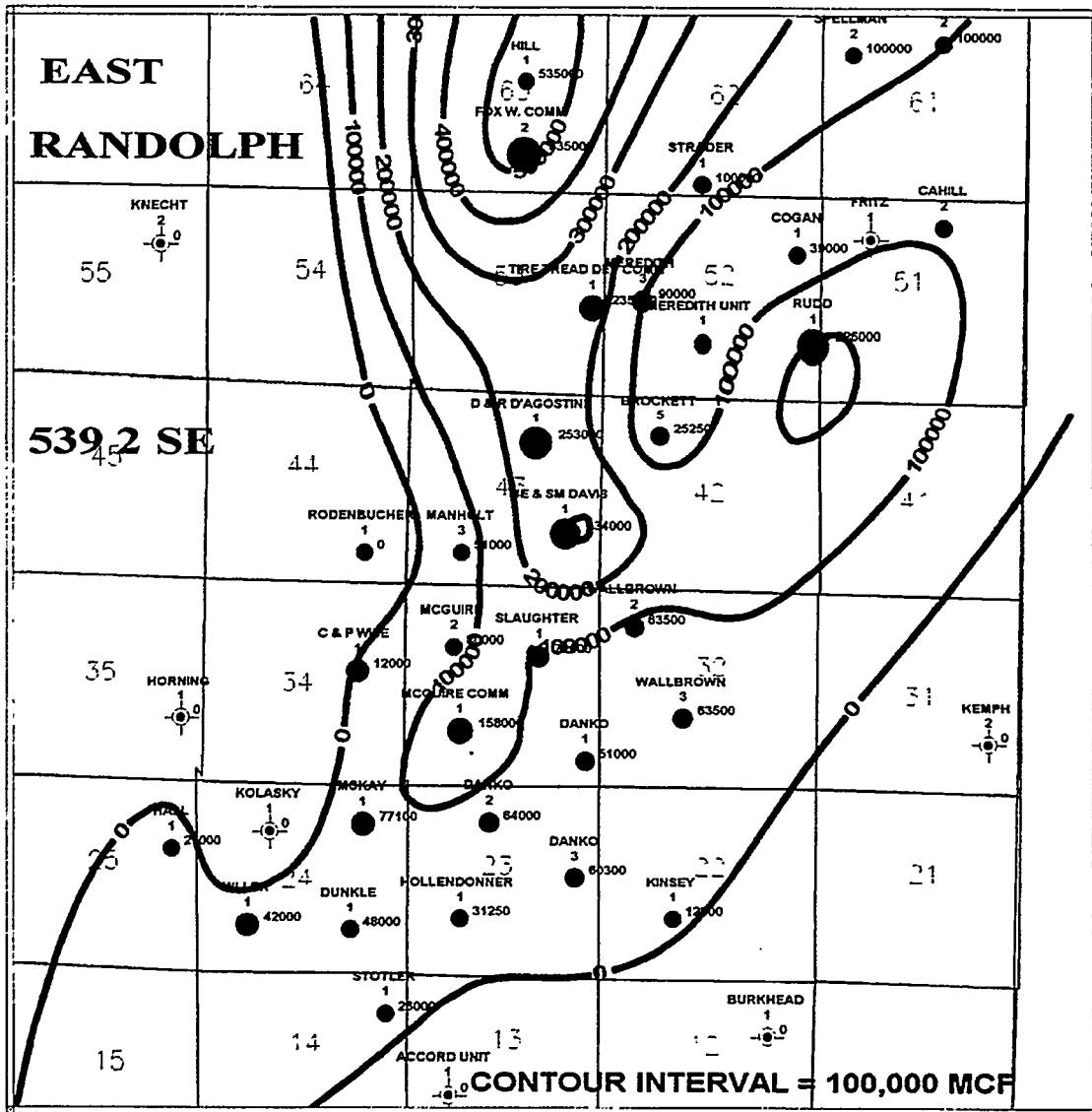


Figure 3-32 Contoured Estimated Ultimate Recovery of Oil from East Randolph Field



LEGEND

- OIL WELL
- ☀ GAS WELL
- ⊖ DRY AND ABANDONED

BDM-Oklahoma, Inc.

EAST RANDOLPH FIELD
CONTOUR EST. ULTIMATE GAS RECOVERY
BUBBLE CUM GAS PRODUCTION

Figure 3-33 Contoured Estimated Ultimate Recovery of Gas from East Randolph Field

3.3 Reservoir Engineering Analysis

3.3.1 Preliminary Data Analysis

Available reservoir and production data were gathered and analyzed to describe the field in terms of pressures, production rates, stimulation effectiveness, and reservoir quality. A single-well reservoir model (the D'Agostine well) was developed to run on BOAST3-PC to assess whether reasonable reservoir parameters could be estimated from the minimal field data. BOAST3-PC, a modified version of BOAST II, is a three-phase 3D black oil simulator developed by Louisiana State University under contract from the U.S. Department of Energy (Mathematical and Computer Services, Inc. 1993).

The composition and properties of reservoir fluids are essential for reservoir characterization. Incomplete fluid characterization can result in formation damage, plugging of perforations, scaling and corrosion of casing and pump rods, channeling of injected fluids, and treatment slug degradation. PVT measurements include solution-gas ratio, viscosity, formation volume factor, and fluid density at various pressures. Several empirical correlations (Beal 1946) have also been developed to estimate PVT values of the oil system based on the oil gravity.

Initial reservoir parameters were analyzed to estimate PVT data based on various published PVT correlations (Beal 1946). The relative permeability and capillary pressure performance for the field were not available, and therefore were predicted using existing data from analogous Marlboro (located a few miles to the south) and West Randolph fields. Well stimulation data for the Belden & Blake wells were evaluated, and fracture gradients for the wells were computed. The resulting single-well model was found to be unstable due to the high initial GOR. This well has the highest GOR in the field, which can be attributed to either initial conditions below the bubble point with an initial gas cap or conditions above the bubble point with the top zone being gas and the other two oil-saturated.

To better define the PVT parameters, a commercially available PVT correlation model was used to predict PVT data based on initial reservoir fluid conditions. It was determined that additional reservoir data were needed to project the reservoir fluids behavior using this model. The PVT correlations in the literature were revisited, and several model data sets were developed, but it was concluded that actual field PVT data were required in order to reasonably simulate the field performance. In addition, it was determined that the pressure data, relative permeability data, and material balance calculations for the field were needed to accurately simulate field performance. Since the field was still in the development stage, it became important to re-examine the material balance calculations and volumetric analyses in order to estimate and update the OOIP value for the field. Table 3-3 lists the initial reservoir data estimated from available log interpretations, collected pressure data, and fluid samples.

Table 3-3 East Randolph Field Reservoir Properties

Depth, ft	7,200	Gross Interval, ft	50
Porosity, %	5-10	Net Pay Thickness, ft	15
Water Saturation, %	30	Oil Gravity, °API	42
Permeability, md	0.5-2.0	Initial Reservoir Pressure, psia	3,100

3.3.2 Pressure Buildup Analysis

The lack of available reservoir engineering data for material balance calculations and simulation study created the need to measure the reservoir pressure at different times during the life of the field and estimate reservoir properties. Well tests sample a much larger volume than do core sampling and well logs, which only measure near-wellbore properties. The pressure measurements were also used to determine individual well drainage areas and interwell connectivity.

A 14-day pressure buildup test was conducted on the McGuire No. 1 well located south of the new core well (McGuire No. 2). Data collected from the test were analyzed separately by BDM-Oklahoma and Belden & Blake. BDM-Oklahoma implemented the Pressure Transient Analysis module of GeoGraphix for analyzing the pressure data. The Horner technique and automatic type curve matching (ATCM) were used for analyzing the pressure buildup data to predict the effective reservoir permeability and formation damage and to estimate the reservoir pressure. Figures 3-34 and 3-35 show Horner plot and automatic type curve matching of pressure and pressure-derivative data, respectively. In addition, the results from applying both techniques are summarized in Table 3-4. The negative skin indicates the existence of induced fractures and that pre-fracture permeability was 0.7 md compared with post-fracture permeability of 1.35 md. The three values for permeability, independently determined, indicate a high confidence in the use of the value for effective permeability.

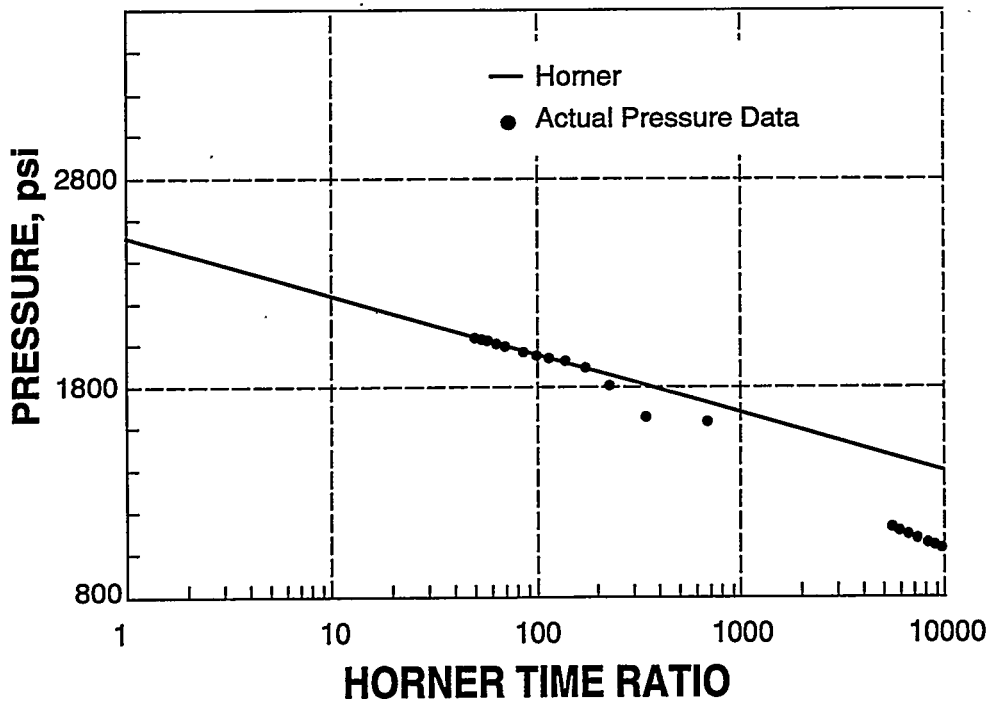


Figure 3-34 Pressure Buildup Analysis Using a Horner Plot for the McGuire No. 1 Well

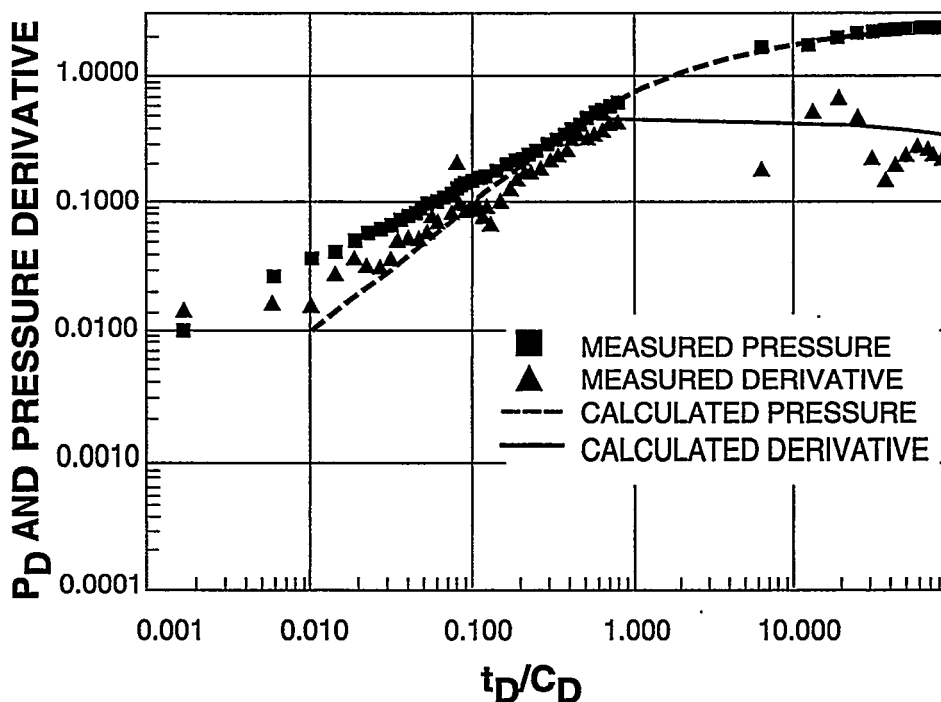


Figure 3-35 Pressure Buildup Analysis Using ATCM for the McGuire No. 1 Well

Table 3-4 Results of Pressure Buildup Data Analysis for the McGuire No. 1 Well

	Horner	ATCM	Belden & Blake
Effective Permeability, md	1.35	1.33	1.37
Skin Factor	-2.09	NA	-2.64
Initial Pressure, psia	2,513*	3,160	2,500*

*False pressure (i.e., pressure extrapolated at Horner time = 1).

3.3.3 PVT Data Analysis

The lack of pressure data and the need to understand the fluid behavior in terms of fluid properties, bubble point pressure, and solution GOR, dictated the need to run PVT analyses on fluid samples from East Randolph field. A surface-recombined fluid sample from McGuire No. 1 was collected by Belden & Blake and shipped to Core Laboratories for analysis.

Core Laboratories performed the following set of analyses:

- Separator gas composition analysis
- Adjusted reservoir fluid composition

- Pressure-volume relations
- Viscosity of reservoir fluid
- Separator flash analysis

At the time when the sample was collected, the average reservoir pressure was estimated at 2,065 psig with the average reservoir temperature reported at 130°F. Table 3–5 summarizes the findings of Core Laboratories after performing PVT analyses of the surface recombined sample.

Table 3–5 Summary of PVT Data Analysis

Average Reservoir Pressure	2,065 psig
Average Reservoir Temperature	130°F
Saturation Pressure	2,075 psig
Average Compressibility	8.74×10^{-6} volume/volume/psi
Reservoir Fluid Viscosity	0.738 cp
Formation Volume Factor	1.221 reservoir bbl/stb
Total Solution GOR	485 scf/stb
Tank Oil Gravity	42° API

3.3.4 Relative Permeability and Capillary Pressure Data Collection

Relative permeability is one of the most important input parameters for reservoir simulation and recovery prediction. Relative permeability data is used in reservoir simulators to predict fluid movement associated with production and injection of fluids. In addition to planning production operations, the data can be used to diagnose formation damage expected under various operational conditions.

Relative permeability is the ratio of the effective permeability of a fluid to the absolute permeability of the rock at a given saturation. Two-phase relative permeability measurements measure the difference in movement of reservoir fluid (such as water and oil) through the rock. Measurements that are obtained are often inaccurately manipulated to obtain good history matching of production data. Reliable relative permeability data are difficult to obtain because they require the native wettability of the core to be maintained, and the saturation history of the recovery process to be simulated.

Capillary pressure is the difference in pressure across the interface between wetting fluids (e.g., oil) and nonwetting fluids (e.g., water). The capillary pressure reflects the pore size distribution and affects the two-phase flow in the rock.

Due to the lack of relative permeability and capillary pressure data from East Randolph field when the project began, the reservoir management project team reviewed available data from analogous reservoirs. The purpose was to generate a set of relative permeability and capillary

pressure data to best describe the fluid behavior for wells producing from East Randolph field. This process is most effective if the flow characteristics, or reservoir quality indices, are about equal (Amaefule et al. 1993). Available gas-water relative permeability data from the Ward No. 1 well in the West Randolph gas field were evaluated and used as a starting point to describe the gas-water relative permeability relationship for zone 2, which is believed to be primarily a gas zone.

In order to describe the oil-water relative permeability relationship for Rose Run zones 3A and 3B, relative permeability and capillary pressure data from Marlboro field, producing from the Clinton reservoir, were evaluated. The Lower Silurian Clinton sand unit, a deltaic sequence of interbedded sandstones, siltstones, and shales, has a range of porosity and permeability similar to that of the Rose Run. In addition, the project team solicited the help of BDM-Oklahoma's Reservoir Characterization Group to evaluate oil and gas relative permeability data for similar millidarcy-range permeable rocks.

The relative permeability and capillary pressure data generated from analogous reservoirs were used as a first approximation in the simulation process of the East Randolph production data. It is worthy to note that the accuracy of the simulation process is dependent on collecting actual relative permeability and capillary pressure data from East Randolph field. From this perspective, core plugs from the McGuire No. 2 infill well were used to experimentally generate the relative permeability and capillary pressure data for the Rose Run reservoir. Results of the special core analyses, including relative permeability and capillary pressure data collection, are reported in Appendix A.

The most reliable relative permeability data are obtained by steady-state methods in which two fluids are injected simultaneously at constant rates or pressures for extended duration until they reach equilibrium (Honarpour and Mahmood 1988). The steady-state methods are more time consuming than unsteady-state techniques because equilibrium attainment may require several hours or days at each saturation level. In addition, these methods require independent measurement of fluid saturation in the core. Their advantages are greater reliability in calculations and the ability to determine relative permeability for a wider range of saturation levels.

Steady-state imbibition and second-drainage oil-water relative permeability measurements were performed at 72°F on a sample from zone 3A. Fluid saturations were monitored using a linear X-ray scanner. Imbibition cycle oil and brine relative permeabilities were measured at six brine fractional flows ranging from 0.05 to 0.975. A brine permeability of 0.037 md was measured at residual oil saturation of 0.45. Second-drainage cycle oil and brine relative permeabilities were measured at six brine fractional flows ranging from 0.975 to 0.05. A permeability to oil of 0.314 md was measured after the second-drainage at residual brine saturation of 0.294. Steady-state imbibition oil-brine relative permeability results, shown in Figure 3-36, illustrate the low oil-water relative permeability, a serious deterrant for achieving waterflood sweep efficiency.

Oil-brine centrifuge tests were performed on samples from zones 3A and 3B. Methods presented by Hassler and Brunner (1945) and Rajan (1986) were used to interpret capillary pressures from

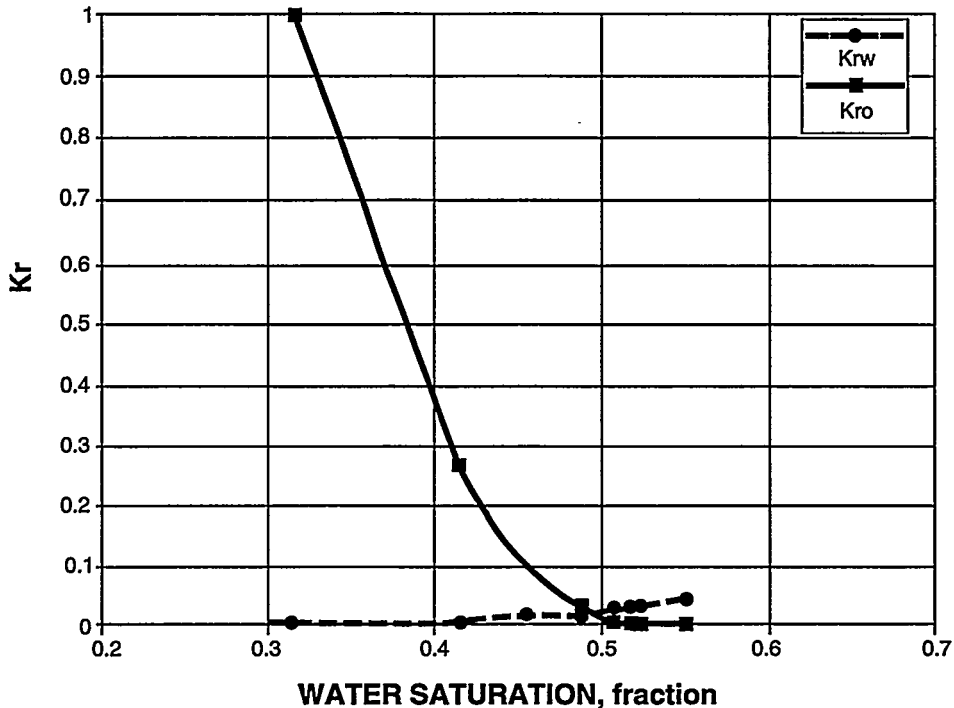


Figure 3-36 Relative Permeability for Oil-brine System, McGuire No. 2 Zone 3A at 7328.3 ft

the centrifuge data. Fluids used during the centrifuge tests were the same as those used in the oil-brine relative permeability tests. The brine-saturated plugs were first centrifuged in oil to yield primary drainage capillary pressure vs. saturation data. The plugs were then centrifuged in brine to obtain first imbibition cycle capillary pressure and saturation data, and finally centrifuged again in oil to yield second-drainage cycle capillary pressure and saturation data. The shape of the capillary pressure curve is considered to be indicative of the rock wettability. Wettability indices were close to 1, indicating that the plugs were preferentially water wet. Oil-water capillary pressure results are shown in Figure 3-37.

In addition, a waterflood susceptibility test was conducted on several plugs from the McGuire No. 2 well (see Fig. 3-38). The plugs were flooded with laboratory oil at a rate of 150 ml/hr to achieve residual brine saturation condition. The residual brine saturation (expressed as a function of pore volume) ranged from 31.5% to 44.9%. Prior to waterflooding the sample, the oil injection rate was reduced to 3 ml/hr. The waterflood was started by switching from oil to brine at 3 ml/hr, yielding an injection rate of 0.53 PV/hr or a linear displacement of 2 ft/day. Residual oil saturations achieved during these tests ranged from 25% to 45%, yielding oil recovery rates from 30% to 58% of OOIP. This suggests that recoveries of 30% to 58% of OOIP could be achieved at high pore volumes of water injected. Injected pore volumes greater than 4 achieved little additional recovery. However the low oil-water relative permeabilities may prohibit injection of the required pore volumes of water.

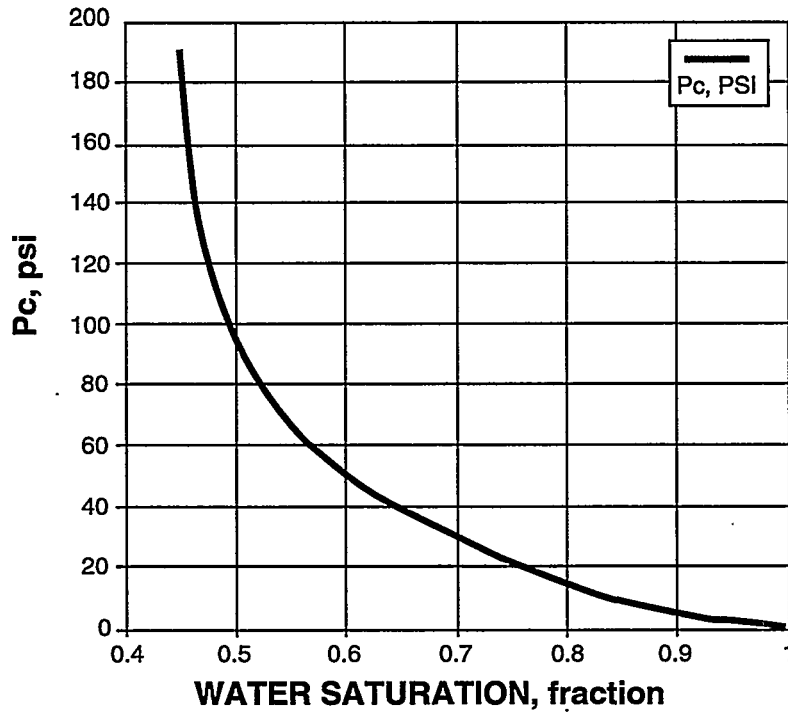


Figure 3-37 Centrifuge Oil-Brine Capillary Pressure, McGuire No. 2 Zone 3A at 7332.2 ft

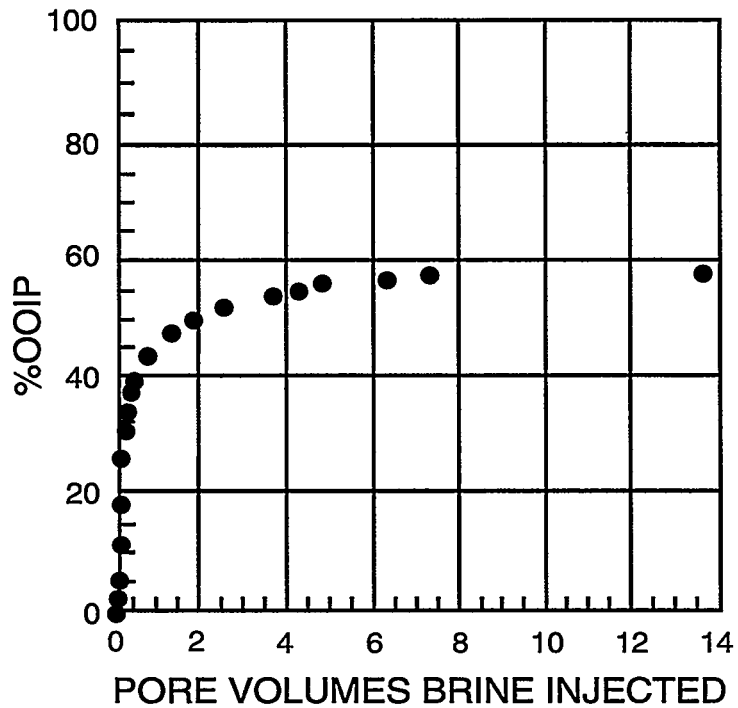


Figure 3-38 Waterflood Susceptibility Test, McGuire No. 2 Coreflood

3.3.5 Volumetrics and Material Balance Calculations

Net sand thickness isopach maps generated with commercially available software, were used to compute OOIP. Porosity and water saturation maps generated from log analysis for the three zones across the field were also used in the process. The values generated were compared with the 4.4 million stb of original oil-in-place originally calculated for the field. Volumetric calculations were performed for each zone to determine each zone's contribution to the total OOIP. Table 3-6 summarizes the results of the volumetric calculations by zone.

Table 3-6 Volumetric OOIP Analysis by Reservoir Zone for East Randolph Field

Zone	Avg. Net Pay, ft	Acreage, ac	Volume bbl/ac-ft	Volume, bbl oil
Rose Run 2	4	2,698	47.4	512,000
Rose Run 3A	6	3,477	240.6	5,020,000
Rose Run 3B	7	3,339	248.1	5,800,000
Total				11,332,000

Zone 2 has a lower OOIP than zones 3A and 3B because zone 2 is thinner, has lower porosity, and is believed to be primarily a gas zone. This assumption was based on log analysis, production data analysis, and material balance calculations.

Material balance calculations using Dwight's OilWat/GasWat material balance software package, were performed using the available production and reservoir pressure data. In addition, PVT data from the McGuire No. 1 well were used as input for the material balance computation.

In the first step, the software predicted OOIP based on available reservoir pressure and cumulative production. In order to predict OOIP, the software required assigning a fractional value representative of the initial gas/oil volume in the reservoir. A sensitivity test using different initial gas/oil volume values was performed, generating a wide range of OOIP values. For example, for an initial gas/oil volume of zero (fraction), the calculated OOIP was 81.6 million stb for East Randolph field. For an initial gas/oil volume of 0.12 (fraction), the OOIP was calculated at 17 million stb, and for an initial gas/oil volume of 0.20, the OOIP was calculated at 11.2 million stb, which correlates with the OOIP value based on volumetrics.

The next step was to implement the pressure match option where both the OOIP and gas/oil volume were known. The software has the capabilities of predicting PVT data based on correlations and initial values. The PVT option was used; the generated values were compared with the PVT data measured at Core Laboratories and were found to be in agreement. Two cases were simulated, the first case with OOIP at 12 million stb and gas/oil volume of 0.17, and the second case with an OOIP of 11.5 million stb and gas/oil volume of 0.15. Results of the pressure match in Figure 3-39 indicated that the gas/oil volume of 0.17 and OOIP of 12 million stb showed the better pressure match. Therefore, by performing the detailed log analyses and geologic mapping, and incorporating reservoir pressure and PVT data, OOIP estimates were increased from 4.4 million stb to 12 million stb. This oil-in-place estimate is the target for the improved recovery process.

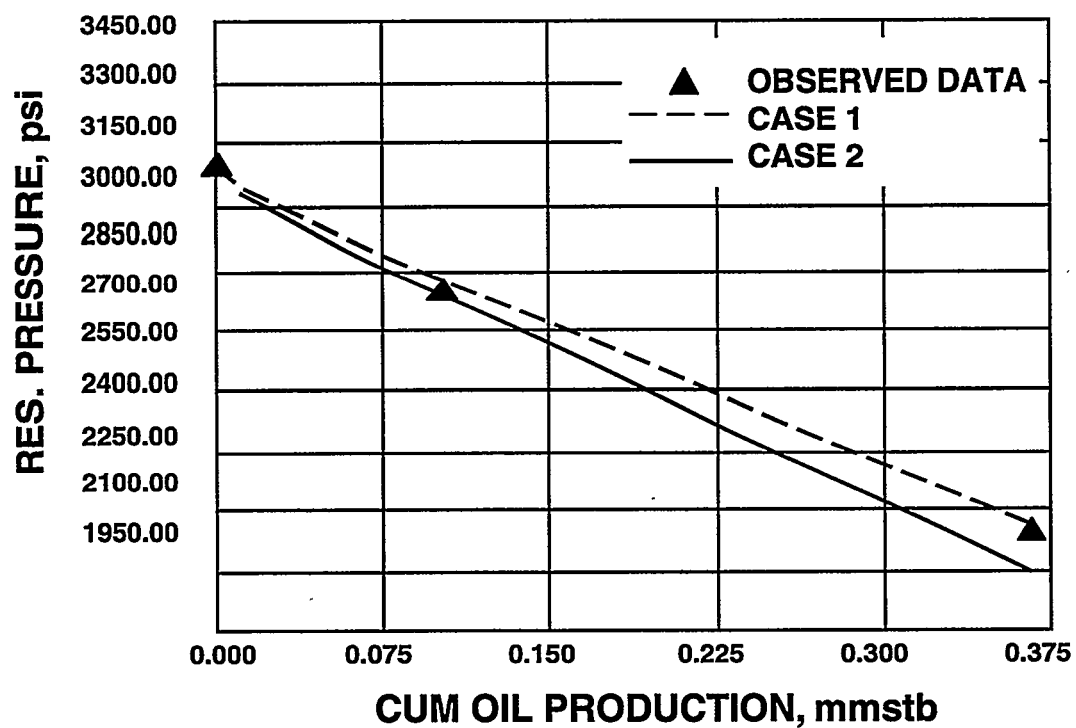


Figure 3-39 Material Balance Pressure Match for East Randolph Field

4.0 RESERVOIR SIMULATION

As previously mentioned, a single-well reservoir simulation study was performed on the D'Agostine No. 1 well in an attempt to match the production and pressure histories. Because of the high GOR in the D'Agostine No. 1 and the lack of PVT, pressure, and sufficient core data, the single-well simulation for the D'Agostine No. 1 was terminated because of the lack and inaccuracy of input data. In the meantime, the efforts of the project team concentrated on collecting additional pertinent data to assist in the simulation process and ultimately in the design of the waterflood or gas re-injection project.

Fluid samples were collected from the McGuire No. 1 and PVT analyses were performed, as mentioned earlier. In addition, a 14-day pressure buildup test was conducted on the McGuire No. 1, and pressure-time data were analyzed to determine the various reservoir parameters necessary for simulation.

The McGuire No. 1 well was selected due to data availability. As results of the pressure buildup test and PVT analyses became available, the project team initiated a single-well model simulation for the McGuire No. 1. Using a phased approach, the first step was to conduct the single-well simulation and predictive study on the McGuire No. 1. The second step was to conduct a sensitivity study on the various simulation parameters using the single-well model to determine if additional data were needed to improve the results of the simulation process. The third step was to perform a full-field simulation study and determine the technical and economic feasibility of implementing waterflooding and/or gas pressure maintenance as improved recovery processes.

4.1 Single-Well Model Simulation of the McGuire No. 1 Well

The first step in the process was to simulate the production and pressure history for the McGuire No. 1 well using BOAST3-PC, which is a 3-D, three-phase fluid-flow black oil model. When simulating the production for the McGuire No. 1, the following assumptions were made:

- The McGuire No. 1 well produces from a drainage area of 60 acso there is no interference from adjacent wells.
- On the basis of the developed geological model, a three-layer system was assumed with the top layer primarily a gas zone and the bottom two layers being oil-producing zones.
- The Core Laboratories PVT data from the McGuire No. 1 well would be used to describe the fluid behavior.
- Relative permeability data would be modified or generated based on available data from similar or nearby reservoirs.
- Implicit pressure calculations for a producing oil well would be made by specifying the well productivity index (PI) and bottomhole flowing pressure.

Results of the single-well history match of cumulative production for oil, gas, and water are in Figures 4-1, 4-2, and 4-3, respectively. History match results indicated that simulated production data are within 10% of the actual data.

In order to validate the presence of high gas saturation in zone 2, the single-well model was simulated with all three zones being oil-producing zones with no free gas. The only gas present in the system is solution gas. Simulation results of this case exhibited reasonably good oil and water history match, as shown in Figures 4-4 and 4-5. The gas match (see Fig. 4-6) was 60% less than the actual gas production. These results indicated that an initial gas saturation must be present in zone 2 in order to arrive at an acceptable match for gas production.

After arriving at a reasonable match of historical production data, the project team developed a base case simulation run to project the primary production for the McGuire No. 1 well to the economic limit and to compare the simulated base case recovery to decline curve projections. Decline curves generated by Belden & Blake for the McGuire No. 1 were used to determine the economic limit and ultimate recovery for the well (see Fig. 4-7).

In addition, the single-well simulation model was used to project the production rate for the McGuire No. 1 to the economic limit. Results of the base case oil and gas production rate simulation vs. the decline curve extrapolations are shown in Figures 4-8 and 4-9, respectively.

A quarter of a 5-spot pattern was simulated to predict the effect of water injection on the McGuire No. 1 by comparing the results to the base case prediction. Preliminary results of this study indicated an incremental recovery of 13,000 stb oil (see Figs. 4-10 and 4-11).

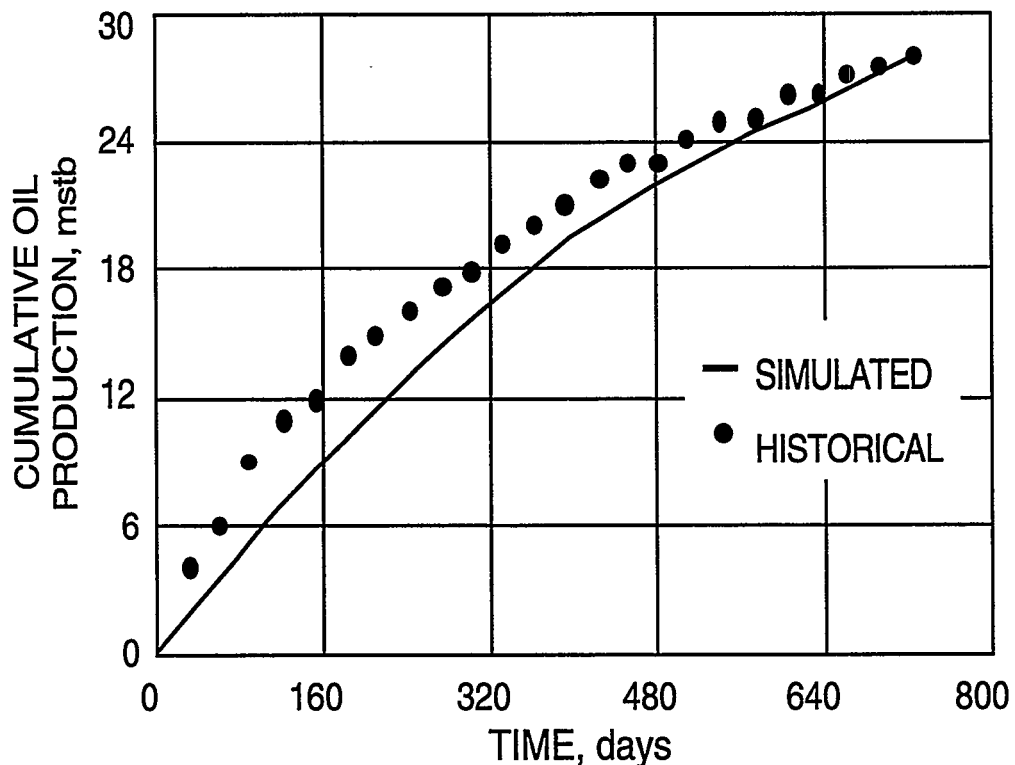


Figure 4-1 History Match of Cumulative Oil Production for the McGuire No. 1 Well

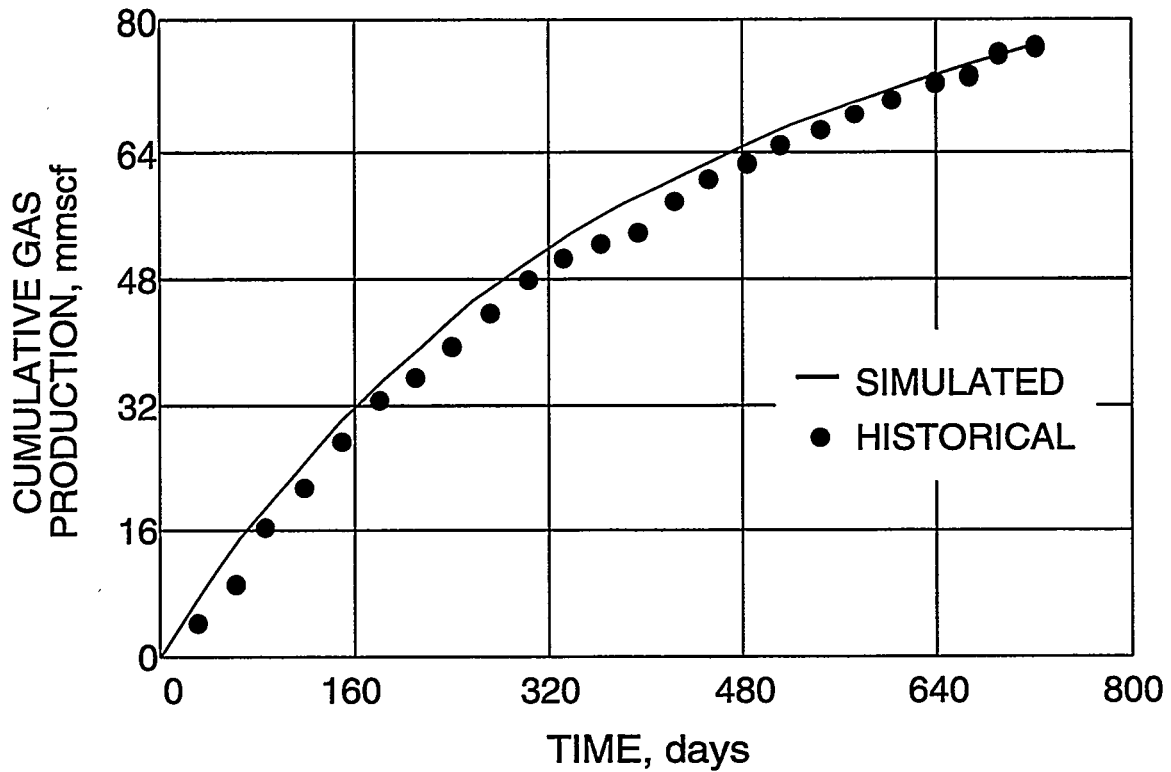


Figure 4-2 History Match of Cumulative Gas Production for the McGuire No. 1 Well

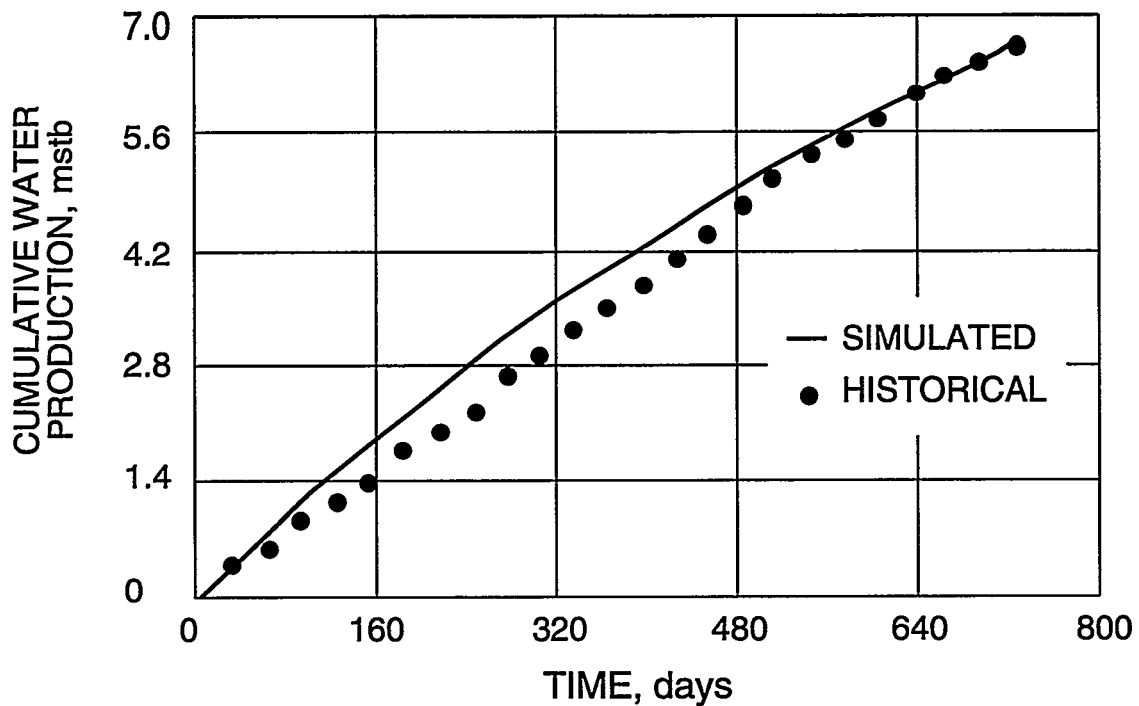


Figure 4-3 History Match of Cumulative Water Production for the McGuire No. 1 Well

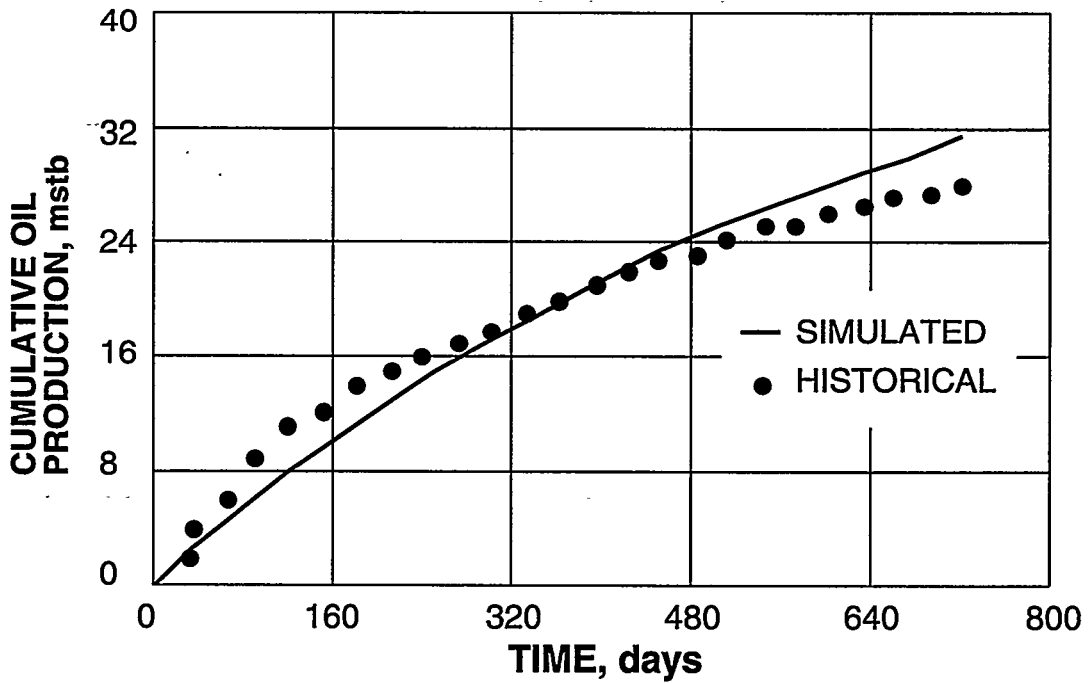


Figure 4-4 History Match of Cumulative Oil Production for the McGuire No. 1 Well (No Free Gas)

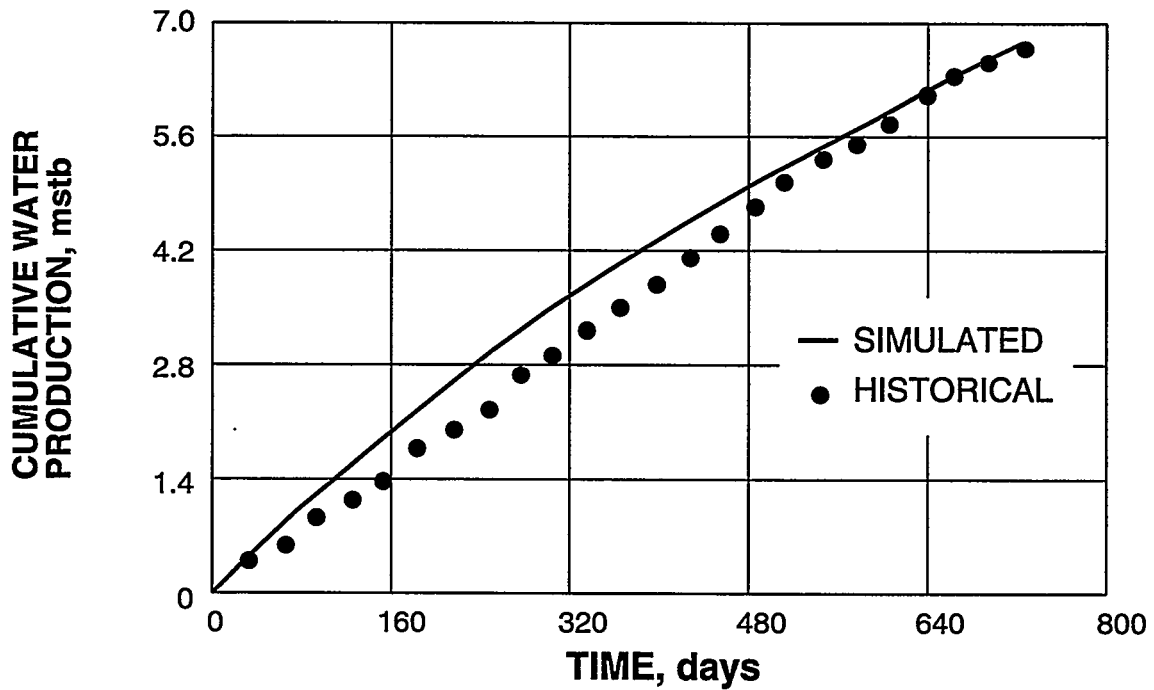


Figure 4-5 History Match of Cumulative Water Production for the McGuire No. 1 Well (No Free Gas)

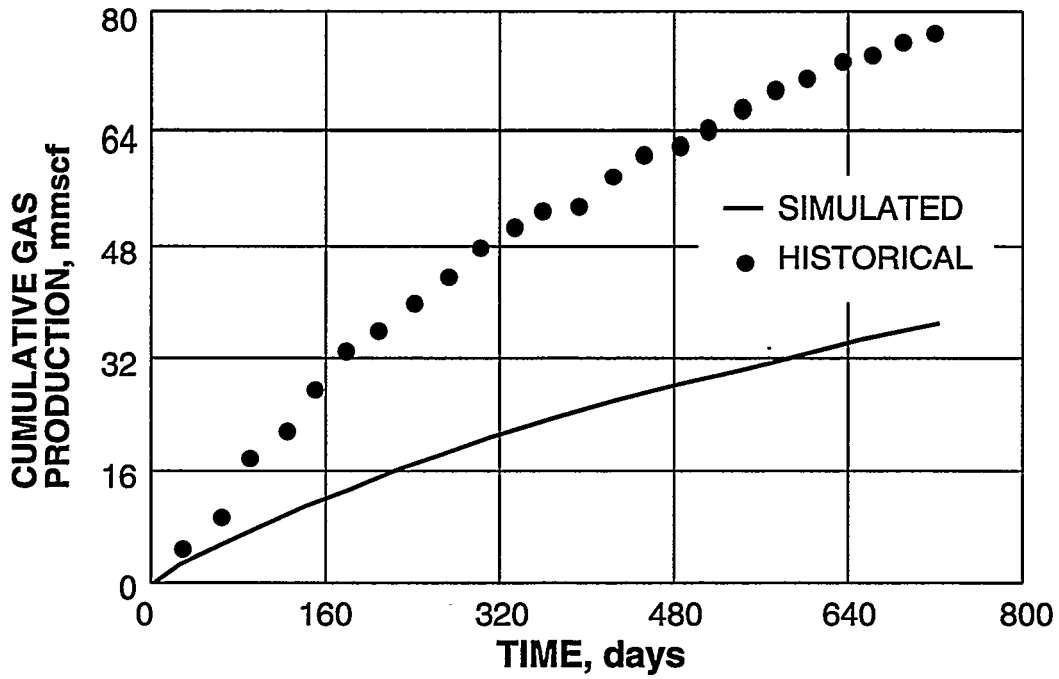


Figure 4-6 History Match of Cumulative Gas Production for the McGuire No. 1 Well (No Free Gas)

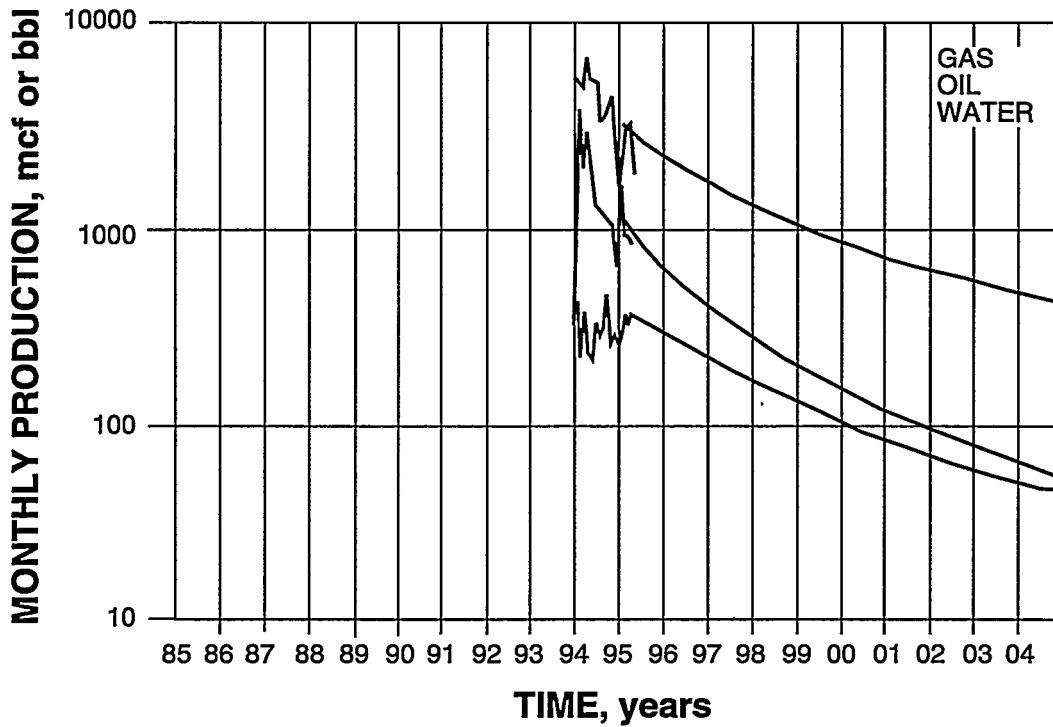


Figure 4-7 Decline Curves for the McGuire No. 1 Well

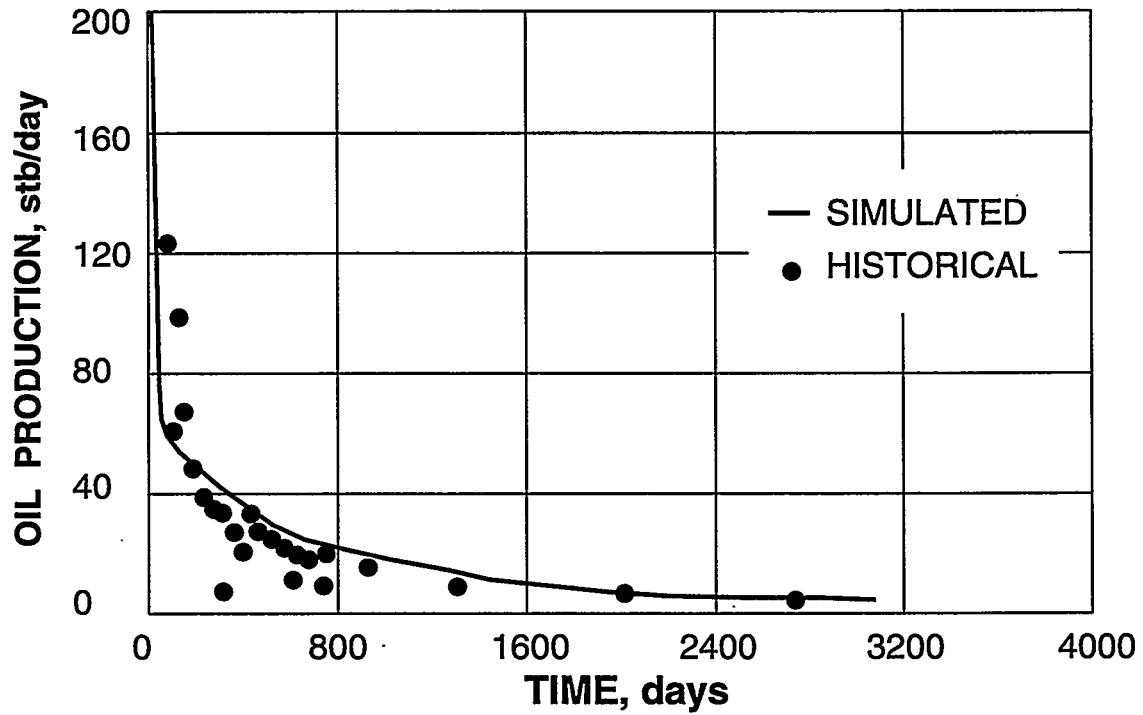


Figure 4-8 Base Case Oil Rate Simulation vs. the Decline Curve Extrapolations

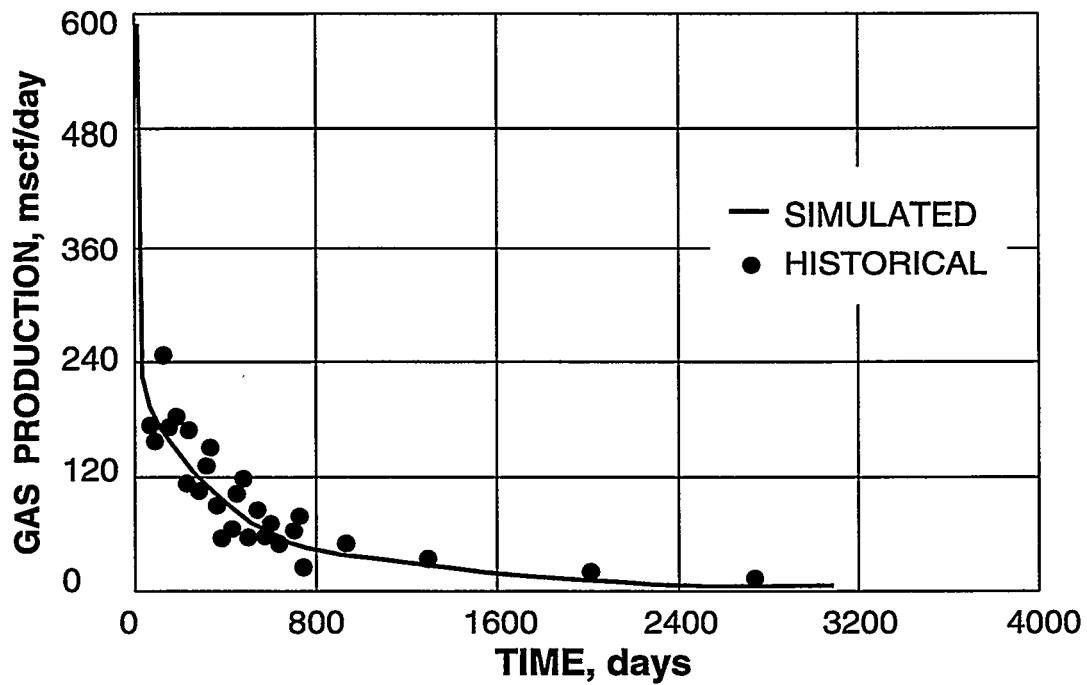


Figure 4-9 Base Case Gas Rate Simulation vs. the Decline Curve Extrapolations

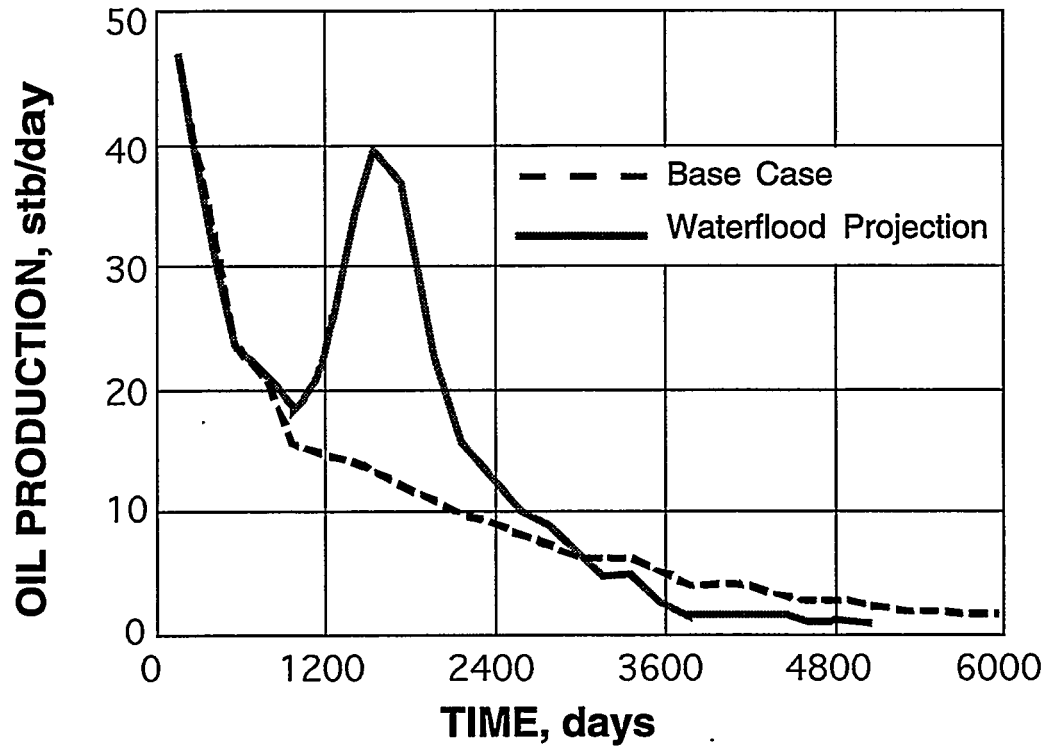


Figure 4-10 McGuire No. 1 Well Oil Production Waterflood

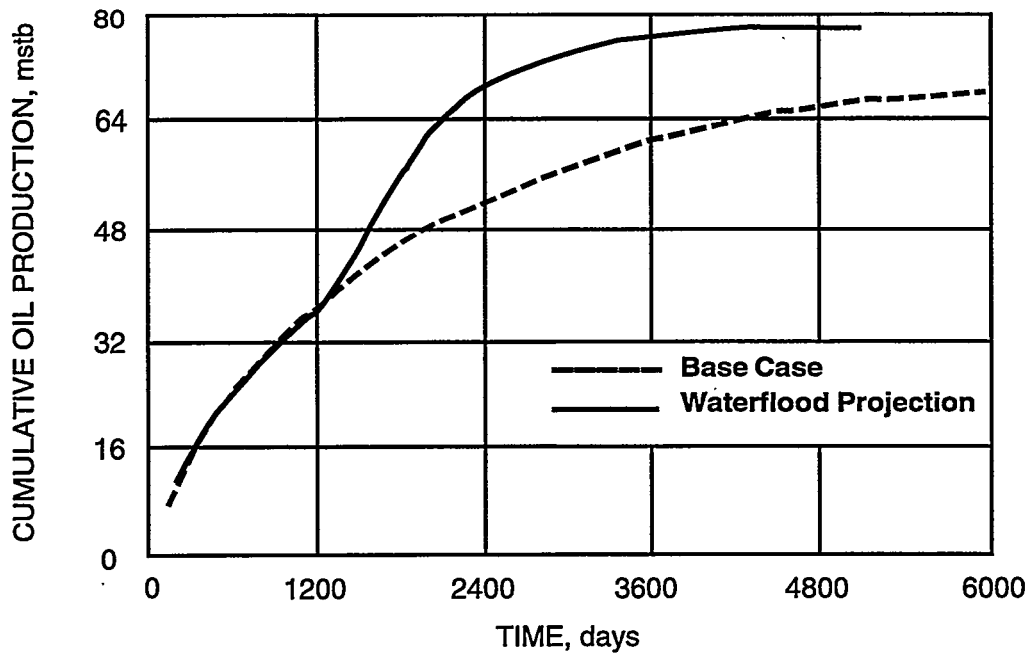


Figure 4-11 McGuire No. 1 Well Cumulative Oil Production Waterflood Projection

Note that these results only reflect the behavior of the McGuire No. 1 well, which has low permeability (1.35 md) compared to permeabilities in nearby wells. Also note that the single-well simulation predicted a reservoir pressure of 2,000 psi (prior to the start of water injection) at the extreme edge/corner of the simulated area. This particular location is representative of the location for the McGuire No. 2 well, which was spudded in June 1996, about the same time as the designed start of the water injection for the McGuire No. 1, and measured a pressure of 2,200 psi.

4.2 Pilot Area Simulation

In April 1996, the reservoir management team visited Belden & Blake in Canton, Ohio, to discuss the status of the project, present the BDM-Oklahoma work, review Belden & Blake's progress, and determine future project and technology transfer activities. During the meeting, BDM-Oklahoma presented the results of the geological modeling of the field and the results of the PVT, pressure analysis, material balance, and single-well numerical simulation efforts. Belden & Blake discussed its recent geologic work, as well as activities related to solving production problems in the field. The reservoir management team discussed a "pilot area" between two fault blocks crosscutting the central portion of the field to simulate in order to define infill drilling, waterflooding, or gas re-injection opportunities.

As more geologic information and reservoir data became available, it became apparent to the reservoir management team, that the pilot area is in production and pressure communication with the rest of the wells in the field. In addition, the faults separating the pilot area from the remaining wells in the field are not sealed enough to prevent pressure communication. From this perspective and on the basis of collected field data, the project team opted to develop a full-field simulation to evaluate the potential for water injection and/or gas repressurization.

4.3 Full-Field Simulation

4.3.1 Model Development

The development of the input data set for the full-field simulation was initiated as more experimental and field data became available. The simulation grid represents an area of the field 20,500 ft wide \times 10,700 ft long and which contains 25 wells. A rotated, nonuniform 65 \times 41 grid using three layers was designed to simulate the area. Values of net pay, porosity, and water saturation were generated for each grid block representing the study area. These values were generated by electronically superimposing computer-generated geological maps and the grid map representing the study area. Saturation values for the pay zones were calculated for various wells so that this data could be mapped and imported into the simulator.

Three steps were anticipated to complete the full-field simulation study. The first step was to history match the production and pressure data from the 25 production wells in the study area. The second step, the baseline prediction, was to project the performance of the field to the

economic limit based on decline curve analysis performed by Belden & Blake for the entire field. The third step was to predict the performance of the field as a result of waterflooding and/or gas re-injection.

4.3.2 History Matching

History matching the actual production and pressure data for the field was accomplished by holding known field and experimental data constant, such as fluid properties and initial oil, water, and gas saturation. In addition, experimentally determined relative permeability and capillary pressure values were not changed or modified. In order to simulate the field performance, two different rock regions were modeled, each having different relative permeabilities and capillary pressure values. Zone 2 was represented by one rock region depicting a three-phase system with an irreducible water saturation of 25%, whereas zones 3A and 3B were represented by a different rock region producing from a two-phase system (oil-water) with an irreducible water saturation of 32%. Figures 4-12, 4-13, and 4-14 show the acceptable full-field history match of cumulative oil production, cumulative gas production, and reservoir pressure, respectively.

A satisfactory history match of water production was not achieved; however, it was decided to accept the results of the water history match and not to tamper with the experimentally determined relative permeability data in order to maintain the integrity and accuracy of predicting the performance and feasibility of waterflooding and gas re-injection.

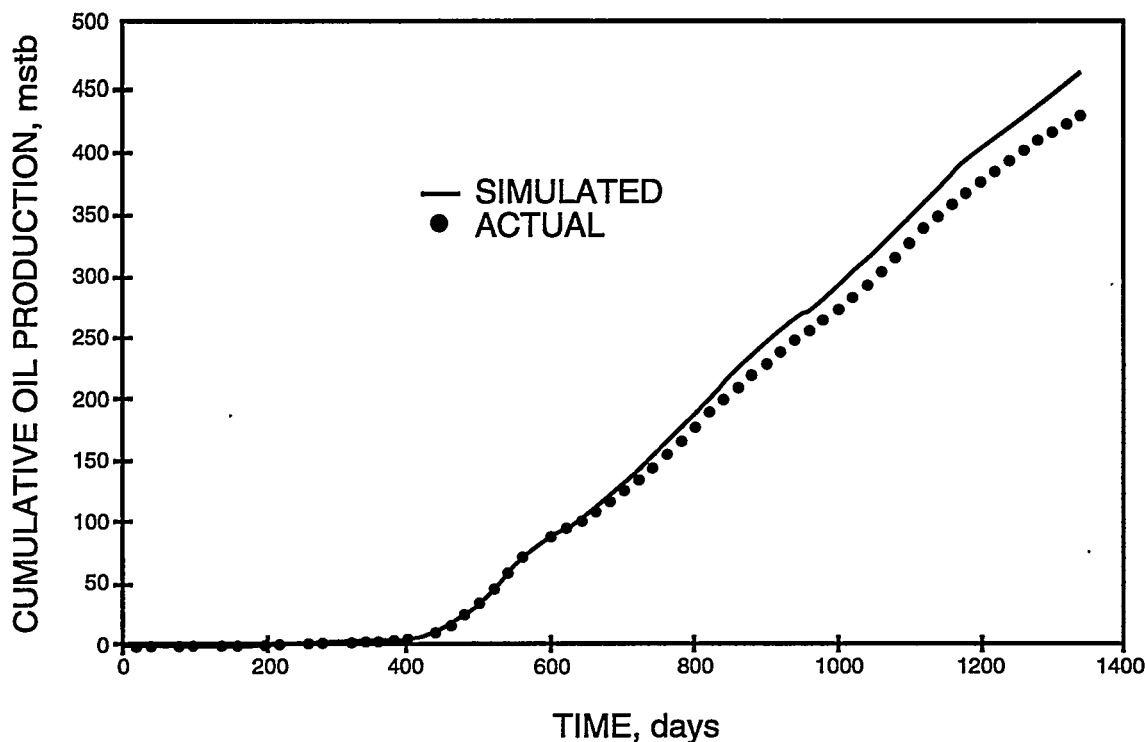


Figure 4-12 Full-Field History Match of Cumulative Oil Production

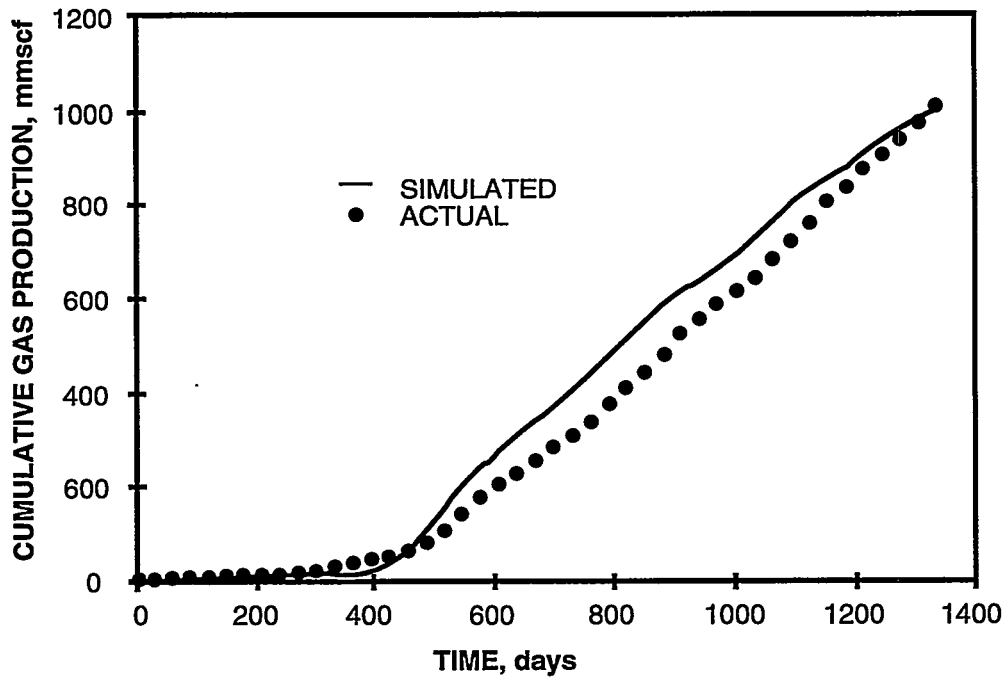


Figure 4-13 Full-Field History Match of Cumulative Gas Production

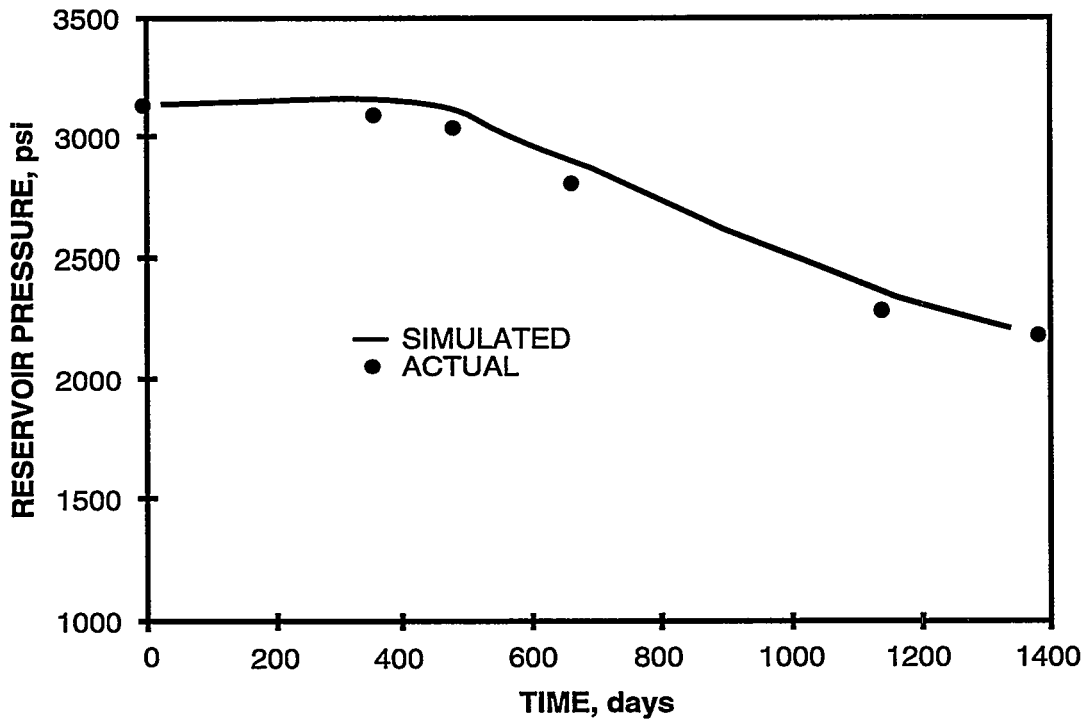


Figure 4-14 Full-Field History Match of Reservoir Pressure

4.3.3 Recovery Process Predictions

Following the history match process for East Randolph field, the reservoir management team of Belden & Blake and BDM-Oklahoma decided to investigate the potential for implementing waterflooding or gas re-injection as potential recovery processes to enhance the overall production from the field. Based on the lack of available CO₂ sources and field economics, no other recovery processes were considered.

As a first step in the prediction process, a baseline case was established by projecting the performance of the reservoir to the economic limit. The economic limit was established based on analyses performed by the field operator using decline curve projections and field operation costs. In addition, the simulation considered the WOR as a screening criteria for reaching the economic limit. The WOR limit for the field was set at 99%. Based on the baseline predictions to the established economic limit, the projected cumulative oil production is 881,000 stb with a cumulative gas production of 4,547 mmcf at an average reservoir pressure of 753 psi after 10 years.

Prior to initiating the simulation predictions for the waterflood and the gas re-injection recovery processes, the project team established a field injection-production pattern based on current and potential future field development and on practical injection and production scenarios. For the simulated field in question, a total of 11 injectors and 17 producers were used to project the potential for the various recovery processes. A line drive pattern was designed using the current 60-ac well spacing.

In the waterflood case, the average injection rate used in the simulation was 200 BWPD in each of 11 injection wells. This value was selected as result of performing various sensitivity analyses on different projected rates and keeping in mind the practical aspects of waterfloods in East Randolph field, including the availability of injection water, the formation breakdown pressure, and the formation injectivity potential.

Similarly, in the gas re-injection case, the average injection rate was selected as a result of rate sensitivity analysis, gas availability, and reservoir limitations. An injection rate of 350 MCFGD in each of 11 wells was used in simulating the gas re-injection recovery process. Note that methane was the gas used in the simulation because of the current limitations of BOAST3. Flue gas might substantially reduce operating costs while maintaining injection performance. Downsides to flue gas, such as corrosion, must also be considered and analyzed.

Simulation results from the two recovery processes indicated that the field has an excellent recovery potential when gas re-injection is implemented. As indicated in Figure 4-15, the field oil production rate was maintained at 350 BOPD compared to a sharp decline for both the baseline case and the waterflood case. Figures 4-16 and 4-17 show the potential for gas re-injection as an optimum recovery process for East Randolph field.

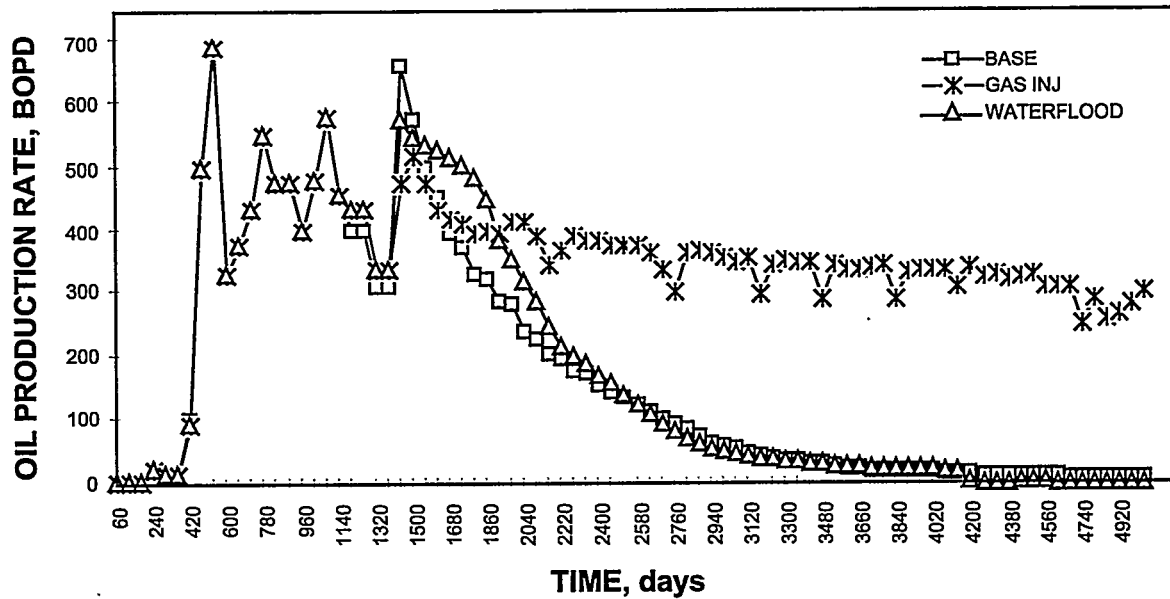


Figure 4-15 East Randolph Field Oil Rate Production as Function of Recovery Process

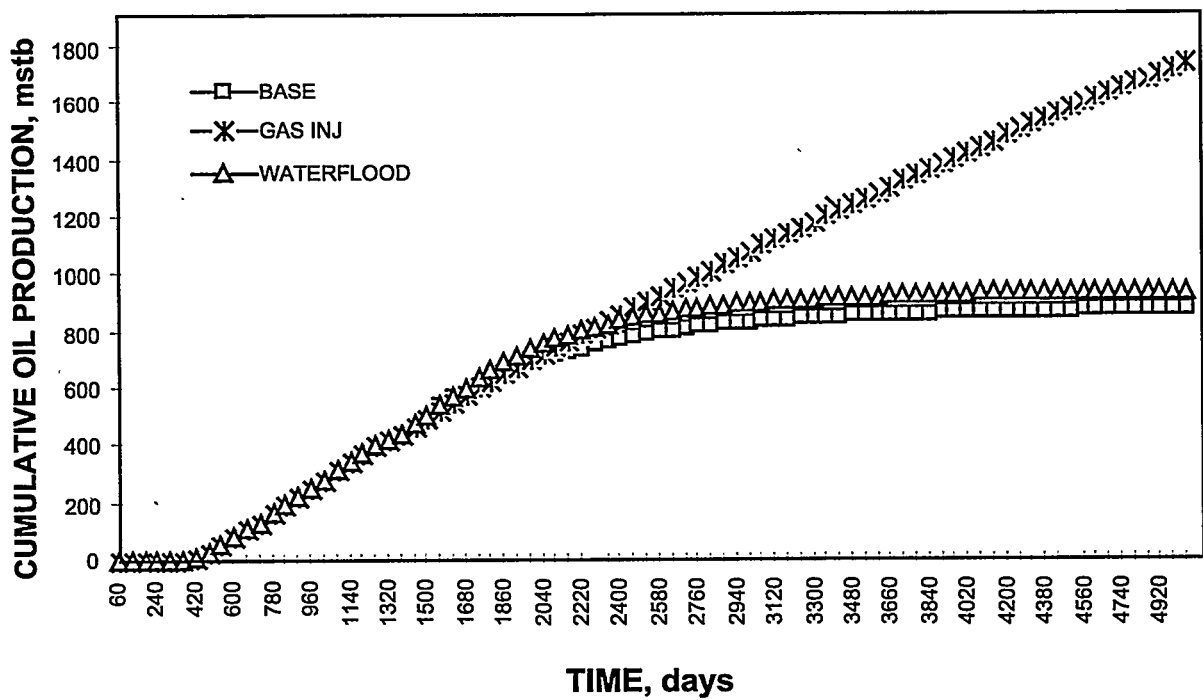


Figure 4-16 East Randolph Field Cumulative Oil Production as Function of Recovery Process

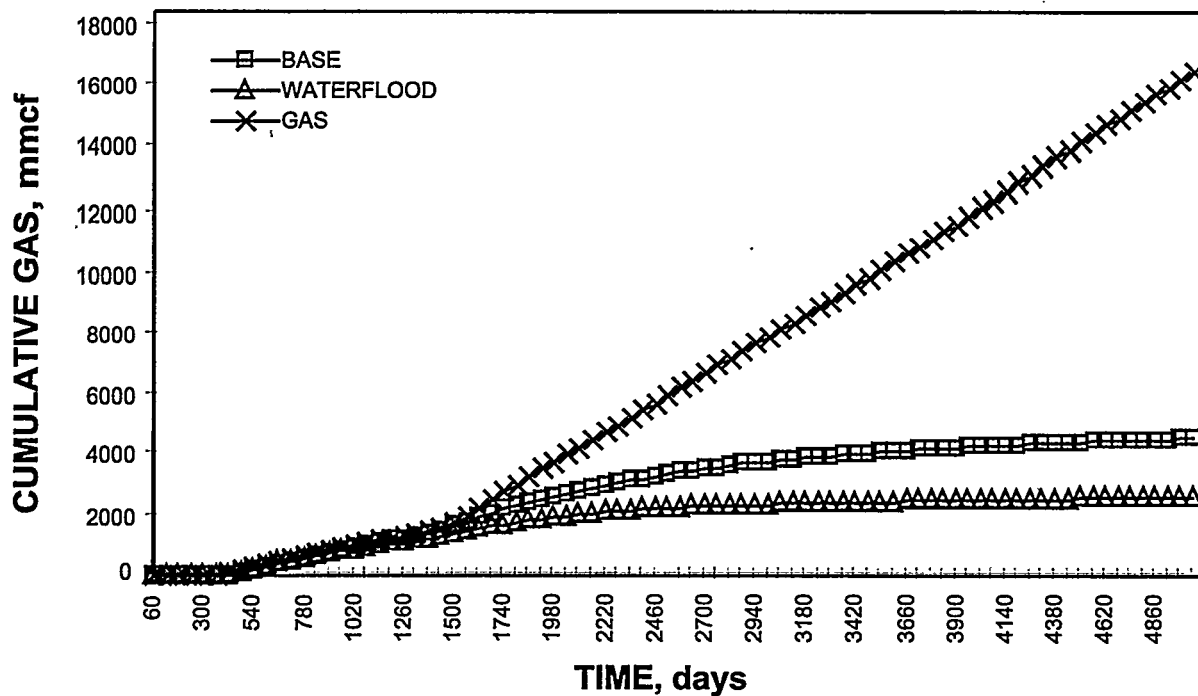


Figure 4-17 East Randolph Field Cumulative Gas Production as Function of Recovery Process

Based on an OOIP of 11 million stb, the baseline projection to the economic limit indicates an oil recovery potential of 8.0% OOIP compared to 8.5% and 16% OOIP for waterflooding and gas re-injection, respectively. The low incremental recovery due to waterflooding is attributed to the low reservoir permeability, the very low formation permeability to water as determined from the special core analyses performed on the McGuire No. 2 core well, and the presence of a high gas saturation in Rose Run zone 2.

Furthermore, results of the simulation study on the two processes indicated that the gas re-injection recovery process, due to gas compressibility and entering into solution, will result in a reservoir pressure maintenance that will stabilize the pressure at approximately 2,400 psi (see Figure 4-18). This pressure is above the reservoir saturation pressure of 2,070 psi.

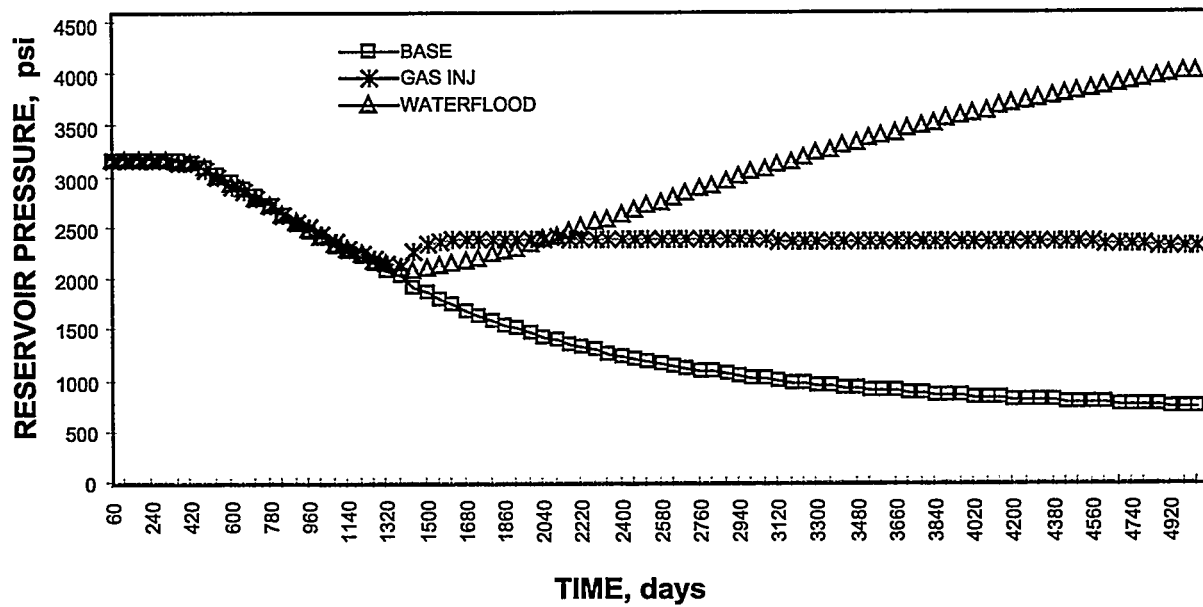


Figure 4-18 East Randolph Field Pressure Performance as Function of Recovery Process

5.0 PRODUCTION ANALYSES

Production operations were evaluated to improve efficiency and optimize recovery. A previous study identified several mechanisms that affect well productivity and determined improvements to current stimulation techniques (Cramer and Thomas 1994). Drill cutting samples and rotary sidewall cores were analyzed to measure porosity, permeability, and the effects of different acid solutions used in stimulation techniques. Results of exposing core samples to various acid solutions indicated that wells treated with hydrochloric acid (HCl) could be susceptible to migrating clays, thus having steeper decline curves. The use of hydrofluoric acid (HF) was found to effectively dissolve the authigenic clays from the pore throats around the wellbore.

If waterflooding is determined to be technically and economically feasible, specific data must be collected and analyzed. Production issues for waterflood facility requirements include injection water sources, pump system and horsepower sizing, gathering lines and tank batteries size and location, water treatment chemicals, water filtering system, and bactericides. Rules and regulations for an enhanced recovery project in Ohio were also researched in order to apply for and conduct a possible pilot test. The approximate capital cost to set up a waterflood pilot is \$200,000; a field-wide waterflood could cost approximately \$1.25 million, in present day dollars.

The optimum water injection pattern was determined to be a staggered, northeast-southwest line drive on approximately 30-ac spacing from injector to producer. This pattern uses the natural northeast-southwest permeability trend determined from core analyses, geologic mapping, and fracture orientation interpretation. Approximately 10–12 injectors among 17 producers would be required for the full field waterflood to effectively sweep the reservoir. Many of the injectors would come from conversions of current producers. Two to four new injectors would be required to provide support for current producers. Wells currently shut in could also be used.

Injection water sources were identified based on estimates of the total water injection required and the amount of current water production from the Rose Run in East Randolph field. Possible sources included water from the Clinton reservoir in nearby fields (such as Marlboro field, several miles to the south). Freshwater wells drilled within the field would provide an alternative source. Water compatibility studies would be performed to determine effects of water chemistry on the productive intervals at reservoir temperatures and pressures. Initial injection rates were estimate at 100–150 BWPD. The rates, at 1,000 psi surface injection pressure to stay below formation parting pressure, would decrease and stabilize at 50–75 BWPD over a 3–6 month period. Reservoir modeling concentrated on water injection into the oil-bearing Rose Run zones 3A and 3B; however, since most wells are also completed and stimulated in zone 2, which contains a high gas saturation, Zone 2 would be a potential water thief zone. Polymer slugs to modify injection profiles in current producers and/or new injectors would need to be investigated.

Paraffin buildup problems were identified in the field in current producers and in surface facilities. The high paraffin content of the oil was confirmed by fluid analyses prior to special core analyses. Laboratory results indicated a paraffin content of 8%-10% by weight. Higher permeability was measured in special core analyses performed by BDM-Oklahoma than in routine core analyses performed by OMNI Lab. The differences were predominantly due to the cleaning procedures performed by each group. OMNI Lab cleaned the core plugs using a combination of toluene and methanol for approximately 24 hr before the plugs were tested for porosity and permeability. BDM-Oklahoma cleaned additional core plugs from the same zone and similar depths for a period of two weeks using repeated cleaning and extraction procedures of toluene and methanol. The longer cleaning period allowed the toluene to dissolve paraffin present in the micropores, therefore measuring higher permeabilities indicative of reservoir conditions.

Results of these experiments were discussed with Belden & Blake to assist its production operations department in controlling and solving the paraffin problem in its wells in the field. The current practice is to dump 300 gal of toluene once a month on the back side while the well is producing. The pumping schedules have been changed to reduce the cooling effect on the toluene. Huber rods have been run with snowball scrapers and rod rotators to cut the paraffin. Additional work may be required to design improved chemical treatment procedures that will help to alleviate paraffin problems.

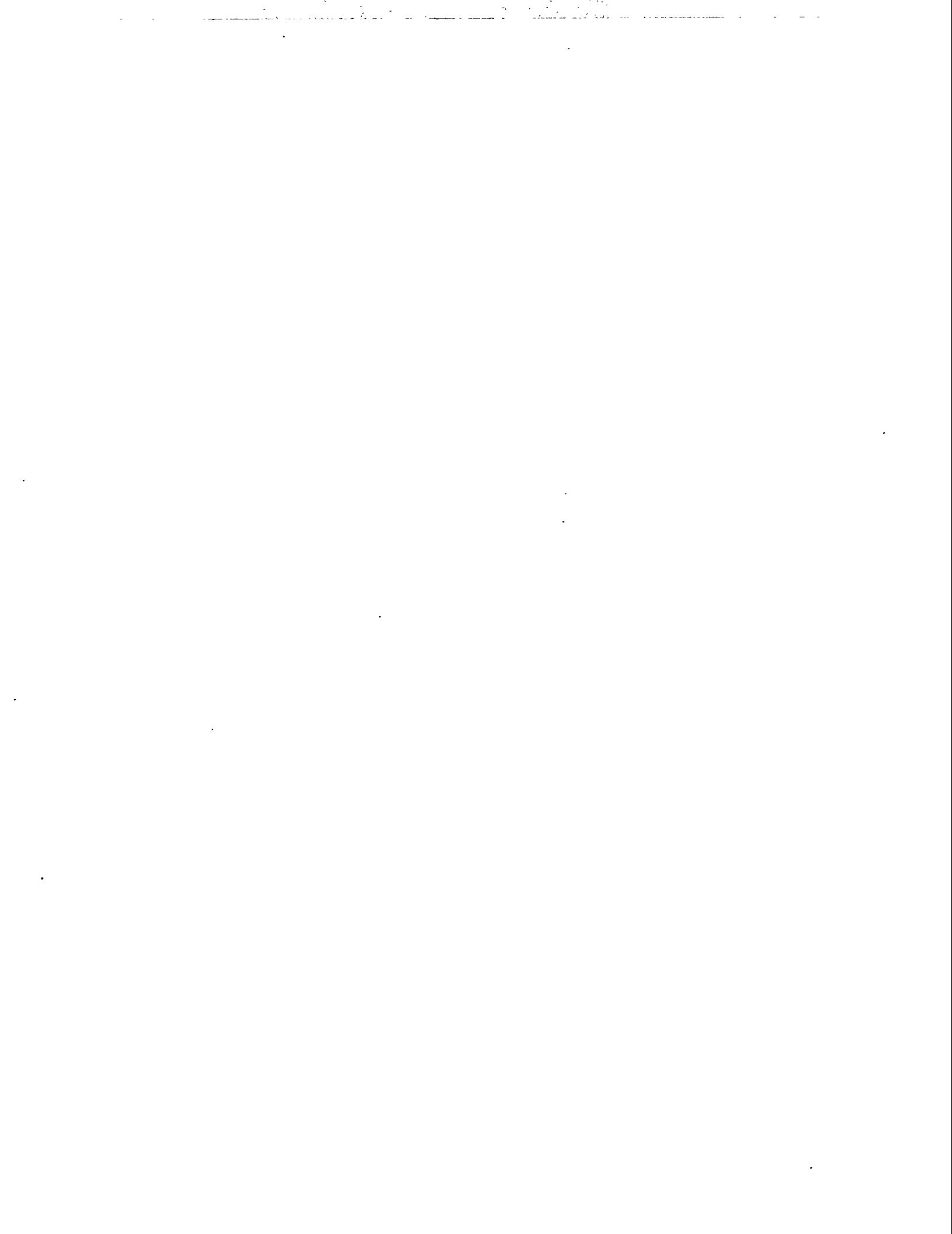
Another treatment option to alleviate paraffin wax crystallization and deposition is the use of microbes. Microbial techniques are a flexible, cost-effective way to improve oil recovery without the use of environmentally-toxic solvents and dispersants (Brown 1992). Microbes specially formulated for reservoir temperature, fluid salinity, and crude oil composition are injected into the reservoir through production and/or injection wells. Microbes live in the water phase and colonize at oil-water interfaces. Oil viscosity is reduced due to the microbial cracking of long-chain, saturated hydrocarbons (alkanes) into short-chain molecules. The microbes produce solvents and surfactants, and remove scale-forming and metallic ions from the formation water. The increase in solvent composition and decrease in wax composition reduces the critical waxing temperature and pressure of the paraffinic oil. Lower interfacial tension mobilizes previously immobile oil, decreasing WORs and increasing oil recovery.

A typical well would be treated once a month with 5 gal of microbe-inoculated water blended with a predetermined amount of lease brine. The procedure is to batch-treat down the casing annulus and flush the bacteria blend with KCl water. This would cost approximately \$350 per treatment per well. The well should be shut in for 24 hr after each treatment to allow the microorganisms to disperse and inoculate the system prior to fluid withdrawal. A net increase of 0.6 BOPD at \$20 oil would pay for the treatment. This does not take into account any decrease in chemical treatment costs and tax credits. The treatment has been applied in several waterfloods that meet screening criteria with oil production increases of 13%-20% (Bryant et al. 1994).

Various production lift methods and on/off time schedules have been evaluated to optimize production operations. Some of the wells were initially flowing for a short period of time after

completion, but subsequently were placed on plunger lift. Due to the relatively high fluid volumes produced from many wells in the central part of the field, rod pumping has proved to be better operationally and economically. In addition, submersible pumps have been considered. The more prolific producers are produced 24 hr/day; marginal producers have varied production schedules in order to maintain reservoir pressure.

Hydraulic fracturing has been extensively studied in East Randolph field as part of the Gas Research Institute field deployment program. An SPE paper (Fairchild et al. 1996) presented several techniques used to design an improved hydraulic fracture treatment. The new technique uses crosslinked fluids to place more sand at higher concentrations in the pay zone and create higher conductivity fractures, with less total fluid volume. Real-time fracture diagnostics and modeling are used to help place proppant and refine the interpretation of reservoir properties and production responses. Field results of the hydraulic fracture stimulation treatments developed have significantly improved field operations. After the crosslinked fluid treatments were applied, daily production data were collected and compared to offset wells that were fracture stimulated with CO₂ foam or polymer gels. The comparison shows the crosslinked fluid treatments result in improved, sustainable oil production.



6.0 ECONOMIC ANALYSES

The economic analysis uses the data collected from the log, core, and fluid analyses integrated with the well tests to determine the most economic strategy for improving oil recovery. The optimum improved recovery process must be technically as well as economically feasible for the field operation to be successful. The improved recovery processes evaluated included a combination of infill drilling, waterflooding, and gas re-injection.

The reservoir simulation work conducted under this project indicated that the most technically viable option for improving recovery in East Randolph field is through the implementation of a gas re-injection project. Waterflooding showed only a marginal recovery increase, but production is accelerated. The predicted production responses for these two improved recovery options were used to assess the economic viability of implementing these processes in the field. Economics were run for three cases: (1) the base case of continued operation of the field to the economic limit, (2) the full-field waterflood case, and (3) the full-field gas-injection case, as discussed in Sections 6.1 through 6.3 of this report.

The fluid volumes predicted from reservoir simulation for waterflooding were incrementally evaluated above the baseline forecast for primary recovery. Approximated costs for the installation of field-wide facilities for waterflooding were incorporated. Profitability indicators were calculated and sensitivity analyses were run to calculate the oil price necessary for the field-wide project to be economic. Table 6-1 summarizes the economic assumptions for the base case (primary recovery), the gas injection case, and the field-wide waterflooding case. As indicated, waterflooding does not generate positive incremental cash flow above primary recovery. Due to the incremental recovery of only 50,000 bbl of oil (approximately 2% of OOIP), waterflooding is not attractive at any oil price.

Natural gas re-injection for pressure maintenance appears to have the most promise, pending a detailed engineering and economic analysis. Full-field reservoir modeling of 350 MCFGD per well injection rate into 11 injectors promotes recovery of an additional 800,000 bbl of oil (8% of OOIP) or more. In addition, not perforating the Rose Run zone 2 sand (which contains a high gas saturation) in future wells will help maintain reservoir pressure.

6.1 Base Case Economics

The assumptions of the base case economics for continued operation of East Randolph field to the economic limit are summarized in Table 6-1. This case assumes an average net revenue interest of 81.25%, which is the typical interest for the various operators in the field. The oil price for the economics was assumed to be constant at \$20/bbl, and the gas price was held constant at \$2.50/mcf. The operating cost for the 24 wells in the field was estimated to be a total of \$25,000/month, and the costs were not escalated. There were no capital investments in this case, and the start date for the case was July 1, 1996. Taxes were handled as required for production in the state of Ohio.

Table 6-1 Economic Assumptions

	Base Case	Gas Injection Case	Waterflooding Case
Oil Price, bbl	\$20.00	\$20.00	\$20.00
Gas Price, mcf	\$2.50	\$2.50	\$2.50
Escalation	No	No	No
Working Interest	100%	100%	100%
Net Revenue Interest	81.25%	81.25%	81.25%
Ad Valorem Tax*	1.0%	1.0%	1.0%
Severance Tax	\$0.10/bbl	\$0.10/bbl	\$0.10/bbl
	\$0.025/mcf	\$0.025/mcf	\$0.025/mcf
Operating Expense/Month	\$25,000**	\$42,000†	\$42,500†
Investment:			
Injector/Compressor System	\$0	\$120,000	\$400,000
Convert 7 Wells to Injection	\$0	\$70,000	\$70,000
Drill 4 Injectors	\$0	\$780,000	\$780,000
Total Investment	\$0	\$970,000	\$1,250,000

*Pre-tax revenues.

**88ths for 24 producers.

†88ths for 17 producers and 11 injectors.

The predicted oil and gas production rates from the base case simulation were used, as discussed in Section 4 and shown in Figure 4-15. Table 6-2 shows the cumulative oil and gas volumes from this simulation case, along with the cumulative undiscounted net cash flow (also see Figure 6-1).

Table 6-2 Base Case Economic Results for a July 1, 1996 Start Date

End of Year	Cumulative Oil Production (bbl)	Cumulative Gas Production (mcf)	Cumulative Net Cash Flow* (\$1,000)
1	175,000	838,000	4,169
2	274,000	1,438,000	6,648
5	396,500	2,473,000	9,769
7	417,000	2,824,000	10,196
10	428,500	3,113,500	10,300

*Net cash flow = undiscounted revenues less royalties, expenses, and investments (before state and federal income tax).

The results of the base case show that the field will reach the economic limit in 2006, with cumulative production for its remaining life of 428,000 bbl of oil and 3.1 bcf of gas. This results in an ultimate recovery from the field at the economic limit of 878,000 bbl of oil and 4.3 bcf of gas. The recovery factor at the economic limit is about 8% of the OOIP of 11 million bbl.

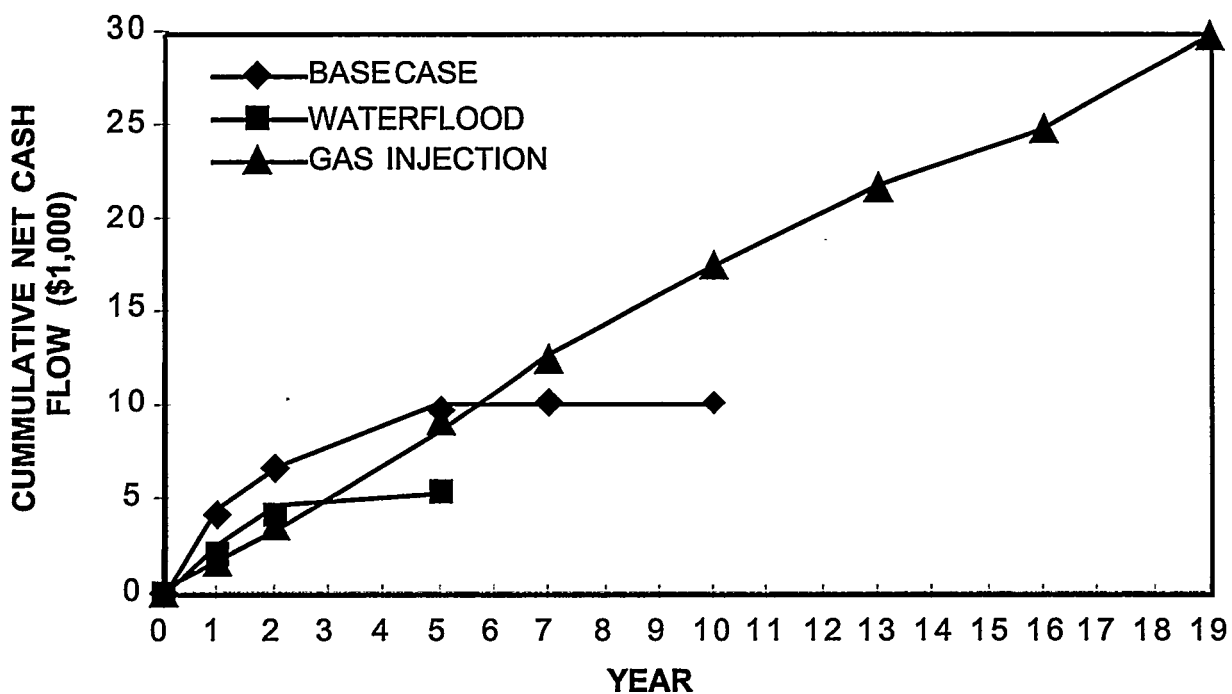


Figure 6-1 Cumulative Undiscounted Net Case Flow Diagram for Improved Recovery Options in East Randolph Field

6.2 Waterflood Economics

The waterflood case assumes that 200 BWPd will be injected in each of 11 injectors. The predicted oil and gas production rates from the base case simulation were used, as discussed in Section 4 and shown in Figure 4-15. Table 6-3 shows the cumulative oil and gas volumes from the simulation case, along with the cumulative undiscounted net cash flow.

Table 6-3 Waterflooding Case Economic Results for a July 1, 1996 Start Date

End of Year	Cumulative Oil Production (bbl)	Cumulative Gas Production (mcf)*	Cumulative Net Cash Flow** (\$1,000)
1	190,500	460,000	1,955
2	325,500	764,000	4,211
5	451,000	1,120,000	5,398

*Only base gas produced above injected volumes. Assumes base gas production is delayed until the economic limit of gas injection is reached (about 15 yr) and is subsequently recovered.

**Net cash flow = undiscounted revenues less royalties, expenses, and investments (before state and federal income tax).

The basic economic assumptions for the waterflood case are summarized in Table 6-1.

The estimated total capital expenditure for the installation of a field wide waterflood in East Randolph Field is \$1,250,000. This includes the cost to convert seven wells to water injection (\$70,000), the cost to drill and complete four additional water injection wells and one source well (\$780,000), and all associated waterflood capital equipment costs (\$400,000). The operating cost for the field under waterflood was estimated to be \$42,500/month, an incremental operating cost of \$17,500/month over the base case.

The results of the waterflood economic analysis show that the capital investment pays out in the first year, but the cash flow is significantly lower than for the base case. Waterflooding is not incrementally economic in East Randolph field. The cumulative net cash flow for the waterflood at the economic limit is half that of the base case. Under the waterflood case, the field will reach the economic limit in 2001, with cumulative production for its remaining life of 451,000 bbl of oil and 1.1 bcf of gas. This results in an ultimate recovery from the field at the economic limit of 900,000 bbl of oil and 2.3 bcf of gas. The recovery factor at the economic limit is 8.5% of the OOIP of 11 million bbl.

6.3 Gas Injection Economics

The gas injection case assumes that 350 mcf/day, supplied from field production and additional sources, of produced gas will be re-injected into each of 11 wells. The predicted oil and gas production rates from the base case simulation were used, as discussed in Section 4 and shown in Figure 4-15. Table 6-4 shows the cumulative oil and gas volumes from this simulation case, along with the cumulative undiscounted net cash flow (see also Figure 6-1).

Table 6-4 Gas Injection Case Economic Results for a July 1, 1996 Start Date

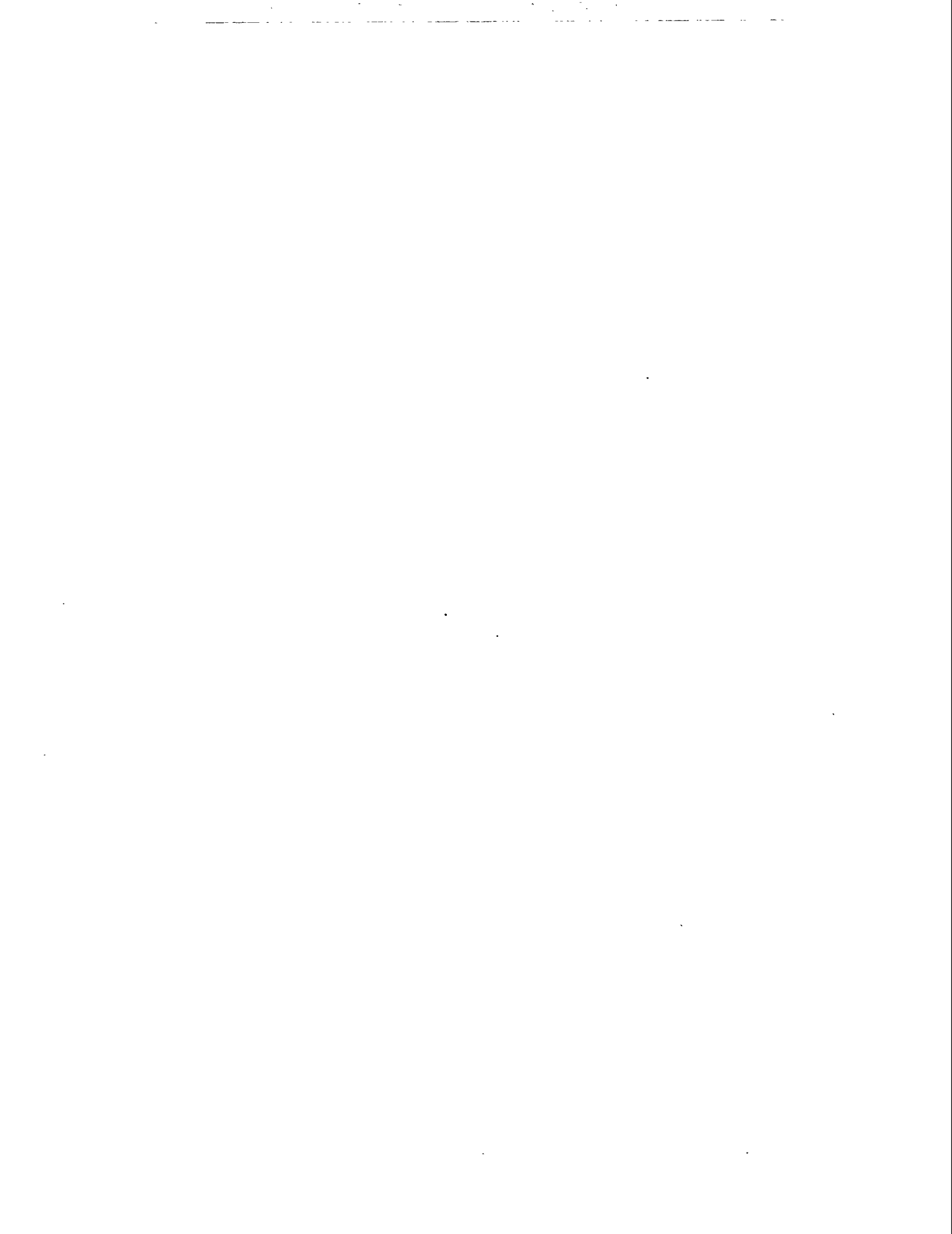
End of Year	Cumulative Oil Production (bbl)	Cumulative Gas* Production (mcf)	Cumulative Net Cash Flow** (\$1,000)
1	160,000	72,000	1,600
2	312,000	144,000	3,600
5	698,000	360,000	9,100
7	937,000	504,000	12,400
10	1,295,000	720,000	17,500
13	1,550,000	936,000	21,600
16	1,775,000	1,152,000	24,800
19	1,925,000	3,300,000	29,800

*Only base gas produced above injected volumes. Assumes base gas production is delayed until the economic limit of gas injection is reached (about 15 yr) and is subsequently recovered.

**Net cash flow = undiscounted revenues less royalties, expenses, and investments (before state and federal income tax).

The basic economic assumptions are summarized in Table 6-1. The estimated total capital expenditures required for the installation of a gas injection project in East Randolph Field is \$970,000. This includes the cost to convert seven wells to gas injection (\$70,000), the cost to drill and complete four additional gas injection wells (\$780,000), and all associated capital equipment costs (\$120,000). The operating cost for the field for the gas injection case was estimated to be \$42,000/month, an incremental operating cost of \$17,000/month over the base case.

The results of the gas injection economic analysis show that the capital investment pays out in the first year and that cash flow is significantly higher than for the base case. Under the gas injection case, the field will reach the economic limit in 2015, with cumulative production for its remaining life of 1.9 million bbl of oil and 3.3 bcf of gas. This results in an ultimate recovery from the field at the economic limit of about 2.4 million bbl of oil and 4.5 bcf of gas. The recovery factor at the economic limit is 16% of the OOIP of 11 million bbl. The economic life and economic recovery from the field can be almost doubled through gas injection.



7.0 APPLICATION OF RESERVOIR MANAGEMENT CONCEPTS

7.1 Defining Reservoir Management Approach

7.1.1 Introduction

From studies of reservoir management under this and other DOE-sponsored field demonstration programs, reviews of the abundant literature on reservoir management, and our past experiences and responsibilities in reservoir management with both major and independent oil companies, the authors have arrived at several important conclusions about the nature of reservoir management. First, every petroleum reservoir being exploited is undergoing reservoir management. Every operator uses either a general philosophy, simple guidelines, or a detailed strategy that governs interaction with the reservoir. Collectively, these diverse approaches can be viewed as reservoir management plans. It is the plan that is at the core of reservoir management. Effective reservoir management is formulating and implementing an appropriate plan that will maximize the reservoir's profitability (or other desired measure of performance) to the operator.

An effective reservoir management plan cannot simply be assumed or transferred from reservoir to reservoir or from operator to operator. A good plan must be custom made for a particular reservoir with a particular operator at a particular time. Building the optimally effective reservoir management plan requires knowledge and consideration of (1) the reservoir system, (2) proven and currently evolving technologies, and (3) the business environment under which the reservoir management plan will be implemented.

7.1.2 Reservoir System

The reservoir system is composed of subsurface reservoir rock, its contained fluids, all wellbores and downhole equipment, and surface equipment and facilities. A thorough knowledge of the reservoir system will include familiarity with past activities during drilling, stimulation, completion, and operation that may have resulted in changes in reservoir properties not otherwise anticipated.

A reservoir characterization model is a complete conceptual 3D model or picture of the subsurface reservoir, including consideration of its lithologies and fluids and their interactions. It is a representation or estimate of reservoir reality, depicting not only the three-dimensional extent or bounds of the reservoir, but the qualitative (presence or absence) and quantitative (magnitude) characteristics of rock, fluid, and other reservoir parameters which affect fluid flow at every location in the volume of the reservoir. The degree of uncertainty associated with placement and magnitude of fluid-flow properties is an important facet of this model.

Reservoir characterization data can come from a wide variety of technologies and cover a wide range of scales. Because a single reservoir characterization model or a small number of such representations is the desired result, and because the necessary data are of both engineering and geological origin, the need for close cooperation between the members of the reservoir management team (i.e., between geoscientists, engineers, and other professionals) in formulating such models is paramount. Data from various technological sources often suggest a number of nonunique interpretations of reservoir reality. It is the duty of the reservoir management team to understand and use the various technological data types in complementary and supplementary fashions to arrive at the most probable range of possible reservoir realities upon which to base reservoir performance predictions. Model construction is not a trivial task, and its successful completion requires continual cooperation and interchange of information and ideas among team members. The task cannot be efficiently accomplished (indeed, it may not be accomplishable at all) if geologists, engineers, and others work on the task sequentially and independently.

An additional important aspect of reservoir knowledge is familiarity with the production and injection infrastructure. Natural processes in the subsurface can interact with wellbore equipment, resulting in problems such as corrosion, scaling, paraffin deposition, etc. Surface processes, such as erosion or flooding, can affect both wells and facilities, and human development activities certainly may affect surface facilities and the use of wellbores. Knowledge of the history of drilling, completion, recompletion, and workover practices in the field, as well as familiarity with current surface and wellbore facilities, is also necessary. Equally important is a knowledge of past production and injection practices in order to be aware of alterations in the natural properties of the reservoir that have resulted from past human activities. Human activities in development and depletion of a reservoir can have a profound influence on the reservoir's basic characteristics and thus on its performance. In some cases, human activities are equivalent to introduction of whole new and often extreme episodes of diagenesis, tectonics, and/or fluid exchange. The nature of these changes is unexpected in many instances and can result in decreased reservoir performance and permanent reservoir damage if not considered. Examples might include situations where stimulation practices have led to communication between reservoir units behind pipe, or where long periods of water injection above formation parting pressure have led to channeling between injection and production wells.

7.1.3 Available Technologies

Successful reservoir management is also dependent on a familiarity with existing and newly developing technologies that are available to characterize reservoirs and to improve operational efficiencies and hydrocarbon recovery. This does not mean that a high-tech approach is necessarily the appropriate one to take. It is much more important to be aware of the wide range of technologies available and the economics involved in assessing and implementing those technologies.

A range of technological knowledge from that of building conceptual/analog and stochastic reservoir characterization models to construction of models from a variety of traditional and newly developing deterministic data sources is appropriate for addressing the reservoir characterization aspects of reservoir management. Familiarity with appropriate techniques and technologies for reducing costs and increasing operating efficiencies through optimization of wellbore and facilities equipment and practices (including modern stimulation and completion practices) will also be critical.

It is also important to be aware of routine application techniques and new techniques, and technologies associated with improved recovery. Secondary techniques include injection of water or gas (immiscible) for pressure maintenance or displacement of hydrocarbons. Advanced secondary recovery techniques include techniques aimed at improving contact with mobile oil, such as infill drilling using vertical and horizontal wells and employing polymers for profile modification and mobility control. Enhanced oil recovery techniques include application of processes to recover immobile oil, such as microbial, alkaline and alkaline-surfactant-polymer, surfactant, steam, in-situ combustion, and miscible and immiscible gas-re-injection.

Maintaining an awareness of appropriate and often rapidly changing technologies in so many areas is a difficult task, especially for smaller organizations. Membership and participation in professional societies, attendance at their meetings, and review of their publications may help; but it is not realistic to assume that any organization will always have (or should have) the necessary depth of knowledge and experience in all the areas that may be required. A realistic target is to obtain enough of a general (screening level) knowledge of available technologies to know when an expert should be consulted for detailed evaluation. Numerous professional societies and organizations like the regional offices of the Petroleum Technology Transfer Council can provide contact with the appropriate consulting expertise.

7.1.4 Business Environment

The reservoir management business environment includes all factors influencing reservoir management decisions aside from the properties of the reservoir itself (including equipment and facilities) and available technologies. Like technology and the reservoir itself, these factors are dynamic rather than static and must be accounted for as such in the reservoir management plan.

Reservoir management business environment factors fall into two categories: those that are external to the operator's organization (i.e., those that affect all operators equally) and those that are internal (i.e., their influences are different in different organizations). External factors include considerations such as market economics, taxes, operational regulations, safety and environmental regulations, and social perceptions. Internal factors include the company or organization's attitude toward risk, its acceptable rate of return, its ability to raise and/or commit capital, its organizational structure (e.g., interdisciplinary team vs. disciplinary approach to reservoir management), its objectives, and its ability to commit to execution of long-term plans (Cole et al. 1993; Wiggins and Startzman 1990).

The organizational structure of reservoir management teams and the interaction dynamics of their members are extremely important aspects of the internal reservoir management business environment. Thakur and Satter (1994) present an excellent discussion on the structure and function of reservoir management teams. Team efforts, performed by multidisciplinary groups sharing common goals, are critical to the success of any reservoir management project. At project inception, team members should share in developing project goals and objectives and aid in developing and assigning project responsibilities for each team member. A team leader with the multidisciplinary insight and management skills to encourage cooperative participation in these and subsequent project activities is a necessity.

The dynamic interaction of the group comprising the reservoir management team makes a strong contribution to the success of the effort. The team leader must be aware that the team members may have varying degrees of technical skill and experience in their own disciplines and may have varying experience in working closely with people from other disciplines. The leader must monitor and nurture the daily interaction of team members. To do so, the team leader must be aware of individual personality traits and differences in rank, must be aware that certain team members may have commitments to other projects that may compete for their time and dedication at inconsistent and often inconvenient intervals (though management should do everything possible to minimize conflicts in priorities), and must realize that occasional disruptions, such as loss or addition of team members, may inevitably occur.

The importance of incorporating both external and internal reservoir management environment factors into the reservoir management plan cannot be overemphasized. A comprehensive plan might specify surveillance criteria for these factors as well as those concerning the reservoir and technology. Significant changes in any of these business environment factors may be just cause for revision of the reservoir management plan.

7.2 Plan Building Process

One of the key objectives in the Reservoir Management Demonstration Program being implemented by BDM-Oklahoma has been to resolve the sequence of considerations that goes into the development of an effective reservoir management plan. At this time, only the broadest categories have been identified, but it is hoped that subsequent work on a variety of reservoir management projects in different contexts will enable the procedures to be defined in greater detail with time.

As currently recognized, the primary steps in plan construction are as follows:

1. Define the target size
2. Locate the target.
3. Identify appropriate technologies.
4. Optimize technology implementation.
5. Optimize operational procedures and technologies.

An ideal plan will also specify its own limitations based on the conditions and assumptions that were incorporated into its development. These steps are very general and should be applicable whether or not improved recovery is being considered as a reservoir management option. In each step, careful attention must be paid to the complete context of reservoir management (i.e., the reservoir system, available technologies, and the business environment).

Defining the target size, whether that target be the recovery of additional petroleum resources or merely saving dollars associated with addressing chronic production problems or spent on inefficient operating procedures, will help to determine the scale and scope of the plan being developed. Multiple targets of the same or different types may be addressed by the same reservoir management plan. In fact, this approach should lead to a plan that will optimize the profitability of the reservoir to the operator on several fronts. Often the target or targets can be defined adequately with existing data, but there are instances in which additional information may have to be collected to reduce uncertainty about the target size to an acceptable level.

In some cases the scope of the reservoir management plan will include the entire field, but more often, certain zones or areas of the field will present the best development of the target situation. Additional data may have to be gathered on a field-wide scale to locate the target or targets accurately. If additional oil recovery is the target, questions such as whether the oil is mobile or immobile may also have to be addressed.

Identifying appropriate technologies to achieve the target may involve gathering yet more information in order to evaluate not only the technical appropriateness of potential technologies, but to arrive at an economic ranking of potentially acceptable technologies as well. For example, when the target is improved recovery, this step will include a first-pass screening evaluation of a wide variety of technologies, followed by an in-depth evaluation of the appropriateness of the resulting top-ranking recovery technologies.

Optimizing an implementation scheme for selected technologies can require major data collection and analysis efforts, especially if recovery technologies are a focus. Reservoir characterization in particular may need to be done in great detail to allow development of models to predict recovery and economic results with a sufficiently low degree of uncertainty. Well placement and completion configurations will be strongly dependent on the results of this modeling optimization. Implementation of new technologies in a reservoir is likely to mean that operational procedures and associated technologies may need to be adjusted for best reservoir performance.

7.3 Summary of the Plan-Building Process for East Randolph Field

Two items of context associated with East Randolph field had an especially important bearing on the development of the reservoir management plan for the reservoir. First, the field has been and continues to be developed by small independent operators. Second, the field has been entirely

developed in the 1990s. In fact, development is still going on as efforts continue to define the productive limits of the field.

In the proposal submitted by the operators, they outlined a list of potential targets or opportunities to pursue as goals for the reservoir management plan to address. The list included:

- Optimumization of development and infill well locations
- Selection and implementation of an improved recovery method
- Optimumization of hydraulic fracturing techniques
- Development of solutions for paraffin buildup problem in producing wells

In the proposal, the operators also suggested project tasks and teaming arrangements that might be used to best address these issues.

A kickoff meeting of all project participants was held at the project outset to further prioritize targets and to assign specific plan development tasks to team members. It was expected that the plan development process would be flexible and capable of changing to accommodate the course suggested by new information obtained.

Reservoir characterization played a major role in arriving at the reservoir management plan for this project, particularly in pursuit of the targets selected as highest priority (i.e., defining development and infill well locations and selecting an optimum secondary recovery method). A series of incremental and sometimes iterative steps was performed in arriving at the final reservoir characterization model employed. The steps involved analysis of existing data, identifying data insufficiencies, obtaining and incorporating new information into the emerging model, and testing the predictive limits of the model.

At the project outset, field limits were not yet accurately defined; pre-project estimates of OOIP were approximately 4.4 million bbl. Although the three productive sandstone intervals (zones 2, 3A, and 3B) in the Rose Run were recognized as such, the high GOR observed for most wells (1,500–2,000 scf/stb) was attributed to conditions in all three sandstone zones.

Initial geologic work with neutron and density logs suggested that the uppermost sandstone (zone 2) had a much higher gas saturation. Analysis of production data showed a correlation between high initial GORs and occurrence of a well-developed upper sandstone (zone 2), further suggesting a possible gas cap. Field-wide work based on logs and previously existing sidewall core analysis data determined structural heterogeneities (faults), vertical layering of rock properties, and horizontal variations in rock properties. Zone mapping and volumetric analysis based on this geologic model yielded an OOIP figure of approximately 11 million bbl. Considering its potential impact on continued development and future recovery, participants considered it important to resolve the discrepancy in OOIP estimates.

In parallel with the initial geological work and as an initial and potentially cost-effective check on reservoir parameters, a single-well reservoir model was developed on one of the highest GOR

wells in the field. PVT parameters input to this model were derived using published correlation techniques from initial reservoir parameters. Relative permeability and capillary pressure data input to the model were taken from analogous nearby fields. Model results were unstable in predicting production and indicated the need for more representative values for PVT and relative permeability parameters, additional field pressure data, and field volumetric information. As a result, a pressure buildup test was run and surface-recombined fluid samples were obtained from an existing field well.

The new PVT data (which indicated only 485 scf/stb), new pressure data, and production data were then used in a material balance calculation. A sensitivity analysis done on gas/oil volume ratios indicated that gas/oil volume ratios in the range of 0.16 to 0.2 would yield OOIP values in the observed range of 13 to 11 million bbl. A gas/oil volume ratio of 0.17 and an OOIP of 12 million bbl yielded a reasonable match with observed field pressure history. This analysis confirmed that the field's high GOR was not just a result of gas coming out of solution.

A second single-well simulation was run using a 3-layer (1 gas layer, 2 oil layers) model, the new PVT data and, again, relative permeability data from analogous fields. This modeling confirmed zone 2 as predominantly a gas zone and accurately predicted reservoir pressure encountered by a subsequently drilled well at the edge of the modeling area. Predictions, however, were still found to be sensitive to relative permeability data, so a recommendation was made that this new information be obtained.

An infill well was drilled and cored, and relative permeability and capillary pressure data were obtained on samples from the whole core (see Appendix A). A CMR log was run to better define water saturation distribution, and an FMI log was run to investigate distribution and orientation of natural fractures. Cleaning the samples for special core analysis also gave insight into the nature of the paraffin deposition problem and the anomalously low measured permeabilities from routine core analysis samples.

As a final step, a full-field simulation was undertaken using all the newly collected information. The simulation study was completed in two steps. The first step, history matching of field production and pressure data, was done holding constant all known field and experimental data. Results of this first step showed a good match with oil and gas production and field pressure data, thus validating the basic model. The second step used the model to predict waterflood and gas re-injection results as potential secondary recovery methods for the field. Simulation results from the two recovery processes indicated that the field has an excellent recovery potential when gas re-injection is implemented. The field oil production rate was maintained at 350 BOPD compared to a sharp decline for the waterflood case. The gas re-injection recovery process will stabilize the reservoir pressure at approximately 2,400 psi, which is above the reservoir saturation pressure of 2,070 psi.

Two important issues had an especially strong influence on development of the reservoir management plan. First, the fact that the field is operated by small independents governed not only the nature of the analyses and improved recovery techniques recommended by the plan,

but also the expenditure of effort and capital in collecting and analyzing data to arrive at the plan. Collection of new information had to be adequately justified. Although mutually supportive evidence from different reliable and cost-effective sources was sought, highly redundant confirmations were avoided. Second, the continued development of the field during formulation of the plan meant that new information had to be considered and incorporated continuously. Rapid development of a plan was necessary to optimize field development and definition activities.

The incremental approach to reservoir description for plan development employed in this project results in an efficiency in data collection. Existing data were analyzed at each step with the objective of determining whether the uncertainty associated with the predictive power of the models based on those data was acceptable. If not, the type and quantity of new data needed to constrain the modeling efforts were identified and obtained after first considering the potential cost-effectiveness of the new information. This approach avoids the collection of unnecessary data and fits very well with the typical independent operator's economic constraints in reservoir characterization.

8.0 TECHNOLOGY TRANSFER

An important aspect of this project was the transfer of information about the methods employed in developing the reservoir management plan, the value of the various analyses, and the technical results and conclusions reached. This information was transferred to independent operators through numerous papers and presentations.

Phillip Salamy prepared a project presentation which was given at the SPE Ohio Section luncheon meeting in Columbus, Ohio, in May 1996. The meeting was well attended, and operators showed real interest in the project. In addition, Salamy met with Belden & Blake the day before the meeting and gave his presentation to the top executives of Belden & Blake at its offices in North Canton, Ohio. The Belden & Blake management are very supportive of this project.

During the fall of 1996, the project team was involved in three significant technology transfer activities which facilitated the transfer of the methods employed, value of using various technologies, and project results to other operators in the region. The first event was the Fourth Annual Technical Canton Symposium, October 8-9, 1996, sponsored by the Ohio Division of Geological Survey. John Thomas of Belden & Blake presented a paper, co-authored with Eugene Safley, on the geologic interpretations and core descriptions of the Rose Run sandstone. The paper was entitled "Improved Reservoir Characterization of the Rose Run Sandstone in the East Randolph Field, Portage County, Ohio."

The second event was the American Association of Petroleum Geologists (AAPG) Eastern Regional Meeting, which was held in Charleston, West Virginia, on October 13-15, 1996. Representatives from BDM-Oklahoma presented a half-day workshop on the Reservoir Management Demonstration Program at this meeting. The attendees were interested in understanding and applying the reservoir characterization techniques in other fields within the Appalachian basin. In addition, two papers were presented by BDM-Oklahoma in the technical sessions. The first paper, "Some Practical Aspects of Reservoir Management," an overview of various aspects of the Reservoir Management Demonstration Program, was presented by Mike Fowler. The second paper, "Improved Reservoir Characterization of the Rose Run Sandstone in the East Randolph Field, Portage County, Ohio," was presented by Eugene Safley and focused on the geologic methods and interpretations conducted under the East Randolph field project.

The third technology transfer event was the Eastern Regional SPE meeting, held in Columbus, Ohio, on October 23-25, 1996. Two papers were presented at this meeting. The first, "Some Practical Aspects of Reservoir Management," an overview of various aspects of the Reservoir Management Demonstration Program, was presented by Mike Fowler. The second, "Application of Reservoir Management to the East Randolph Field: Reservoir Engineering Study," focused on the reservoir engineering aspects of the East Randolph field project. It was presented by Phillip Salamy. (These two papers are reprinted in Appendix B and C, respectively.) The AAPG and SPE

meetings drew participants from the Appalachian, Illinois, and Michigan basins, so the methods employed and results of the project were well publicized.

A paper entitled "The Role of Reservoir Characterization in the Reservoir Management Process as Reflected in the Department of Energy Reservoir Management Program" was presented by Mike Fowler at the Fourth International Reservoir Characterization Conference in Houston, Texas, on March 2-4, 1997. The conference was sponsored by the U.S. Department of Energy, BDM-Oklahoma, and AAPG. The paper showed that reservoir characterization efforts should be appropriately scaled by considering the context of the reservoir management strategy being considered.

Eugene Safley will present the final results of this project at the AAPG Eastern Regional Meeting in Lexington, Kentucky in September 1997.

Several of the papers presented at regional conferences are available on the Internet on the National Petroleum Technology Office's homepage (www.npto.doe.gov) under the link "Get the latest news on NPOT projects and events." The papers, "Some Practical Aspects of Reservoir Management" by Mike Fowler and "Application of Reservoir Management to the East Randolph Field: Reservoir Engineering Study" by Phillip Salamy, are complete with graphics for operators to review the techniques used and analyze results of the project. Additional papers concerning methodologies, value, and results achieved will be put on the Web in the future.

9.0 REFERENCES

- Amaefule, J. O., M. Altunbay, D. Tiab, D. G. Kersey, and D. K. Keelan. 1993. Enhanced Reservoir Description: Using Core and Log Data to Identify Hydraulic (Flow) Units and Predict Permeability in Uncored Intervals/Wells. SPE Paper 26436 presented at the 1993 68th SPE Annual Technical Conference and Exhibition, October 3-6, Houston, TX.
- Beal, C. 1946. The Viscosity of Air, Water, Natural Gas, Crude Oil and Its Associated Gases at Oil Field Temperatures and Pressures. *Transactions of AIME* 165: p. 94-115.
- Brown, F. G. 1992. Microbes: The Practical and Environmental Safe Solution to Production Problems, Enhanced Production, and Enhanced Oil Recovery. SPE Paper 23955 presented at the 1992 SPE Permian Basin Oil and Gas Recovery Conference, March 18-20, Midland, TX.
- Bryant, R. S., A. K. Stepp, K. M. Bertus, and T. E. Burchfield. 1994. Microbial Enhanced Waterflooding Field Tests. SPE/DOE Paper 27751 presented at the SPE/DOE Ninth Symposium on Improved Oil Recovery, April 17-20, Tulsa, OK.
- Cole, E. L., R. S. Sawin, and W. J. Weatherbie. 1993. Reservoir Management Demonstration Project. *The University of Kansas, Energy Research Center, Technology Transfer Series* 93-5.
- Cole, E. L., M. L. Fowler, S. Jackson, M. P. Madden, T. K. Reeves, S. P. Salamy, and M. A. Young. 1994. *Geological and Production Characteristics of Strandplain/Barrier Island Reservoirs in the United States*. DOE Report No. NIPER/BDM-0227
- Cole, G. A., R. J. Drozd, R. A. Sedivy, and H. I. Halpern. 1987. Organic Geochemistry and Oil-Source Correlations, Paleozoic of Ohio. *AAPG Bulletin* 71 (7): p. 788-809.
- Coogan A. H. and M. U. Maki. 1986. Trapping Configurations for Cambrian Rose Run Production in Ohio. SPE Paper 15922 presented at the SPE Eastern Regional Meeting, November 12-14, Columbus, OH.
- Cramer, J. W. and J. B. Thomas. 1994. Rose Run Stimulation: A Case History of Problem Identification, Research, Planning, Implementation, and Evaluation. SPE Paper 29189 presented at 1994 Eastern Regional Conference and Exhibition, November 8-10, Charleston, WV.
- Dewan, J. T. 1983. *Essentials of Modern Open-Hole Log Interpretation*. Tulsa, OK: PennWell Publishing.
- Fairchild, Jr., N. R., J. Mills, and D. D. Wood. 1996. GRI Advanced Stimulation Technologies Improve Production in Rose Run Formation. SPE Paper 37360 presented at the 1996 SPE Eastern Regional Meeting, October 23-25, Columbus, OH.
- Folk, R. L. 1974. *Petrology of Sedimentary Rocks*. Austin, TX: Hemphill Publishing Company.

- Fowler, M. L., M. A. Young, E. L. Cole, and M. P. Madden. 1996. Some Practical Aspects of Reservoir Management. SPE Paper 37333 presented at the 1996 SPE Eastern Regional Meeting, October 23–25, Columbus, OH.
- Goldring, R. and P. Bridges. 1973. Sublittoral Sheet Sandstones. *Journal of Sedimentary Petrology* 43: p. 736–747.
- Guo, G. and S. George. 1996. *An Analysis of Surface and Subsurface Lineaments and Fractures for Oil and Gas Exploration in the Mid-Continent Region*. DOE Report No. NIPER/BDM-0223.
- Harper, J. A. 1989. Effects of Recurrent Tectonic Patterns on the Occurrence and Development of Oil and Gas Reservoirs in Western Pennsylvania. *Northeastern Geology* 11: p. 225–245.
- Hassler, G. and E. Brunner. 1945. Measurement of Capillary Pressures in Small Core Samples. *Transactions of AIME* 160: p. 114.
- Hine, A. C. 1977. Lily Bank, Bahamas: History of an Active Oolite Sand Shoal. *Journal of Sedimentary Petrology* 47: p. 1554–1582.
- Honarpour, M. and S. M. Mahmood. 1988. Relative Permeability Measurements: An Overview. SPE Paper 18565 Technology Today Series.
- Jackson, S., M. M. Chang, and M. Tham. 1993. Data Requirements and Acquisition for Reservoir Characterization. DOE Report No. NIPER-615.
- Janssens, A. 1973. Stratigraphy of the Cambrian and Lower Ordovician Rocks in Ohio. *Ohio Division of Geological Survey Bulletin* 64.
- Johnson, H. D., 1978, Shallow Siliciclastic Seas, in Reading, H. G., ed. *Sedimentary Environments and Facies*. New York: Elsevier, p. 207–258.
- Klein, G. deV. 1970. Deposition and Dispersal Dynamics of Intertidal Sand Bars. *Journal of Sedimentary Petrology* 40: p. 1095–1127.
- Mathematical and Computer Services, Inc. 1993. *BOAST 3—A Modified Version of BoastII with Post Processors B3PLOT and COLORGRID—Users Guide*. Prepared for Louisiana State University under Contract with US DOE. Contract No. DE-AC22-92BC14831.
- McCormac, M. P. and M. E. Wolfe. 1996. Ohio 1995 Oil and Gas Activity and Exploration Highlights. *Oil & Gas Journal* April 15.
- Miall, A. D. 1984. *Principals of Sedimentary Basin Analysis*. New York: Springer-Verlag.
- Moyer, C. C. 1995. Geology and Log Responses of the Rose Run Sandstone in Randolph Township, Portage County, Ohio. Paper presented at the Third Annual Technical Canton Symposium, Canton, OH.

- Rajan, R. 1986. Theoretically Correct Analytical Solution for Calculating Capillary Pressure-Saturation from Centrifuge Experiment. Paper presented at the SPWLA 27th Annual Logging Symposium, June 9-13.
- Read, J. F. 1989. Controls on Evolution of Cambrian-Ordovician Passive Margin, U.S. Appalachians. In Crevello, P. D., et al., eds. *Controls on Carbonate Platform and Basin Development*. Society of Economic Paleontologists and Mineralogists Special Publication.
- Reinech, H. E. and F. Wunderlich. 1968. Classification and Origin of Flaser and Lenticular Bedding. *Sedimentology* 11: p. 99-104.
- Riley, R. A., J. A. Harper, M. T. Baranoski, C. A. Laughrey, and R. W. Carlton. 1993. *Measuring and Predicting Reservoir Heterogeneity in Complex Deposystems: The Late Cambrian Rose Run Sandstone of Eastern Ohio and Western Pennsylvania*. Morgantown, WV: Appalachian Oil and Natural Gas Research Consortium.
- Ringrose, P. S., K. S. Sorbie, F. Feghi, G. E. Pickup, and J. L. Jensen. 1991. Relevant Reservoir Characterization: Recovery Process, Geometry, and Scale. *Proceedings of the European IOR Symposium*: p. 15-25.
- Ryder, R. T., R. C. Burruss, and J. R. Hatch. 1991. *Geochemistry and Selected Oil and Source Rock Samples From Cambrian and Ordovician Strata, Ohio-West Virginia-Tennessee, Part of the Appalachian Basin*. U. S. Geological Survey Open File Report 91-434.
- Saleri, N. G., R. M. Toronyi, and D. E. Snyder. 1991. Data and Data Hierarchy. SPE Paper 21369 presented at Middle East Oil Technical Conference and Exhibition, Manama, Bahrain: p. 279-292.
- Schlumberger. 1989. *Log Interpretation—Principles/Applications*. Houston: Schlumberger Educational Services.
- Schrider, L. A., R.J. Watts, and J. A. Wasson. 1970. An Evaluation of the East Canton Oil Field Waterflood. SPE Paper 2764 presented at the SPE Eastern Regional Meeting, November 6-7, 1969, Columbus, OH.
- Shinn, A. E., 1983, Tidal Flat Environment. In Scholle, P. A., et al., eds., *Carbonate Depositional Environments*. AAPG Memoir 33: p. 171-211.
- Tearpock, D. J. and R. E. Bischke. 1991. *Applied Subsurface Geologic Mapping*. Englewood Cliffs, New Jersey: Prentice Hall.
- Teufel, L. W. and J. C. Lorenz. 1992. Control of Fracture-Reservoir Permeability by Spatial and Temporal Variations in Stress Magnitude and Orientation. *AAPG Annual Meeting Program and Abstracts*: p. 131.

Thomas, J. B. and L. E. Safley. 1996. Improved Reservoir Characterization of the Rose Run Sandstone in East Randolph Field, Portage County, Ohio. Paper presented at the Fourth Annual Technical Canton Symposium, October 8–9, Canton, OH.

Wiggins, M. L. and R. A. Startzman. 1990. An Approach to Reservoir Management. SPE Paper 20747 presented at the 1990 65th Annual Technical Conference and Exhibition, September 23–26, New Orleans, LA.

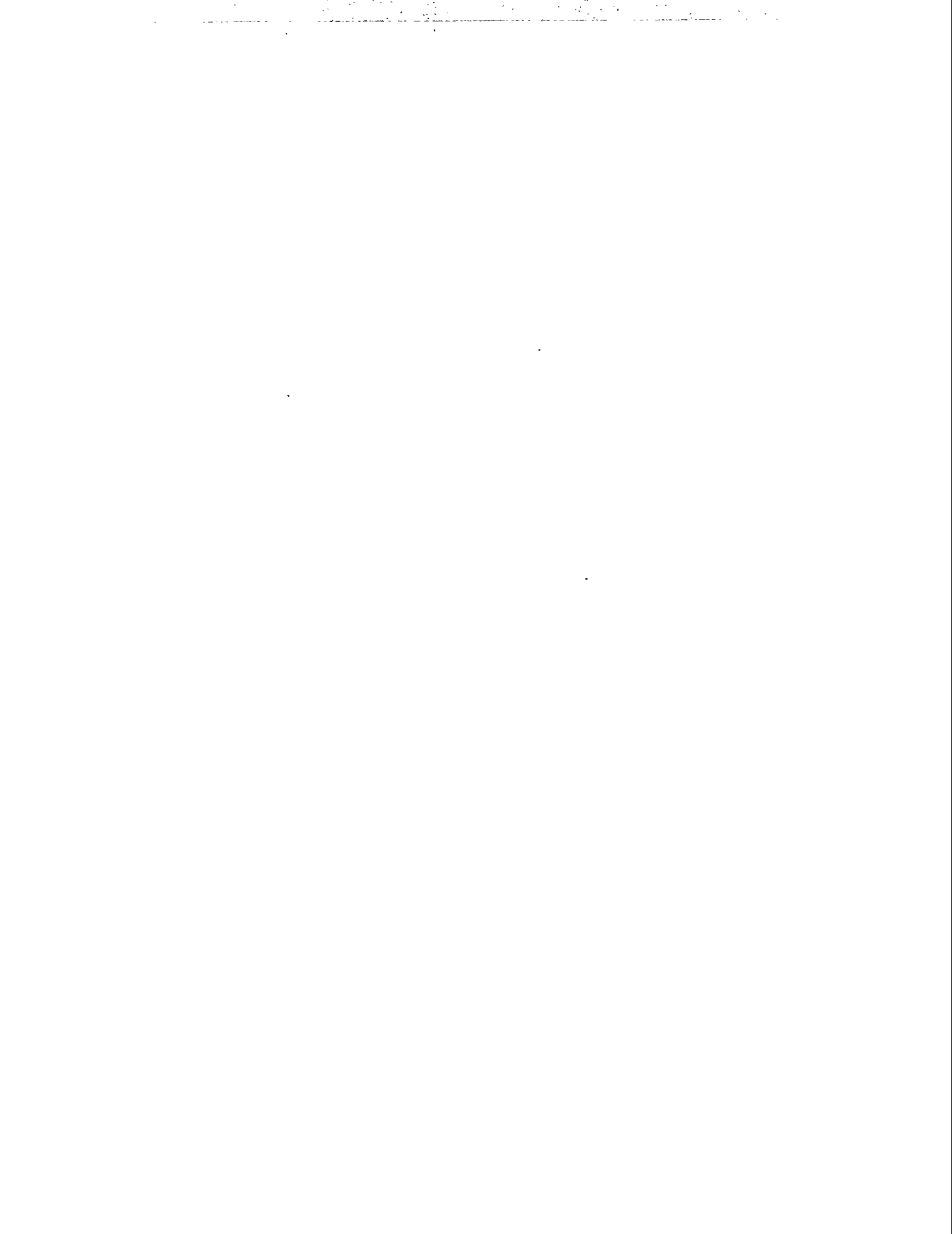
Wilson, J. L. 1983. Middle Shelf Environment. *In* Scholle, P. A., et al., eds., *Carbonate Depositional Environments*. AAPG Memoir 33: p. 297-345.

Thakur, G. C. and A. Satter. 1994. Integrated Petroleum Reservoir Management—A Team Approach. Tulsa, OK: PennWell Publishing Company.

APPENDIX

A

SPECIAL CORE ANALYSES



This report describes results from tests conducted by Dan Maloney at BDM-Oklahoma on core plugs from the McGuire No. 2 well. Plugs tested by BDM-Oklahoma were cut from whole core sections by OMNI Laboratories of Houston, Texas. Sample locations were specified by Eugene Safley of BDM-Oklahoma. Tests by BDM-Oklahoma were conducted at the NIPER facility in Bartlesville, Oklahoma.

Plugs received by BDM-Oklahoma were labeled according to depth; depths used in this report are those provided with the core plugs. When the plugs were first received, Eugene Safley indicated that plug and log depths may differ by about 4 ft.. Core, log, and reservoir depths should be correlated when comparing core, log, and reservoir descriptions.

Summary of Results

Core Plug Cleaning. BDM-Oklahoma cleaned plugs by multiple extraction/soak cycles using toluene and methanol solvents. Toluene was used to remove oil and paraffin from the plugs. Methanol was used to remove the toluene, which sometimes leaves outer plug surfaces oil-wet. The rigorous cleaning techniques employed by BDM-Oklahoma provided routine permeability and porosity results that were, for some plug depths, higher than those measured by OMNI Labs.

Test Fluids. Synthetic brine and oil were used for BDM-Oklahoma core analyses. Synthetic fluids were prepared considering chemical compositions and characteristics of the reservoir fluids. The paraffin content of the crude oil was such that it could not be used for room-temperature corefloods.

Routine Gas Permeability (k_g) and porosity (ϕ) Measurements. Gas permeabilities and porosities exhibited considerable variability. For the group of plugs tested, permeabilities ranged from submillidarcy values to about 17 md. Porosities ranged from about 0.7% to 11%. Cracks were visually evident in two plugs and were suspected in two other plugs. At reservoir stress conditions, these cracks are probably closed and do not provide for increased permeability beyond that contributed by the rock matrix. For the plugs measured, it appears that samples with porosities less than about 4% have permeabilities of 0.01 md or less at reservoir conditions.

Water Permeability (k_w) and Porosity Measurements at Simulated Reservoir Stress Conditions. Pore volumes for most of the plugs were reduced by 4% to 6% as the net confining pressure changed from 300 psig to 4,250 psig. Brine permeabilities measured when the plugs were subjected to 4,250 psig net confining pressure were, on average, about seven times lower than gas permeabilities measured with minimal confining pressure.

Moveable Oil from Waterflood Susceptibility, Steady-State, and Capillary Pressure Tests. Residual brine saturations that were achieved in the laboratory during oilfloods of four brine saturated plugs (in dynamic displacement and centrifuge tests) ranged from 31.5% to 44.9%. Residual oil

saturations achieved during low-rate brinefloods and centrifuge tests for the same four plugs ranged from 25% to 45%. In these tests, oil recoveries ranged from 30% to 58% of OOIP.

Wettability Indices. From centrifuge tests on two plugs using synthetic brine and oil, U.S. Bureau of Mines wettability indices were close to 1, indicating that the plugs were preferentially water-wet.

Pore Size Descriptions from Mercury Intrusion Tests. Mercury intrusion tests were performed on samples from four plugs. Plug 7319.1 was found to be predominantly microporous, with a median pore diameter of 0.0098 μm . Median pore diameters for the other plugs ranged from 0.4 to 2.9 μm . Pore size descriptions indicate that the rock is susceptible to plugging if injected fluids are not filtered to remove fine particles.

Nuclear Magnetic Resonance (NMR) Measurements. NMR measurements suggest that cleaning techniques employed by BDM-Oklahoma may not have completely removed all paraffin from the plugs. Pore size distributions from NMR interpretations appear to be consistent with results from mercury intrusion tests.

Test Descriptions and Results

Core Plug Cleaning

BDM-Oklahoma cleaned 15 core plugs in preparation for routine and special core analyses. After being placed in extractors, the plugs were soaked in toluene for 5 days. The plugs were extracted with hot toluene for 8 hours, followed by a 16-hour soak period. Extraction and soak cycles were repeated 5 times. The toluene was then replaced with methanol and the plugs were allowed to soak for 2 days before extracting for 8 hours. The methanol was then replaced by toluene, and the plugs underwent two more cycles of soaking for 16 hours and extracting for 8 hours before a final methanol extraction. They were then dried in a 50°C forced air oven.

Test Fluids

Routine core analyses were conducted using nitrogen for gas permeability measurements and helium for porosity measurements. Gas permeabilities are interchangeably expressed as k_g and k_a in this report.

A synthetic brine was prepared following a reservoir water analysis provided by Belden & Blake. Sodium iodide was added to the brine to substitute for some of the other sodium salts in order that X-ray techniques could be used to determine fluid saturation contents of core plugs during flow tests. Synthetic brine constituents expressed by weight percentages were 6.470% NaI, 14.395% NaCl, 9.300% CaCl_2 , 0.332% KCl, and 69.503% water. The brine was filtered through a 0.45- μm filter. The viscosity and density of the brine at laboratory temperature (74°F) were 1.949 cp and 1.236 g/cm³, respectively.

A sample of stock tank crude oil was provided by Belden & Blake. The crude oil was filtered through a 0.45- μm filter. Crude oil viscosities were measured at temperatures ranging from 67° to 128°F. Results are shown in Figure A-1. The data trend appears to change slope at 85°F. At room temperature, paraffin from the crude oil coated everything that was exposed to the oil. Although the paraffin seems to go back into solution when the oil is heated to temperatures about 85°F, it is certainly problematic at room temperature conditions. For this reason, the paraffin content of the crude oil made it unsuitable for room-temperature tests. A laboratory oil was used for special core analysis measurements to avoid problems induced by paraffin buildup. The oil consisted of 8.1% bromodecane and 91.9% Soltrol 200 by weight. Soltrol 200 is an isoparaffinic oil product of Phillips Petroleum Company. At laboratory temperature (74°F), the viscosity and density of the oil were 4.156 cp and 0.814 g/cm³, respectively. The viscosity of the synthetic oil at 74°F was close to that of the crude oil at 120°F.

The interfacial tension of the synthetic brine and synthetic oil was 26.8 dyn/cm at 74°F.

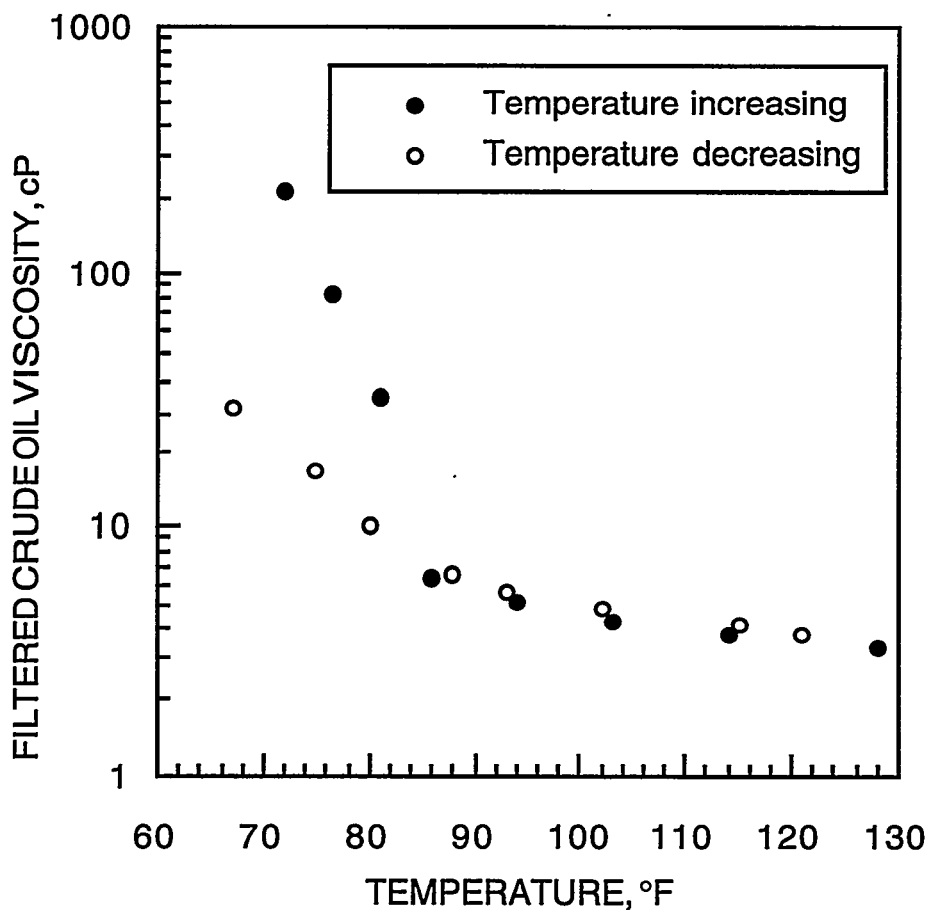


Figure A-1 Viscosities Measured on a Filtered Sample of the Reservoir Crude Oil During Increasing and Decreasing Temperature Cycles

Routine Property Measurements

BDM-Oklahoma's routine permeability and porosity measurements were made using nitrogen (permeability) and helium (porosity) gases. Plugs were subjected to 100 psig confining pressure during routine tests. Results are shown in Table A-1. Table A-1 also includes routine property results from OMNI Labs for comparison. Please note that more rigorous cleaning techniques are likely responsible for some of the higher permeabilities measured at BDM-Oklahoma.

Table A-1 Routine Permeability and Porosity Results

Sample Depth, ft	Gas Permeability, md	Helium Porosity, %	Lab
7318.10	<0.01	0.7	BDM
7319.10	0.01	1.7	BDM
7321.45	0.06	5.1	OMNI
7322.20	0.17	7.0	OMNI
7323.10	8.58	2.1	BDM
7327.00	1.02	11.2	OMNI
7328.30	3.04	10.9	BDM
7328.50	1.74	8.6	OMNI
7330.30	12.99	7.9	BDM
7330.95	1.20	7.3	OMNI
7332.30	5.81	10.8	BDM
7332.80	0.80	9.9	OMNI
7333.10	3.76	11.1	BDM
7335.60	7.09	1.2	BDM
7336.00	<0.01	2.8	OMNI
7339.20	8.46	3.8	BDM
7339.90	<0.01	3.3	OMNI
7342.40	1.98	7.9	OMNI
7343.00	16.59	8.4	BDM
7344.00	11.60	0.9	BDM
7346.35	<0.01	2.6	OMNI
7348.30	2.13	10.0	BDM
7348.85	0.54	8.8	OMNI
7349.30	1.73	10.6	BDM
7349.80	<0.01	3.5	OMNI
7350.30	0.02	4.2	BDM
7352.30	<0.01	1.8	BDM

Figure A-2 is a plot of data from Table A-1 for plugs with permeabilities of 0.01 md or greater. Four of the plugs, from depths of 7323.1, 7335.6, 7339.2, and 7344.0 ft, had porosities less than 4% but gas permeabilities of about 10 md. Cracks were visually evident in two of the plugs (7335.6 and 7344.0). The other two plugs are suspected to contain cracks as well. Plugs 7323.1 and 7335.6 were essentially impermeable to brine when subjected to 4,250 psig confining pressures. From these considerations, it appears that samples with porosities less than about 4% have permeabilities of 0.01 md or less at reservoir conditions.

Figures A-3 and A-4 show permeability and porosity data from OMNI and BDM-Oklahoma plotted against depth. Lines on the graphs that link data points are included to show changes in measured results with depth rather than to infer values between measurements. Results for plugs 7323.1, 7335.6, 7339.2, and 7344.0 are not included in these two figures because permeabilities for these samples are believed to be nonrepresentative. The high permeabilities and low porosities for these four plugs suggest the presence of high permeability cracks, as described in the previous paragraph. These cracks are probably closed at reservoir stress conditions.

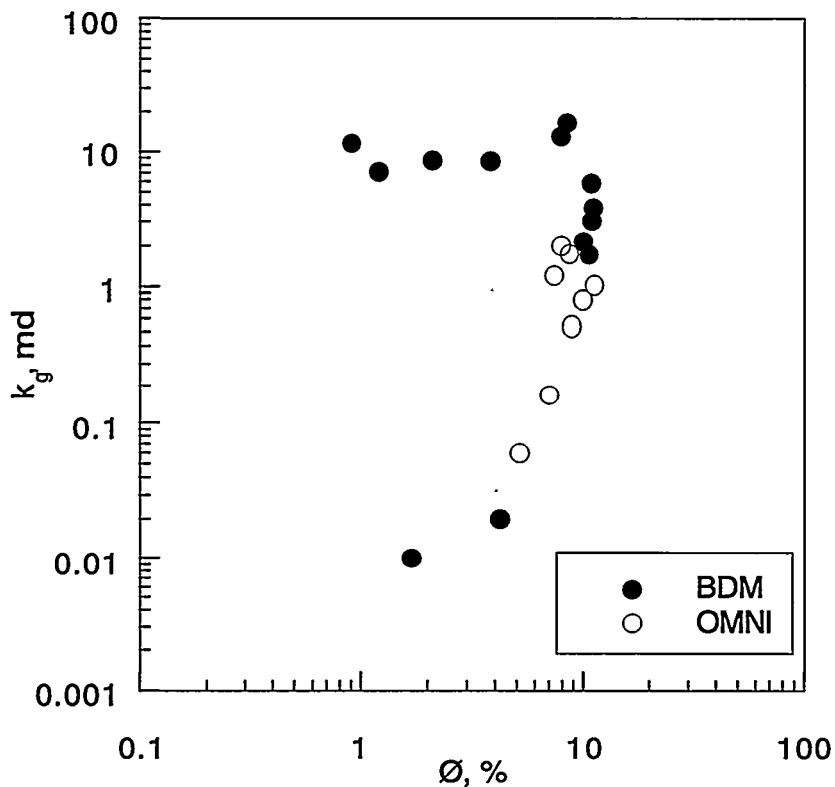


Figure A-2 Gas Permeabilities from OMNI and BDM-Oklahoma Labs. BDM-Oklahoma measurements were performed with 100 psig confining pressure.

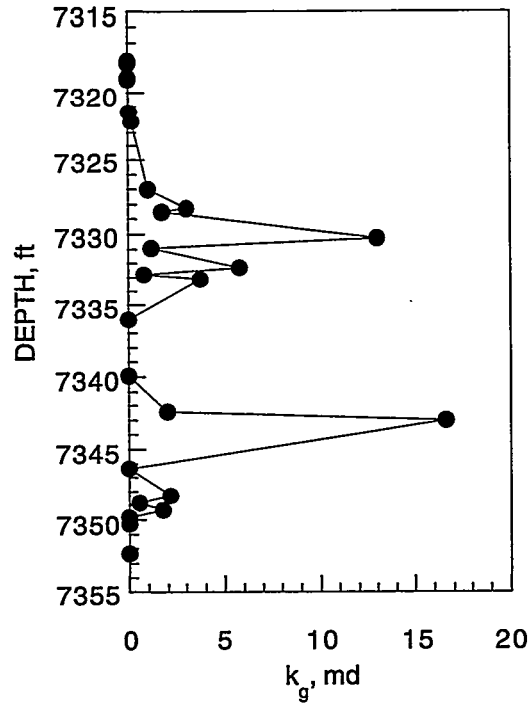


Figure A-3 Gas Permeabilities from Routine Property Measurements by Depth

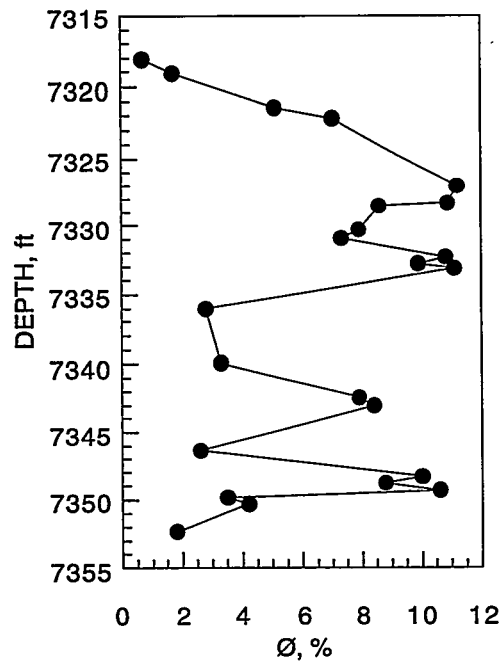


Figure A-4 Porosities from Routine Property Measurements by Depth

Brine Permeability Measurements

Eight core plugs from the McGuire No. 2 core were selected for brine permeability measurements. The plugs were saturated with brine by first placing the dry plugs in a pressure vessel, which was then evacuated using a vacuum pump. Next, degassed brine was introduced to the evacuated vessel. After the vessel filled with brine, the brine pressure was increased to 1,000 psig and maintained overnight. The pressure was then gradually reduced to atmospheric conditions. The brine-saturated plugs were then available for "squeeze-out" and brine permeability measurements. Plug pore-volume measurements were double-checked by dividing differences between brine-saturated and dry weights by the density of the brine. Pore volumes measured in this manner were similar to those previously established by helium measurements.

Plugs were individually loaded into coreholders. As confining pressure was slowly increased in steps, volumes of brine squeezed out of the plugs were measured. Brine volumes produced as the confining pressure was first increased from 0 psig to 300 psig were attributed primarily to surface effects when the coreholder sleeve and core end-pieces firmly seal against the rock sample. For stresses greater than 300 psig, brine volumes squeezed out of a plug were considered to result from pore volume compression. The plugs were ultimately subjected to 4,250 psig net confining pressure, simulating reservoir rock-stress conditions.

Figure A-5 shows apparent decrease in pore volume vs. confining pressure results for the eight core plugs. Analysis of Figure A-5 indicates that pore volumes for most of the plugs were reduced by 4-6% as the confining pressure changed from 300 psig to 4,250 psig.

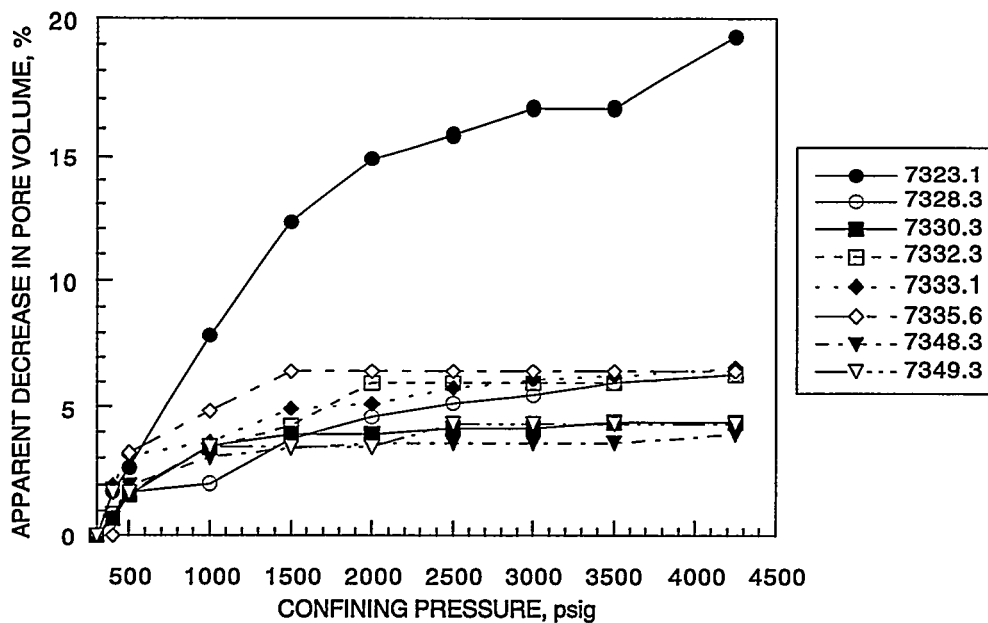


Figure A-5 Changes in Pore Volumes with Stress Interpreted from Squeeze-Out Measurements.

Brine permeability tests were performed with 4,250 psig net confining pressure applied to the plugs. Permeabilities for each plug were calculated using rate and pressure drop measurements from four different injection rates. Table A-2 shows permeability and porosity measurements from routine (low-pressure) gas measurements as well as from brine permeability and porosity measurements at simulated reservoir stress conditions (4,250 psig net confining pressure). Permeabilities for plugs 7323.1 and 7334.6 were too low to be measured.

Figure A-6 shows measured brine permeabilities from 4,250 psig net confining pressure conditions plotted against gas permeabilities measured with 100 psig confining pressure. The correlation equation shown is suggested for estimating brine permeabilities using gas permeability data (within the range of measurements shown).

Table A-2 Petrophysical Properties of Selected Plugs at 100 and 4,250 psi Net Confining Pressure

Plug	100 psig					4,250 psig			
	GV, cm ³	PV, cm ³	BV, cm ³	k _a , md	φ, %	PV, cm ³	k _w , md	φ, %	
7318.1	53.463	0.36	53.819	<0.01	0.7				
7319.1	53.555	0.94	54.497	0.01	1.7				
7323.1	53.012	1.14	54.152	8.58	2.1	0.92	<0.01	1.7	
7328.3	47.962	5.85	53.816	3.04	10.9	5.48	0.81	10.3	
7330.3	50.027	4.32	54.347	13.0	7.9	4.13	1.92	7.6	
7332.3	48.679	5.87	54.554	5.81	10.8	5.50	0.72	10.2	
7333.1	48.723	6.07	54.793	3.76	11.1	5.67	0.424	10.4	
7335.6	52.676	0.62	53.295	7.09	1.2	0.58	<0.01	1.1	
7339.2	53.321	2.09	55.416	8.46	3.8				
7343.0	50.667	4.67	55.341	16.59	8.4				
7344.0	53.962	0.49	54.452	11.6	0.9				
7348.3	49.949	5.57	55.523	2.13	10.0	5.35	0.386	9.7	
7349.3	48.820	5.78	54.601	1.73	10.6	5.53	0.147	10.2	
7350.3	53.970	2.34	56.307	0.02	4.2				
7352.3	55.227	0.99	56.217	<0.01	1.8				

GV = grain volume

PV = pore volume

BV = bulk volume

k_a = gas permeability

k_w = brine permeability

φ = porosity

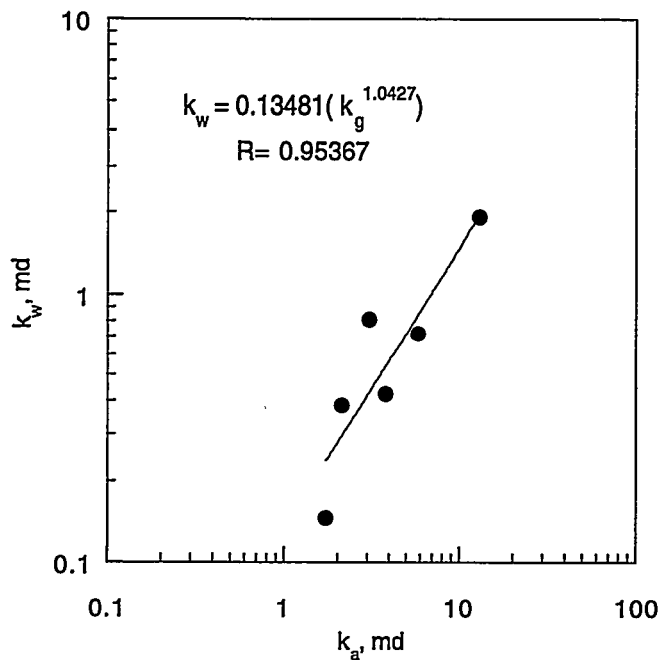


Figure A-6 Comparison of Brine Permeability Measurements (4,250 psig Confining Pressure) with Air Permeability Measurements (100 psig Confining Pressure)

Waterflood Susceptibility Test

A waterflood susceptibility test was conducted on plug 7333.1. The brine-saturated plug was placed in a coreholder, then subjected to 4,250 psig net confining pressure. Brine was injected through the plug at several rates ranging from 10 ml/hr to 40 ml/hr. Pressure drops were measured across the total length of the plug and across a 2.54-cm section near the center of the plug. Figure A-7 shows pressure drop and flow rate results from brine permeability measurements. The slopes of the best-fit lines through the data sets are also shown on the figure. Permeabilities to brine, calculated from pressure-drop and flow-rate data, were 0.238 md across the total length and 0.404 md across the center section. The permeability of the plug toward its center was higher than the permeability of the whole sample.

The plug was flooded with the laboratory oil at a rate of 150 ml/hr to achieve a residual brine saturation condition. The residual brine saturation, expressed as a fraction of pore volume, was 0.405. The permeability of the sample to oil was measured using techniques similar to those described for brine permeability measurements. The permeability of the sample to oil was 0.887 md across the entire length, and 1.741 md across the center section.

As stated in a previous section of this report, the permeability of the sample to gas under conditions of low confining pressure was 3.76 md. With 4,250 psig net confining pressure, permeabilities across the center section of the plug were 0.40 md for brine with $S_w = 1.000$, and 1.74 for oil with $S_{wr} = 0.405$. For water-wet samples, it is not uncommon for the permeability of

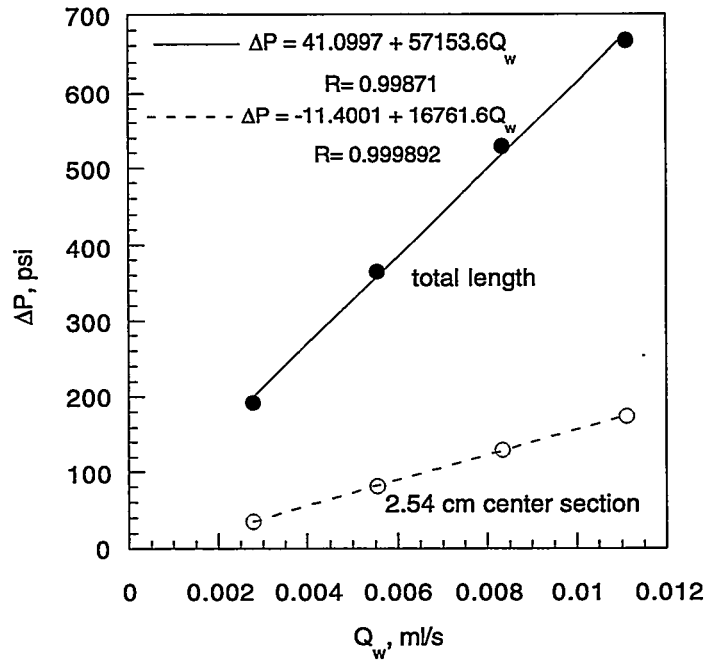


Figure A-7 Pressure Drop and Rate Data from Brine Permeability Measurements on Plug 7333.1

the sample to oil at a residual brine saturation condition to be higher than the permeability of the sample to brine when completely brine saturated.

Prior to waterflooding the sample, the oil injection rate was reduced to 3 ml/hr. The waterflood was started by switching injection from oil to brine at the 3 ml/hr rate. For this plug, 3 ml/hr yields an injection rate of 0.53 pore volumes per hour, or a linear displacement rate of 2 ft/day. In-situ saturations, production histories, and pressure histories were recorded with time throughout the test.

Figure A-8 shows saturation profiles within the sample at various times during the test. As shown in the figure, brine reached the outlet face of the sample after about 0.61 hours of brine injection. The higher than average brine saturation buildup at the outlet end of the sample toward the end of the test may have resulted because of capillary end effects.

Figure A-9 shows changes in bulk brine saturation vs. pore volumes of brine injected in detail for the first 2 pore volumes of injection. Figure A-10 shows changes in bulk brine saturation for the duration of the test. Figures A-11 and A-12 show oil recovery results as functions of brine throughput. Overall, 57.6% of the original oil in place was recovered by the waterflood.

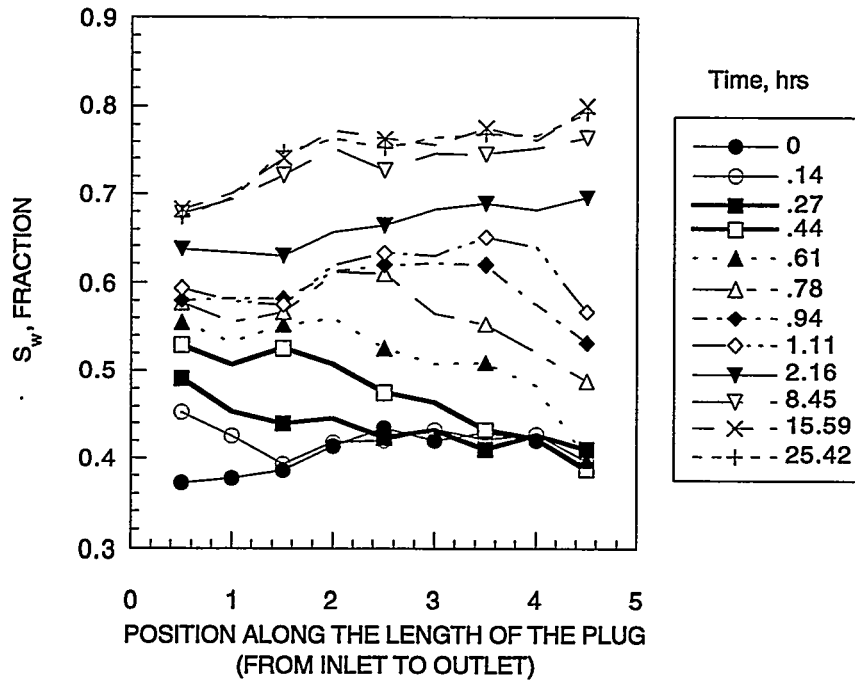


Figure A-8 Saturation Profiles during the Waterflood Test on Plug 7333.1. The inlet was at position 0. The flow direction was from inlet to outlet.

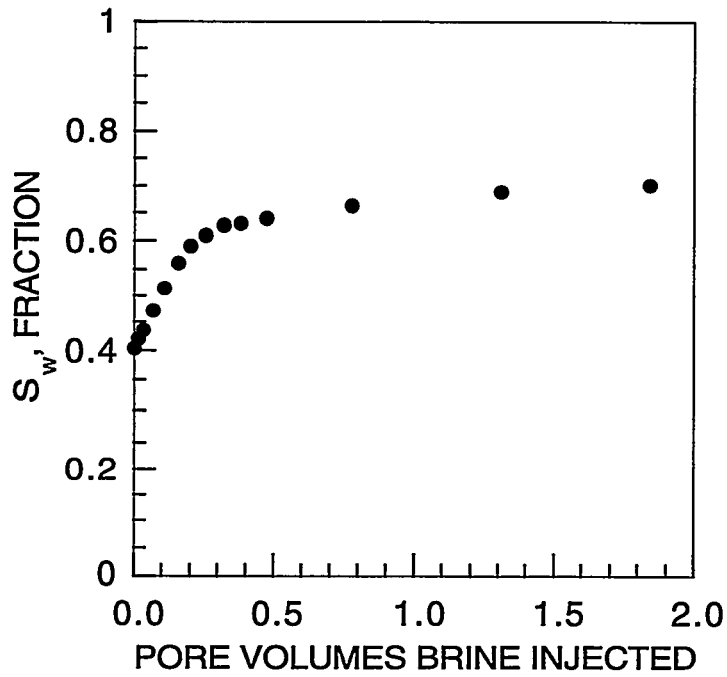


Figure A-9 Bulk Brine Saturation Changes during the First 2 Pore Volumes of Brine Injection

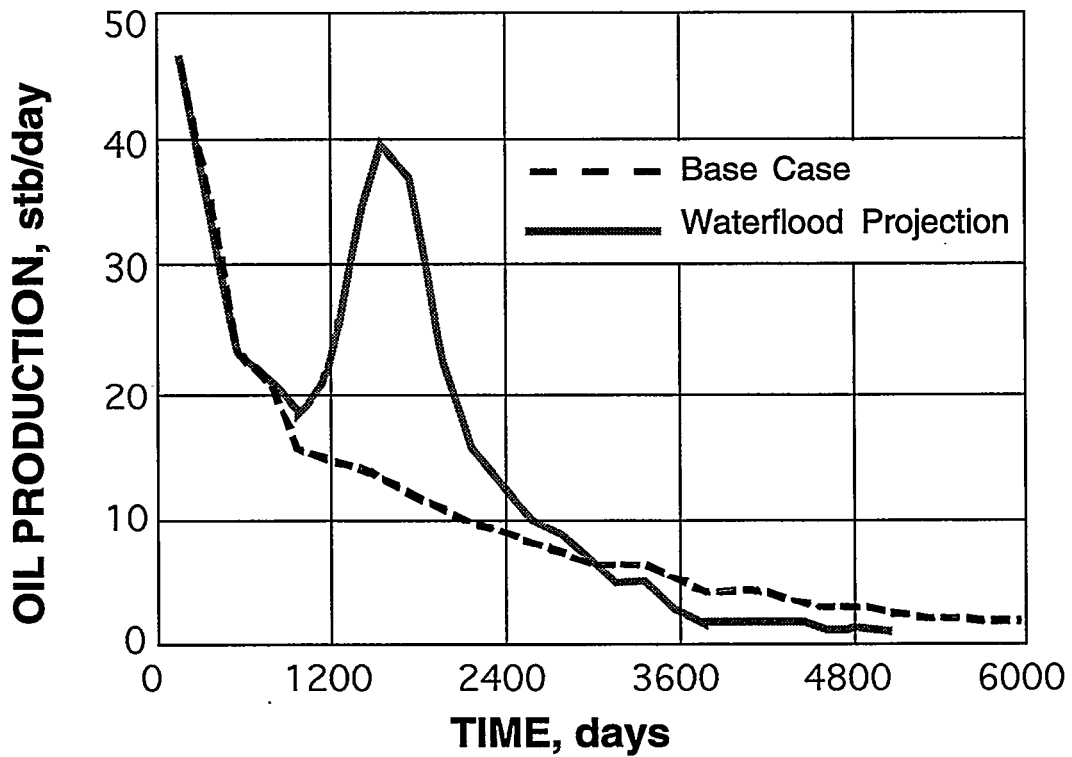


Figure A-10 Bulk Brine Saturation Changes throughout the Test

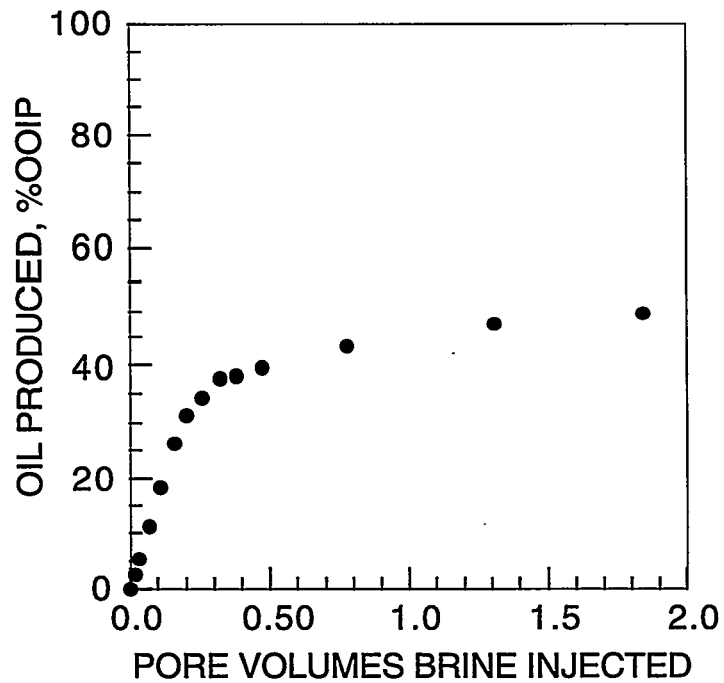


Figure A-11 Oil Recovery during the First 2 Pore Volumes of Brine Injection

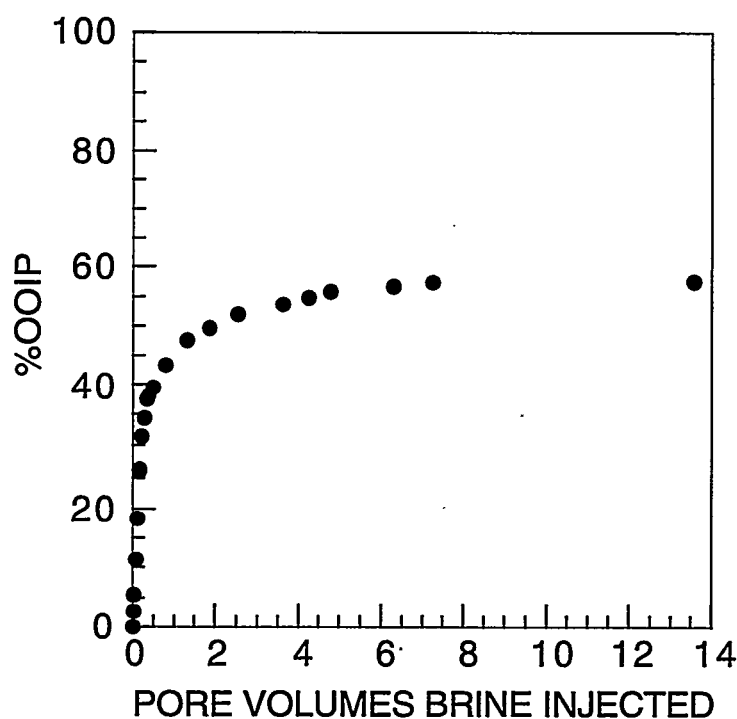


Figure A-12 Oil Recovery throughout the Test

Steady-State Oil-Brine Relative Permeability Measurements

Steady-state imbibition and second-drainage oil-water relative permeability measurements were performed at 74°F on sample 7328.3 from the zone 3A sand. Fluid saturations were monitored using a linear X-ray scanner. End-point relative permeabilities and two-phase permeability results from six oil-water fractional flow ratios are reported.

Sample 7328.3 (length 5.07 cm, diameter 3.68 cm) was placed inside a coreholder and confined at a pressure of 4,250 psig. Pressure taps on the side of the coreholder permitted differential pressures to be measured across a 2.54-cm segment near the middle of the core. Test fluids consisted of tagged test brine (6.47% NaI, 14.40% NaCl, 9.30% CaCl₂, and 0.33% KCl by weight in water), untagged brine (6% KCl by weight in water), and tagged oil (Soltrol 220 doped with bromodecane to have similar X-ray absorption characteristics as the test brine). Scans of the plug saturated with tagged and untagged brine were used to obtain an X-ray calibration. Note that the test brine was similar in composition to the reservoir brine. Its viscosity and density at 74°F were, respectively, 1.95 cp and 1.236 g/cm³. The test oil had a viscosity of 4.16 cp and a density of 0.814 g/cm³ at 74°F.

The permeability to tagged brine was measured to be 0.806 md. As previously described, routine (100 psig net confining pressure) permeability and porosity results measured with gas were,

respectively, 3.04 md and 10.9%. More than 30 pore volumes of oil were injected at rates up to 25 ft/day, producing differential pressures up to 580 psi, to reach a residual brine saturation of 0.315. An oil permeability of 0.810 md was measured at this condition. Imbibition cycle oil and brine relative permeabilities were measured at six brine fractional flows ranging from 0.05 to 0.975. Saturations were measured using the X-ray scanner. A brine permeability of 0.037 md was measured at the residual oil saturation of 0.450. Second-drainage-cycle oil and brine relative permeabilities were measured at six brine fractional flows ranging from 0.975 to 0.05. A permeability to oil of 0.314 md was measured after the second drainage at a residual brine saturation of 0.294. Relative permeability results are shown in Tables A3 and A4 and Figure A-13. Values have been normalized with respect to the absolute brine permeability of 0.806 md.

Table A-3 Sample 7328.3 Steady-State Imbibition Oil/Brine Relative Permeability Results

f_w , fraction	$S_{w, ave}$, fraction	k_{rw} , fraction	k_{ro} , fraction
0.000	0.315	0.00e+00	1.01e+00
0.050	0.415	6.56e-03	2.66e-01
0.200	0.455	2.01e-02	1.72e-01
0.500	0.488	1.79e-02	3.82e-02
0.900	0.507	2.97e-02	7.04e-03
0.950	0.517	3.21e-02	3.60e-03
0.975	0.522	3.28e-02	1.79e-03
1.000	0.550	4.65e-02	0.00e+00

Table A-4 Sample 7328.3 steady-state second-drainage oil/brine relative permeability results

f_w , fraction	$S_{w, ave}$, fraction	k_{rw} , fraction	k_{ro} , fraction
1.000	0.550	4.65e-02	0.00e+00
0.950	0.526	2.99e-02	3.35e-03
0.900	0.507	2.63e-02	6.24e-03
0.500	0.474	1.40e-02	2.98e-02
0.200	0.455	5.24e-03	4.48e-02
0.050	0.398	1.66e-03	6.90e-02
0.025	0.407	1.20e-03	9.51e-02
0.000	0.294	0.00e+00	3.90e-01

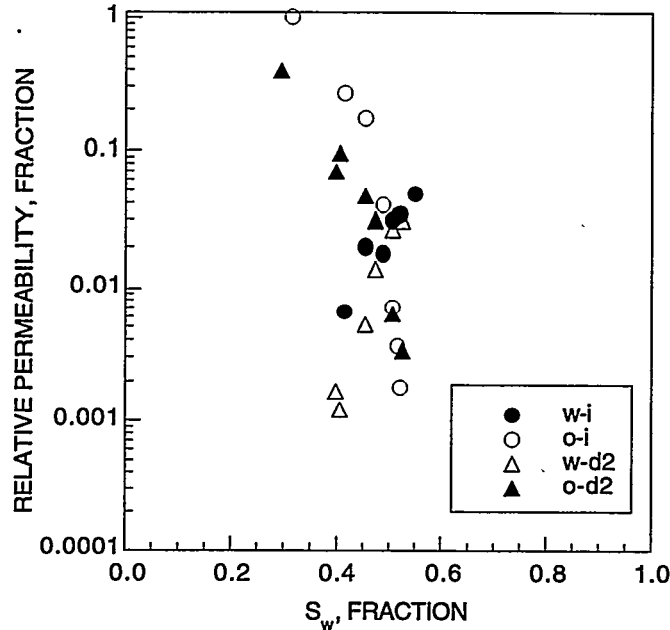


Figure A-13 Steady-State Oil-Brine Relative Permeability Results for Plug 7328.3. Results are normalized with respect to the brine permeability of 0.806 md at $S_w = 1.000$.

Oil-Brine Capillary Pressure and Wettability Measurements

Oil-brine centrifuge tests were performed on sample 7332.3 from the zone 3A sand and sample 7349.3 from the zone 3B sand. Hassler and Brunner (1945) and Rajan (1986) methods were used to interpret capillary pressures from the centrifuge data. The results are reported in Tables A-5 and A-6.

Fluids used during the centrifuge tests were the same as those used in the oil-brine relative permeability tests. The densities of the brine and oil were 1.236 g/cm^3 and 0.814 g/cm^3 , respectively.

The lengths of samples 7332.3 and 7349.3 were 5.09 cm and 5.06 cm, respectively. The distance from the center of rotation to the core bottom during the drainage (oil-displacing-brine) cycles was 8.60 cm. The distance from the center of rotation to the core bottom during the imbibition (brine-displacing-oil) cycle was 16.68 cm.

The brine-saturated plugs were centrifuged in oil at eight centrifuge speeds for up to 24 hours per speed to yield primary drainage capillary pressure vs. saturation data. Care was taken to ensure that the plugs were at equilibrium before increasing the centrifuge speed. The plugs were centrifuged in brine at eight speeds for up to 24 hours to obtain first imbibition cycle capillary pressure and saturation data; they were then centrifuged again in oil at eight speeds for up to 24 hours to yield second drainage cycle capillary pressure and saturation data. NMR measurements were taken of the brine-saturated plugs at the start of the tests and at the end of each centrifuge cycle.

Table A-5 Sample 7332.3 Centrifuge Oil-Brine Capillary Pressure/Wettability Results

Primary Drainage Cycle				Cycle Imbibition				Second Drainage Cycle			
P _c		S _w fraction		P _c		S _w fraction		P _c		S _w fraction	
psi	avg	HB	RJ	psi	avg	HB	RJ	psi	avg	HB	RJ
0.00	1.000	1.000	1.000	0.00	0.449	0.449	0.449	0.00	0.725	0.725	0.725
0.19	1.000	1.000	1.000	-0.44	0.630	0.692	0.680	1.19	0.725	0.725	0.725
1.32	0.971	0.939	0.956	-3.09	0.696	0.716	0.713	1.32	0.725	0.725	0.725
4.66	0.905	0.815	0.851	-10.88	0.715	0.717	0.716	4.66	0.687	0.645	0.661
18.62	0.766	0.629	0.682	-30.20	0.715	0.716	0.716	18.62	0.617	0.562	0.586
51.73	0.601	0.480	0.538	-59.19	0.715	0.717	0.717	51.73	0.537	0.475	0.507
87.43	0.561	0.405	0.464	-97.84	0.715	0.721	0.720	87.43	0.535	0.423	0.459
132.43	0.471	0.349	0.407	-146.15	0.715	0.725	0.724	132.43	0.461	0.380	0.419
186.75	0.449	0.305	0.362	-204.13	0.725	0.730	0.728	186.75	0.440	0.343	0.384
						avg	HB	RJ			
Second Drainage Cycle Area:						15.37	18.52	17.17			
Imbibition Cycle Area:						2.05	1.84	1.61			
Wettability = log(A _{d2} /A _i):						0.88	1.00	1.03			

HB = Hassler-Brunner (1946) method.

RJ = Rajan (191986) method.

Table A-6 Sample 7349.3 Centrifuge Oil-Brine Capillary Pressure/Wettability Results

Primary Drainage Cycle				Imbibition Cycle				Second Drainage Cycle			
P _c		S _w fraction		P _c		S _w fraction		P _c		S _w fraction	
psi	avg	HB	RJ	psi	avg	HB	RJ	psi	avg	HB	RJ
0.00	1.000	1.000	1.000	0.00	0.414	0.414	0.414	0.00	0.591	0.591	0.591
0.19	1.000	1.000	1.000	-0.44	0.556	0.587	0.581	0.19	0.591	0.591	0.591
1.32	0.979	0.979	0.995	-3.07	0.591	0.596	0.595	1.32	0.591	0.591	0.591
4.64	0.965	0.828	0.870	-10.81	0.591	0.592	0.593	4.64	0.591	0.591	0.591
18.55	0.770	0.607	0.668	-30.04	0.591	0.589	0.590	18.55	0.538	0.463	0.493
51.53	0.575	0.439	0.505	-58.86	0.591	0.589	0.589	51.53	0.453	0.392	0.420
87.10	0.519	0.360	0.424	-97.31	0.591	0.591	0.591	87.10	0.432	0.375	0.397
131.93	0.437	0.302	0.364	-145.34	0.591	0.593	0.593	131.93	0.412	0.372	0.387
186.03	0.414	0.258	0.317	-203.01	0.591	0.597	0.596	186.03	0.396	0.378	0.386
						avg	HB	RJ			
Second Drainage Cycle Area:						9.78	4.53	6.54			
Imbibition Cycle Area:						0.09	1.09	0.88			
Wettability = log(A _{d2} /A _i):						2.03	0.62	0.87			

HB = Hassler-Brunner (1946) method.

RJ = Rajan (191986) method.

Centrifuge data was analyzed using PORCAP analysis software developed by Dr. Doug Ruth of the University of Manitoba. Face saturations were determined using the Hassler and Brunner (1945) and Rajan (1986) methods. Note that the validity of the Hassler-Brunner method breaks down when the core length is not significantly smaller than the distance between the core bottom and the axis of rotation. As this is the case for the drainage cycles, the face saturations determined using the Rajan method probably are more realistic. Capillary pressure and saturation data were used to calculate areas and wettability indices. Oil-water capillary pressure and wettability results are shown in Tables A-5 and A-6.

USBM wettability indices for both plugs were close to 1, indicating that, for the rock-fluid systems used, rock samples were preferentially water-wet.

Mercury Injection Tests

Mercury injection tests were performed on samples from plugs 7319.1, 7330.3, 7332.3, and 7349.3. Small pieces trimmed from the ends of the plugs were sent to another laboratory for standard mercury-intrusion pore-size measurements. For these tests, the plugs are first subjected to a vacuum. Mercury is then forced into the rock pores during controlled experiments in which 10 seconds of equilibrium time is allowed during each pressure and volume measurement. Data results were obtained for mercury injection pressures to 60,000 psia.

Table A-7 provides a summary of mercury intrusion results. Plug 7319.1 was found to be predominantly microporous, with a median pore diameter of 0.0098 μm and average pore diameter of 0.0089 μm . Results for the other three plugs ranged from 2.9 to 0.4 μm for median pore diameters and 0.03 to 0.025 μm for average pore diameters. Intrusion results are graphically displayed in Figures A-14 through A-17. The figures show incremental mercury intrusion in milliliters per gram of sample vs. pore diameter results. They can be used to gain a sense of the pore size distributions within the samples.

Table A-7 Summary of Mercury Intrusion Results

Sample	Apparent density, g/cm^3	Grain density, g/cm^3	Median pore diameter, μm	Average pore diameter, μm	ϕ , %
7319.1	2.7825	2.6644	0.0098	0.0089	4.2451
7330.3	2.6988	2.2964	2.9364	0.0318	14.9106
7332.3	2.7207	2.3675	0.4971	0.0251	12.9816
7349.3	2.7036	2.3306	0.4254	0.0289	13.7952

From these results, it appears that the samples are highly susceptible to plugging. Fluids injected into the rocks should be finely filtered to avoid permeability degradation by plugging.

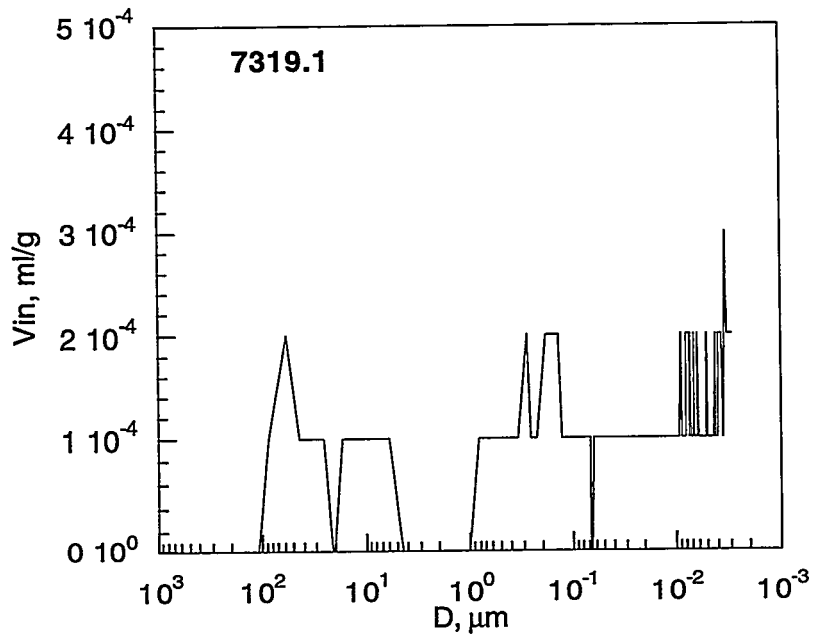


Figure A-14 Incremental Mercury Intrusion for Sample 7319.1. The total intrusion at 60,000 psia injection pressure was 0.0159 ml/g. V_{in} = volume of mercury injected; D = pore diameter.

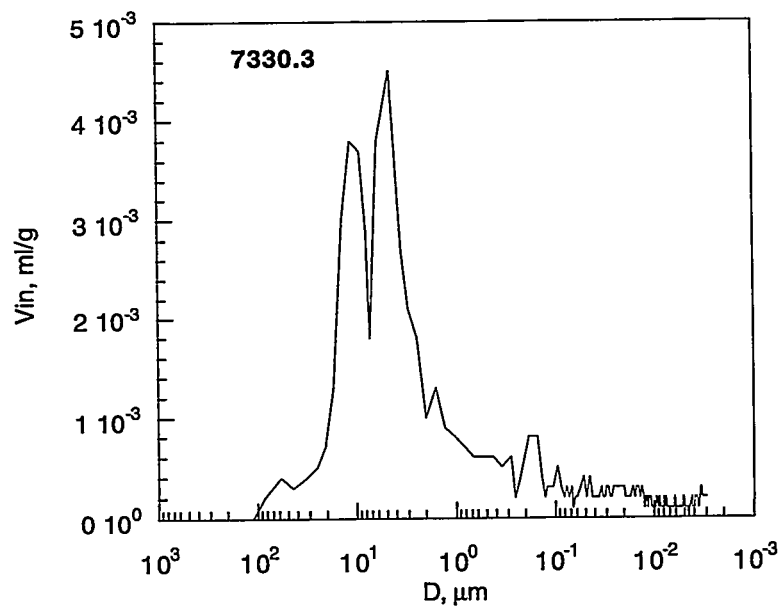


Figure A-15 Incremental Mercury Intrusion for Sample 7330.3. The total intrusion at 60,000 psia injection pressure was 0.0649 ml/g. V_{in} = volume of mercury injected; D = pore diameter.

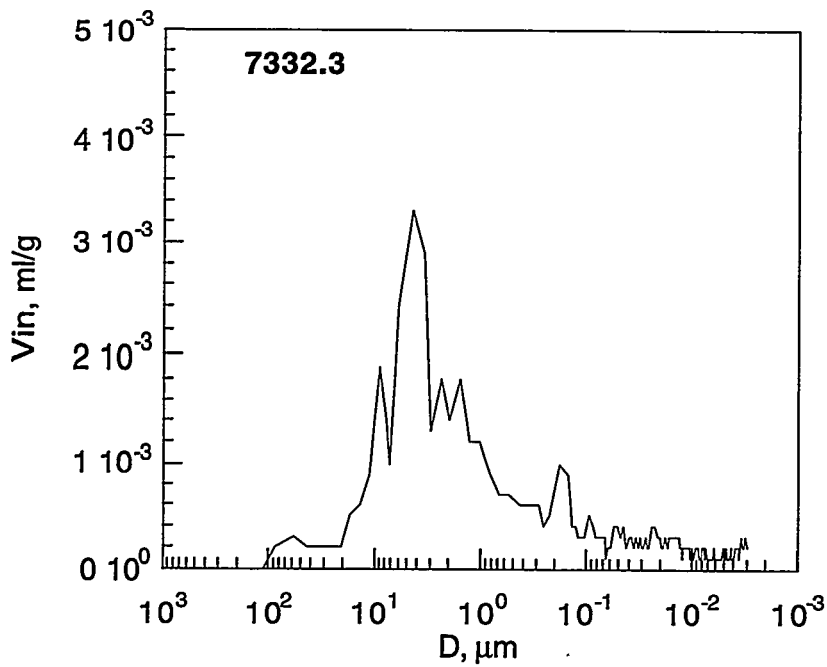


Figure A-16 Incremental Mercury Intrusion for Sample 7332.3. The total intrusion at 60,000 psia injection pressure was 0.0548 ml/g. V_{in} = volume of mercury injected; D = pore diameter.

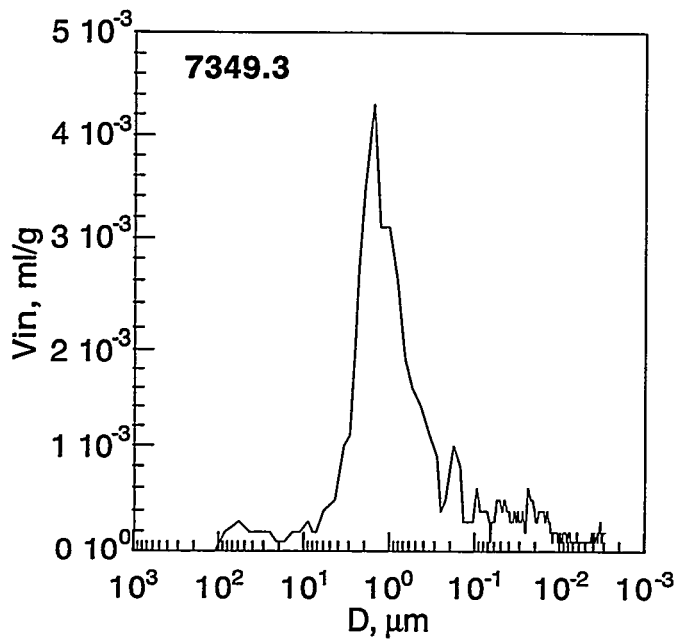


Figure A-17 Incremental Mercury Intrusion for Sample 7349.3. The total intrusion at 60,000 psia injection pressure was 0.0592 ml/g. V_{in} = volume of mercury injected; D = pore diameter.

Low-Field NMR Experiments on Belden & Blake Core Plugs

A MARAN-2 low-field NMR instrument was used for the measurements reported in this section. The instrument has a 500-gauss permanent magnet and operates at 2.1 MHz proton frequency. The sample probe can hold a sample up to 1.57 in. in diameter. Samples tested were of 1.5-in. nominal diameter.

Core plugs were wrapped with Saran Wrap for NMR measurements. Preliminary experiments on brine-saturated core plugs showed that wrapping the saturated core plugs in Saran Wrap provides an adequate barrier to fluid loss for several days. The proton content of the Saran Wrap has such a short spin-spin relaxation time (T_2) that no interference with the signal from the fluid is detectable.

The clean dry core plugs were weighed and then saturated with the synthetic laboratory brine (30.5% dissolved solids, 1.2365 g/ml density, previously described) under vacuum. The saturated core plugs were then removed from the brine, wiped to remove surface moisture, and wrapped in a previously weighed square of Saran Wrap before weighing. The weight of absorbed brine was obtained by difference. The volume of the absorbed brine was obtained using the density and the brine weight. The volume of the core plug was calculated from measurements of diameter and length at several points. A gravimetric/volumetric porosity value was thus obtained for each saturated core plug. The gravimetric porosity values obtained were very close to the values obtained on the dry core plugs using helium gas in a rock-grain volume apparatus.

Amplitude measurements on the brine-saturated core plugs were made using a simple 90° radio-frequency (RF) pulse followed by signal acquisition to develop a relationship between rock porosity and the specific NMR response. The signal amplitude was sampled at 256 points and extrapolated to zero time (the center of the RF pulse) to eliminate effects of signal relaxation during acquisition. A number of scans (64–256) were accumulated to improve signal-to-noise ratios. The delay between scans was chosen to allow complete recovery of the sample magnetic moment for quantitative results. At least 5 sets of measurements were made and averaged for each sample. The specific NMR response was obtained by dividing the average signal amplitude by the bulk volume of the core plug. The resulting value was referenced to 64 scans for analysis. (The NMR measurement is quantitative, so taking the ratio of 64 to the number of scans was all that was required.)

While the core plugs were in the sample probe, T_1 and/or T_2 relaxation-time measurements were also made. The Carr-Purcell-Meiboom-Gill (CPMG) pulse sequence was used for the T_2 measurements, where a single 90° RF pulse is followed by a string of N (delay- 180° RF pulse-delay) components, where the delay is fixed for a given experiment. At the end of each of the N components, an echo of the initial RF signal is formed; the amplitude of this echo signal is measured as a function of the total time from the initial 90° RF pulse. The amplitude of the echo signal decays as a function of the T_2 relaxation time for the sample. Typically, the delay was set from 70 to 400 μ s with $N = 2,048$ for an experiment. The entire sequence was repeated 256–1,024 times to accumulate signal at each echo for an improved signal-to-noise ratio. The T_2 experiment

is considerably faster than a T_1 experiment, and much of the same information is contained in the results.

An inversion recovery pulse sequence was used for the T_1 measurements, where a 180° RF pulse is used to invert the sample magnetic moment. Following a variable delay, a 90° RF pulse immediately followed by signal acquisition is used to determine the extent of recovery of the sample magnetic moment as a function of delay time. A sequence of 64 delay times ranging from 0.05 ms to several seconds was used to span the sample T_1 relaxation process for each sample. At each delay time, a number of scans were accumulated to improve the signal-to-noise ratio. These T_1 measurements took several hours for each sample.

Following the NMR experiments on the brine saturated core plugs, two core plugs (7332.3 and 7349.3) were centrifuged in the synthetic laboratory oil (previously described) to simulate primary drainage to residual brine conditions. The centrifuge used could achieve drainage to a capillary pressure equivalent of 100 psi. Because the amount of brine displaced by the oil during centrifugation was measured, the relative saturations of the brine and oil phases present after centrifugation could be calculated. Following the centrifuge experiments, a second set of NMR measurements was performed on the brine/oil-saturated core plugs. Following the primary drainage cycle and the sequence of NMR experiments for the samples, the core plugs were centrifuged in brine in an imbibition experiment to residual oil and an additional set of NMR data collected. An additional set of NMR experiments was made following a secondary drainage run in the centrifuge.

NMR Results and Discussion

From specific response measurements on brine saturated porous rock reported previously, a linear relationship exists between NMR specific response (SR) and rock porosity (Tomutsa et al. 1996). For measurements adjusted to a uniform number of 64 scans, the following equation gives the quantitative relationship between rock porosity (ϕ) and SR:

$$\phi = (SR - 36)/7861$$

In this equation, the SR value is corrected for the average noise from the NMR measurement and divided by the noise corrected specific response for bulk brine (7,861) to calculate the fractional NMR porosity.

Table A-8 shows the results from measurements on the 12 brine-saturated Belden & Blake samples expressed as percent porosity. Also included for comparison in Table A-8 are the porosity values obtained from measurements using a helium rock-grain volume apparatus and the gravimetric porosity value from the weight/density of the brine required to saturate each core plug. A bar graph comparing the three porosity values for each core plug is shown in Figure A-18. As Figure A-18 illustrates, the porosity values obtained by the three methods are in good agreement. However, the NMR porosity value is higher in essentially every case. From the known history of cleaning and porosity measurements on the core plugs, there is some indication that the plugs may contain some paraffin incompletely extracted by cleaning

procedures. Because the NMR measurement responds to all proton-containing material in the pore space, this residual paraffin would appear as elevated NMR porosity above the amount determined from the weight of saturating brine in the gravimetric porosity value.

Table A-8 Routine Permeability and Porosity Results

Sample Depth, ft	Air Permeability, md	Helium Porosity, %	Gravimetric Porosity, %	NMR Porosity, %
7323.1	8.58	2.1	2.34	2.74
7328.3	3.04	10.9	10.97	11.2
7330.3	12.99	7.9	8.15	8.14
7332.3	5.81	10.8	10.24	10.7
7333.1	3.76	11.1	11.04	11.5
7335.6*	7.09	1.2	1.32	1.63
7339.2	8.46	3.8	3.71	4.71
7343.0	16.59	8.4	8.39	8.70
7344.0*	11.60	0.9	1.23	1.39
7348.3	2.13	10.0	10.24	10.6
7349.3	1.73	10.6	10.6	11.3
7352.3	<0.01	1.8	2.06	2.50

*Indicates visible presence of fractures along the longitudinal axis of plug

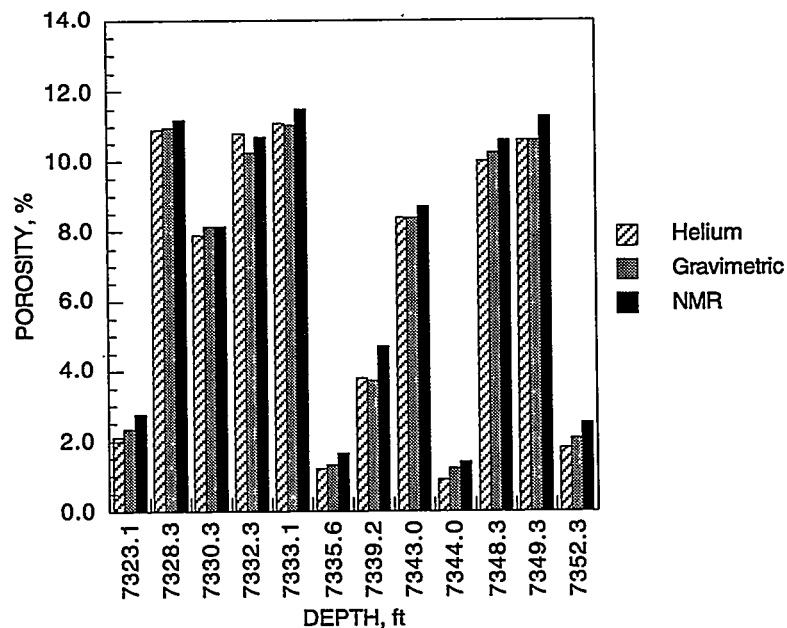


Figure A-18 Helium, Gravimetric, and NMR Porosity Measurements for the Belden & Blake Sandstone Core Plugs

The results of the T_2 relaxation experiments on one- and two-phase fluid systems in the core plugs are illustrated in Figures A-19 and A-20, which show data for the 7,332 and 7,349 samples, respectively, plotted as the spin echo amplitude (using a logarithmic scale) vs. the time to echo in milliseconds. The echo amplitudes for some of the data sets in both figures have been multiplied by a factor of 2 (imbibition, or "i" on Figure A-19) or a factor of 4 (second drainage, or "2nd d" on Figure A-19) to provide a clear distinction between the data for the different experiments. This has no effect on the slope of the plots, which determines the relaxation time values in each case. Also shown in Figure A-19 is the T_2 relaxation data for a sample of brine saturated synthetic ceramic rock (echo amplitude multiplied by a factor of 8). The relaxation process is an exponential decay of the perturbed sample magnetic moment back to the equilibrium state in the fixed magnetic field of the NMR instrument. The magnetic moment for a bulk homogeneous liquid relaxes at a characteristic rate determined by the properties of the liquid, such as viscosity and chemical composition, and the quality of the external magnetic field. The value of the T_2 relaxation time can be obtained from the slope of the semilog plot of echo amplitude (EA) vs. time shown in Figures A-19 and A-20, where

$$EA = A \cdot \exp(-t/T_2)$$

As Figure A-19 shows, only the data for the brine-saturated ceramic core plug approximate a uniform slope indicative of a single characteristic relaxation time for the water in the porous environment. The data for the brine-saturated 7332 sample are strongly curved, whereas the data

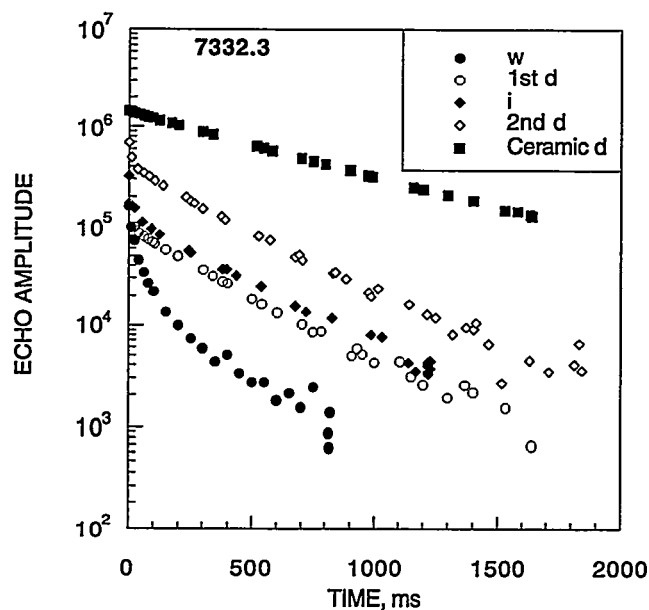


Figure A-19 T_2 Relaxation Data for Brine- and Oil/Brine-Saturated Sample of Belden & Blake Sandstone (7332.3 ft) and Brine-Saturated Ceramic. The oil/brine data show a prominent two-component character to the relaxation process, whereas the ceramic data show a nearly linear one-component relaxation. w = brine-saturated plug; 1st d = first drainage cycle; i = imbibition; 2nd d = second drainage cycle, ceramic d = ceramic drainage cycle.

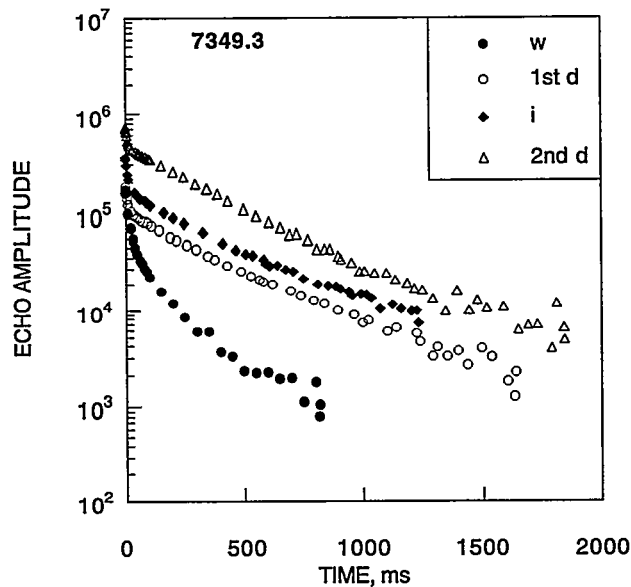


Figure A-20 T_2 Relaxation Data for Brine- and Oil/Brine-Saturated Sample of Belden & Blake Sandstone (7349.3 ft). The oil/brine data again show a prominent two-component character to the relaxation process similar to that for the 7332.3-ft sample. w = brine-saturated plug; 1st d = first drainage cycle; i = imbibition; 2nd d = second drainage cycle.

for the two-phase experiments (first drainage, imbibition, and second drainage) seem to have an approximately linear more slowly relaxing region and a second region of much higher slope at short echo time, indicating fast relaxation. Figure A-20 shows that the T_2 data from the experiments for the 7349 core plug are similar to those for the 7332 core plug.

For liquids in porous rock, the relaxation rate is strongly enhanced by contact between the fluid molecules and the pore surface where most of the relaxation occurs (Straley et al. 1994). The properties of the rock grain surface in the pores, the ratio of pore surface area to pore volume, and the degree of contact between a given fluid and the pore surface thus control the relaxation in porous rock. If the rock is assumed to be generally uniform in composition throughout the sample, then the variation in relaxation rate evident in the data in Figures A-19 and A-20 can only be explained by variations in pore surface area to volume ratios or by variations in contact between the fluids and the rock grain surface. For the brine-saturated 7332 and 7349 samples, the only variable to explain the nonuniform relaxation rate is a variation in the ratio of surface area to volume that implies that the T_2 data is a strong indicator of the variation in pore size within the samples.

Some investigators have used a sum of two or three exponentials to more closely fit the actual variations in relaxation rate exhibited for fluids in porous rock (Kenyon et al. 1988). In fact, the data for the two-phase brine/oil systems from samples 7332 and 7349 can be fitted to within 92% to 98% with two components or 98% to 99% with three components. The results for one-, two-,

and three-exponent fits to the T_2 relaxation data for the four experiments on the two core plugs are shown in Table A-9. The entries in the table for each sample give the fitted value of the T_2 relaxation time in milliseconds, followed in parentheses by the percentage this component of the fit contributes to the total experimental relaxation data. A one-exponent fit to the ceramic data achieves 95% agreement with the data.

Table A-9 One-, Two-, and Three-Exponent Fits to T_2 Relaxation Data

Sample	One	Two Exponent		Three Exponent		
	Exponent					
7332 w	57.9 (70%)	166.0 (24%)	19.0 (66%)	263.0 (12%)	51.0 (38%)	10.0 (47%)
7332 1st d	289.0 (63%)	317.0 (52%)	9.5 (43%)	395.0 (31%)	197.0 (24%)	7.9 (43%)
7332 i	253.0 (45%)	336.0 (35%)	14.0 (57%)	375.0 (31%)	74.0 (13%)	10.0 (54%)
7332 2nd d	300.0 (62%)	325.0 (57%)	9.3 (41%)	408.0 (34%)	200.0 (26%)	7.4 (39%)
7349 w	66.2 (67%)	144.0 (29%)	16.5 (62%)	221.0 (15%)	51.0 (36%)	8.8 (46%)
7349 1st d	354.0 (60%)	377.0 (55%)	8.4 (40%)	431.0 (41%)	209.0 (16%)	7.1 (41%)
7349 i	342.0 (50%)	399.0 (42%)	13.0 (50%)	430.0 (39%)	75.0 (11%)	8.7 (48%)
7349 2nd d	346.0 (63%)	365.0 (59%)	7.7 (39%)	434.0 (39%)	228.0 (22%)	6.4 (38%)
Ceramic d	688.0 (95%)	715.0 (87%)	237.0 (11%)	732.0 (82%)	311.0 (15%)	8.2 (3%)

w = brine-saturated plug; d = drainage; i = imbibition.

As discussed above, the T_2 relaxation data contain information about the variation in pore size in the porous rock. By using a sum of several exponential terms, the relaxation data for any fluid saturated porous rock can be closely fitted. By extending this process further, a distribution of exponentials using many terms can be fitted to the relaxation data (Howard and Kenyon 1992; Howard et al. 1993).

Software for this fitting of a distribution of exponentials to the relaxation data was obtained with the MARAN low-field NMR instrument. It can be applied to both T_1 and T_2 relaxation data with up to 127 terms used for the fit. Figures A-21 and A-22 show the results of the distributed exponential fit to the T_2 relaxation data for the different experiments for the two core plug samples using 127 terms for each fit. In the figures, the plot for each sample shows the relative amplitude each term contributes to the fit at each fitted value of the time. Because of the strong connection between pore size and the relaxation process, the resulting distribution of relaxation terms is believed to represent the actual distribution of pore sizes within the rock sample. Comparisons of such distributions of relaxation time with mercury porosimetry data for porous rock have shown a strong correlation between pore throat size distributions and T_1 - T_2 distributions of exponentials (Howard et al. 1993).

Figure A-21 shows that the distributed exponentials fit for the brine-saturated ceramic rock has a relatively narrow band around 700–800 ms with a much smaller band at about 8 ms. This agrees with the result that the relaxation data was closely fit using just one exponent and implies that the ceramic rock contains a very uniform pore size. Considering the ceramic rock was made using a well-graded sample of silica grains pressed and sintered together, this finding is reasonable.

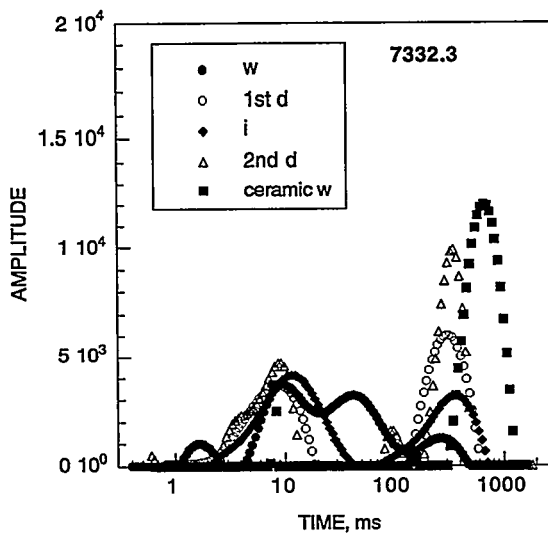


Figure A-21 Distributed Exponential Fits to the T_2 Relaxation Data for the Brine and Oil/Brine Saturated Sample of Belden & Blake Sandstone (7332.3 ft) and the Brine Saturated Ceramic. The oil/brine data show the bi-modal character with the band at longer time representing the oil relaxation. The ceramic data shows a narrow band at longer time consistent with its nearly single component relaxation. w = brine-saturated plug; 1st d = first drainage cycle; i = imbibition; 2nd d = second drainage cycle, ceramic d = ceramic drainage cycle.

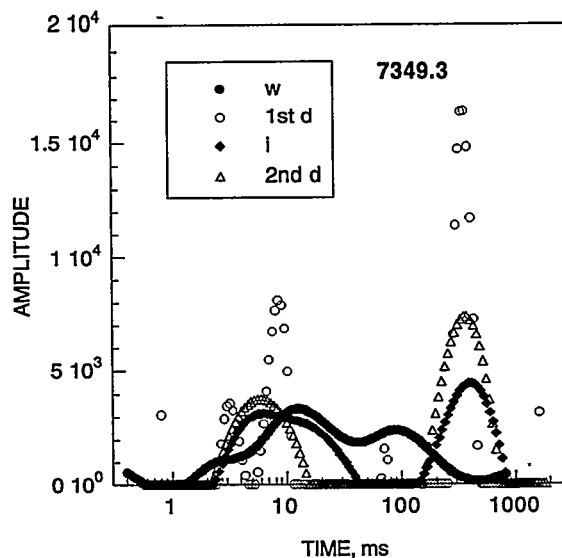


Figure A-22 Distributed Exponential Fits to the T_2 Relaxation Data for the Brine and Oil/Brine Saturated Sample of Belden & Blake Sandstone (7349.3 ft). The oil/brine data show the bi-modal character with the band at longer time representing the oil relaxation. w = brine-saturated plug; 1st d = first drainage cycle; i = imbibition; 2nd d = second drainage cycle.

In contrast, the distributed exponentials fit for the brine saturated 7332 and 7349 samples is much broader, with four regions evident in the distribution shown in Figure A-21 and three regions in Figure A-22. This implies that the 7332 sample contains a broad distribution of pore sizes with four size ranges represented, whereas the 7349 sample contains a broad distribution with three size ranges of pores. Also, because the distribution is shifted to shorter times, the pores could be smaller than those in the ceramic sample. However, natural sandstones contain materials such as clays and shales that are known to enhance relaxation and could shift the distribution to shorter times independently of small average pore sizes. The 7332 sandstone had a measured porosity of 10.7% with an air permeability of 5.81 md, whereas the 7349 sandstone had a measured porosity of 11.3% with an air permeability of 1.73. The lower permeability for the 7349 sample is consistent with the distribution of relaxation times not extending to as long a time as evident in Figures A-21 and A-22, implying smaller pore sizes at the upper end compared to the results for the 7332 sample.

Figures A-21 and A-22 show the distributed exponentials fit for the two-phase brine/oil saturated sample data for both the 7332 and 7349 samples. In every case, the fits are separated into two distinct bands implying two basic relaxation regimes, which was evident in Figures A-19 and A-20 for these samples. The best interpretation is that the band at longer relaxation times from 100 to 700 ms is the oil phase contained in the larger pores, whereas the band at shorter times from 2 to 50 ms is the water retained in the smaller pores or existing as a film wetting the grain surfaces in the larger pores. The area under the bands is a measure of the relative fraction of the fluid in that regime. For both the 7332 and 7349 samples, the primary drainage (oil/brine) data shows the larger area to be in the longer time band, implying a higher oil saturation (54% oil/46% brine for 7332 and 57% oil/43% brine for 7349). From the centrifuge data for the 7332 sample, the relative volumes of oil and brine in the sample were 3.31 ml and 2.47 ml following primary drainage. In the data for the imbibition (brine/oil) experiments, the band at shorter time is larger, implying a lower oil saturation (39% oil/61% brine for 7332 and 44% oil/56% brine for 7349). In the data for the second drainage (oil/brine) experiments, the band at longer time is larger, implying a higher oil saturation (59% oil/41% brine for both 7332 and 7349). From experiments reported in the literature for many different sandstones, the brine in pores having a relaxation time shorter than 31-35 ms is considered to be immovable or irreducible water (Straley et al. 1994). This is consistent with the interpretation given above for the two-phase relaxation data from the 7332 and 7349 samples.

References

- Hassler, G. and E. Brunner. 1945. Measurement of Capillary Pressures in Small Core Samples. *Transactions of AIME* 160: p. 114.
- Howard, J. J. and W. E. Kenyon. 1992. Determination of Pore Size Distribution in Sedimentary Rocks by Proton Nuclear Magnetic Resonance. *Marine and Petroleum Geology* 9: p. 139-145.
- Howard, J. J., W. E. Kenyon, and C. Straley. 1993. Proton Magnetic Resonance and Pore Size Variations in Reservoir Sandstones. *SPE Formation Evaluation*: p. 194-200.

- Kenyon, W. E., P. I. Day, C. Straley, and J. F. Willemsen. 1988. A Three-Part Study of NMR Longitudinal Relaxation Properties of Water-Saturated Sandstones. *SPE Formation Evaluation*: p. 622-636.
- Rajan, R. 1986. Theoretically Correct Analytical Solution for Calculating Capillary Pressure-Saturation from Centrifuge Experiments. Paper J presented at the SPWLA 27th Annual Logging Symposium, June 9-13.
- Straley, C., D. Rossini, H. Vinegar, P. Tutunjian, and C. Morriss. 1994. Core Analysis by Low Field NMR. Paper SCA-9404 presented at the International Symposium of the Society of Core Analysts, September 12-14, Stavanger, Norway.
- Tomutsa, L., D. Doughty, and S. Swan. 1996. Imaging Techniques Applied to the Study of Fluids in Porous Media. DOE Report No. NIPER/BDM-0279, September.

APPENDIX B

SPE 37334

**APPLICATION OF RESERVOIR MANAGEMENT
TECHNIQUES TO THE EAST RANDOLPH FIELD,
PORTAGE COUNTY OHIO: RESERVOIR ENGINEERING
STUDY**

*report
removed*

APPENDIX C

SPE 37333 SOME PRACTICAL ASPECTS OF RESERVOIR MANAGEMENT

*Report
Number*